X-ray Diffraction and Density Functional Theory Provide Insight into Vanadate Binding to Homohexameric Bromoperoxidase II and the Mechanism of Bromide Oxidation

Madlen Radlow, Mirjam Czjzek, Alexandra Jeudy, Jerome Dabin, Ludovic Delage, Catherine Leblanc, Jens Hartung

X-Ray-Diffraction and Density Functional Theory Provide Insight into Vanadate Binding to Homohexameric Bromoperoxidase II and the Mechanism of Bromide Oxidation

Madlen Radlow[a], Mirjam Czjzek[b], Alexandra Jeudy[c], Jerome Dabin[b], Ludovic Delage[b], Catherine Leblanc[b,c]*, and Jens Hartung[a]*

[a] Fachbereich Chemie, Organische Chemie, Technische Universität Kaiserslautern, Erwin-Schrödinger-Straße, D-67663 Kaiserslautern, Germany

[b] Sorbonne Université, CNRS, UMR 8227, Integrative Biology of Marine Models, Station Biologique de Roscoff, CS 90074, F-29688 Roscoff cedex, France

[c] Sorbonne Université, CNRS, FR 2424, Station Biologique de Roscoff, CS 90074, F-29688 Roscoff cedex, France

* Corresponding authors. Phone, +33-298292362; fax, +33-298292324; e-mail, catherine.leblanc@sb-roscoff.fr. Phone, +49-631-205-2431; fax, +49-631-205-3921; e-mail, hartung@chemie.uni-kl.de for JH.

Abbreviations: $V_{Br}PO$ = vanadate(V)-dependent bromoperoxidase; $V_{Br}PO$(*Ge*X) = $V_{Br}PO$-isoenzyme X = I, II,... from genus *G*, specified by epithet *e*; *An* abbreviates *Ascophyllum nodosum*, *Am Acaryochloris marina*, *Ci Curvularia inaequalis*, *Co Corallina officinalis*, *Cp Corallina pilulifera*, and *Ld Laminaria digitata*.

Keywords: activating hydrogen peroxide; hydrogen bond strength; ionic hydrogen bonds; orthovanadate; protein structure.

Abstract: X-ray diffraction of crystals from native *Ascophyllum nodosum* bromoperoxidase II (E.C. 1.11.1.18) reveals at a resolution of 2.26 Ångström details of vanadate co-factor binding and homohexameric protein organization. The enzyme is built from three dimers, being interwoven and tightened at the interfaces by hydrogen bond-clamped guanidinium stacks and regularly arranged water molecules. These structural elements are considered to contribute stabilizing the structure as documented by dynamic light scattering and full enzymatic activity up to a temperature of 90 °C. Every monomer binds one equivalent of orthovanadate in a cavity formed from side chains of three histidines, two arginines, one lysine, serine, and tryptophan. Binding of the co-factor occurs primarily by hydrogen bonding, as deduced from a density functional theory-based thermochemical model (B3LYP/6-311++G**). Guanidinium thereby is the strongest attractor, enhancing in a positive cooperative manner binding of histidine, lysine and serine. Activating hydrogen peroxide in density functional theory occurs in side-on coordinated orthovanadium peroxoic acid, an oxidant converting bromide with almost no energy barrier into hydrogen bonded hypobromous acid.

1. Introduction

The crystal structure of the *Ascophyllum nodosum* bromoperoxidase I [V_{Br}PO(*An*I), EC 1.11.1.18] was the first to grant insight into a class of metalloenzymes utilizing orthovanadate as co-factor for activating hydrogen peroxide. [1,2,3] The peroxide is the terminal oxidant for converting bromide into electrophilic bromine,[4] which adds chemical reactivity to nature's inventory for transforming nucleophilic hydrocarbons into brominated secondary metabolites.[5,6,7,8]

Orthovanadate exists in micromolar pH-neutral solution predominantly as twofold protonated anion, $H_2VO_4^-$, and between pH 3.8 and 3.5 as metastable orthovanadium acid (H_3VO_4; pK_a 3.5, 7.8, 12.5).[9] More acidic dilute solutions cause orthovanadium acid to degrade into the *cis*-dioxidovanadium(V) cation (VO_2^+). At concentration above micromolar autocondensation becomes sufficiently rapid to effectively convert orthovanadates into linear, cyclic, and polycyclic isopolyorthovanadates.[10,11,12,13] Hydrogen peroxide interferes with orthovanadate equilibria, providing in pH-neutral aqueous solution mono-, di-, tri-, and tetraperoxidoorthovanadates, depending on concentration and vanadate-peroxide-ratio.[14,15]

Protein binding alters orthovanadate chemistry. Interacting with amino acid side chains prevents orthovanadate from condensing to isopolyorthovanadates, may induce faster reaction with hydrogen peroxide, and has the potential to restrict peroxide chemistry to a three-membered cyclic intermediate, referred to as the *peroxo state* in bromoperoxidases (Scheme 1).[16,17,18,19] Bromoperoxidase proteins also affect rate of oxygen atom transfer to bromide and protonation of the hypobromite oxygen, ending with restoring the *resting state* at the active site.[1,4,8,20] In case no suitable organic acceptor is present hypobromous acid reduces excessive

hydrogen peroxide providing singlet dioxygen (Scheme 1).[21]

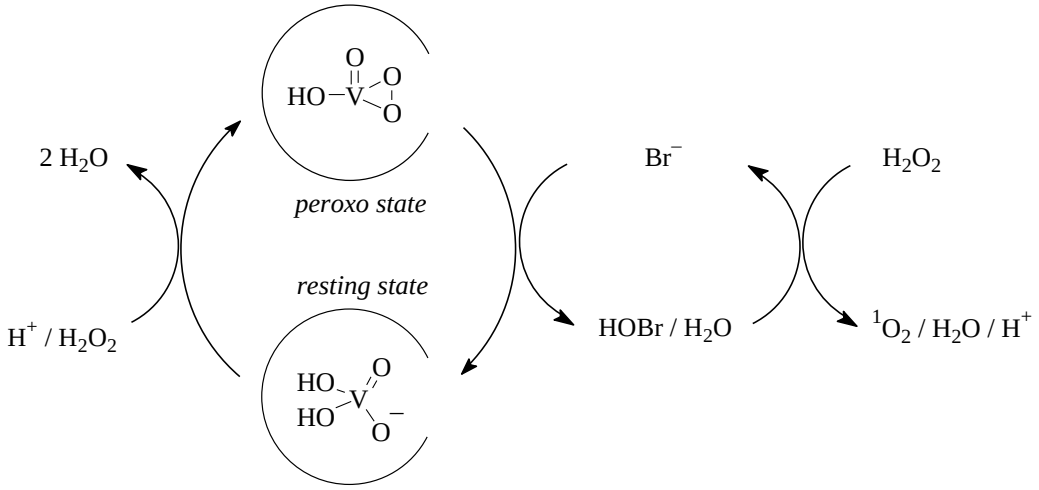

Scheme 1. Proposed intermediates and products in vanadate-dependent bromoperoxidase-catalyzed oxidation of bromide by hydrogen peroxide [for the sake of simplicity, the bromoperoxidase protein is symbolized by a partially open circle and bonding interactions (vide infra) are omitted].[1,2,16,]

Functional groups modifying orthovanadate reactivity and selectivity in the *A. nodosum* bromoperoxidase I are delivered from side chains of in total three histidines, two arginines, one lysine, serine, and tryptophan.[1,22,23,24,25] Principal attraction between co-factor and protein in this enzyme arise from covalent bonding between vanadium and nitrogen from a proximal histidine side chain.[1] A second histidine nucleus serves as general acid/base-catalyst for accelerating the rate of co-factor peroxidation leading to the *peroxo state*.[20,26] This model complies with mechanistic interpretation of orthovandate binding and oxidative chemistry of a chloroperoxidase from the fungus *Curvularia inaqualis,* [27,28,29] bromoperoxidases from *Corallina* red algae,[30,31] an iodoperoxidase from the bacterium *Zobellia galactanivorans*,[32]and

a haloperoxidase from the cyanobacterium *Acaryochloris marina*.[33]

As understanding of orthovanadate interaction with nitrogen compounds progressed and theory for describing peroxide chemistry of vanadate(V) compounds advanced, [15,34] we became aware that alternatives for co-factor bonding and the pathway for activating hydrogen peroxide by haloperoxidases exist.[34,35] In order to find out whether these alternatives apply to explain properties of marine bromoperoxidases, we investigated the solid state structure of the second *Ascophyllum nodosum* bromoperoxidase [V_{Br}PO(*An*II)] by X-ray diffraction and supplemented this information by thermochemical data on co-factor bonding and reactivity derived from an electronic structure model. We chose V_{Br}PO(*An*II) to start with, since the protein shares 61% primary structure homology with a bromoperoxidase from *Laminaria digitata* [V_{Br}PO(*Ld*)] and 41% with the *A. nodosum* bromoperoxidase I [V_{Br}PO(*An*I)].[36,37]

The information gained from our study reveals that bromoperoxidase II is a homohexamer, binding one equivalent of orthovanadate per subunit. Disulfide bonds link monomers into covalently connected dimers. Three dimers align to a cyclic homohexamer, being rigidified at interfaces by interwoven peptide chains and tightened by prolyl carboxamide-clamped guanidinium stacks from arginine side chains in addition to accurately aligned water molecules. In a shallow sterically unobstructed cavity coated by side chains from three histidines, two arginines, one lysine, serine, and tryptophan orthovanadate binds in typical hydrogen bonding distances to donor and acceptor groups. Thermochemical data from isodesmic substitutions on a density functional level of theory (B3LYP/6-311++G**) imply that orthovanadate interacts with the protein primarily through hydrogen bonding and Coulomb attraction, differing from the structure model proposed for isoenzyme I. Particularly

strong attractors for the co-factor in the new model are *N*-methylguanidinium groups, mimicking arginine side chains. Interaction with *N*-methylguanidinium furthermore strengthens in positive cooperative manner hydrogen bonding between the co-factor and weaker donors, such as amino from the side chain of lysine and hydroxy from serine. *N*-Methylguanidinium also affects acid/base-equilibria, rendering vanadium-bound hydroxy groups more acidic.

The reagent for oxidizing bromide at the active site in the electronic structure model is a side-on conformer of orthovanadium peroxoic acid. Anionic alternatives fail to attain adequate electrophilicity. In side-on conformation orthovanadium peroxoic acid transfers the outer and almost uncharged peroxidic oxygen with virtually no activation energy to bromide. From conserved orthovanadate binding sites we feel that the new mechanism is able to explain the chemistry of bromoperoxidases in a quite general manner.

2 Results and Discussion

2.1 X-ray crystal structure of V_{Br}PO(*An*II)

(*i*) *Crystallogenesis*. Vanadate-dependent bromoperoxidase II from *Ascophyllum nodosum*, abbreviated V_{Br}PO(*An*II), crystallizes from a solution of polyethylene glycol (PEG), bis(2-hydroxyethyl)amino[tris(hydroxymethyl)]methane (Tris), and sodium chloride in space group $P2_1$ (monoclinic). Substituting potassium rhodanide for sodium chloride under otherwise identical conditions furnished hexagonal crystals of V_{Br}PO(*An*II) ($P6_1$; Supporting Information). Superimposing atoms from respective dimers obtained from both types of

crystals provides a root-mean-square-deviation of 0.24 Ångström (Å). In the following we therefore restricted ourselves to summarize data from the higher in quality structure model obtained from monoclinic V_{Br}PO(*An*II)-crystals.

(*ii*) *Structure solution and quality of the model*. Given primary sequence homology of 41%, we started from atomic coordinates of the V_{Br}PO(*An*I)-crystal structure (PDB-code 1QI9)[1], replaced step-by-step amino acid side chains of the original structure by residues from the V_{Br}PO(*An*II)-protein sequence translated from a full length cDNA-clone,[36] and solved and refined the new structure after every substitution step. By this approach we obtained a three-dimensional structure model of V_{Br}PO(*An*II) displaying details at a resolution of 2.26 Å. The quality factor R_{cryst} of the model is 0.170 (R_{free} = 0.236; Supporting Information).

(*iii*) *Constitution and packing of V_{Br}PO(AnII)*. The crystal structure of bromoperoxidase II is composed of six identical subunits (Figure 1), verifying predictions from gel filtration.[36] The unit cell comprises one entire homohexamer, leading to a Mathew's coefficient V_M of 2.26 and 45.7% solvent content. Hexamers form infinite stacks of trigonal symmetry along *c* (Supporting Information).

Every chain, labelled alphabetically from *A* to *F*, comprises one molecule of orthovanadate. Disulfide bridges connect thiol groups from cysteine(Cys)-41 and Cys-77 from one chain to Cys-77 and Cys-41 of the proximal, linking chain *A* to chain *F*, *B* to *C*, and *D* to *E*. Disulfide bridges within every chain are formed from Cys-117 to Cys-126, from Cys-474 to Cys-502, and from Cys-603 to Cys-613.

Converging chains of *N*-terminal peptides are interwoven at dimer-dimer interfaces in catenane-type manner. Guanidinium stacks between arginine side chains tighten interfaces by

hydrogen bond-clamping between prolyl carboxamide and guanidinium groups, supplemented by arrays of hydrogen-bonded water molecules for overcoming like/like-repulsion (Figures 2–4).[38,39]

Three dimers stack in petal-like anticlockwise helicity to an esthetical homohexamer.[40] Inside the hexamer, when viewed from above, pairs of antiparallel helices form a triangular channel, having a maximum height of 37.6 Å above the perpendicular bisector (Figure 1).

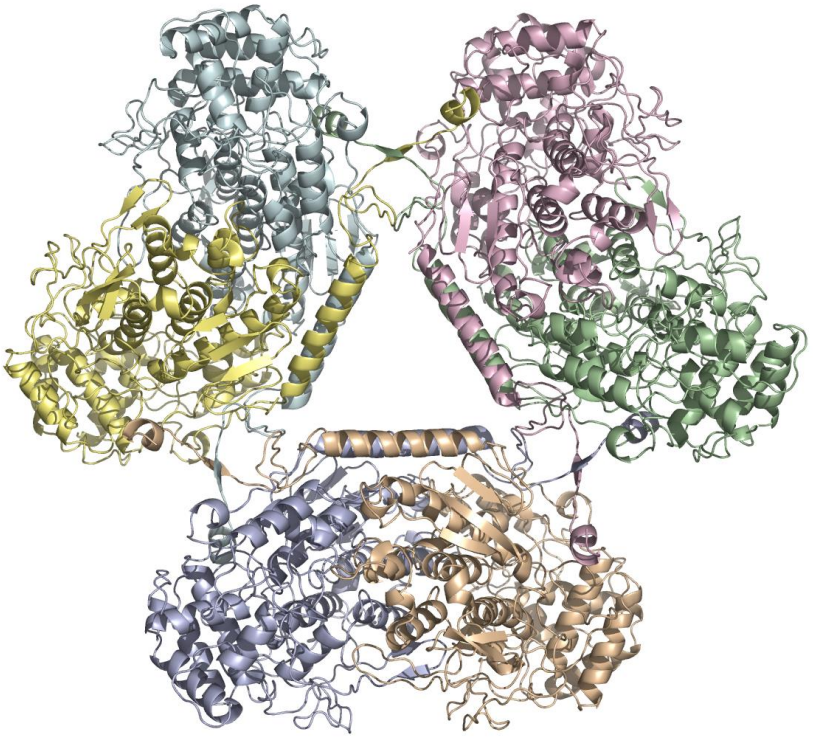

Figure 1. Ribbon-drawing showing the V_{Br}PO(*An*II)-homohexamer in the solid state at 100 K (colors were used to distinguish chains; chain *A* is drawn in yellow, *B* in magenta, *C* in green, *D* in orange, *E* in blue, and *F* in turquoise).

(*iv*) *Peptide bond conformations*. The fraction of peptide bonds in a monomer adopting dihedral angles φ[H,N,C(O),C^{α}] and ψ[O,C,C^{α},N] close to equilibrium values is 96.6%. 3.3% of peptide dihedral angles are located in less favorable but still allowed regions of the Ramachandran-chart, and 0.1% are offset from equilibrium φ/ψ-dihedral angles in the static picture of the crystal structure. Outlier conformations are peptide bonds formed by leucine-89 in chain *B* and glyine-223 in chain *C*.

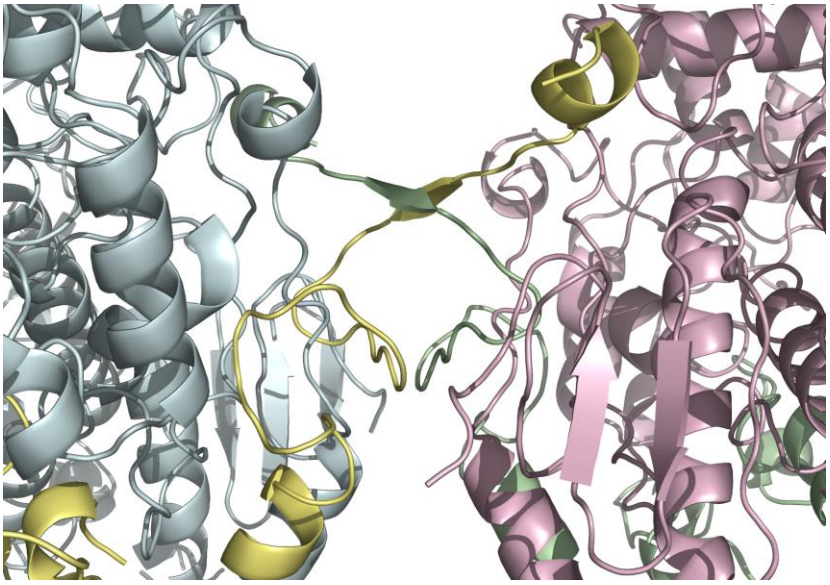

Figure 2. Interlaced peptide chains at the homodimer/homodimer-interface (for color coding, see legend of Figure 1).

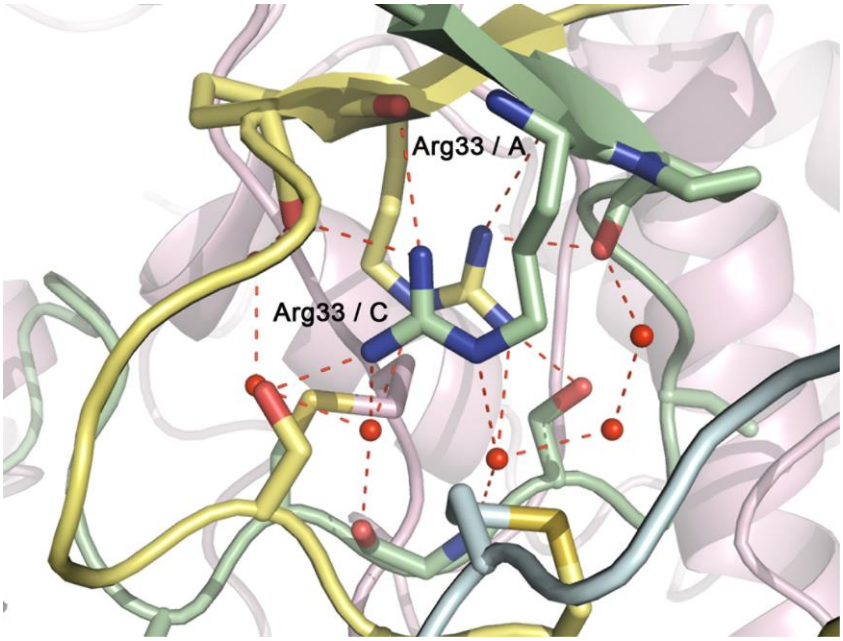

Figure 3. View along the guanidinium-guanidinium axis of arginines from two convergent peptide chains at the interface of a homodimer, displaying arrays of hydrogen-bonded water molecules (red dot for oxygen; hydrogens are omitted).

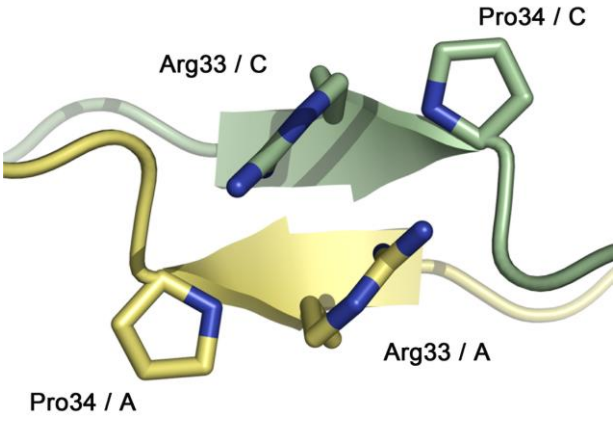

Figure 4. Stacking of guanidine-groups from arginine-side chains and hydrogen bonding between guanidinium and prolyl carboxamide groups.

3.2 Primary structure

The peptide chain of wild-type V_{Br}PO(*An*II) is built from 595 amino acids, agreeing in all but six positions with the primary sequence of the inner segment of a protein encoded by *A. nodosum* cDNA (for alignment, refer to the Supporting Information).[40] The protein sequence derived from cloned cDNA comprises 641 amino acid residues. Position 22 to 616 of the latter match with the protein identified from the crystal structure. For reasons of coherence, we applied the same numbering for the matching sequence, starting with position number 22 for the wild-type protein.

Differences between the two protein sequences are seen for valine-68 in chain *A* of the V_{Br}PO(*An*II)-crystal structure, which is an alanine in the translated cDNA-derived protein. Isoleucine-87 in the experimental structure is valine in the translated protein, methionine-103 is a valine, valines-203 and 204 are both alanines, and methionine-327 in the encoded protein is a leucine. Additional electron density points to an insertion between asparagine-396 and isoleucine-398 in the experimental structure. The nature of residue X-397 remained unidentified in the experimental structure, given insufficient local resolution.

Carbon-termini located before residue 22 and amino-termini beyond residue 616 of all six protein chains were not defined by electron density patterns and are therefore not modelled in the crystal structure.

3.3 Secondary structure

Folding of the protein chain leads to α-helical (18) and η-helical (7) segments, β-strands

(14), and sheets arising from two (2), three (1), and four (1) turned β-strands. The segment starting from position 24 to 206 contains 12 out of 25 helices (48%, 12 α and 2 η), which is followed by the most extended coiled region (position 207 to 276), being interrupted by a short η-helix (3 amino acids) and a segment of two β-strands comprising three amino acid residues each. The third quarter of the protein chain, ending at position 449, is characterized by a non-systematic alternation of seven medium-sized α-helices (8 to 14 amino acid residues), three short η-helices (3 to 4 residues), a β-strand (2 residues), and a turn having coiled segments in between. The final quarter of the chain, begins with glycine-450 and is built from three extended α-helical regions (19 to 23 residues), with the first being separated from the second by a sheet of four anti-parallel β-strands, connected by three turns (positions 479 to 511). Position 515 marks the beginning of the most extended helical domain, being interrupted at position 533 to 537 by a short coiled fragment. The final part of the chain contains a short η-helix (three residues), two sheets composed of two β-strands, and a combination of a turn and a β-sheet ending at proline-615.

In summary, 40% of the bromoperoxidase II solid state secondary structure are composed of helices, 10% of β-strands, 4% of turns, and 46% of coiled region. This information differs from a secondary structure model developed for the enzyme in tris-hydrogen chloride-buffered solution (pH 8.0), predicting 51% α-helices, 27% coils, 17% turns, and 5% β-strands.[36,41] Both models predict helical domains as dominating secondary structures (40–51%) but differ regarding proportions of coiled segments. Packing of helices in the solid state may occur tighter than coiled segments, which may be starting point for explaining secondary structural differences of the bromoperoxidase II-protein in solid and liquid phase.

2.4 On thermal stability

Dynamic Light Scattering (DLS)-signals remain invariant, when heating solutions of V_{Br}PO(*An*II) in intervals from room temperature to 90 °C. In the on-gel *ortho*-dianisidine assay oxidative activity of V_{Br}PO(*An*II) remains constant throughout the same temperature interval (Supporting Information).

In controls performed with isoenzyme V_{Br}PO(*An*I) DLS-signal change, specified by an increase in *Z*-average diameter from 24.97 to 37.93, as temperature of the solution reached 70°C. An increasing *Z*-average diameter indicates protein aggregation. The changes recorded in DLS-experiments correlate with fading enzymatic activity in the *ortho*-dianisidine assay, starting to decline at 70 °C and fading at 80 °C (Supporting Information).

V_{Br}PO(*An*II) is located at the extracellular surface, and is heat resistant even close to the boiling point of water. This stability is advantageous for an organism living in the intertidal zone, particularly during low tide when exposed to sunlight. V_{Br}PO(*An*I) occurs inside the algal tissue and copes less well with heat.[42] The differences correlate in our opinion with strength of forces holding protein chains – disulfide bonds for both enzymes for linking monomers, but in addition covalent bonds from interwoven chains in homohexameric bromoperoxidase II.

2.5 Co-factor binding

(*i*) *Orthovanadate binding site*. In the topographic center of every monomer, a well-accessible shallow cavity opens, hosting one molecule of orthovanadate (Figures 5 and 6). The

cavity is coated by functional groups from nine amino acid side chains: tryptophane-371 and lysine-374, constituents of α-helix 12 (α_{12}), arginine-382 from the coil between α_{12} and α_{13}, histidine-444 and serine-449 located in the coil bridging helices α_{15} and α_{16}, glycine-450 and histidine-451 from helix α_{16}, arginine-530 from α_{17}, and histidine-536 from the coil connecting helices α_{17} and α_{18} (Figures 6 and 7, and the Supporting Information).

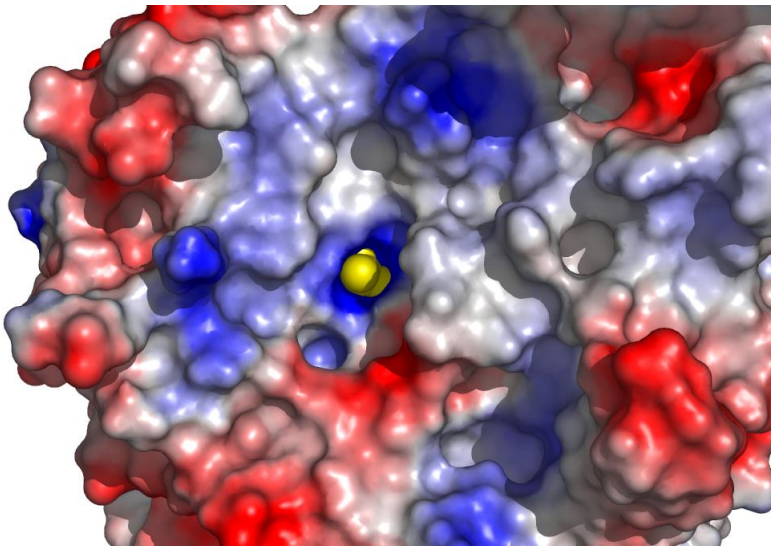

Figure 5. Modelled surface polarization of a V_{Br}PO(*An*II)-monomer (negatively polarized surface areas are depicted in blue, positively polarized areas in red; vanadate is drawn in yellow; for comments on the role of charged surfaces, see section 2.7).[43]

(*ii*) *Amino acid side chains next to orthovanadate*. Closest neighbors to orthovanadate oxygen O1 are guanidinium nitrogens $N^{\eta 1}$ and $N^{\eta 2}$ from arginine-382, $N^{\eta 1}$ from the guanidinium side chain of arginine-530, and N^{τ} from histidine-536. Vanadate oxygen O2 is positioned next to N^{ζ} from the amino group of lysine-374 and N^{τ} from the heterocyclic ring of histidine-444. Proximal heteroatoms to vanadate oxygen O3 are nitrogen N^{τ} from the

imidazole ring of histidine-444, N^{π} from the heterocyclic side chain of histidine-451, and $N^{\eta 1}$ from the guanidinium group of arginine-530.[47,44] Vanadate oxygen O4 is located next to O^{γ} from serine-449, N^{π} from histidine-451, and N^{τ} from the terminus of histidine-536 (Figure 7).

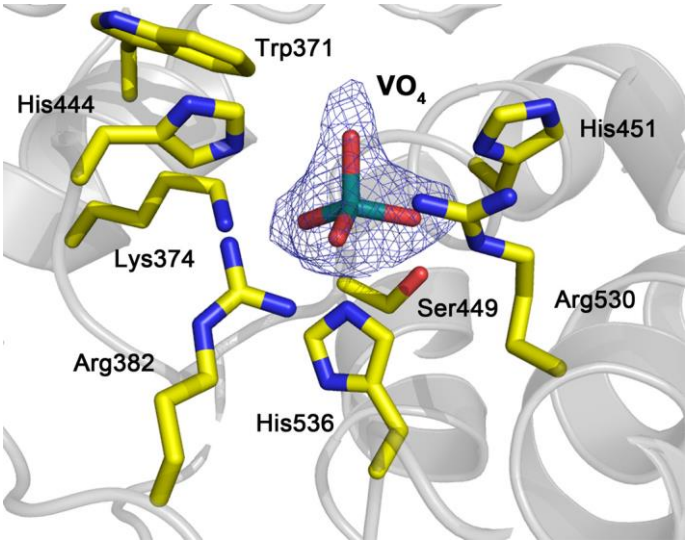

Figure 6. View of the vanadate binding site in V_{Br}PO(*An*II), displaying proximal amino acid side chains in color and the protein backbone in gray.

Proline-448 in combination with serine 449 and glycine-450 induces a distinctive turn within the protein chain.[45] Glycin-450 furthermore marks the beginning of α_{16}, the second longest α-helix continuing at position 451 with one of prominent histidine side chains. The proline-serine-glycine segment, according to our interpretation, defines the bottom of vanadate binding cavity.

In the structure model from unconstrained refinement, vanadate oxygens O1–O4 are separated on average by 3.0 ±0.3 Å (standard deviations hereafter are in most instances printed as subscripts, succeeding a mean value, i.e. 3.0 ±0.3 Å is equivalent to 3.0_3 Å) from closest

heteroatoms of amino acid side chains. Some distances are shorter than sums of associated van der Waals-radii (3.04 Å for two oxygens and 3.07 Å for one oxygen and one nitrogen), pointing to hydrogen bonding between nucleophilic heteroatoms. [46,47] Contacts O^{γ}(Ser-449),O^{4} (2.60 Å) and N^{ζ}(Lys-374),O^{2} (2.70 Å) point to particularly strong hydrogen bonds, being probably superimposed by a salt bridge for orthovanadate binding to the Lysine-374 side chain.

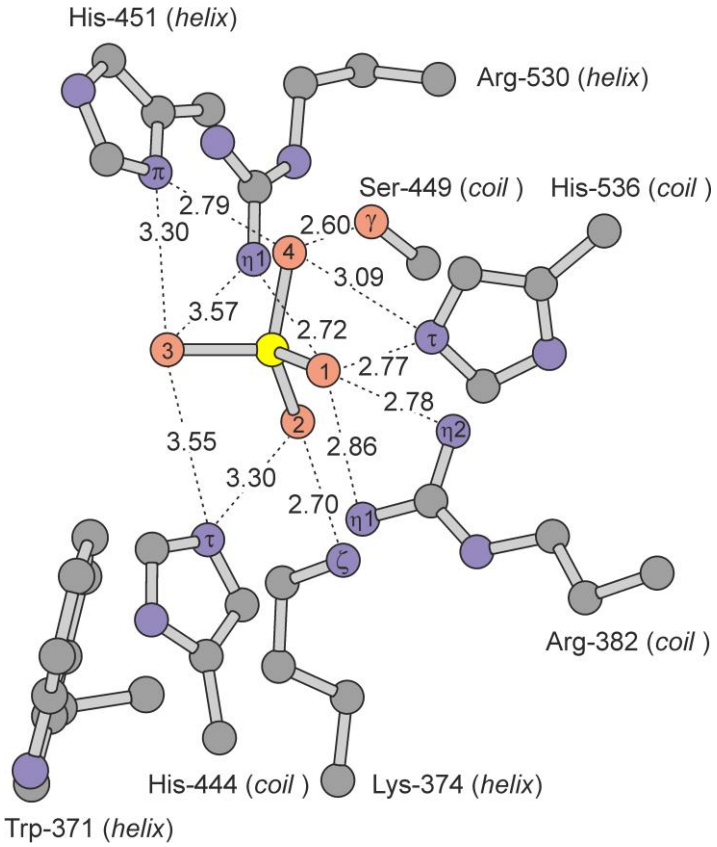

Figure 7. Distances between orthovanadate oxygens O1–4 and heteroatoms of amino acid side chains at the co-factor binding site [all values in Å; the O1,N^{τ}–distance for His-444 (3.81 Å) was omitted from the graphic for reasons of clarity; *coil* and *helix* specify secondary structure elements hosting the amino acid side chain; for labelling of atoms, refer to the text].

(*iii*) *Nitrogen-vanadium distances*. Closest distances between vanadium and nitrogen at the co-factor binding site vary from 3.0 to 3.7 Ångström (Table 1). Separations of this dimension are beyond limits for attractive interactions, when argued on the basis of crystallographic data from organometallic references [σ(V,N) = 2.11$_2$ Å].[48,49,50] Nitrogen bonding to vanadium, according to this interpretation, is not primarily relevant for co-factor bonding.

In isoenzyme V_{Br}PO(*An*I), experimental electron density from diffraction analysis was interpreted as σ-bonding and trigonal bipyramidal configuration at vanadium [V,N$^{\tau}$(His-468 = 2.11 Å].[1] The derived distance of 2.11 Å was hereafter treated as constraint feature during structure data refinement according details of the deposited PDB-file.

In the deeper cavity of V_{Br}PO(*An*I) supramolecular interactions may become more intense, having the potential to direct vanadate closer to nitrogen from a histidine side chain than in less constrained environment of V_{Br}PO(*An*II).

Table 1. Summary of distances between and imidazole-nitrogens and vanadium at the co-factor binding site

entry	histidine-position	nitrogen [a]	$d_{V,N}$ / Å
1	444	N$^{\tau}$	3.66
2	451	N$^{\pi}$	3.84
3	536	N$^{\tau}$	2.97

[a] τ = tele (remote from alkyl substitution at C4 of the imidazole core); π = pros (proximal to C4).

(*iv*) *Common structure motifs of orthovanadate-binding sites in haloperoxidases*. All marine bromoperoxidases structurally characterized thus far comprise conserved orthovanadate binding sites (Table 2).[1,30,31] In iodoperoxidase I from the bacterium *Zobellia galactanivorans* [V_IPO(*Zg*I)] and chloroperoxidase I from the fungus *Curvularia inaequalis* [V_{Cl}PO(*Ci*I)], the first histidine is replaced by a phenylalanine. In the V_{Cl}PO(*Ci*I), two additional arginines are located close to the co-factor. In the haloperoxidase from *Acaryochloris marina* [V_XPO(*Ac*I)], the proximal serine is replaced by alanine.

For understanding relevant roles, the seven prominent amino acid side chains play in bromoperoxidase chemistry we extended the crystallographic part of the study by thermochemical and molecular orbital-theoretical analysis on co-factor bonding to truncated amino acid side chains, electronic requirements and energetics of compound meeting demands for the *peroxo state*, and essentials for bromide oxidation by this intermediate. Atomic distances from the bromoperoxidase II-crystal structure served as reference for assessing the method providing in addition a first model for predicting a bromide binding site (sections 2.6–2.8).

Table 2. Summary of amino acid side chains forming co-factor-binding sites in crystal structures of vanadate-dependent haloperoxidases [a]

V_{Hal}PO(*Ge*X) [b]	Arg1-*psn.*	Arg2-*psn.*	His1-*psn.*	His2-*psn.*	His3-*psn.*	Lys- *psn.*	Ser- *psn.*	*s*AS1- *psn.* [c]	*s*AS2- *psn.* [c]
V_{Br}PO(*An*I) [d]	349	480	411	418	486	341	416	Trp-338	Gly-417
V_{Br}PO(*An*II)	382	530	444	451	536	374	449	Trp-371	Gly-450
V_{Br}PO(*Cp*I) [e]	406	545	478	485	551	398	483	Arg-395	Gly-484
V_{Br}PO(*Co*I) [f]	407	546	479	486	552	399	484	Arg-396	Gly-485
V_{I}PO(*Zg*I) [g]	331	410	(Phe-353)	360	416	324	358	Trp-321	Gly-359
V_{Cl}PO(*Ci*I) [h]	360	490	(Phe-397)	404	496	353	402	Trp-350	Asp-292
V_{X}PO(*Am*I) [i]	436	588	513	520	594	428	(Ala-518)	(Val-593)	Gly-519

[a] *psn*. = *p*rimary sequence *n*umber. [b] See abbreviations. [c] *s*AS = supplementary amino acid considered important for describing the vanadate binding site. [d] Bromoperoxidase I from *Ascophyllum nodosum* (1QI9).[1] [e] Phosphate-exchanged wild type bromoperoxidase I from *Corallina pilulifera* (1UP8).[30] [f] Phosphate-exchanged mutated bromoperoxidase I from *Corallina officinalis* (1QHB).[31] [g] Iodoperoxidase I from *Zobellia galactanivorans* (4CIT)). [27] [h] Chloroperoxidase I from *Curvularia inaequalis* (1IDQ).[27] [i] Phosphate-exchanged recombinant haloperoxidase (unspecified) from *Acaryochloris marina* (5LPC).

2.6 A thermochemical model for co-factor bonding to the bromoperoxidase II-protein

(*i*) *Approach*. For determining strength of co-factor bonding we defined an isodesmic reaction describing substitution of water from hydrated orthovanadates by molecules covering functional groups of prominent amino acid side chains at the bromoperoxidase II-binding site. Methanol in this model serves as mimic for the serine side chain, imidazole for the side chain of histidine, methylamine and methylammonium for lysine, and *N*-methylguanidinium for arginine. From orientation of the tryptophan-371-side chain we concluded that the heterocyclic N,H-group is not involved in hydrogen bonding to the co-factor and omitted indole from the study.

In an isodesmic reaction, numbers of bonds broken and formed and thus the number of chemical events occurring on both sides of a equation is the same.[51] Possible aberration in molecular energies arising from the physical model used for mathematically describing chemical bonding largely cancels in an isodesmic reaction while calculating energy difference by subtraction.[52,53] The precision for predicting accordingly thermochemical data from theory nowadays comes close to the experiment, given an adequate theory exists for precisely calculating molecular energies.

(*ii*) *Structure and energy of hydrogen bonds toward orthovanadium compounds*. A theory for reproducing experimental bond lengths between vanadium and second row elements in trialkyl orthovanadates with a precision of 97% and above is Becke's three parameter Lee-Yang-Parr hybrid functional[54,55] (B3LYP) in combination with a triple ζ-basis set, specified as 6-311++G**.[34,56,57,58,59] For securing that B3LYP/6-311++G**-theory also reproduces hydrogen bond strengths of interest, we calculated association energies in clusters comprising

four to eight water molecules (Figure 8).[60] The mean value per hydrogen bond in these clusters is –21±2 kJ mol^{-1}, matching with the value of 23±2 kJ mol^{-1} reported for the experimental hydrogen bond strength in liquid water.[61]

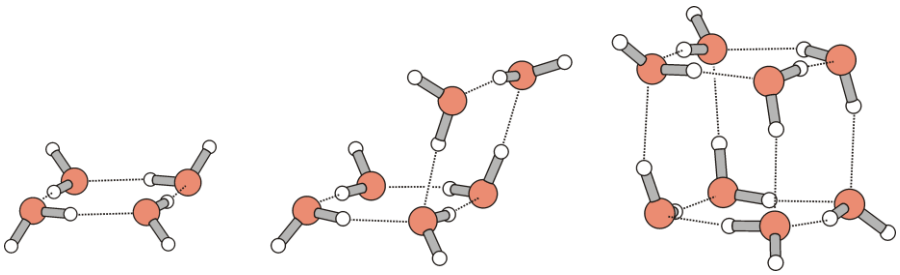

–89.3 *–149.4* *–225.9*

7.6 **20.5** **30.2**

Figure 8. Association energy for water in clusters (B3LYP/6-311++G**; zero-point vibrational energy-corrected reaction energies for zero Kelvin, $\Delta_R E$, are printed in italics; Gibbs free energy referring to a temperature of 298.15 Kelvin and a pressure of 1 atmosphere, ΔG^0, are printed in bold; all energies are given in kJ mol^{-1}; oxygens in the Figure are depicted in red and hydrogens in white).

(*iii*) *Hydrating orthovanadium acid*. A co-factor suitable for converting hydrogen peroxide into an electrophile is orthovanadium acid. Positive charges from side chains of arginine-382 and arginine-530 are expected to kinetically stabilize the acid for preventing hydrolysis to the *cis*-dioxidovanadium(V) cation.[62] Anionic orthovanadate-derived peroxides, as will become apparent in the following, are less electrophilic than hydrogen peroxide. Dihydrogen orthovanadate, on the other hand, is the most likely configuration of the *resting state* in bromoperoxidase II.

In the calculated minimum structure of orthovanadium acid, all protons point toward oxido oxygen O^A, similar to configuration of orthophosphorous acid (H_3PO_4) in the solid state.[63,64] Water preferentially accepts a proton from the acidic hydroxy group in orthovanadium acid and forms in hydrate **1a*1*** a second weaker bond with oxido oxygen O^A (O^B,O^W = 2.773 Å and O^W,O^A = 3.009 Å in **1a*1***). A second water molecule adds to monohydrate **1a*1*** similar to the first (O^B,O^W = 2.786$_6$ Å and O^W,O^A = 3.02$_2$ Å in **1a$_2$**), while the third merely forms a monovalent hydrogen bond with the non-hydrated hydroxy group of dihydrate **1a*2*** (Scheme 2).

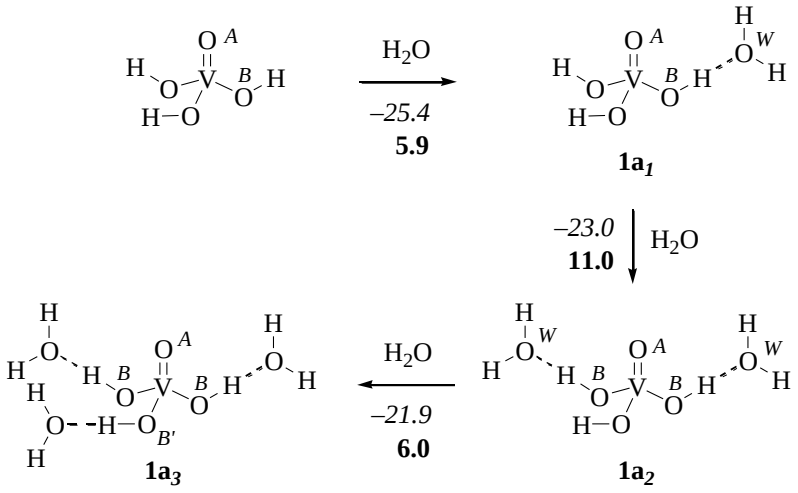

Scheme 2. Calculated hydrogen bond energies between water and orthovanadium acid (reaction energies, $\Delta_R E$, are printed in italics, Gibbs free energy differences for standard conditions, ΔG^0, in bold; all energies in kJ mol^{-1}).

The energy gained by hydrating orthovanadium acid gradually declines from –25.4 kJ mol^{-1} for the first water molecule via –23.0 kJ mol^{-1} for the second to –21.9 kJ mol^{-1} for the third. Energy differences of 2 kJ mol^{-1} and below come close to the limit of the chosen theory

for predicting absolute reaction energies. We therefore consider sequential hydration as independent events, occurring with averaged hydrogen bond energy of 23±2 kJ mol^{-1}, which is close to the hydrogen bond strength of water (Figure 8).[47]

(*iv*) *Hydrating dihydrogen orthovanadate*. Dihydrogen orthovanadate, the most likely configuration of the bromoperoxidase II-*resting state*, adopts in density functional theory C_2-symmetry. Bonds between vanadium and hydroxy oxygen O^B (V,O^B = 1.864 Å) are longer than bonds between vanadium and oxido oxygens O^A and O^C (V,O^A = V,O^C = 1.623 Å). Delocalizing nonbonding electron pairs from formally anionic oxygen O^C into vacant *d*-orbitals at vanadium, equilibrates lengths and renders oxido oxygens O^A and O^C in natural bond order (NBO)-theory[65] indistinguishable.

Water binds to dihydrogen orthovanadate **2a** in chelating manner across oxido oxygens O^A and O^C (O^A/O^C···O^W = 2.949 Å). The strength of this interaction exceeds the value for hydrating orthovanadium acid by factor 2.3 (Scheme 3).

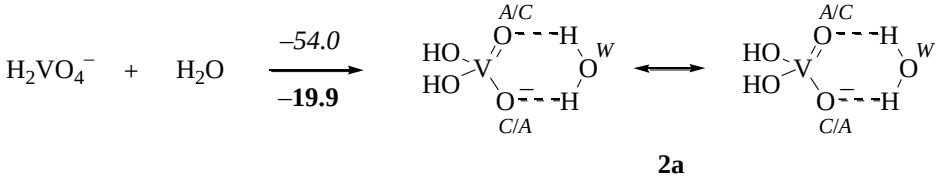

Scheme 3. Hydrogen bonding between water and dihydrogen orthovanadate [reaction energies ($\Delta_R E$) are printed in italics, Gibbs free energy differences for standard conditions (ΔG^0) in bold; all energies in kJ mol^{-1}].

(*v*) *Hydrogen bonding of amino acid side chain mimics to orthovanadium acid*.

Methanol, imidazole, and methylamine bind to orthovanadium acid preferentially as hydrogen bond acceptors, leading to monovalent adducts **1b**–**1d**. Methylammonium and *N*-methylguanidinium form in calculated minimum structures **1e**–**1f** chelated hydrogen bonds with two hydroxy oxygens (O^B). In a second local minimum of similar energy, *iso*-**1f**, *N*-methylguanidinium forms a bifurcated hydrogen bond with O^B (Table 3).

Table 3. Calculated reaction energies for substituting water from orthovanadium acid monohydrate (**1a*1***) by amino acid side chain mimics H_nX [a]

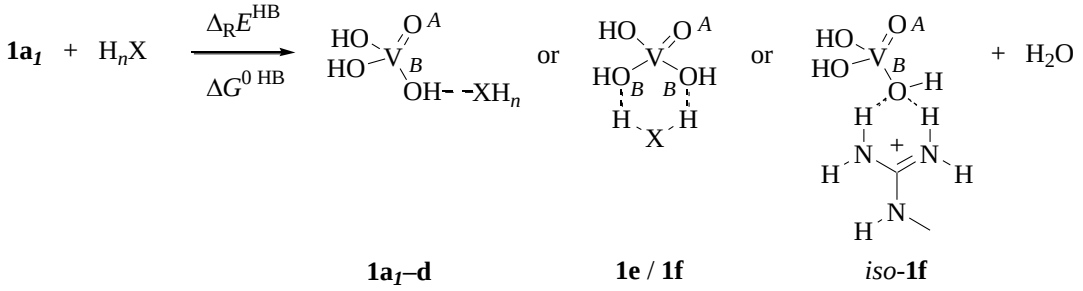

1a*1*–d **1e** / **1f** *iso*-**1f**

entry	H_nX / compd. **1**	$\Delta_R E^{HB}$ / kJ mol^{-1} [b]	$\Delta G^{0\,HB}$ / kJ mol^{-1} [c]	d(O,X) / Å [d]
1	CH_3OH / **1b**	–3.9	–0.1	2.735
2	imidazole / **1c**	–18.3	–13.2	2.708
3	CH_3NH_2 / **1d**	–17.1	–15.7	2.702
4	$CH_3NH_3^+$ / **1e**	–57.8	–50.0	2.850
5	*N*-methylguanidinium / **1f**	–41.4	–31.3	2.94_1
6	*N*-methylguanidinium / *iso*-**1f**	–35.7	–30.4	2.95_1

[a] Definition of relative hydrogen bond strengths: $\Delta_R E^{HB} = \Sigma(E_{products}) - \Sigma(E_{substrates})$ and $\Delta_R G^{0\,HB} = \Sigma(G^0_{products}) - \Sigma(G^0_{substrates})$. [b] For 0 K, zero-point vibrational energy-corrected. [c] For 298.15 K and 1 atm. [d] For entries 5 and 6: mean value; the subscript gives the standard deviation for the last digit from the mean value.

The experimental oxygen-oxygen distance between O^{γ} in serine-449 and vanadate oxygen O4 is 5% shorter than the calculated distance in methanol-adduct **1b**. In imidazole-adduct **1c**, the predicted nitrogen-oxygen distance is 2% shorter than experimental distance between O1 and N^{τ} in histidine-536. For the methylamine adduct to orthovanadium acid (i.e. **1d**), calculated and experimental nitrogen-oxygen distances match (Table 3 and Figure 7). From this information we concluded that the selected density functional method reproduces distances from protein crystallography in desired precision.

Thermochemically, isodesmic substitution of water at orthovanadium acid is thermoneutral for the reaction with methanol, exergonic for methylamine and imidazole as acceptors, and markedly exothermic for substitution by *N*-methylguanidinium and methylammonium (Table 3).

(*vi*) *Hydrogen bonding to dihydrogen orthovanadate*. Dihydrogen orthovanadate attracts methanol and imidazole as donor providing monovalent adducts **2b** and **2c** as minimum structures. Methylamine, methylammonium, and *N*-methylguanidinium form chelated hydrogen bonds across oxido oxygens O^{A} and O^{C} in calculated structures **2d**–**f** (Table 4). No evidence was seen for a local minimum displaying a bifurcated hydrogen bond between *N*-methylguanidinium and dihydrogen orthovanadate.

Distances between orthovanadate oxygens and heteroatoms from hydrogen bond donating groups from theory are well in accord with data from the V_{Br}PO(*An*II)-crystal structure for imidazole adduct **2c** (1% shorter compared to O1, N^{τ}-His-536), methylammonium adduct **2e** (3% shorter compared to O2,N^{ζ}-Lys-374) and *N*-methylguanidinium adduct **2f** (3% shorter compared to average value for $N^{\eta 1}$ and N^{η} from Arg-382; Table 4, entries 4 and 5).

Close to target limit is the oxygen-oxygen distance for hydrogen bonded methanol (5% longer in **2b**), compared to O4,O^{γ} in the solid state structure. Hydrogen bonding methylamine of exceeds the experimental O2,N^{ζ}-distance by 17%, indicating that this does reflect structure of lysine-374 to the co-factor adequately (vide infra).

Table 4. Energies for substituting water from hydrated dihydrogen orthovanadate by bromoperoxidase II-binding site mimics

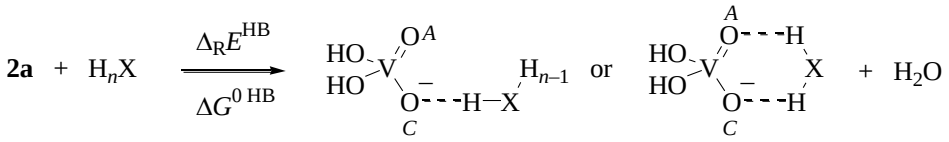

2b / **2c** **2d–f**

entry	H_nX / compd. **2**	$\Delta_R E^{HB}$ / kJ mol^{-1} [b]	$\Delta G^{0\,HB}$ / kJ mol^{-1} [c]	d(O,X) / Å [d]
1	CH_3OH / **2b**	0.6	0.9	2.737
2	imidazole / **2c**	–31.8	–26.6	2.758
3	CH_3NH_2 / **2d**	23.9	25.3	3.17_1
4	$CH_3NH_3^+$ / **2e**	–435.4 [d]	–429.1	2.63_7
5	*N*-methylguanidinium / **2f**	–382.7 [d]	–370.2	2.73_1

[a] For definition of $\Delta_R E^{HB}$ and $\Delta G^{0\,HB}$, see footnote [a] of Table 3. [b] For 0 K, zero-point vibrational energy-corrected. [c] For 298.15 K and 1 atm. [d] For entries 4 and 5: mean values; the subscript gives the standard deviation for the last digit.

Replacing water from hydrated dihydrogen orthovanadate by methylamine is endothermic (23.9 kJ mol^{-1}), thermoneutral for methanol, and exothermic for imidazole (–31.8

kJ mol^{-1}). *N*-Methylammonium and *N*-methylguanidinium form salt bridges superimposing hydrogen bonds. Distances between nitrogens and oxido oxygens O^A and O^C predicted by theory for adduct **2e** match with the O2,N^{ζ}-contact in the crystal structure.

(*vii*) *Cooperative effects*. *N*-Methylguanidinium in combination with methanol, methylamine, and imidazole (i.e. **1g**$_2$, *iso*-**1g**$_2$–**1i**$_2$) form stronger hydrogen bonds with orthovanadium acid than predicted from individual contributions (Table 5, entries 1, 4–6, and Figure 9). Positive cooperativity arises from a stabilizing effect of *N*-methylguanidinium on the accepting non-bonding electron pair at O^B. Increased electron attraction at O^B is forwarded to substituents at vanadium, strengthening hydrogens toward donors. The hydroxy group not involved in chelated *N*-methylguanidinium binding becomes for the same reason more acidic, as seen in dihydrogen orthovanadates **2h**$_2$ and **2h**$_2$ formed upon binding methylamine or imidazole (Table 5, entries 2 and 3; Figure 5).

Two donors, for instance imidazole *and* methylamine, bind weaker to orthovanadium acid than predicted from the sum of individual contributions. Imidazole in combination with methylamine thus is an instance of negative cooperativity (Table 5, entry 8).

Considering isodesmic substitution of three water molecules from trihydrate **1a**$_3$ by *N*-methylguanidinium, imidazole, and methylamine (or methanol) as thermochemical model for co-factor attraction by the bromoperoxidase II protein in aqueous solution provides a Gibbs free energy difference of –112±9 kJ mol^{-1} (Table 5, entries 10 and 12). The modelled equilibrium constant for hydrolytically displacing the side chin mimics would be 2.4×10^{-20}. An experimental constant for orthovanadate dissociating from the protein of V_{Br}PO(*An*I) is 55 nanomolar.[16] Cooperative hydrogen bonding, in summary is sufficiently strong explaining

experimental affinity for orthovanadate to a bromoperoxidase protein.

Table 5. Calculated energies for substituting three molecules of water from trihydrate **1a*3*** by three amino acid side chain mimics [a]

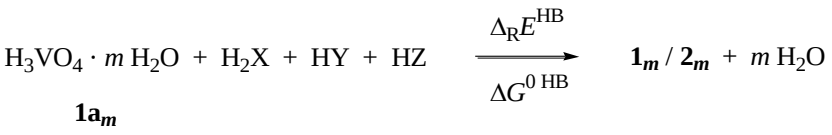

entry	**1a**$_m$	**1**$_m$ / **2**$_m$	H_2X	HY	HZ	$\Delta_R E^{HB}$	$\Delta G^{0\,HB}$	$\Delta\Delta_R E$	$\Delta\Delta G^0$
1	**1a*2***	**1g*2***	*N*mg	MeOH	–	–71.6	–60.2	–26.3	–28.8
2	**1a*2***	**2h*2***	*N*mg	imH	–	–113.1	–90.0	–50.4	–47.5
3	**1a*2***	**2i*2***	*N*mg	$MeNH_2$	–	–97.6	–78.2	39.1	–31.2
4	**1a*2***	*iso*-**1g*2***	*N*mg	–	MeOH	–72.3	–58.6	–27.0	–27.2
5	**1a*2***	*iso*-**1h*2***	*N*mg	–	imH	–108.6	–90.1	–50.1	–43.1
6	**1a*2***	*iso*-**1i*2***	*N*mg		$MeNH_2$	–96.1	–80.5	–37.6	–33.5
7	**1a*2***	**1j*2***		imH	MeOH	–21.1	–12.8	1.1	0.6
8	**1a*2***	**1k*2***		imH	$MeNH_2$	–28.4	–21.6	7.0	7.3
9	**1a*2***	**1m*2***		MeOH	$MeNH_2$	–20.5	–15.1	0.6	0.7
10	**1a*3***	**1n*3***	*N*mg	imH	MeOH	–130.7	–105.3	–67.1	–60.7
11	**1a*3***	*iso*-**1n*3***	*N*mg	MeOH	imH	–127.0	–102.2	–63.4	–57.6
12	**1a*3***	**1o*3***	*N*mg	imH	$MeNH_2$	–145.7	–118.7	–68.9	–58.5
13	**1a*3***	*iso*-**1o*3***	*N*mg	$MeNH_2$	imH	–146.1	–118.1	–69.3	–57.9

[a] All energies in kJ mol^{-1}; H_2X: *N*mg = *N*-methylguanidinium; HY, HZ: imH = imidazole, MeOH = methanol, $MeNH_2$ = methylamine; $\Delta\Delta_R E = \Delta_R E^{HB}$ for *multiple* substitution (*multiple*) – $\Sigma\Delta_R E^{HB}$ for *mono*substitution (mono); $\Delta\Delta G^0 = \Delta G^{0\,HB}$ *multiple* – $\Sigma\Delta G^{0\,HB}$ *mono*.

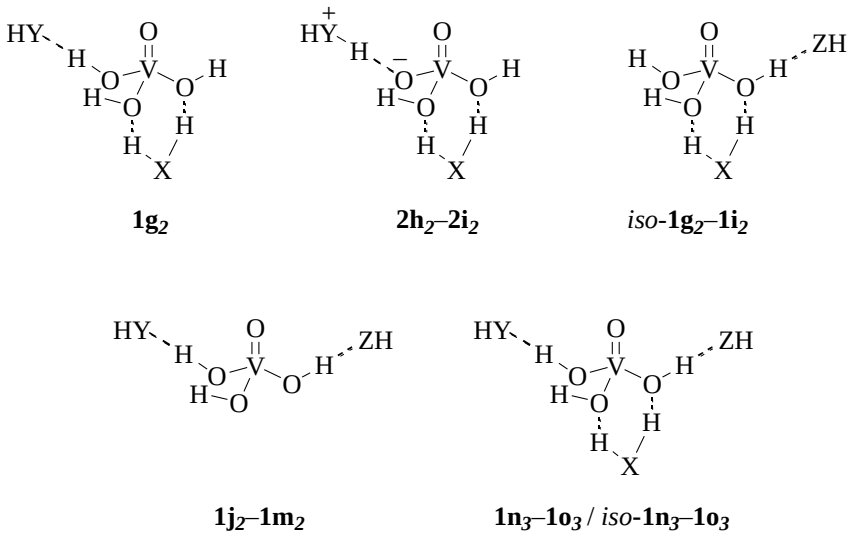

Figure 9. Structure formulas of orthovanadium acid, hydrogen bonded to two (**1g*2***, *iso*-**1g*2***–**1m*2***) and three amino acid side mimics [**1n*3***–**1o*3***, and *iso*-**1n*3***–**1o*3***; the descriptor *iso* for structures **1g**–**1i**, and **1n**–**1o** refers to *iso*(mer)s having HY and HZ interchanged with respect to position of H_2X] and twofold hydrogen-bonded dihydrogen orthovanadates **2i*2*** and **2j*2***.

(*viii*) *A model for protonating dihydrogen orthovanadate*. Side chains from lysine and histidine bear functional groups able protonating in acid-base equilibria dihydrogen orthovanadate.

The side chain of lysine (pK_a 10.53) is similarly basic as methylamine (pK_a 10.66).[66] In molar solution 2.1% of methylamine is protonated at room temperature. The fraction of methylammonium increases upon diluting to micromolar solution to 99.9%. Imidazole (pK_a 6.95) is less basic than methylamine. The fraction of imidazolium in in molar solution of imidazole therefore is markedly smaller (0.03%). Diluting an imidazole solution to micromolar raises the percentage of imidazolium to 25.7% (for 25 °C).

Protonating dihydrogen orthovanadate is endergonic by 39.0 kJ mol^{-1} utilizing methylammonium as acid and 18.0 kJ mol^{-1} for the reaction with imidazolium, when calculated from pK_a-values tabulated for a temperature of 25 °C.

In model calculations referring to the gas phase, the hydrogen-bonded proton is spontaneously released from imidazolium starting from input structure **2p** to oxido oxygen $O^{A/C}$ in final product **1c**. Methylammonium form hydrogen-bonded adduct **2d** with dihydrogen orthovanadate existing as local minimum. After crossing a shallow barrier, methylammonium transfers the hydrogen-bonded proton along the path of an exergonic N,H-stretching vibration toward oxido oxygen $O^{A/C}$ (Scheme 4).

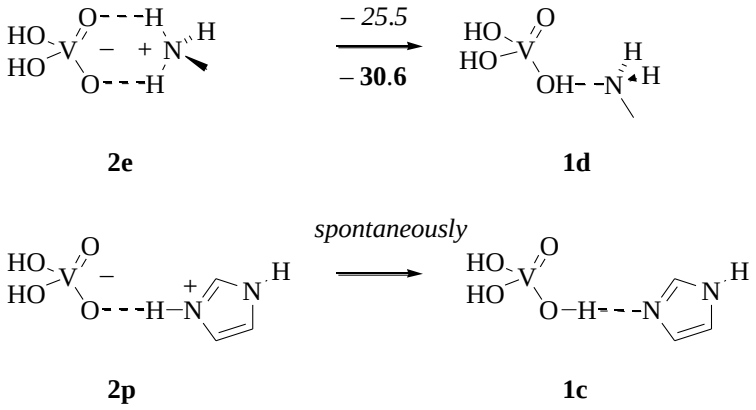

2e **1d**

2p **1c**

Scheme 4. Reactivity of dihydrogen orthovanadate toward methylammonium [top; *d*(O,N) = 2.702 Å in **1d** and 2.63$_7$ Å in **2d**] and imidazolium (bottom; *spontaneously* means that unconstrained energy function minimization provides adduct **1c** from input structure **2p** without proceeding through a local minimum).

At the site in bromoperoxidase II, dihydrogen orthovanadate may encounter a situation in between diffusion-controlled solution chemistry and gas phase reactions. Imidazolium is the

stronger and more effective N,H-acid for protonating the co-factor. Lysine-374, however, may take over the role for effectively picking up a proton from water to and converting the closest available imidazole nitrogen, which is the side chain from histidine-444 into an imidazolium group. A distance of 2.70 Å between N^{ζ} from lysine-374 and vanadate oxygen O2 is in line with the closest nitrogen-oxygen contact in calculated methylammonium adduct to dihydrogen orthovanadate (cf. 2.63$_7$ Å in **2e**, Table 4, entry 4).

(*ix*) *Nitrogen bonding to vanadium*. Imidazole in some reactions is a Brønsted-base in others as Lewis base.[48,49,50] Nitrogen-bonding to vanadium has been put forward as principal driving force for binding orthovanadate other haloperoxidase proteins.[1,29,32]

In the electronic structure model, imidazole adds to orthovanadium acid vicinal to oxido oxygen O^A (*iso*$_{cis}$-**1c**), as already described by others,[67] and also opposite to O^A (*iso*$_{trans}$-**1c**; Scheme 5). Both adducts pose local minima on the orthovanadium acid/imidazole-potential energy surface, with hydrogen-bonded adduct **1c** marking the global minimum, 28.3 kJ mol^{-1} in Gibbs free energy below Lewis-acid/base adduct *iso*$_{trans}$-**1c**.

Bonds between vanadium and nitrogen in imidazole adducts *iso*$_{cis/trans}$-**1c** are long and weak (Table 6), reflecting small stabilizing effects of the metal on the non-bonding electron pair of at nitrogen (NBO-analysis, Supporting Information). The energy gained from σ(V,N)-bonding in *iso*$_{trans}$-**1c** (119 kJ mol^{-1}) and *iso*$_{cis}$-**1c** (215 kJ mol^{-1}) remains below the value needed for compensating structural changes imposed by adding the Lewis base to the metal, for instance lengthening of vanadium-oxygen bonds and widening of O,V,O-angles.

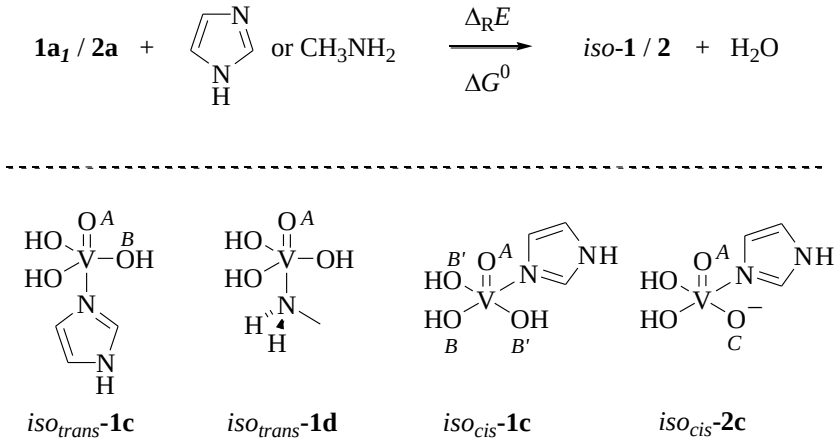

Scheme 5. Pentacoordinated adducts between nitrogen bases and orthovanadium compounds (B3LYP/6-311++G**).

Table 6. Calculated reaction energies for preparing Lewis-acid/base adducts from hydrated orthovanadates and nitrogen compounds

entry	conversion [a]	$\Delta_R E$ / kJ mol^{-1} [b]	ΔG^0 / kJ mol^{-1} [c]	d(V,N) / Å	α(O,V,N) / deg [d]
1	**1a$_1$** → *iso$_{trans}$*-**1c**	4.8	15.1	2.403	178.1
2	**1a$_1$** → *iso$_{cis}$*-**1c**	21.3	35.0	2.291	91.8
3	**1a$_1$** → *iso$_{trans}$*-**1d**	3.3	9.3	2.400	178.5
4	**2** → *iso$_{cis}$*-**2c**	101.8	114.1	2.337	86.1_3

[a] $\Delta_R E$ and $\Delta G°$ refer to the stoichiometry specified in Tables 3 and 4. [b] For 0 K; zero-point vibrational energy-corrected. [c] For 298.15 K and 1 atm. [d] O^A for entries 1–3; mean value for O^A and O^C for entry 4; subscript indicates standard deviation for the last digit; deg = degrees.

σ-Bonding of nitrogen from imidazole to vanadium in dihydrogen orthovanadate occurs in the electronic structure model exclusively proximal to one of the oxido oxygens $O^{A/C}$,

leading to *iso*$_{cis}$-**2c**.[67] Substituting water from hydrate **2a** via σ(V,N)-bonding is endergonic (114 kJ mol^{-1}), because vanadium in an anionic orthovanadate destabilizes the non-bonding electron pair at nitrogen (NBO-analysis, Supporting Information).

The principles described for σ-bonding donor atoms to vanadium in orthovanadates extend to other Lewis-bases. Methylamine, for instance forms local minimum *iso*$_{trans}$-**2d** when added opposite to oxido oxygen O^{A} in orthovanadium acid, 25.0 kJ mol^{-1} higher in Gibbs free energy than hydrogen-bonded adduct **2d**.

Imidazole and methylamine, in conclusion, will seek alternatives to vanadium binding when existing.

2.7 Hydrogen bonding to bromide

(*i*) *Bromide – a competitive bromoperoxidase II-inhibitor*. Steady state kinetic data reveal weaker affinity of bromide toward bromoperoxidase II than hydrogen peroxide and a competitively inhibiting effect at higher concentration.[36] Three orthogonally arranged non-bonding electron pairs put bromide into a position to interact in similar manner with amino acid side chains as dihydrogen orthovanadate. A smaller ionic radius of 1.95 Å,[68] compared to 2.92 Å for the VO_4^--tetrahedron in sodium metavanadate hydrate,[69] implies weaker interaction with a static binding site. Half of hydrogen bond donating side chains reside in coiled regions offering to some extent structural flexibility for responding to variation in size of a hosted anion. For testing the hypothesis that an abandoned co-factor binding site attracts bromide, we calculated structure and heats of formation of hydrogen bonded adducts of amino acid side

chain mimics to bromide from isodesmic substitutions.

(*ii*) *Hydrated bromide*. In the minimum structure calculated for hydrated bromide **3a*1*** oxygen and bromine are separated by 3.346 Å, similar to reference data found in crystal structures of sodium bromide dihydrate (e.g. Br,O = 3.36 Å)[70] and inside a cryptand cavity (3.28_1 Å).[71]

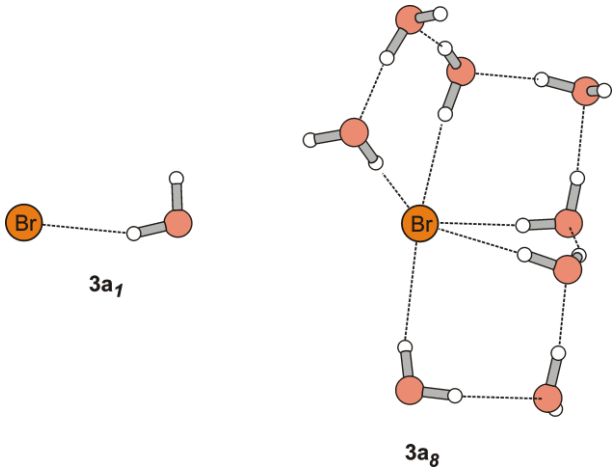

–48.8 *–320.0*

–28.9 **–62.5**

Figure 10. Calculated minimum structures and hydration energies for bromide by one molecule of water (left) and eight water molecules (right; $\Delta_R E$ are printed in italics, ΔG^0 in bold; all values in kJ mol^{-1}; oxygens are depicted in red and hydrogens in white).

In aqueous solution, bromide is surrounded on average by seven to eight water molecules, at a mean experimental oxygen-bromine distance of 3.1_2 Å.[72] The electronic structure model places bromide at the periphery of a octahydrate cluster **3a*8***, similar to minimum structures calculated for hepta- and octahydrated chloride.[73,74] The mean oxygen-bromine distance in the static model of octahydrate **3a*8*** according to theory is 3.3_2 Å (Figure

10).

Peripheral hydrogen atoms of octahydrate **3a**$_{8}$ are positively charged, finding negatively polarized counterparts on the surface of the bromoperoxidase protein at the outer rim of the co-factor binding cavity (Figure 5). For steric reasons, bromide needs to strip off solvating water molecules in order to bind inside the cavity for being oxidized. A possible desolvating mechanism is substitution by hydrogen bond donating amino acid side chains.

(*iii*) *Hydrogen bonding of bromide to side chain mimics*. Bromide forms monovalent hydrogen bonds with methanol, imidazole, methylamine, and methylammonium (adducts **3b**–**e**). Theory predicts a bifurcated hydrogen bond for *N*-methylguanidinium binding to bromide (**3f**).

The calculated distance between bromine and nitrogen in hydrogen bonded methylamine **3d** is 12% larger than reported for bromide bonding to a secondary amine (Br,N = 3.262 Å).[75] A thermochemical reference is the gas phase reaction between ammonia and bromide (ΔG^0 = –31 kJ mol^{-1}), which is 20% more exergonic than predicted by theory (–25 kJ mol^{-1}; Supporting Information).[76] From this data we concluded that theory reproduces bromine-oxygen distances more reliably than bromine-nitrogen distances in anionic hydrogen bonds and underestimates strengths of hydrogen bonding the halide.

Substituting water from hydrated bromide **3a**$_{1}$ is endothermic for methylamine, thermoneutral for methanol, and exergonic for imidazole (Table 7). Methylammonium and *N*-methylguanidinium form strong salt bridges superimposing hydrogen bonding, similar to interactions between dihydrogen orthovanadate and cationic side chain mimics.

Table 7. Calculated energies for substituting water in hydrated bromide **3a*1*** by amino acid mimics for the bromoperoxidase II- binding site

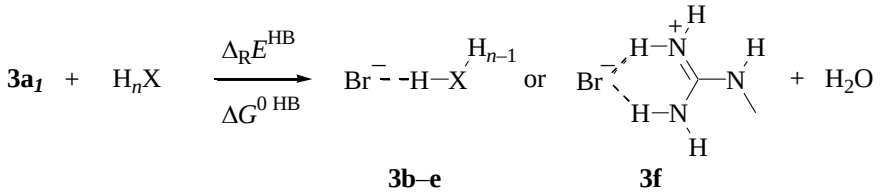

entry	H_nX / **3**	$\Delta_R E^{HB}$/ kJ mol^{-1} [a]	$\Delta G^{0\,HB}$ kJ mol^{-1} [b]	d(Br,X) / Å [c]
1	CH_3OH / **3b**	–2.6	0.4	3.352
2	imidazole / **3c**	–36.5	–30.9	3.300
3	CH_3NH_2 / **3d**	21.1	23.2	3.638
4	$CH_3NH_3^+$ / **3e**	–434.5	–428.2	3.002
5	*N*-methylguanidinium / **3f**	–372.8	–363.8	3.20_2

[a] Referring to 0 K; zero-point vibrational energy-corrected. [b] Referring to 298.15 K and 1 atm. [c] For entry 5: mean value; the subscript gives the standard deviation for the last digit.

Placing bromide at the position occupied by vanadium in the bromoperoxidase II-crystal structure furnishes a cluster having the halide separated by 3.9_5 Å from hydrogen bond donating heteroatoms (Figure 11). Edge lengths of a triangle spanned by three donating histidine nitrogens (5.53 Å × 5.85 Å × 6.81 Å) hosting bromide in the approximate center are strikingly similar to a triangular plane spanned by three water molecules in the calculated minimum structure of bromide octahydrate **3a*8*** (5.74 Å × 5.85 Å × 7.75 Å; Figure 11 and the Supporting Information). In a cavity like this, one face of hydrogen-bonded bromide is accessible for an approaching oxidant, a compound formed from hydrogen peroxide and the co-factor (section 2.8). Binding bromide prevents dihydrogen orthovanadate from being

charged with hydrogen peroxide, thus preventing the halide from being oxidized.[36]

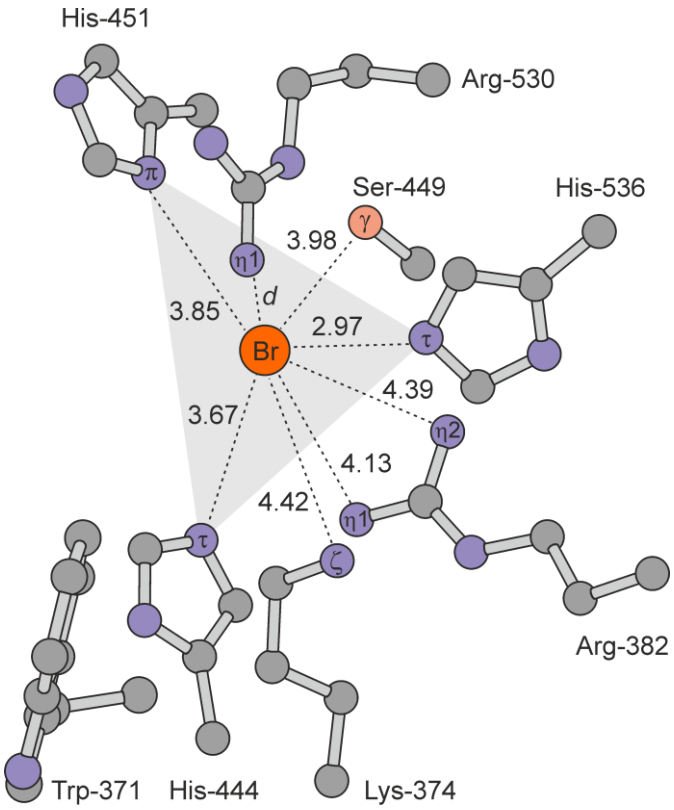

Figure 11. Bromine heteroatom distances calculated for a structural model having bromide bound at the crystallographic of vanadium in the V_{Br}PO(*An*II)-structure, hosting the halide in a triangular plane (shaded) formed by three hydrogen bond-donating histidine side chains (*d* = 3.42 Å; oxygens are drawn in red, nitrogens in blue, and carbons in gray; hydrogens on protein side chains are omitted for the sake of clarity).

2.8 A mechanism for oxidizing bromide

(*i*) *Resting state and active form of the co-factor*. Protonating dihydrogen orthovanadate in the *resting state* provides orthovanadium acid as more electrophilic configuration of the co-

factor. Electrophilicity is the perquisite for activated hydrogen peroxide to serve as oxidant for bromide.

(*ii*) *Activating hydrogen peroxide*. Hydrogen peroxide is a nucleophile substituting in exergonic reaction hydroperoxy for hydroxy in orthovanadium acid to give orthovanadium peroxoic acid (**4**) (*step A* in Scheme 6). In the ground state the hydroperoxy group binds as monovalent substituent in gauche conformation to vanadium, specified hereafter as *end-on*-**4** (V,O^D,O^P,H = 106.9 °, O^A,V,O^D,O^P = 179.2 °). Oxygens in hydroperoxides are distinguished as proximal (O^P) and distal (O^D). The proximal oxygen binds hydrogen and the distal in peroxoic acid *end-on*-**4** to vanadium (Scheme 6).[77]

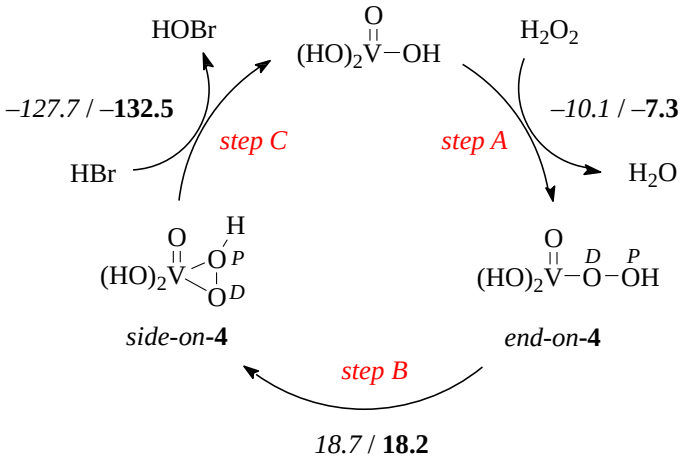

Scheme 6. Calculated (B3LYP/6-311++G**) energies ($\Delta_R E$ for 0 K; printed in italics) and Gibbs free-energy differences (ΔG^0; printed in bold; all energies in kJ mol^{-1}) for bromoperoxidase elementary reactions (for details on *steps A–C*, refer to the text).

Oxidative strength of a peroxide toward a nucleophilic reductant gradually rises with the affinity of the σ^*(O,O)-orbital for accepting electrons. The more substituents stabilize a

peroxide group by accepting electrons, the lower the σ^*(O,O)-orbital energy will be. The dimension used in molecular orbital theory for orbital energies is electron volts [1 electron volt (eV) per molecule corresponds to 96.485 kilojoules per mole]. Stabilizing virtual orbitals increases reactivity toward nucleophiles, classifying peroxides with stabilized σ^*(O,O)-orbital as electrophilic oxidants.

In orthovanadium peroxoic acid *end-on*-**4** the σ^*(O,O)-orbital is 0.7 electron volts lower in energy than in hydrogen peroxide. Vanadium substitution exerts an electron withdrawing effect, as evident from Pauling electronegativities of 2.20 for hydrogen and 2.47 as equilibrated value for the $(HO_2)V{=}O$-unit.[78,79]

(*iii*) *Strengthening electrophilicity*. In gauche conformation of peroxoic acid *end-on*-**4**, the *p*-type non-bonding electron pair at O^P overlaps to some extent with the $\sigma^*(V,O^A)$-orbital. This secondary interaction increases upon shortening the V,O^P-distance, for instance during thermal motion or in response to structural changes inside the bromoperoxidase binding cavity. At a distance of 2.270 Å a full $\sigma(V,O^P)$-bond develops, directing the hydroperoxy group approximately orthogonal to oxido oxygen O^A [O^A,V,O^D,O^P = 70.7 °]. The energy gained by $\sigma(V,O^P)$-bonding in conformer *side-on*-**4** cannot fully account for strain imposed by the three-membered peroxide group. Conformer *side-on*-**4** therefore poses a local but not an absolute minimum, situated 18.7 kJ mol^{-1} in Gibbs free energy above ground state *end-on*-**4** (*step B* in Scheme 6).

Structural dissymmetry differentiates partial charges at peroxide oxygens, becoming more negative at the distal oxygen (–0.3 compared to –0.2 in *end-on*-**4**) and less at the proximal (–0.1 compared to –0.2 in *end-on*-**4**). The second σ-bond formed to vanadium

stabilizes occupied and virtual orbitals of the peroxide group, making *side-on*-**4** an even stronger electrophile than ground state *end-on*-**4**.

Reducing the V,O^P-distance below the equilibrium value of *side-on*-**4** provides at a distance of 1.876 Å, 53.0 kJ mol^{-1} in Gibbs free energy above ground state of *end-on*-**4**, an intermediate specified as *side-on*-$\mathbf{4}^{acitvated}$. Close contact between vanadium and O^P have almost entirely cancelled negative partial charge (–0.04) and stabilized the σ^*(O,O)-orbital by a total of 1.4 electron volts compared to hydrogen peroxide (Figure 12). A nucleophile approaching at O^P experiences full electrophilicity and little to no Coulomb repulsion making *side-on*-$\mathbf{4}^{acitvated}$ an ideal candidate for the *peroxo state* of bromoperoxidase II.

Alternatives for the *peroxo state* are hydroperoxy hydrogen orthovanadate (**5**) and peroxo metavanadate (**6**).[27] A σ^*(O,O)-orbital energy well above the value of hydrogen peroxide, characterizes **5** as nucleophilic oxidant (Figure 12). Peroxide **6**, synthetically accessible from peroxoic acid **4** by eliminating one molecule of water, is a strong electrophile, as judged by relative σ^*(O,O)-orbital energy of –1.2 electron volts, but 1.8-fold higher in Gibbs free energy than peroxoic *side-on*-$\mathbf{4}^{acitvated}$, and therefore a second best option for the *peroxo state* (Scheme 7).

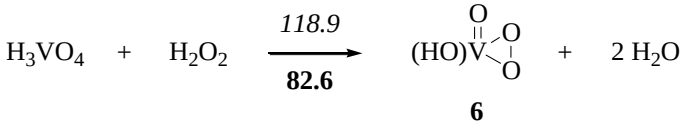

6

Scheme 7. Calculated (B3LYP/6-311++G**) reaction energy ($\Delta_R E$ for 0 K, figure printed in italics) and Gibbs free-energy difference (ΔG^0 figure printed in bold; all energies in kJ mol^{-1}) for preparing metavanadium peroxoic acid (**6**) from orthovanadium acid.

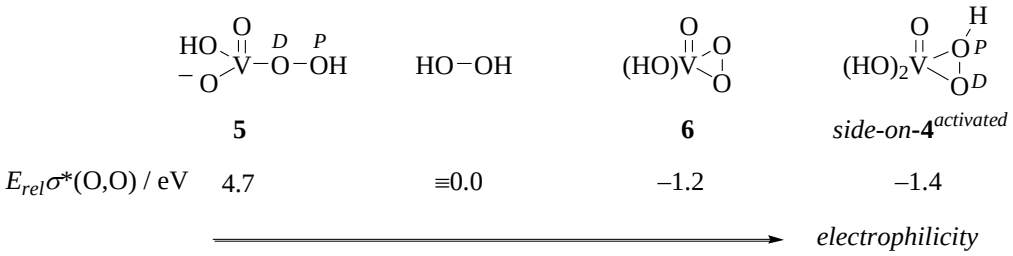

Figure 12. Relative σ^*(O,O)-orbital energies (NBO-values, Supporting Information) and electrophilicity of peroxides [1 electron Volt per molecule corresponds to to 96.485 kilojoules per mole].

Activating hydrogen peroxide by orthovanadium compounds occurs in the electronic structure model via endergonic peroxides. In reaction theory, endergonic products form in a rate determining step. Hydrogen peroxide binding is one of the rate determining steps in steady state kinetics of V_{Br}PO(*An*II).

The energy required for forming the *peroxo state* is delivered by the succeeding reaction: oxygen atom transfer. When stored in the protein, for example, as metastable secondary structure, a fraction of the energy released from bromide oxidation may be used in the next reaction cycle for mediating conformational change from end-on to the activated side-on structure of peroxoic acid **4**. A trigger for releasing strain from a peptide chain possibly is a change in hydrogen bonding prerequisites as the co-factor undergoes transformation from the *resting state* to the *peroxo state*.

(*iv*) *Oxidizing bromide*. The least negatively charged peroxide oxygen, O^P, is the site preferentially approached by bromide in peroxide *side-on*-**4** in the electronic structure model

(Scheme 8). An ancillary hydrogen bond guides the reductant along a trajectory extending the oxygen-oxygen bond almost linearly. Transition structure O^P-**7** reflects these movements by coupled trajectories of Br,O^P-bond formation and O^P,O^D-dissociation giving rise to a single diagnostic negative mode of vibration.

Bromide is separated in transition structure O^P-**7** by 2.402 Å from O^P, exceeding the σ(O,Br)-bond in hypobromous acid by 29% (Table 8). Transferring electrons from bromide into the σ*(O,O)-orbital reduces the bond order of the peroxide group, as evident from widening of the σ(O^P,O^D)-bond by 24% compared to *side-on*-**4**. The barrier for oxidizing bromide from octahydrate **3a**$_8$ is 34.4 kJ mol^{-1} starting from ground state *side-on*-**4**, and –0.4 kJ mol^{-1} starting from peroxoic acid *side-on*-**4**^{activated}.

Upon approaching distal oxygen O^D bromide, experiences a barrier which is 13.6 kJ mol^{-1} higher in Gibbs free energy than for the alternative pathway via O^P. Transferring O^D provides a pentavalent mixed anhydride of orthovanadium acid and hypobromous, which is higher in energy than hydrogen bonded hypobromous acid to dihydrogen orthovanadate (i.e. **2q**; Supporting Information).

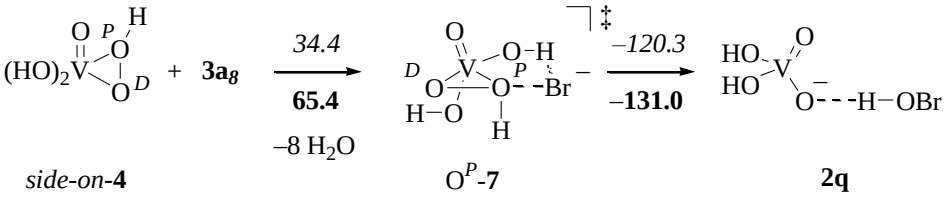

Scheme 8. Calculated lowest in energy pathway for the transferring an oxygen atom from the side-on conformer of peroxoic acid **4** to bromide (reaction energies at 0 K printed in italics and Gibbs free energy-differences at 298.15 K in bold; all energies in kJ mol^{-1}; dashed lines mark attractive interactions).

Table 8. Calculated energy barriers and parameters for characterizing transition structures of bromide oxidation by transferring proximal oxygen (O^P) and the distal (O^D)

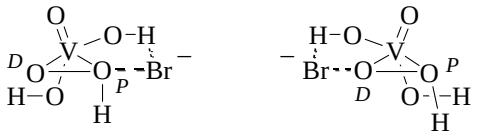

O^P-**7** O^D-**7**

Entry	**7**	$\Delta G^{0‡}$ / kJ mol^{-1}	$d(O^P,O^D)$ [a] / Å	d(O,Br) [b] / Å	α(O,O,Br) / deg	$\omega(O^A,V,O^D,O^P)$ / deg
1 [c]	**7**-O^P	≡0.0	1.820	2.402	168.8	79.3
2 [d]	**7**-O^D	13.6	1.664	2.658	169.5	75.1

[a] Bond dissociation leads to a negative vibrational mode at –289 cm^{-1} for entry 1 and –219 cm^{-1} for entry 2. [b] $d(O^P,Br)$ for entry 1 and $d(O^D,Br)$ for entry 2. [c] Br,O^B = 3.618 Å, Br,H,O^B = 144.0 °. [d] Br,O^B = 3.116 Å, Br,H,O^B = 154.4 °.

(*v*) *Energy budget*. The Gibbs free energy change for converting bromide and a proton or directly hydrogen bromide with hydrogen peroxide into water and hypobromous acid is –130.5 kJ mol^{-1}, based on tabulated standard heats of formation for the gas phase.[80,81] The electronic structure method provides a value of –121.6 kJ mol^{-1} in Gibbs free energy for the reaction, securing coherence between experiment and theory data for the conclusive step. Parts of the energy released are required for activating hydrogen peroxide in the rate-determining step, as outlined above.

3. Concluding Remarks

Solving the crystal structure of the *Ascophyllum nodosum* bromoperoxidase II [V_{Br}PO(*An*II)] provided unique opportunity for developing a thermochemistry-based model for co-factor bonding and the mechanism for oxidizing bromide.

The three dimensional structure reveals details not accessible from solution studies. The question on how the enyzme retains full catalytic activity, even when stored ex-vivo in buffered solution for months or when heated close the boiling point of water, now may be related to secondary and tertiary structural elements in a tightly bound homohexamer, exerting remarkable structural features at the dimer-dimer interfaces. Catenane-type linking in this region, for instance, explains why an earlier attempt to reductively break disulfide bonds in order to obtain measuring masses by spectrometry – an approach successfully pursued for analyzing isoenzyme V_{Br}PO(*An*I) [82] – had failed for bromoperoxidase II.[36]

The crystal structure furthermore clarifies that all subunits of the enzyme are accessible for binding orthovanadate. Analytical data gained from ICP-MS-experiments of bromoperoxidase II in solution had suggested that only three out of six monomers were loaded with the co-factor.[36]

Binding orthovanadate to the V_{Br}PO(*An*II)-protein in the solid state occurs in a shallow well accessible cavity, explaining the ease chelators remove vanadate, and the swiftness externally administered sodium orthovanadate restores oxidative ability of the protein after co-factor loss.[36] Amino acid residues binding orthovanadate in bromoperoxidase II match with structural motifs found in all previously investigated bromoperoxidases, although it needs to

be noted at this point that only the V_{Br}PO(AnI)- structure contained orthovanadate in the solid state, all others had phosphate exchanged for vanadate.[30,31]

Driven by the idea that a conserved bromoperoxidase binding site fulfills all requirements for turning nucleophilic orthovanadate, existing in aqueous solution as mixture of mono- and structurally diverse oligomers, into a reactive electrophile specifically activating hydrogen peroxide for oxidizing bromide, we noted three essentials pursuing this hypothesis with the aid of an assessed electronic structure method: (*i*) cooperative (anionic) hydrogen bonding, (*ii*) environment for gaining maximum electrophilicity, and (*iii*) a possible role in bromide binding.

(*i*) *Hydrogen bonding*. Co-factor binding in the new model entirely relies on hydrogen bonding and Coulomb attraction, with guanidinium groups from arginine side chains serving as strongest attractors for dihydrogen orthovanadate ($H_2VO_4^-$), the proposed configuration of the *resting state*. Cooperative hydrogen bonding to arginine-, histidine- and lysine models is in density functional theory sufficiently strong for explaining an experimental dissociation constant.[2] Vanadium bonding to nitrogen, as proposed for isoenzyme V_{Br}PO(*An*I), play no significant role in isoenzyme II.

(*ii*) *Electrophilicity*. Peroxido derivatives of dihydrogen orthovanadate are nucleophiles. Gaining electrophilicity for activating hydrogen peroxide requires an uncharged co-factor and derived *peroxo state*. Our proposal based for the electrophilic co-factor is orthovanadium acid (H_3VO_4). Positive charges from arginine side chains are ideal prerequisites for stabilizing this otherwise metastable compound. Electrophilicity of orthovanadium acid extends to the derived peroxoic acid, which converts when conformationally properly aligned bromide with virtually

no activation energy into hypobromous acid.

(*iii*) *A dual binding site*? A model based on hydrogen bonding and Coulomb attraction provides options for the co-factor to shift position, for example in response to structural changes when converted into the *peroxo state*. Once the co-factor leaves position, bromide may slip in, binding with lower affinity when argued on the basis of ionic radii. Strong attractors for bromide in the density functional theory model are side chains from arginine and histidine. If bromide bound before orthovanadium acid was converted into the derived peroxoic acid, the halide remained unchanged. Experimentally, bromide competitively inhibits hydrogen peroxide turnover at elevated concentration.

The proposed option for bromide being temporally hosted at the orthovanadate binding poses a step toward unraveling the origin of halide specificity by haloperoxidases. Validating this hypothesis and securing roles side chains from prominent amino acids play for co-factor binding and chemical reactivity needs to be addressed in upcoming studies, for instance, by preparing bromoperoxidase mutants and correlating changes imposed by substituting amino acids to kinetic data, which however was beyond the scope of this investigation. A second aspect worth being revisited is bromoperoxidase model chemistry, putting this time emphasis on thermochemical data for hydrogen bonding, and shaping orthovanadium reactivity by this type of attraction.

4. Materials and Methods

4.1 Bromoperoxidase purification

The bromoperoxidase structurally characterized in this article was isolated from *Ascophyllum nodosum* (knotted wrack), collected in April 2012 in Roscoff/Brittany (France, 48° 43’ N, 3° 58’ W). Lyophilizing and milling furnished algal powder, which was subjected to a liquid-liquid-partitioning process developed by Vilter,[83] and refined by Schulz, Wischang, and Radlow for separating bromoperoxidase II.[36] Dialyzing the crude bromoperoxidase precipitate against an aqueous solution of sodium orthovanadate (pH 9) furnished a mixture of peroxidases, which was chromatographed to give a fraction containing 10 milligrams of native V_{Br}PO(*An*II). This sample was ultracentrifuged for raising V_{Br}PO(*An*II)-concentration to 15.5 mg mL^{-1} (220 µL) in one sample and to 19.6 mg mL^{-1} (220 µL) in the second. A stock solution of V_{Br}PO(*An*I), for conducting comparative biochemical experiments, was obtained from the same algal material following the procedure described by Vilter.[83]

Proper protein folding in all samples was monitored and verified by Dynamic light scattering (DLS), using a Zetasizer Nano ZS (Malvern Instruments). All samples of V_{Br}PO(*An*I) and V_{Br}PO(*An*II) used in this study showed single DLS-signals.

4.2 Crystallization

Parameters for growing bromoperoxidase crystals were screened by adding solutions of V_{Br}PO(*An*II) to PACT- and JCSG+-formulations (Quiagen) using a Honeybee nanodrop robot (Cartesian). Conditions identified from the screening were used to grow crystals for diffraction analysis. For crystallogenesis, a droplet of 1 µL volume containing native V_{Br}PO(*An*II) (8 mg mL^{-1}) and 0.5 µL of a reservoir solution were combined at a temperature of 18 °C using the hanging drop vapor diffusion method. The first reservoir solution was prepared from sodium

chloride (0.1 M), Tris-HCl (0.01 M, pH 5.5), and 25 % PEG 3350, leading to monoclinic crystals. A second reservoir solution, prepared from potassium rhodanide (0.15 M), Tris (0.01 M, pH 7.5) and 19 % PEG 3350 furnished hexagonal crystals. For growing the latter, we used a droplet of 2 µL volume containing the dissolved enzyme, and 1 µL of the reservoir solution. Crystals obtained by both approaches were soaked in the mother liquor with glycerol as cryoprotecting agent. Likewise prepared crystals were collected and cryocooled for being transported.

4.3 Data collection, model building, structure solution, and refinement

Data from diffraction analysis of V_{Br}PO(*An*II)-crystals were collected under cryocooled conditions on Beamline ID23-2 at the European Synchrotron Radiation Facility (ESRF, Grenoble/France), equipped with a 225 mm-MarMosaic detector, using a wavelength of 0.873 nm. X-ray diffraction data were scaled with Scala.[84] For structure solution and refinement, we used the programs MolRep and Phaser, being implemented in the CCP4i-software.[85] Starting from the model of V_{Br}PO(*An*I) (PDB code 1QI9) shows 41% sequence homology, the structure of V_{Br}PO(*An*II) was manually built with *Coot* and refined with REFMAC5 (version 5.8).[86,87] As primary structure used for solving the bromoperoxidase II-crystal structure, we used a protein sequence (EBI UniProtKB: accession No. K7ZUA3) derived from a translated full length cDNA cloned in a previous study.[36] Water molecules were automatically added with WARP implemented in REFMAC5 and verified manually. Data collection and refinement parameters have been deposited at the Protein Data Bank, Research Collaboratory for Structural Bioinformatics (PDB code 5AA6; see also, the Supporting Information).

4.4 Electronic structure methods

For analyzing thermochemistry and hydrogen bonding of orthovanadium acid we used Becke's three parameter Lee-Yang-Parr hybrid functional[54,55] (B3LYP) in combination with a triple ζ-basis set, specified in the applied Gaussian03-suite of program (Revision E.01)[88] as 6-311++G**. The basis set adds polarization and diffuse functions to energy functions of the 6-311G basis. For hydrogen, the 6-311G basis corresponds to the Pople-6-311G-basis set. For oxygen, nitrogen, and carbon the 6-311G-basis applies the McLean-Chandler (12s,9p) → (621111,52111)-basis set.[89] For vanadium, the 6-311G basis uses Wachters-Hay all electron basis, developed calculating energy functions of 3d-orbitals,[90,91] corrected by scaling factors recommended by Raghavachari and Trucksrow.[92] This parametrization in combination with B3LYP-hybrid functional considering electron correlation provides energies prevents relativistic effects from electron attraction by the vanadium nucleus to become significant.[93] Energies for all compounds in this article refer to minimum structures on potential energy surfaces, being computationally obtained from energy function minimizations applying the ultrafine grid in combination with the tight option. Minima were identified as such by absence of imaginary normal modes in calculated vibrational spectra. Gibbs free energies (*G*) were calculated with the thermochemical model implemented in Gaussian03, without frequency scaling. Thermochemical corrections refer a temperature of 298.15 Kelvin and a pressure of 1 atmosphere. Gibbs free energies from density functional theory were corrected for zero-point vibrational energy contributions, thermal factors, and molecular entropy. For translating results from density functional theory into a more descriptive bonding model, we analyzed electron

population by B3LYP/6-31G*-single point calculations in natural bond orbital (NBO)-theory, using B3LYP/6-311++G**-minimized structures as input (Supporting Information).

Data deposition

Atomic coordinates and structure parameters have been deposited in the Protein Data Bank (www.rcsb.org, PDB code 5AA6).

Supporting Information Available: Instrumentation, details on molecular graphics, reagents and enzyme purification, crystallogenesis and crystallographic data, protein sequence alignment, thermostability studies, atomic coordinates and molecular energies from density functional theory, and structure references. This material is available free of charge via the Internet at http://pubs.acs.org.

Acknowledgements.

† This work is part of the Ph.D. thesis of M.R. and was supported by the State Rheinland-Pfalz (NanoKat), the Association of European Marine Biological Laboratories (ASSEMBLE Research Infrastructure Action under the FP7 "Capacities" Specific Program, grant agreement no. 227799), and the European Synchrotron Radiation Facility (ESRF). Parts of this work were supported by the Centre National de la Recherche Scientifique and by the French National Research Agency investment expenditure program IDEALG (ANR-10-BTBR-02-04-11). Crystal structure determination was performed at the crystallography platform of the Station

Biologique de Roscoff, supported by the Centre National de la Recherche Scientifique and Université Pierre et Marie Curie, Paris 06. We are indebted to the staff of the European Synchrotron Radiation Facilities (ESRF) (Grenoble, France), beamline ID23-2, for technical support during X-ray data collection and treatment. We appreciate and acknowledge helpful advice on purification of the bromoperoxidase II protein by D. Wischang and H. Vilter. We furthermore thank J.-B. Fournier for technical assistance in concentration and ultracentrifugation of bromoperoxidase samples, and both two reviewers in the course of peer-review process for their helpful and constructive comments.

References

(1) Weyand, M., Hecht, H.-J., Kieß, M., Liaud, M.-F., Vilter, H., and Schomburg, D. (1999) X-ray structure determination of a vanadium-dependent haloperoxidase from Ascophyllum nodosum at 2.0 Å resolution. *J. Mol. Biol*. *293*, 595–611.

(2) Tromp, M.G., Olafsson, G. Krenn, B.E., and Wever, R. (1990) Some structural aspects of vanadium bromoperoxidase from *Ascophyllum nodosum*. *Biochim. Biophys. Acta 1040*, 192–198.

(3) Vilter, H. (1984) Peroxidases from *Pheaophyceae*: a vanadium(V)-dependent peroxidase from *Ascophyllum nodosum*. *Phytochemistry 23*, 1387–1390.

(4) Butler, A., and Walker J.V. (1993) Marine haloperoxidases. *Chem. Rev*. 93, 1937–1944.

(5) Butler, A, and Carter-Franklin, J.N. (2004) The role of vanadium bromoperoxidase in the biosynthesis of halogenated marine natural products. *Nat. Prod. Rep. 21*, 180–188.

(6) Vaillancourt, F.H., Yeh, E., Vosburg, D.A., Garneau-Tsodikova, S., and Walsh, C.T. (2006) Nature's inventory of halogenation catalysts: oxidative strategies predominate. *Chem. Rev*. *106*, 3364–3378.

(7) Gribble, G.W. (2003) The diversity of naturally produced organohalogens. *Chemosphere 52*, 298–297.

(8) Wischang, D., and Hartung J. (2012) Bromination of phenols in bromoperoxidase-catalyzed oxidations. *Tetrahedron 68*, 6456–9463.

(9) Schwarzenbach, G., and Geier, G (1963) Die Raschacidifizierung und –Alkalisierung von Vanadaten. *Helv. Chim. Acta 46*, 906–926.

(10) Petterson, L., Hedman, B., Nenner, A.-M., and Andersson I. (1985) Multicomponent polyanions. 36. Hydrolysis and redox equilibria of the H^+–HVO_4^{2-} system in 0.6 M Na(Cl). A complementary potentiometric and ^{51}V NMR study at low vanadium concentrations in acidic solution. *Acta Chem. Scand*. *A39* 499–506.

(11) Ehde, P.M., Andersson, I., and Petterson L. (1986) Multicomponent polyanions. 40. Potentiometric and ^{51}V NMR study of equilibria in the H^+–$H_2VO_4^-$–$C_2O_4^{2-}$ system in 0.6 M Na(Cl) medium. *Acta Chem. Scand*. *A40* 486–499.

(12) Tracey, A.S., Jaswal, J.S., and Angusdunne, S.J. (1995) Influences of pH and ionic-strength on aqueous vanadate equilibria. *Inorg. Chem. 34*, 5680–5685.

(13) Rossotti, F.J.C., and Rossotti, H. (1956) Equilibrium studies of polyanions I. isopolyvanadates in acidic media. *Acta. Chem. Scand*. *10*, 957–984.

(14) Clague, M.J. and Butler, A. (1995) On the mechanism of *cis*-dioxovanadium(V)-catalyzed oxidation of bromide by hydrogen peroxide: evidence for a reactive, binuclear vanadium(V) peroxo complex. *J. Am. Chem. Soc. 117*, 3475–3484.

(15) Jaswal, J.S., and Tracey, A.S. (1991) Formation and decomposition of peroxovanadium(V) complexes in aqueous solution. *Inorg. Chem*. *30*, 3718–3722.

(16) Butler, A., and Sandy, M. (2009) Mechanistic considerations of halogenating enzymes. *Nature 460*, 848–854.

(17) Jones, C.W. (1999) Activation of hydrogen peroxide using inorganic and organic species. In *Applications of hydrogen peroxide and its derivatives*, pp 37–77, RSC-Clean Technology Monographs, Cambridge.

(18) Rehder, D. (2007) Vanadate-dependent haloperoxidases. In *Bioinorganic Vanadium Chemistry*, pp.105–116, Wiley, Chichester.

(19) Crans, D.C., Smee, J.J., Gaidamauskas, E., and Yang, L. (2004) The chemistry and biochemistry of vanadium and the biological activities exerted by vanadium Compounds. *Chem. Rev*. *104*, 849-902.

(20) de Boer, E., and Wever, R. (1988) The reaction mechanism of the novel vanadium-bromoperoxidase. A steady-state kinetic analysis. J. Biol. Chem. 263, 12326–12332.

(21) Everett R.R., Soedjak H.S., and Butler, A. (1990) Mechanism of Dioxygen Formation Catalyzed by Vanadium Bromoperoxidase. *J. Biol. Chem*. *265*, 15671–15679.

(22) Butler, A. (1999) Mechanistic consideration of the vanadium haloperoxidases. *Coord. Chem. Rev. 187*, 17–35.

(23) Raugei, S., and Carloni, P. (2006) Structure and function of vanadium haloperoxidases. *J. Phys. Chem. B. 110*, 3747–3758.

(24) Renirie, R., Charnock, J.M., Garner, C.D., and Wever, R. (2010) Vanadium K-edge XAS studies on the native and the peroxo-forms of vanadium chloroperoxidase from *Curvularia inaqualis*. *J. Inorg. Biochem. 104*, 657–664.

(25) Zampella, G., Fantucci, P., Pecoraro, V.L., and De Gioia, L (2005) Reactivity of peroxo forms of the vanadium haloperoxidase cofactor. A DFT investigation. *J. Am. Chem. Soc. 127*, 953–960.

(26) Zampella, G., Fantucci, P., Pecoraro, V.L., and De Gioia L (2006) Insight into the catalytic mechanism of vanadium haloperoxidases. DFT investigation of vanadium cofactor reactivity. *Inorg. Chem. 45*, 7133–7143.

(27) Schijndel, J.W., Simons, L.H., Vollenbroek, E.G., and Wever, R. (1993) The vanadium chloroperoxidase from the fungus, *Curvularia inaequalis*. Evidence for the involvement of a histidine residue in the binding of vanadate. *FEBS Lett. 336*, 239–243.

(28) Messerschmidt A., Prade L., and Wever, R. (1997) Implications for the catalytic mechanism of the vanadium-containing enzyme chloroperoxidase from the fungus *Curvularia inaequalis* by X-ray structures of the native and peroxide form. *Biol. Chem. 378*, 309–315.

(29) Messerschmidt A., and Wever, R. (1996) X-ray structure of a vanadium-containing enzyme: chloroperoxidase from the fungus *Curvularia inaequalis*. *Proc. Natl. Acad. Sci. USA 93*, 392–396.

(30) Littlechild, J., Rodriguez, E.G., and Isupov, M. (2009) Vanadium containing bromoperoxidase – Insights into the enzymatic mechanism using X-ray crystallography. *J. Inorg. Biochem*. 103, 617–621.

(31) Isupov, M.N., Dalby, A.R., Brindley, A.A., Izumi, Y., Tanabe, T. Murshudov, G.N., and Littlechild, J.A. (2000) Crystal structure of dodecameric vanadium-dependent bromoperoxidase from the red algae *Corallina officinalis*. *J. Mol. Biol*. *299*, 1035–1049.

(32) Fournier J-B, Rebuffet E, Delage L, Grijol R, Meslet-Cladière L, Rzonca, J., Potin, P., Michel, G., Czjzek, M., and Leblanc, C. (2014) The bacterial vanadium iodoperoxidase from the marine flavobacteriaceae *Zobellia galactanivorans* reveals novel molecular and evolutionary features of halide specificity in this enzyme family. *Appl. Environ. Microbiol. 80*, 7561-7573.

(33) Frank, A., Seel, C.J., Groll, M., and Gulder T. (2016) Characterization of a cyanobacterial haloperoxidase and evaluation of its biocatalytic halogenation potential. *ChemBioChem. 17*, 2028–2032.

(34) Dönges, M., Amberg, M., Niebergall, M., and Hartung J. (2015) Activating *tert*-butyl hydroperoxide by chelated vanadates for stereoselectively preparing sidechain-functionalized tetrahydrofurans. *J. Inorg. Biochem*. *147*, 204–220.

(35) Jaswal, J.S., and Tracey, A.S. (1993) Reactions of mono- and diperoxovanadates with peptides containing functionalized side chains. *J. Am. Chem. Soc. 115*, 5600–5607.

(36) Wischang, D., Radlow, M., Schulz, H. Vilter H., Viehweger, L. Altmeyer, M.O., Kegler, C., Herrmann, J., Müller, R., Gaillard, F., Delage, L., Leblanc, C., and Hartung, J. (2012)

Molecular cloning, structure and reactivity of the second bromoperoxidase from *Ascophyllum nodosum*. *Bioorg. Chem*. *44*, 25–34.

(37) Wischang, D., Radlow, M., and Hartung J. (2013) Vanadate-dependent bromoperoxidase from *Ascophyllum nodosum* in the synthesis of brominated phenols and pyrroles. *Dalton Trans*. *42*, 11926–11940.

(38) Mason, P.E., Neilson, G.W., Enderby, J.E., Saboungi, M.-L., Dempsey, C.E., MacKerell, Jr., A.D., and Brady, J.W. (2004) The structure of aqueous guanidinium chloride solutions. *J. Am. Chem. Soc*. *126*, 11462–11470.

(39) Vazdar, M., Vymětal, J., Heyda, J., and Jungwirth, P. (2011) Like-charge guanidinium pairing from molecular dynamics and ab initio calculations. *J. Phys. Chem. A 115*, 11193–11201.

(40) Cahn, R.S., Ingold, C.K., and Prelog, V. (1966) Specification of molecular chirality. *Angew. Chem. Int. Ed. Engl*. *5*, 385–415.

(41) Whitmore, L., and Wallace B.A. (2008) Protein secondary structure analyses from circular dichroism spectroscopy: methods and reference databases. *Biopolymers 89*, 392–400.

(42) Krenn, B.E., Tromp, M.G.M., and Wever, R. (1989) The brown alga *Ascophyllum nodosum* contains two different vanadium bromoperoxidases. *J. Biol. Chem*. *264*, 19287–19292.

(43) PyMOL molecular graphics system, version 1.3r1 (Schrödinger, LLC).

(44) Dixon, H.B.F., Cornish-Bowden, A., Liebecq, C., Loening, K.L., Moss., G.P., Reedijk. J., Velick, S.F., and Vliegenthart J.F.G. (1984) Nomenclature and symbolism for amino acids and peptides. *Eur. J. Biochem. 138*, 9–37.

(45) Weber, M., Tome, L., Otzen, D., and Schneider, D. (2012) A Ser residue influences the structure and stability of a Pro-kinked transmembrane helix dimer. *Biochim. Biophys. Acta 1818*, 2103–2107.

(46) Bondi, A. (1964) Van der Waals volumes and radii. *J. Phys. Chem. 68*, 441–451.

(47) Jeffrey, G.A. (1997) An introduction to hydrogen bonding. Oxford University Press.

(48) Vergopoulos, V., Priebsch, W., Fritzsche, M., and Rehder, D. (1993) Binding of L-histidine to vanadium. Structure of *exo*-[VO_2{*N*-oxidonaphthal)-His}]. *Inorg. Chem. 32*, 1844–1849.

(49) Cornman, C.R., Kampf, J., Lah, M.S., and Pecoraro, V.L. (1992) Modeling vanadium bromoperoxidase: synthesis, structure, and spectral properties of vanadium(IV) complexes with coordinated imidazole. *Inorg. Chem. 31*, 2035–2043.

(50) Kanamori, K., Nishida, K., Miyata, N., and Okamoto, K.-i. (1998) Synthesis and characterization of a peroxovanadium(V) complex containing *N*-carboxymethylhistidine as a model for the vanadium haloperoxidase enzymes. *Chem. Lett*. pp 1267–1268

(51) Takhistov, V.V., and Ponomarev, D.A. (1994) Isodesmic reactions and thermochemistry of ions. *J. Mass Spectrom. 29*, 395–412.

(52) Hehre, W.J., Ditchfield, R., Radom, L., and Pople, J.A. (1970) Molecular orbital theory of the electronic structure of organic compounds. V. Molecular theory of bond separation. *J. Am. Chem. Soc. 92*, 4796–4801.

(53) Forseman, J.B., and Frisch, Æ (2015) Studying reaction mechanisms. In *Exploring Chemistry With Electronic Structure Methods*, 3rd ed., Gaussian, Inc, Pittsburg, PA, pp 227–274.

(54) Becke, A.D. (1993) Density functional thermochemistry. III. The role of exact exchange. *J. Chem. Phys. 98* 5648–5652.

(55) Lee, C., Yang, W., and Parr, R.G. (1988) Development of the Colle-Salvetti correlation-energy formula into a functional of the electron density. *Phys. Rev., B37* 785–789.

(56) Bagno, A., Conte, V., Di Furia, F., and Moro, S. (1997) Ab initio calculations on water-peroxovanadium clusters, $VO(O_2)(H_2O)_n^+$ (n = 1–5). Implications for the structure in aqueous solution. *J. Phys. Chem. A 101*, 4637–4640.

(57) Adão, P., Pessoa, J.C., Henriques, R.T., Kuznetsov, M.L., Avecilla, F., Maurya, M.R., Kumar, U., and Correia, I. (2009) Synthesis, characterization, and application of vanadium-salan complexes in oxygen transfer reactions. *Inorg. Chem. 48*, 3542–3561.

(58) Geethalakshmi, K.R., Waller, M.P., Thiel, W., and Bühl, M. (2009) ^{51}V NMR chemical shifts salculated from QM/MM models of peroxo forms of vanadium haloperoxidases. *J. Phys. Chem. B 113*, 4456–4465.

(59) Conte, V., Coletti, A., Floris, B., Licini, G., and Zonta, C. (2011) Mechanistic aspects of vanadium catalysed oxidations with peroxides. *Coord. Chem. Rev. 255*, 2165–2177.

(60) Kim, J., Majumdar D., Lee, H.M., and Kim, K.S. (1999) Structures and energetics of the water heptamer: comparison with the water hexamer and octamer. *J. Chem. Phys. 110*, 9128–9134.

(61) Suresh, S. J., and Naik, V. M. (2000) Hydrogen bond thermodynamic properties of water from dielectric constant data. *J. Chem. Phys. 113*, 9727–9732.

(62) Harms, M. J., Schlessman, J. L., Sue, G.R., and Garcia-Moreno E., B. (2011) Arginine residues at internal positions in a protein are always charged. *Proc. Natl. Acad. Sci*. *108*, 18951–18959.

(63) Vijayakumar, M., Liyu, Li, Graff, G., Liu, L., Zhang, H., Yang, Z., and Hu, J.Z. (2011) Towards understanding of the poor stability of V5+ electrolyte solution in Vanadium Redox Flow Batteries. *J. Power Sources 196*, 3666–3672.

(64) Dickens, B., Prince, E., Schroeder, L.W., and Jordan T.H. (1974) A refinement of the crystal structure, $H_3PO_4 \cdot ½\ H_2O$ with neutron diffraction data. *Acta Cryst*. *B30* 1470–1473.

(65) Glendening, E.D., Badenhoop, J.K., Reed, A.E., Carpenter, J.E., Bohmann, J.A., Morales, C.M., and Weinhold, F. (2009) NBO 5.9 http://www.chem.wisc.edu/~nbo5. Theoretical Chemistry Institute, University of Wisconsin, Madison, WI.

(66) Grimsley, G.R., Scholtz, J.M., and Pace, C.N. (2009) A Summary of the measured p*K* values of the ionizable groups in folded proteins. *Protein Sci*. *18*, 247–251.

(67) Bangesh, M., and Plass W. (2005) TD-DFT studies on the electronic structure of imidazole bound vanadate in vanadium containing haloperoxidases (VHPO). *THEOCHEM 725*, 163–175.

(68) Fumi, F.G., and Tosi, M.P. (1964) Ionic sizes and born repulsive parameters in the NaCl-type alkali halides – I. The Huggins-Mayer and Pauling Forms. *J. Phys. Chem*. *Solids 25*, 31–43.

(69) Marumo, F., Sobe, I., and Iwai, S. (1974) α Form of sodium metavanadate. *Acta Cryst. B30*, 1628–1630.

(70) Haar, W.R., and Carpenter, G.B. (1964) The crystal structure of sodium bromide dihydrate. *Acta Cryst*. *17*, 730–732.

(71) Saeed, M.A., Pramanik, A.,Wong, B.,Haque, S.A., Powell, D.R.,Chand D.K., and Hossain M.A. (2012) Self-assembly of ordered water tetramers in an encapsulated $[Br(H_2O)_{12}]^-$ complex. *Chem. Commun*. *48*, 8631–8633.

(72) D'Angelo, P., Migliorati, V., and Guidoni, L. (2010) Hydration properties of the bromide aqua ion: the interplay of first principle and classical molecular dynamics, and X-ray absorption spectroscopy. *Inorg. Chem*. *49*, 4224–4231.

(73) Pereara, L., and Berkowitz, M.L. (1994) Structures of $Cl^-(H_2O)_n$, and $F^-(H_2O)_n$ (n = 2,3,...15) clusters. Molecular dynamics computer simulations. *J. Chem. Phys*. *100*, 3085–3093.

(74) Ishibashi, C., Iwata, S., Onoe, K., and Matsuzawa, H. (2015) Hydrogen-bonded networks in hydride water clusters, $F^-(H_2O)_n$, and $Cl^-(H_2O)_n$: cubic form of $F^-(H_2O)_7$, and $Cl^-(H_2O)_7$. *J. Phys. Chem. A. 119*, 10241–10253.

(75) Das, M.C., and Bharadwaj, P.K. (2007) Molecular ice with hybrid water-bromide network around a cryptand with a bromide ion included in the cavity to form a host-within-a host-like structure. *Eur. J. Org. Chem*. pp 1229–1232.

(76) Evans, D.H., Keesee, R.G., and Castleman, A.W. (1987) The association of ammonia with halide ions in the gas phase. *J. Chem. Phys. 86*, 2927–2931.

(77) Hartung J., and Svoboda, I. (2006) The structural chemistry of acyclic organic peroxides. In *The Chemistry of Peroxides* (Rappaport, Z. Ed.), vol. 2, pp, 93–144, Wiley, Chichester.

(78) Sanderson, R.T. (1955) Partial charges on atoms in organic compounds. *Science 121*, 207–208.

(79) Bratsch, S.G. (1984) Electronegativity equalization with Pauling units. *J. Chem. Educ. 61*, 588–589.

(80) Cox, J.D., Wagman, D.D., and Medvedev, V.A. (1989) Committee on Data for Science and Technology (CODATA) Key Values for Thermodynamics, Hemisphere Publishing Corp., New York. In CRC Handbook of Chemistry and Physics (Lide, D.R., Ed.), 78th ed., pp. 5–5 and 5–18, CRC Press, Boca Raton.

(81) Denis, P.A. (2006) Thermochemistry of the hypobromous and hypochlorous acids, HOBr and HOCl. *J. Phys. Chem. A 110*, 5887–5892.

(82) Vilter, H.(1995) Vanadium-dependent haloperoxidases, Marcel Dekker, Inc., New York. In Metal Ions in Biological Systems, Vol. 31, pp. 325–362.

(83) Vilter, H. (1994) Extraction of proteins from sources containing tannins and anionic mucilages. *Methods Enyzm. 228*, 665–672.

(84) Murshudov, G.N., Vagin, A.A., and Dodson, E.J. (1997) Refinement of macromolecular structures by the maximum-likelihood method: *Acta Cryst. D53*, 240–255.

(85) Winn, M., Ballard, C., Cowtan, K., Dodson, E., Emsley, P., Evans, P., Keegan, R., Krissinel, E., Leslie, A., McCoy, A., McNicholas, S., Murshudov, G., Pannu, N.,

Potterton, E., Powell, H., Read, R., Vagin, A., and Wilson, K. (2011) Overview of the CCP4 suite and current developments. *Acta Cryst. D67*, 235–242.

(86) Emsley, P., Lohkamp, B., Scott, W.G., and Cowtan, K. (2010) Features and development of Coot. *Acta Cryst. D66*, 486–501. http://dx.doi.org/10.1107/S0907444910007493.

(87) Murshudov, G.N., Skubak, P., Lebedev, A.A., Pannu, N.S., Steiner, R.A., Nicholls, R.A., Winn, M.D., Long F., and Vagin, A.A. (2011) REFMAC5 for the refinement of macromolecular crystal structures. *Acta Cryst. D67*, 355–367.

(88) Frisch, M.J., Trucks, G.W., Schlegel, H.B., Scuseria, G.E., Robb, M.A., Cheeseman, J.R., Montgomery, Jr., J.A., Vreven, T., Kudin, K.N., Burant, J.C., Millam, J.M., Iyengar, S.S., Tomasi, J., Barone, V., Mennucci, B., Cossi, M., Scalmani, G., Rega, N., Petersson, G.A., Nakatsuji, H., Hada, M., Ehara, M., Toyota, K., Fukuda, R., Hasegawa, J., Ishida, M., Nakajima, T., Honda, Y., Kitao, O., Nakai, H., Klene, M., Li, X., Knox, J. E., Hratchian, H.P., Cross, J.B., Bakken, V., Adamo, C., Jaramillo, J., Gomperts, R., Stratmann, R.E., Yazyev, O., Austin, A.J., Cammi, R., Pomelli, C., Ochterski, J.W., Ayala, P.Y., Morokuma, K., Voth, G.A., Salvador, P., Dannenberg, J.J., Zakrzewski, V.G., Dapprich, S., Daniels, A.D., Strain, M.C., Farkas, O., Malick, D.K., Rabuck, A.D., Raghavachari, K., Foresman, J.B., Ortiz, J.V., Cui, Q., Baboul, A.G., Clifford, S., Cioslowski, J., Stefanov, B.B., Liu, G., Liashenko, A., Piskorz, P., Komaromi, I., Martin, R.L., Fox, D.J., Keith, T., Al-Laham, M.A., Peng, C.Y., Nanayakkara, A., Challacombe, M. Gill, P.M.W., Johnson, B., Chen, W., Wong, M.W., Gonzalez, C., and Pople, J.A. (2004). Gaussian, Inc., Wallingford CT, 2004.

(89) McLean, A.D., Chandler, G.S. (1980) Contracted Gaussian basis sets for molecular calculations. I. Second row atoms, *Z* = 11–18. *J. Chem. Phys. 72*, 5639–5648.

(90) Wachters, A.J.H. (1970) Gaussian basis set for molecular wavefunctions containing third-row atoms. *J. Chem. Phys. 52*, 1033–1036.

(91) Hay, P.J. (1977) Gaussian basis sets for molecular calculations. The representation of 3*d* orbitals in transition-metal atoms. *J. Chem. Phys. 66*, 4377–4384.

(92) Raghavachari, K., and Trucks, G.W. (1989) Highly correlated systems. Excitation energies of first row transition metals Sc–Cu. *J. Chem. Phys. 91*, 1062–1065.

(93) Neese, F. (2009) Prediction of molecular properties and molecular spectroscopy with density functional theory: From fundamental theory to exchange-coupling. *Coord. Chem. Rev. 253*, 526–563.

Table of Contents (TOC) Graphic

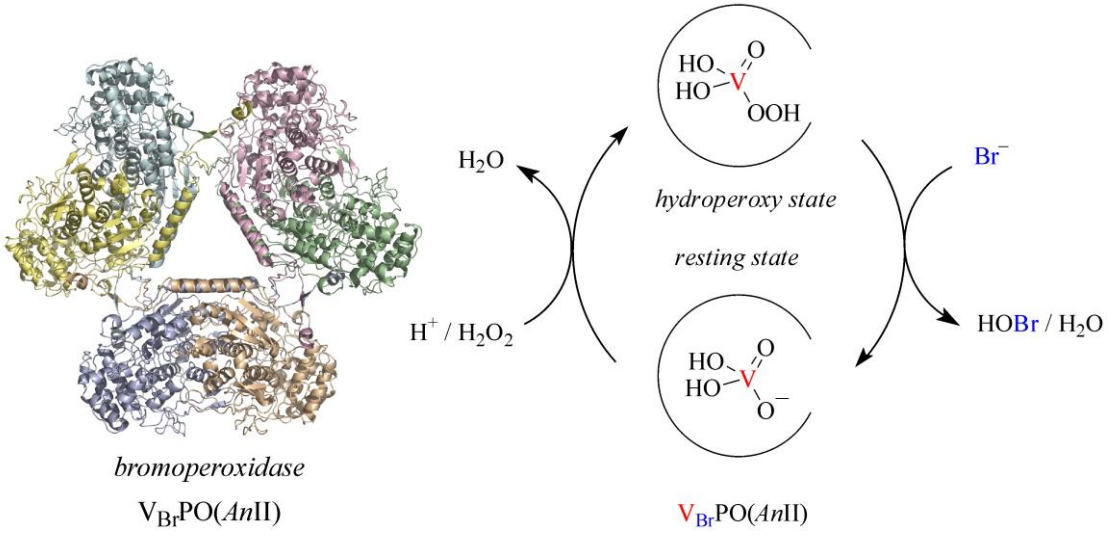

Supporting Information for

X-Ray-Diffraction and Density Functional Theory Provide Insight into Vanadate Binding to Homohexameric Bromoperoxidase II and the Mechanism of Bromide Oxidation

Madlen Radlow,[a] Mirjam Czjzek [b], Alexandra Jeudy [c], Jerome Dabin [b], Ludovic Delage[b], Catherine Leblanc [b]*, and Jens Hartung[a]*

[a] Fachbereich Chemie, Organische Chemie, Technische Universität Kaiserslautern, Erwin-Schrödinger-Straße, D-67663 Kaiserslautern, Germany

[b] Sorbonne Université, CNRS, UMR 8227, Integrative Biology of Marine Models, F-29688, Roscoff cedex, France

[c] Sorbonne Université, CNRS, FR 2424, Station Biologique de Roscoff, F-29688 Roscoff cedex, France

Contents

1 General Remarks

1.1 Numbering of compounds

Compounds in the *Supplementary data* are numbered according to the systematic used in the associated article.

1.2 References

The list of references provided in section 9 refers to the *Supplementary data* refers and is independent from the associated article.

1.3 Molecular graphics for displaying details associated with the bromoperoxidase II-crystal structure

Ball-and stick models displaying distances between vanadate oxygens and heteroatoms of surrounding amino acid side chains, and the hydrogen bonding donating environment for capturing bromide at the co-factor binding side were processed with the molecule editor of the HyperChem 8.0-software,[1] and the ChemPlus-add-on (Version 1.6) to the HyperChem 4.5-software[2] starting from atomic coordinates of the V_{Br}PO(*An*II)-structure.

Data from X-ray diffraction analysis were scaled with SCALA.[3] The structure solved and and Phase by MOLREP[4] and PHASER, which are implemented in the the CCP4-software.[5] The structure of V_{Br}PO(*An*II) was built manually from the V_{Br}PO(*An*I) (PDB code 1QI9, 41 % identity) using the COOT-software[6] and refined with REFMAC5[7],[8],[9] (version 5.8). Water molecules were automatically added with REFMAC5 and verified visually. Global view and detailed figures of the V_{Br}PO(*An*II) homohexamer were generated with the PyMOL molecular graphics system, version 1.3r1 (Schrödinger, LLC).

2 Instrumentation

2.1 European Synchroton Radiation Facility

Diffraction data for the native V_{Br}PO(*An*II) enzyme were collected on the beamline ID23-2 at the European Synchrotron Radiation Facility (ESRF, Grenoble/France) equipped with a 225mm MarMosaic detector to a resolution of 2.26 Å and a wavelength of 0.873 nm.

2.2 Nanodrop-Robot Honeybee

The crystallization screening was undertaken with the nanodrop-robot Honeybee (Cartesian) using the commercial screens PACT and JCSG+ (Quiagen, Les Ulis, France). The best conditions were optimized in 24-well Limbro plates by the hanging-drop vapour diffusion method to obtain crystals for synchrotron radiation diffraction.

2.3 Dynamic Light Scattering (DLS)

Proper protein folding in all samples was monitored and verified by DLS, using a Zetasizer Nano ZS (Malvern Instruments, Orsay, France). For recording melting curves, solutions of V_{Br}PO(*An*I) and V_{Br}PO(*An*II) (45 µg in 60 µL) were heated in intervals of 5 °C from 10 °C to 90 °C. For every temperature three DLS-measurements were performed, following an equilibration time of 5 minutes. Denaturation is apparent from increasing protein size, caused by non-specific aggregation of unfolded polypeptide chains, as evident from *Z*-average diameter. The temperature of denaturation defines the protein melting point (TM).

3 Reagents, Enzyme Purification and activity

3.1 Bromoperoxidase purification

V_{Br}PO(*An*II) was isolated and purified from Ascophyllum nodosum (knotted wrack) collected in April 2012 in proximity to Roscoff/Brittany (France, 48°43'N, 3°58'W). The alga was lyophilized and subjected to an improved liquid-liquid-partitioning process. (The crude solution was enriched with a $(NH_4)_2SO_4$ step gradient (15 % → 0 %) using Phenyl Sepharose™ 6 FF as stationary phase. After pooling the two relevant fractions accumulated with V_{Br}PO(*An*I) and V_{Br}PO(*An*II), the enzymes were concentrated by hydrophobic interaction chromatography (HIC) using a $(NH_4)_2SO_4$ linear gradient (15 % → 0 %). $(NH_4)_2SO_4$ weight percent was pursued by conductivity measurement. The characteristic band at 280 nm was used for detection of bromoperoxidases. Dialysis and chromatography furnished 10 milligrams of native V_{Br}PO(*An*II)-protein, which was concentrated and ultracentrifugated leading to samples containing 15.5 mg mL^{-1} and 19.6 mg mL^{-1} of V_{Br}PO(*An*II). Dynamic light scattering (DLS)-studies showed single peaks for the two samples

3.2 Bromoperoxidase activity thermostability

Nine aliquots from solutions of V_{Br}PO(*An*I) and V_{Br}PO(*An*II) (400 ng in 10 μL) were heated in intervals of 10 °C from 20 °C to 100 °C using a GeneAmp® PCR System 2700 (Applied Biosystems). Following the protocol described for DLS-measurements, protein samples were equilibrated for 5 minutes at every temperature. Sample withdrawn for determining bromoperoxidase activity at a given temperature, were kept on ice before loading the sample on a 10%-polyacrylamide native gel. After electrophoresis, developed polyacrylamide native gels were incubated for 1 hour at room temperature with a solution of 100 mM bis(2-hydroxyethyl)amino[tris(hydroxymethyl)]methane hydrochloride (Tris-HCl; pH 7.4), 0.1 mM 3,3'-dimethoxybiphenyl-4,4'-diamin (*ortho*-dianisidine) and 10 mM potassium bromide. For detecting bromoperoxidase activity, 0.45 mM hydrogen peroxide was added, indicating peroxidase activity by a brownish-orange spot enzyme.[10]

4 Crystallogenesis and Crystallographic Data

4.1 Crystallogenesis

The crystallization screening with the nanodrop-robot Honeybee (Cartesian) using the commercial screens PACT and JCSG+ (Quiagen, Les Ulis, France) provided crystallization conditions, which were optimized in the hanging-drop vapour diffusion method. The crystals were grown at 20 C from droplets composed of 1 µL of native V_{Br}PO(*An*II) (8 mg mL^{-1}) and 0.5 µL of reservoir solution containing NaCl (0.1 M), Bis-(2-hydroxyethyl)-amino-tris-(hydroxymethyl)-methane (0.01 M, pH 5.5), and PEG 3350 (25 %) furnished monoclinic crystals. Hexagonal crystals were obtained from KSCN (0.15 M), Bis-(2-hydroxyethyl)-amino-tris-(hydroxypropyl)-methane (0.01 M, pH 7.5) and PEG 3350 (19 %) as reservoir solution with a drop of 2 µl enzyme and 1 µl of reservoir solution. The crystals were collected and transported under cryocooled conditions soaking single crystals in the reservoir solution with glycerol as cryoprotect solution. The diffraction data were collected on the beamline ID23-2 at the synchrotron ESRF (Grenoble, France).

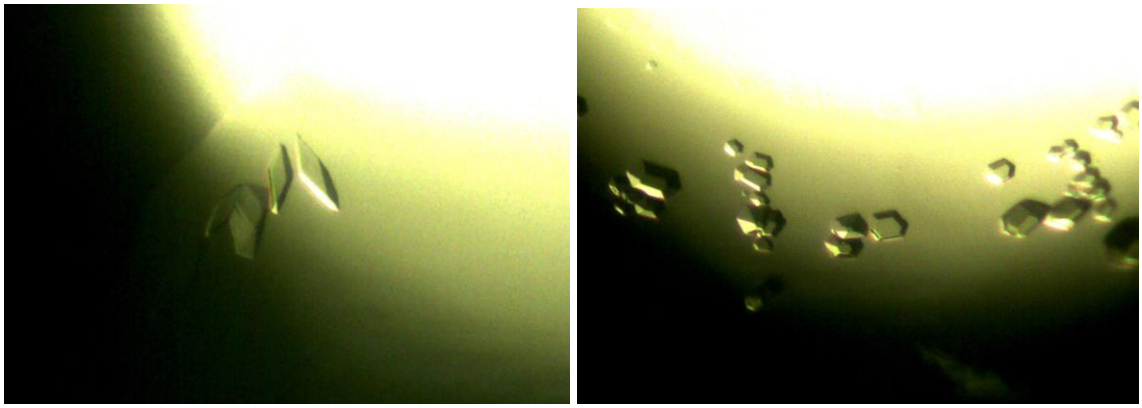

Figure S1. Photograph of monoclinic V_{Br}PO(*An*II)-crystals in the reservoir solution on the left and hexagonal crystals on the right (photographed through a microscope with 120-times magnification).

4.2 Data from diffraction analysis

Table S1. Summary of diffraction analysis data for native V_{Br}PO(*An*II) [a]

entry	data collection	monoclinic crystal	hexagonal crystal
1	wavelength / nm [b]	0.8729	0.8729
2	space group	$P2_1$	$P6_1$
3	unit cell dimension / Å	a = 67.8	a = 139.2
		b = 236.8	b = 139.2
		c = 118.0	c = 357.0
4	unit cell angles [c] / deg	β = 93.74	$\alpha = \beta = \gamma = 90°$
5	maximum resolution / Å	2.26	3.62
6	completeness / %	98.62	99.86
7	redundancy	4.0	5.8
8	mean I/σ (I) [d]	7.0	4.8
9	R_{merge} [e]	0.18	0.21

[a] Values in parentheses refer to the high resolution limit. [b] Wavelength of synchrotron radiation. [c] For remaining angles: $\alpha = \gamma = 90$ degrees. [d] Signal-to-noise ratio. [e] Error in measured intensities of equivalent reflections.

Table S2. Summary of data refinement and conformational analysis for peptide bonds from diffraction analysis of the monoclinic $V_{Br}PO(AnII)$-crystal [a]

entry	refinement parameter	value(s)
1	resolution range (Å)	70.0–2.26
2	number of reflections / unique	681260 / 161755
3	final R_{cryst}	0.1646
4	R_{free}	0.2323
5	figure of merit	0.8236
6	number of protein residues	3480 / 3576
7	number of water molecules	2331
8	number of vanadate ions	6
9	overall B factor ($Å^2$)	34.54
10	$B_{average}$ [a]/ Molecule/ $Å^2$	19.37
11	$B_{average}$ [a]/ Solvent / $Å^2$	20.93
12	$B_{average}$ [a]/ Vanadate/ $Å^2$	23.15
13	φ / $\psi_{favored}$ [b] (number/percent)	3345 / 96.15
14	φ / $\psi_{allowed}$ [b] (number/percent)	102 / 2.93
15	φ / $\psi_{outlier}$ [b] (number/percent)	32 / 0.92
16	root mean square deviation bond lengths / Å	0.0123
17	root mean square deviation bond angles / deg	1.6427

[a] Debye-Waller-factor. [b] Ramachandran φ/ψ-dihedral angle analysis using the program MolProbity.[11]

4.3 Packing of V_{Br}PO(*An*II) in the solid state

Table S3. Details for packing of bromoperoxidase II-molecules in the unit cell

value

entry	parameter	value
1	Z	2
2	molecules per asymmetric unit	6
2	mass per V_{Br}PO(*An*II)-hexamer [a] / Da	405336
2	volume of unit cell / m^3	$1.8945\ 10^{-24}$
4	$\rho_{calculated}$ / kg m^{-3}	4263.36

[a] Includes one $H_2VO_4^-$ per monomer; mass per monomer 67439 Da.[12]

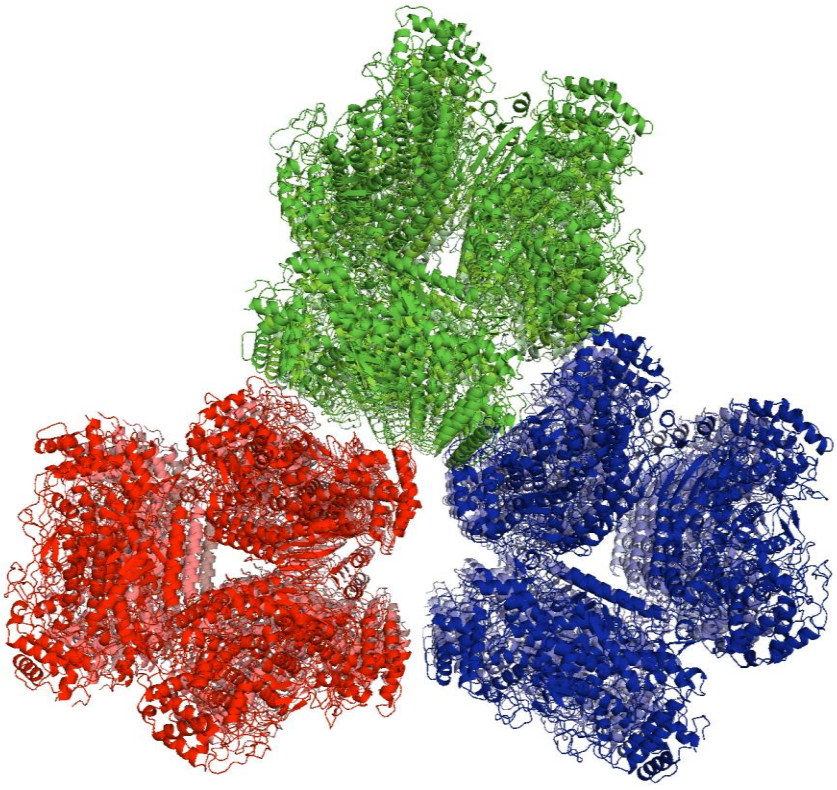

Figure S2. View along *c* for visualizing packing of V_{Br}PO(*An*II)-homohexamers in the solid state

5 Protein Sequence Alignment and Amino Acid-Statistics

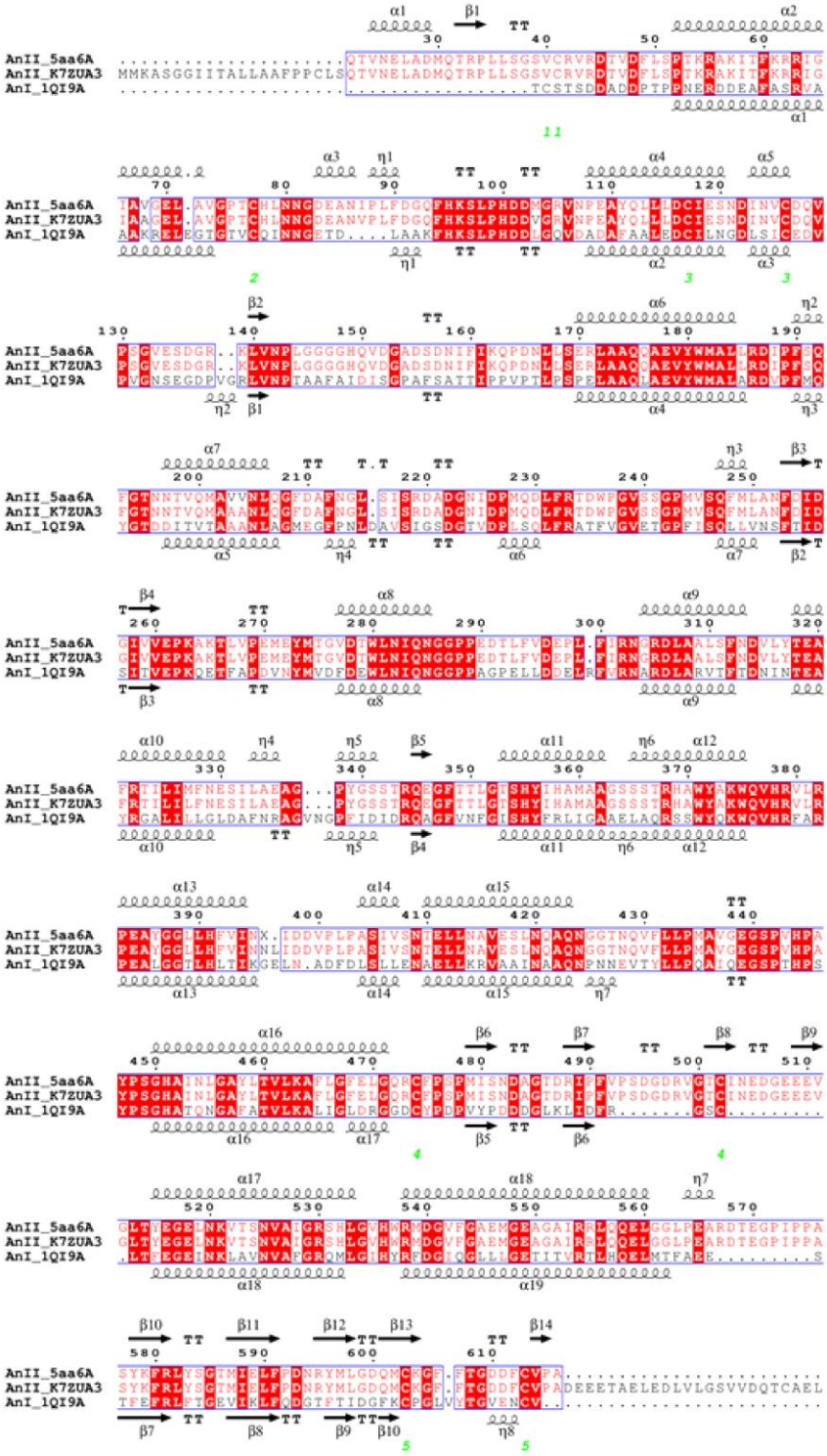

Figure S3. Aligning *A. nodosum* bromoperoxidase sequences (for details, see page 10).

Addenda to the legend for Figure S3 (page 9): Aligned sequences of protein chain A from the crystal structure of V_{Br}PO(*An*II) (PDB ID 5AA6; AnII_5aa6a; top), the protein expressed from the translated sequence of cloned V_{Br}PO(*An*II)-cDNA (EBI UniProtKB ID K7ZUA3; AnII_K7ZUA3; center) and the crystal structure of V_{Br}PO(*An*I) (PDB ID 1QI9; AnI_1QI9A; bottom). The protein alignment was constructed using ESPript software[13] showing the positions of α-helices (squiggles), β-strands (arrows), β-turns (TT letters) and disulfide bridges (green pairs of digits) based on the two threedimensional structures of V_{Br}PO(*An*II) (PDB ID 5AA6) and V_{Br}PO(*An*I) (PDB ID 1QI9).

Table S4. Amino acid sequence of V_{Br}PO(*An*II), as deduced from crystal structure [a]

pos.	amino acid sequence					
22	QTVNELADMQ	TRPLLSGSVC	RVRDTVDFLS	PTKRAKITFK	RRIGIAVGEL	AVGPTCHLNN
82	GDEANIPLFD	GQFHKSLPHD	DMGRVNPEAY	QLLLDCIESN	DINVCDQVPS	GVESDGRKLV
142	NPLGGGGHQV	DGADSDNIFI	KQPDNLLSER	LAAQQAEVYW	MALLRDIPFS	QFGTNNTVQM
202	AVVNLQGFDA	FNGLSISRDA	DGNIDPMQDL	FRTDWPGVSS	GPMVSQFMLA	NFDIDGIVVE
262	PKAKTLVPEM	EYMTGVDTWL	NIQNGGPPED	TLFVDEPLFI	RNGRDLAALS	FNDVLYTEAF
322	RTILIMFNES	ILAEAGPYGS	STRQEGFTTL	GTSHYIHAMA	AGSSSTRHAW	YAKWQVHRVL
382	RPEAYGGLLH	FVINXIDDVP	LPASIVSNTE	LLNAVESLNQ	AQNGGTNQVF	LLPMAVGEGS
442	PVHPAYPSGH	AINLGAYLTV	LKAFLGFELG	QRCFPSPMIS	NDAGTDRIPF	VPSDGDRVGT
502	CINEDGEEEV	GLTYEGELNK	VTSNVAIGRS	HLGVHWRMDG	VFGAEMGEAG	AIRRLQQELG
562	GLPEARDTEG	PIPPASYKFR	LYSGTMIELF	PDNRYMLGDQ	MCKGFFTGDD	FCVPA

[a] The first amino acid was conventionally numbered according to the cDNA-translated protein sequence (see Figure S3, above); Amino acids associated with the vanadate binding site are colored in blue, cysteine residues involved in intramolecular disulfide bridging are colored in yellow, cysteins marked in red form intermolecular disulfide bonds.

Table S5. Amino acid composition of the *A. nodosum* bromoperoxidase II-protein, derived from the translated sequence of the cloned $V_{Br}PO$(*An*II) cDNA (EBI UniProtKB ID K7ZUA3) [a]

entry	amino acid	code	total	% / mol/mol	% /*w*/*w*
1	Ala	A	52	8.11	5.71
2	Cys	C	10	1.56	1.49
3	Asp	D	45	7.02	7.39
4	Glu	E	40	6.24	7.26
5	Phe	F	31	4.84	6.31
6	Gly	G	62	9.67	5.74
7	His	H	13	2.03	2.49
8	Ile	I	31	4.84	5.01
9	Lys	K	14	2.18	2.52
10	Leu	L	64	9.98	10.35
11	Met	M	18	2.81	3.31
12	Asn	N	34	5.30	5.54
13	Pro	P	38	5.93	5.39
14	Gln	Q	25	3.90	4.50
15	Arg	R	29	4.52	6.23
16	Ser	S	38	5.93	4.92
17	Thr	T	33	5.15	4.85
18	Val	V	44	6.86	6.35
19	Trp	W	6	0.94	1.51
20	Tyr	Y	14	2.18	3.13

[a] 641 amino acids; molecular weight of 69511 g mol^{-1}; predicted p*I* = 4.33.

6 Thermostability studies

DLS experiments revealed a high capacity of temperature resistance for both V_{Br}PO(*An*I) and V_{Br}PO(*An*II) proteins (Figure S4, Panel A). V_{Br}PO(*An*I) was stable up to 70°C whereas AnII was not denatured up to 90°C, the maximum temperature authorized by the DLS device. V_{Br}PO(*An*I) exhibited a Melting Temperature value between 70°C and 75°C, corresponding to a strong increase of the Z-average diameter from 24.97 to 37.93 and showing the beginning of protein aggregation. Moreover, PAGE gels (Figure S4, Panel B) showed a significant diminution of bromoperoxidase activity at 70°C and a drastic abolition at 80°C for V_{Br}PO(*An*I). By contrast, V_{Br}PO(*An*II) exhibited a stronger heat tolerance, remaining still partially active until 90°C, and was fully denatured after 100°C .

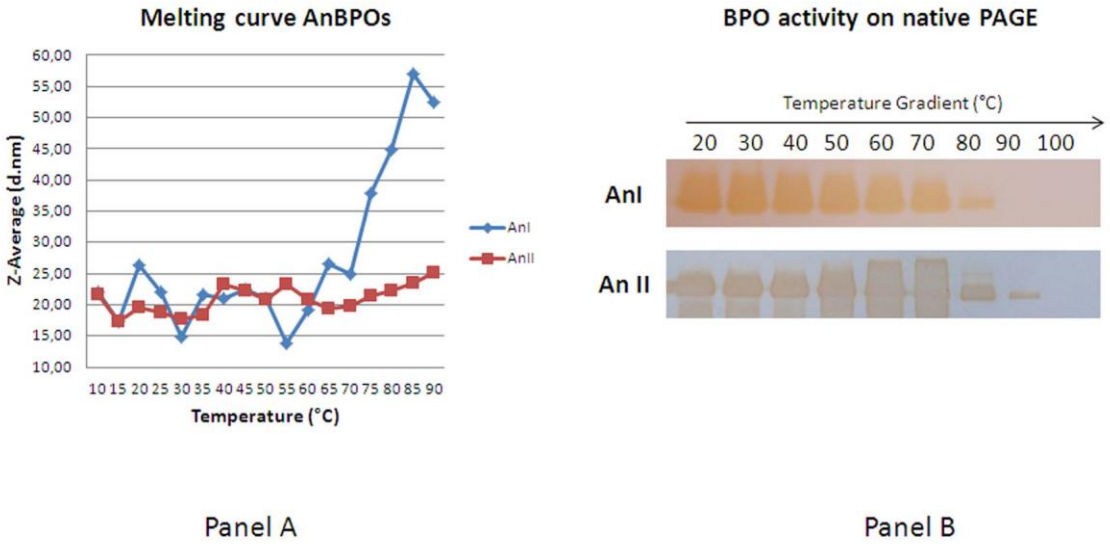

Figure S4. Thermostability of V_{Br}PO-enzymes. Melting curves of V_{Br}PO(*An*I) and V_{Br}PO(*An*II) using DLS-method (panel A) and enyzmytic activity as evident from *o*-dianisidine coloration on native PAGE (Panel B) [AnBPO = *Ascophyllum nodosum* bromoperoxidase; AnI = V_{Br}PO(*An*I); AnII = V_{Br}PO(*An*II), BPO = bromoperoxidase].

7 Molecular Modelling

7.1 Electronic structure methods

All structures and energies reported in the associated article were computed with the density functional/Hartree-Fock-hybrid model B3LYP, in combination with the basis set 6-311++G(d,p) implemented in Gaussian03-suite of program (Revision E.01).[14]

To secure that energy function minimization provided a global structure minimum structure, we prviously scanned potential energy surfaces by continously incrementing dihedral angles of conformationally flexible entities, for instance the H,O,V,O^A-dihedral angle in orthovanadium acid and derived peroxoic acids. The energy minimum from the conformational search served as input for a second energy function minimization, which was performed without symmetry constraints or constrained internal coordinates, using the Bernie-algorithm in combination with the tight-option for minimization routines and the ultrafine grid for integration algorithms.

Minimum structures used for calculating thermochemical properties show exclusively posivitve vibrational normal modes, as specified by the *n*umber zero for *imag*inary modes (Nimag = 0). Transition structures are chracterized by exactly one negative mode of vibration (Nimag = 1). The negative mode of vibration in transition structures describes the reaction coordinate of bond forming, as evident from vibration animations using the MOLDEN-software.[15]

Gibbs free energies referring to physical chemical standards (298.15 Kelvin, 1 atmosphere), abbreviated as $G°$, were calculated on the basis of the thermochemical model implemented in Gaussian03, using unscaled frequency calculations. Likewise obtained Gibbs free energies consider zero-point correction, thermal correction, and molecular entropy.

For translating results from density functional theory calculations into molecular models, single point NBO-population analyses[16] on the B3LYP/6-31G*-level of theory were conducted using atomic coordinates from B3LYP/6-311++G**-minimized structures.

All energies from σ(O,O)-, σ*(O,O)-, σ(O,Br), and σ*(O,Br)-orbitals discussed in the associated article are taken from NBO-population analysis.

7.2 Molecular Graphics

Ball-and-stick graphics displayed in sections 7.3–7.10 were generated with thie ChemPlus add-on (Version 1.6) to HyperChem 4.5.[2] Atomic coordinates for the graphics are taken from B3LYP/6-311++G(d,p)-minimized energy functions archived in Gaussian03-logfiles. Transforming Gaussian logfiles into HyperChem input was achieved by the Open-Babel-feeware.[17] The selected color code depicts carbon in gray, oxygen in red, nitrogen in blue, vanadium in yellow, hydrogen in white, and bromide in orange.

7.3 Orthovanadium acid and hydrogen-bonded adducts

7.3.1 Orthovanadium acid

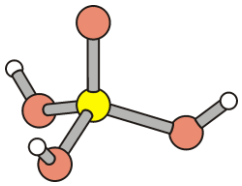

Figure S5. Minimum structure of orthovanadium acid having all hydrogens positioned toward multiply bonded oxido oxygen (all-*syn*-conformation).

(*i*) B3LYP/6-311++G**//B3LYP/6-311++G**

Standard orientation:

Center Number	Atomic Number	Atomic Type	Coordinates (Angstroms) X	Y	Z
1	23	0	0.000000	0.000000	0.027767
2	8	0	0.000000	0.000000	1.596654
3	8	0	0.000000	1.677284	-0.561099
4	8	0	1.452570	-0.838642	-0.561099
5	8	0	-1.452570	-0.838642	-0.561099
6	1	0	-0.000352	2.446734	0.018161
7	1	0	2.119110	-1.223062	0.018161
8	1	0	-2.118758	-1.223672	0.018161

```
Zero-point correction=                          0.043521 (Hartree/Particle)
Thermal correction to Energy=                   0.050709
Thermal correction to Enthalpy=                 0.051653
Thermal correction to Gibbs Free Energy=        0.014104
Sum of electronic and zero-point Energies=          -1246.940727
Sum of electronic and thermal Energies=             -1246.933538
Sum of electronic and thermal Enthalpies=           -1246.932594
Sum of electronic and thermal Free Energies=        -1246.970143

Version=AM64L-G03RevE.01\State=1-A\HF-1246.9842473\RMSD=1.947e-10\
RMSF=1.363e-05\PG=C03 [C3(V1O1),X(H3O3)]\NImag=0\\@.
```

(*ii*) NBO-analysis – B3LYP/6-31G*// B3LYP/6-311++G**

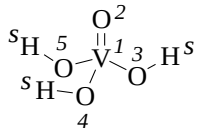


```
=======================================================================
No. (Occupancy) Bond orbital/ Coefficients/ Hybrids
=======================================================================
 1. (1.92324) BD (1) V  1- O  2
    (28.98%) 0.5383* V  1  s(28.30%)   p(0.05%)    d(71.37%)   f(0.28%)
    (71.02%) 0.8427* O  2  s(11.63%)   p(88.18%)   d(0.19%)
 2. (1.98494) BD (2) V  1- O  2
    (22.62%) 0.4756* V  1  s(0.00%)    p(1.11%)    d(98.70%)   f(0.20%)
    (77.38%) 0.8796* O  2  s(0.00%)    p(99.89%)   d(0.11%)
 3. (1.98488) BD (3) V  1- O  2
    (22.62%) 0.4756* V  1  s(0.00%)    p(1.11%)    d(98.69%)   f(0.20%)
    (77.38%) 0.8797* O  2  s(0.00%)    p(99.89%)   d(0.11%)
 4. (1.97440) BD (1) V  1- O  3
    (19.02%) 0.4361* V  1  s(23.36%)   p(0.54%)    d(75.94%)   f(0.16%)
    (80.98%) 0.8999* O  3  s(14.67%)   p(85.25%)   d(0.08%)
 5. (1.97440) BD (1) V  1- O  4
    (19.01%) 0.4360* V  1  s(23.39%)   p(0.53%)    d(75.91%)   f(0.16%)
    (80.99%) 0.8999* O  4  s(14.67%)   p(85.25%)   d(0.08%)
 6. (1.97427) BD (1) V  1- O  5
    (19.10%) 0.4370* V  1  s(23.36%)   p(0.54%)    d(75.94%)   f(0.16%)
    (80.90%) 0.8995* O  5  s(14.59%)   p(85.33%)   d(0.08%)
23. (1.97474) LP (1) O  2  s(88.39%)   p(11.61%)   d(0.00%)
24. (1.95032) LP (1) O  3  s(59.64%)   p(40.30%)   d(0.06%)
25. (1.81299) LP (2) O  3  s(0.00%)    p(99.93%)   d(0.07%)
26. (1.95035) LP (1) O  4  s(59.64%)   p(40.30%)   d(0.06%)
27. (1.81352) LP (2) O  4  s(0.00%)    p(99.93%)   d(0.07%)
28. (1.95005) LP (1) O  5  s(59.75%)   p(40.19%)   d(0.06%)
29. (1.81161) LP (2) O  5  s(0.00%)    p(99.93%)   d(0.07%)
=======================================================================
```

Second order perturbation theory analysis of Fock-matrix for *syn*/*syn*/*syn*-orthovanadium acid in NBO-basis(threshold for printing: 0.50 kcal/mol)

Donor NBO (i)	Acceptor NBO (j)	kcal/mol	a.u.	a.u.
23. LP (1) O 2	94. BD*(1) V 1- O 2	2.45	1.14	0.048
23. LP (1) O 2	97. BD*(1) V 1- O 3	1.65	1.06	0.039
23. LP (1) O 2	98. BD*(1) V 1- O 4	1.66	1.06	0.039
23. LP (1) O 2	99. BD*(1) V 1- O 5	1.65	1.06	0.039
24. LP (1) O 3	94. BD*(1) V 1- O 2	5.04	0.81	0.058
24. LP (1) O 3	96. BD*(3) V 1- O 2	9.20	0.62	0.069
24. LP (1) O 3	98. BD*(1) V 1- O 4	0.95	0.73	0.024
24. LP (1) O 3	99. BD*(1) V 1- O 5	0.95	0.73	0.024
25. LP (2) O 3	95. BD*(2) V 1- O 2	5.42	0.25	0.033
25. LP (2) O 3	98. BD*(1) V 1- O 4	9.42	0.36	0.052
25. LP (2) O 3	99. BD*(1) V 1- O 5	9.45	0.36	0.052
26. LP (1) O 4	94. BD*(1) V 1- O 2	5.04	0.81	0.058
26. LP (1) O 4	95. BD*(2) V 1- O 2	6.89	0.62	0.060
26. LP (1) O 4	96. BD*(3) V 1- O 2	2.30	0.62	0.034
26. LP (1) O 4	97. BD*(1) V 1- O 3	0.95	0.73	0.024
26. LP (1) O 4	99. BD*(1) V 1- O 5	0.94	0.73	0.024
27. LP (2) O 4	95. BD*(2) V 1- O 2	1.36	0.25	0.017
27. LP (2) O 4	96. BD*(3) V 1- O 2	4.05	0.25	0.029
27. LP (2) O 4	97. BD*(1) V 1- O 3	9.41	0.36	0.052
27. LP (2) O 4	99. BD*(1) V 1- O 5	9.43	0.36	0.052
28. LP (1) O 5	94. BD*(1) V 1- O 2	5.04	0.81	0.058
28. LP (1) O 5	95. BD*(2) V 1- O 2	6.93	0.62	0.060
28. LP (1) O 5	96. BD*(3) V 1- O 2	2.31	0.62	0.034
28. LP (1) O 5	97. BD*(1) V 1- O 3	0.95	0.73	0.024
28. LP (1) O 5	98. BD*(1) V 1- O 4	0.95	0.73	0.024
29. LP (2) O 5	95. BD*(2) V 1- O 2	1.36	0.25	0.017
29. LP (2) O 5	96. BD*(3) V 1- O 2	4.08	0.25	0.029
29. LP (2) O 5	97. BD*(1) V 1- O 3	9.44	0.36	0.052
29. LP (2) O 5	98. BD*(1) V 1- O 4	9.45	0.36	0.052

Natural bond orbital (NBO)-energies

NBO	Occupancy	Energy
1. BD (1) V 1- O 2	1.92324	-0.60266
2. BD (2) V 1- O 2	1.98494	-0.37606
3. BD (3) V 1- O 2	1.98488	-0.37605
4. BD (1) V 1- O 3	1.97440	-0.54966
5. BD (1) V 1- O 4	1.97440	-0.54983
6. BD (1) V 1- O 5	1.97427	-0.54806

7.3.2 Monohydrated orthovanadium acid – adduct 1a$_1$

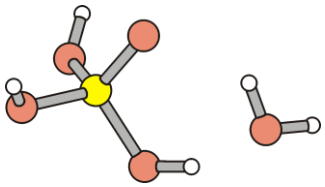

Figure S6. Minimum structure of hydrogen bonded water to the all-*syn*-conformer of orthovanadium acid.

B3LYP/6-311++G//B3LYP/6-311++G****

Standard orientation:

Center Number	Atomic Number	Atomic Type	Coordinates (Angstroms) X	Y	Z
1	8	0	-3.033811	0.074134	0.072366
2	1	0	-3.762245	-0.551353	0.133595
3	1	0	-2.561198	0.025892	0.914358
4	23	0	0.519394	-0.002490	-0.009976
5	8	0	-0.305616	-0.005635	1.337984
6	8	0	-0.642229	-0.045998	-1.326835
7	8	0	1.506176	1.475509	-0.112485
8	8	0	1.578378	-1.431796	-0.083784
9	1	0	-1.593812	-0.024612	-1.089723
10	1	0	1.505838	2.167400	0.557089
11	1	0	1.642175	-2.089764	0.616156

Zero-point correction= 0.068265 (Hartree/Particle)
Thermal correction to Energy= 0.078543
Thermal correction to Enthalpy= 0.079487
Thermal correction to Gibbs Free Energy= 0.033150
Sum of electronic and zero-point Energies= -1323.387658
Sum of electronic and thermal Energies= -1323.377380
Sum of electronic and thermal Enthalpies= -1323.376436
Sum of electronic and thermal Free Energies= -1323.422774

Version=AM64L-G03RevE.01\State=1-A\HF-1323.4559234\RMSD=5.023e-09\
RMSF=1.498e-07\PG=C01 [X(H5O5V1)]\NImag=0\\@.

7.3.3 Twofold hydrated orthovanadium acid – adduct $1a_2$

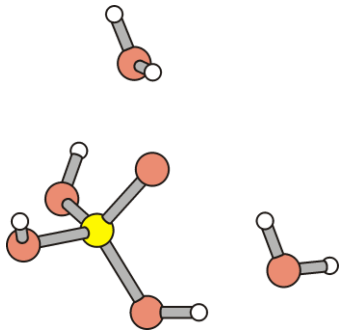

Figure S7. Minimum structure two hydrogen bonded water molecules to the all-*syn*-conformer of orthovanadium acid.

B3LYP/6-311++G//B3LYP/6-311++G****

Standard orientation:

Center Number	Atomic Number	Atomic Type	Coordinates (Angstroms) X	Y	Z
1	23	0	0.006373	-0.618070	0.045971
2	8	0	0.008374	0.607267	-0.972537
3	8	0	1.448056	-0.491264	1.046040
4	8	0	-1.443654	-0.492717	1.032027
5	8	0	0.014144	-2.166016	-0.836954
6	1	0	2.049314	0.263707	0.878404
7	1	0	-2.071509	0.231247	0.824810
8	1	0	-0.035734	-2.242853	-1.795128
9	8	0	2.576383	1.819850	-0.038143
10	1	0	3.405263	1.934107	-0.513056
11	1	0	1.878931	1.799088	-0.708097
12	8	0	-2.679596	1.704099	-0.139439
13	1	0	-2.854407	2.570636	0.240550
14	1	0	-1.908093	1.809939	-0.712753

```
Zero-point correction=                          0.093116 (Hartree/Particle)
Thermal correction to Energy=                   0.106403
Thermal correction to Enthalpy=                 0.107347
Thermal correction to Gibbs Free Energy=        0.053401
Sum of electronic and zero-point Energies=          -1399.833784
Sum of electronic and thermal Energies=             -1399.820497
Sum of electronic and thermal Enthalpies=           -1399.819553
Sum of electronic and thermal Free Energies=        -1399.873499

Version=AM64L-G03RevE.01\State=1-A\HF-1399.9268997\RMSD=5.092e-09\
RMSF=2.396e-07\PG=C01 [X(H7O6V1)]\NImag=0\\@.
```

7.3.4 Threefold hydrated orthovanadium acid – adduct $1a_3$

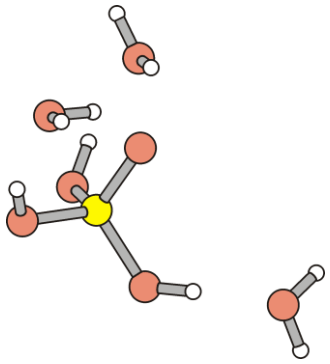

Figure S8. Minimum structure of three hydrogen bonded water molecules to the all-*syn*-conformer of orthovanadium acid.

B3LYP/6-311++G//B3LYP/6-311++G****

Standard orientation:

Center Number	Atomic Number	Atomic Type	Coordinates (Angstroms) X	Y	Z
1	8	0	-1.558456	2.726566	1.031913
2	1	0	-1.294608	1.902206	1.466755
3	1	0	-2.477184	2.874843	1.276062
4	23	0	-0.031373	-0.035495	-0.572434
5	8	0	-0.349409	0.028493	0.993641
6	8	0	-0.619359	1.463291	-1.295163
7	8	0	-0.892023	-1.425444	-1.237319
8	8	0	1.696783	-0.202942	-0.854704
9	1	0	-1.027235	2.119457	-0.694710
10	1	0	-1.436801	-1.950885	-0.617740
11	1	0	2.391173	-0.221492	-0.165583
12	8	0	-2.086527	-2.342602	1.142504
13	8	0	3.759501	-0.179507	1.021908
14	1	0	-1.882092	-3.154676	1.615998
15	1	0	-1.551526	-1.647937	1.554313
16	1	0	4.639110	-0.172504	0.629681
17	1	0	3.756675	0.524529	1.678972

```
Zero-point correction=                          0.117591 (Hartree/Particle)
Thermal correction to Energy=                   0.134293
Thermal correction to Enthalpy=                 0.135237
Thermal correction to Gibbs Free Energy=        0.070867
Sum of electronic and zero-point Energies=          -1476.279356
Sum of electronic and thermal Energies=             -1476.262653
Sum of electronic and thermal Enthalpies=           -1476.261709
Sum of electronic and thermal Free Energies=        -1476.326079

Version=AM64L-G03RevE.01\State=1-A\HF-1476.3969464\RMSD=3.944e-09\
RMSF=3.583e-07\PG=C01 [X(H9O7V1)]\NImag=0\\@.
```

7.3.5 Methanol bonding to orthovanadium acid – adduct 1b

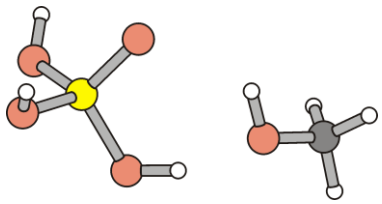

Figure S9. Minimum structure of hydrogen bonded methanol to the all-*syn*-conformer of orthovanadium acid.

B3LYP/6-311++G//B3LYP/6-311++G****

Standard orientation:

Center Number	Atomic Number	Atomic Type	Coordinates (Angstroms) X	Y	Z
1	23	0	-0.980501	0.019246	-0.008284
2	8	0	-0.187737	-0.059509	1.356400
3	8	0	0.201266	-0.117940	-1.298159
4	8	0	-2.154026	-1.317583	-0.105766
5	8	0	-1.837996	1.576597	-0.128892
6	1	0	1.139040	-0.256543	-1.029930
7	1	0	-2.259782	-1.986021	0.578964
8	1	0	-1.831373	2.245540	0.563359
9	8	0	2.553598	-0.483117	0.048690
10	1	0	2.122421	-0.395919	0.908012
11	6	0	3.758807	0.287546	0.029263
12	1	0	3.560362	1.352012	0.191741
13	1	0	4.200596	0.156795	-0.957936
14	1	0	4.466579	-0.071395	0.782556

Zero-point correction= 0.097128 (Hartree/Particle)
Thermal correction to Energy= 0.108768
Thermal correction to Enthalpy= 0.109713
Thermal correction to Gibbs Free Energy= 0.058353
Sum of electronic and zero-point Energies= -1362.665900
Sum of electronic and thermal Energies= -1362.654259
Sum of electronic and thermal Enthalpies= -1362.653315
Sum of electronic and thermal Free Energies= -1362.704674

Version=AM64L-G03RevE.01\State=1-A\HF-1362.7630277\RMSD=4.022e-09\
RMSF=5.643e-07\PG=C01 [X(C1H7O5V1)]\NImag=0\\@.

7.3.6 Imidazole bonding to orthovanadium acid – adduct 1c

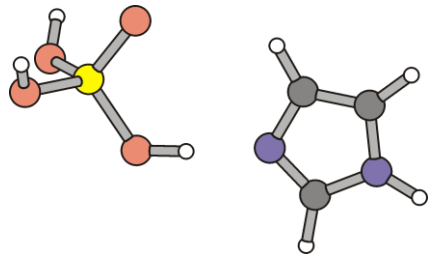

Figure S10. Minimum structure of hydrogen bonded imidazole to the all-*syn*-conformer of orthovanadium acid.

B3LYP/6-311++G//B3LYP/6-311++G****

Standard orientation:

Center Number	Atomic Number	Atomic Type	Coordinates (Angstroms) X	Y	Z
1	23	0	1.911637	-0.001294	0.000000
2	8	0	1.278336	1.444476	-0.000058
3	8	0	0.630236	-1.180709	0.000014
4	8	0	2.925466	-0.204423	-1.462107
5	8	0	2.925409	-0.204337	1.462158
6	1	0	-0.343299	-0.927751	0.000009
7	1	0	3.062160	0.510801	-2.091228
8	1	0	3.062140	0.510948	2.091201
9	7	0	-1.962137	-0.398347	0.000004
10	6	0	-2.340774	0.927754	-0.000013
11	6	0	-3.705569	1.018454	-0.000015
12	7	0	-4.160363	-0.285509	0.000003
13	6	0	-3.073395	-1.102360	0.000014
14	1	0	-3.142177	-2.178659	0.000023
15	1	0	-5.124097	-0.580385	0.000016
16	1	0	-4.375140	1.861332	-0.000022
17	1	0	-1.606895	1.717314	-0.000021

```
Zero-point correction=                          0.116267 (Hartree/Particle)
Thermal correction to Energy=                   0.128687
Thermal correction to Enthalpy=                 0.129631
Thermal correction to Gibbs Free Energy=        0.074477
Sum of electronic and zero-point Energies=          -1473.169398
Sum of electronic and thermal Energies=             -1473.156978
Sum of electronic and thermal Enthalpies=           -1473.156034
Sum of electronic and thermal Free Energies=        -1473.211188

Version=AM64L-G03RevE.01\State=1-A\HF-1473.2856653\RMSD=6.037e-09\
RMSF=3.906e-07\NImag=0\PG=C01 [X(C3H7N2O4V1)]\\@.
```

7.3.7 Methylamine bonding to orthovanadium acid – adduct 1d

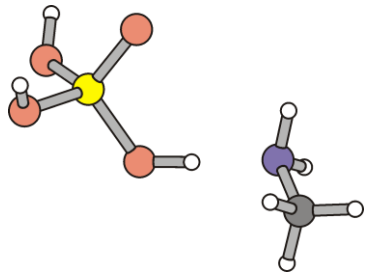

Figure S11. Minimum structure of hydrogen bonded methylamine to the all-*syn*-conformer of orthovanadium acid.

B3LYP/6-311++G//B3LYP/6-311++G****

Standard orientation:

Center Number	Atomic Number	Atomic Type	Coordinates (Angstroms) X	Y	Z
1	23	0	1.027043	0.018054	0.000687
2	8	0	0.628505	-0.174202	1.515786
3	8	0	-0.407217	-0.140579	-0.975449
4	8	0	1.739015	1.645267	-0.222855
5	8	0	2.221296	-1.232715	-0.461167
6	1	0	-1.319173	-0.329902	-0.578648
7	1	0	1.903134	2.240178	0.515531
8	1	0	2.580824	-1.859616	0.174292
9	7	0	-2.817328	-0.610438	0.151542
10	6	0	-3.776998	0.483498	-0.087379
11	1	0	-3.192576	-1.496955	-0.172881
12	1	0	-2.630288	-0.716497	1.144821
13	1	0	-3.947354	0.580543	-1.160751
14	1	0	-3.343316	1.420359	0.265802
15	1	0	-4.742757	0.336546	0.408991

Zero-point correction= 0.109942 (Hartree/Particle)
Thermal correction to Energy= 0.121606
Thermal correction to Enthalpy= 0.122550
Thermal correction to Gibbs Free Energy= 0.070076
Sum of electronic and zero-point Energies= -1342.787025
Sum of electronic and thermal Energies= -1342.775361
Sum of electronic and thermal Enthalpies= -1342.774417
Sum of electronic and thermal Free Energies= -1342.826891

Version=AM64L-G03RevE.01\State=1-A\HF-1342.8969665\RMSD=5.945e-09\
RMSF=1.743e-07\PG=C01 [X(C1H8N1O4V1)]\NImag=0\\@.

7.3.8 Methylammonium bonding to orthovanadium acid – adduct 1e

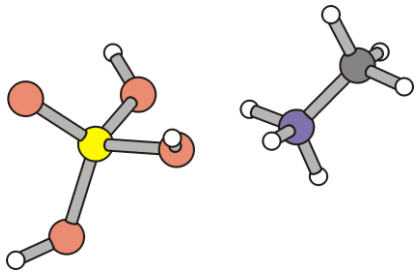

Figure S12. Minimum structure of hydrogen bonded methylammonium to the all-*syn*-conformer of orthovanadium acid (chelated hydrogen bonds).

B3LYP/6-311++G//B3LYP/6-311++G****

Standard orientation:

Center Number	Atomic Number	Atomic Type	Coordinates (Angstroms) X	Y	Z
1	23	0	-1.051542	0.000000	-0.085588
2	8	0	-2.096667	0.000012	-1.236568
3	8	0	0.078860	1.407809	-0.191784
4	8	0	-1.858257	-0.000013	1.467578
5	8	0	0.078859	-1.407808	-0.191803
6	1	0	-0.085022	2.182024	-0.746005
7	1	0	-2.807123	-0.000011	1.652478
8	1	0	-0.085020	-2.182016	-0.746037
9	1	0	1.835322	0.815071	0.349488
10	7	0	2.442914	0.000001	0.552801
11	1	0	1.835327	-0.815076	0.349499
12	6	0	3.693871	-0.000001	-0.278389
13	1	0	4.271442	-0.892460	-0.047015
14	1	0	3.408306	-0.000012	-1.328110
15	1	0	4.271433	0.892468	-0.047031
16	1	0	2.654814	0.000008	1.552611

```
Zero-point correction=                           0.125062 (Hartree/Particle)
Thermal correction to Energy=                    0.136578
Thermal correction to Enthalpy=                  0.137522
Thermal correction to Gibbs Free Energy=         0.087482
Sum of electronic and zero-point Energies=          -1343.142323
Sum of electronic and thermal Energies=             -1343.130807
Sum of electronic and thermal Enthalpies=           -1343.129863
Sum of electronic and thermal Free Energies=        -1343.179902

Version=AM64L-G03RevE.01\State=1-A\HF-1343.2673847\RMSD=6.598e-09\
RMSF=9.373e-08\PG=C01 [X(C1H9N1O4V1)]\NImag=0\\@.
```

7.3.9 *N*-Methylguanidinium bonding to orthovanadium acid I – adduct 1f

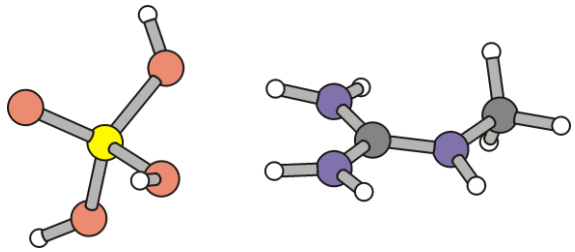

Figure S13. Minimum structure of the chelated adduct of *N*-methylguanidinium with the all-*syn*-conformer of orthovanadium acid.

B3LYP/6-311++G//B3LYP/6-311++G****

Standard orientation:

Center Number	Atomic Number	Atomic Type	Coordinates (Angstroms) X	Y	Z
1	23	0	-2.106518	-0.062844	-0.006515
2	8	0	-3.454574	0.005162	-0.781828
3	8	0	-1.242947	1.516361	-0.091379
4	8	0	-2.377045	-0.505604	1.669624
5	8	0	-0.981605	-1.245586	-0.773434
6	1	0	-1.654982	2.298702	-0.480206
7	1	0	-3.219256	-0.690841	2.104917
8	1	0	-1.244907	-1.781095	-1.532927
9	1	0	0.688065	1.426772	-0.100783
10	7	0	1.708571	1.436009	-0.102686
11	6	0	2.439062	0.317039	-0.037734
12	7	0	1.855900	-0.873410	-0.187730
13	7	0	3.761415	0.396224	0.162181
14	1	0	2.159847	2.336733	-0.104257
15	6	0	4.679716	-0.743419	0.138359
16	1	0	4.140473	1.296664	0.411355
17	1	0	2.370684	-1.717856	0.001703
18	1	0	0.868445	-0.972988	-0.429646
19	1	0	4.578944	-1.300679	-0.795321
20	1	0	5.695833	-0.358439	0.192167
21	1	0	4.522260	-1.407715	0.992869

Zero-point correction= 0.162330 (Hartree/Particle)
Thermal correction to Energy= 0.177452
Thermal correction to Enthalpy= 0.178396
Thermal correction to Gibbs Free Energy= 0.119178
Sum of electronic and zero-point Energies= -1492.006896
Sum of electronic and thermal Energies= -1491.991774
Sum of electronic and thermal Enthalpies= -1491.990830
Sum of electronic and thermal Free Energies= -1492.050049

Version=AM64L-G03RevE.01\State=1-A\HF-1492.1692264\RMSD=4.112e-09\
RMSF=3.038e-07\PG=C01 [X(C2H11N3O4V1)]\NImag=0\\@.

7.3.10 *N*-Methylguanidinium bonding to orthovanadium acid II – adduct *iso*-1f

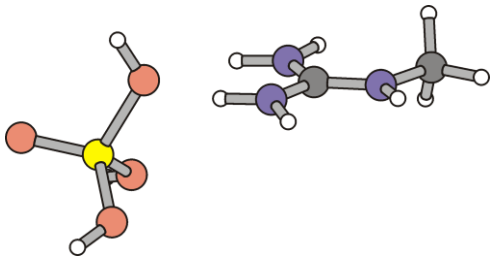

Figure S14. Minimum structure of the bifurcated adduct of *N*-methylguanidinium with the all-*syn*-conformer of orthovanadium acid.

B3LYP/6-311++G//B3LYP/6-311++G****

Standard orientation:

Center Number	Atomic Number	Atomic Type	Coordinates (Angstroms) X	Y	Z
1	23	0	-2.121059	0.070491	-0.035982
2	8	0	-3.477642	0.059079	0.730102
3	8	0	-0.748719	-0.196317	1.156160
4	8	0	-2.063937	-1.231486	-1.223236
5	8	0	-1.861931	1.625931	-0.822837
6	1	0	-0.982674	-0.312612	2.086469
7	1	0	-2.769783	-1.859822	-1.421744
8	1	0	-2.467919	2.377719	-0.826725
9	1	0	0.792420	-1.388501	0.526925
10	7	0	1.760467	-1.457653	0.226586
11	6	0	2.497798	-0.341490	0.165010
12	7	0	3.759533	-0.382543	-0.273880
13	7	0	1.948619	0.809330	0.558840
14	1	0	2.084682	-2.323271	-0.172960
15	1	0	2.473369	1.667609	0.572848
16	1	0	0.975028	0.814077	0.852038
17	6	0	4.640334	0.782039	-0.384756
18	1	0	4.144731	-1.285900	-0.502417
19	1	0	4.848567	1.219223	0.595317
20	1	0	4.211626	1.534178	-1.051165
21	1	0	5.583017	0.451117	-0.814867

```
Zero-point correction=                           0.161912 (Hartree/Particle)
Thermal correction to Energy=                    0.177463
Thermal correction to Enthalpy=                  0.178407
Thermal correction to Gibbs Free Energy=         0.116906
Sum of electronic and zero-point Energies=          -1492.004716
Sum of electronic and thermal Energies=             -1491.989165
Sum of electronic and thermal Enthalpies=           -1491.988220
Sum of electronic and thermal Free Energies=        -1492.049721

Version=AM64L-G03RevE.01\State=1-A\HF-1492.1666275\RMSD=3.534e-09\
RMSF=2.132e-07\PG=C01 [X(C2H11N3O4V1)]\NImag=0\\@.
```

7.4 Dihydrogen orthovanadate and hydrogen-bonded adducts

7.4.1 Dihydrogen orthovanadate

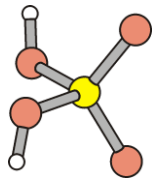

Figure S15. Minimum structure of dihydrogen orthovanadate.

(*i*) B3LYP/6-311++G**//B3LYP/6-311++G**

Standard orientation:

Center Number	Atomic Number	Atomic Type	Coordinates (Angstroms) X	Y	Z
1	23	0	0.000000	0.092320	0.000000
2	8	0	-0.341257	0.996315	1.304286
3	8	0	1.469981	-0.992034	0.371566
4	8	0	-1.469980	-0.992034	-0.371570
5	8	0	0.341256	0.996322	-1.304282
6	1	0	2.038583	-1.095962	-0.396757
7	1	0	-2.038585	-1.095961	0.396751

```
Zero-point correction=                          0.032627 (Hartree/Particle)
Thermal correction to Energy=                   0.039242
Thermal correction to Enthalpy=                 0.040186
Thermal correction to Gibbs Free Energy=        0.002499
Sum of electronic and zero-point Energies=          -1246.421014
Sum of electronic and thermal Energies=             -1246.414399
Sum of electronic and thermal Enthalpies=           -1246.413455
Sum of electronic and thermal Free Energies=        -1246.451142

Version=AM64L-G03RevE.01\State=1-A\HF-1246.453641\RMSD=5.773e-09\
RMSF=1.226e-07\PG=C01 [X(H2O4V1)]\NImag=0\\@.
```

(*ii*) NBO-analysis – B3LYP/6-31G*// B3LYP/6-311++G**

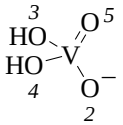


```
=======================================================================
No. (Occupancy) Bond orbital/ Coefficients/ Hybrids
=======================================================================
1.  (1.94315) BD (1) V  1- O  2
    (27.33%) 0.5227* V  1  s(19.89%)   p(0.27%)    d(79.63%)   f(0.21%)
    (72.67%) 0.8525* O  2  s(11.00%)   p(88.85%)   d(0.15%)
2.  (1.90287) BD (2) V  1- O  2
    (16.85%) 0.4104* V  1  s(0.01%)    p(32.15%)   d(67.24%)   f(0.60%)
    (83.15%) 0.9119* O  2  s(0.12%)    p(99.80%)   d(0.08%)
3.  (1.94623) BD (1) V  1- O  3
    (13.20%) 0.3633* V  1  s(28.21%)   p(14.22%)   d(57.32%)   f(0.24%)
    (86.80%) 0.9317* O  3  s(14.44%)   p(85.48%)   d(0.08%)
4.  (1.94221) BD (1) V  1- O  4
    (12.96%) 0.3599* V  1  s(29.12%)   p(14.08%)   d(56.56%)   f(0.24%)
    (87.04%) 0.9330* O  4  s(14.44%)   p(85.48%)   d(0.08%)
5.  (1.95820) BD (1) V  1- O  5
    (27.98%) 0.5289* V  1  s(21.37%)   p(0.43%)    d(77.98%)   f(0.23%)
    (72.02%) 0.8487* O  5  s(11.01%)   p(88.84%)   d(0.15%)
6.  (1.97741) BD (2) V  1- O  5
    (15.93%) 0.3992* V  1  s(0.82%)    p(2.55%)    d(96.41%)   f(0.23%)
    (84.07%) 0.9169* O  5  s(0.54%)    p(99.39%)   d(0.07%)
7.  (1.90309) BD (3) V  1- O  5
    (16.87%) 0.4107* V  1  s(0.00%)    p(32.17%)   d(67.23%)   f(0.60%)
    (83.13%) 0.9118* O  5  s(0.11%)    p(99.81%)   d(0.08%)
23. (1.97711) LP (1) O  2  s(88.35%)   p(11.65%)   d(0.00%)
24. (1.71275) LP (2) O  2  s(0.55%)    p(99.38%)   d(0.07%)
25. (1.97432) LP (1) O  3  s(61.37%)   p(38.59%)   d(0.04%)
26. (1.88058) LP (2) O  3  s(0.34%)    p(99.59%)   d(0.07%)
27. (1.97432) LP (1) O  4  s(61.37%)   p(38.59%)   d(0.04%)
28. (1.88058) LP (2) O  4  s(0.34%)    p(99.59%)   d(0.07%)
29. (1.97711) LP (1) O  5  s(88.35%)   p(11.65%)   d(0.00%)
=======================================================================
```

Second order perturbation theory analysis of Fock-matrix for *anti*/*syn*-dihydrogen orthovanadate in NBO-basis(threshold for printing: 0.50 kcal/mol)

Donor NBO (i)	Acceptor NBO (j)	kcal/mol	a.u.	a.u.
23. LP (1) O 2	92. BD*(1) V 1- O 2	0.83	1.04	0.027
23. LP (1) O 2	94. BD*(1) V 1- O 3	3.72	1.10	0.059
23. LP (1) O 2	95. BD*(1) V 1- O 4	2.46	1.11	0.048
23. LP (1) O 2	96. BD*(1) V 1- O 5	1.52	1.05	0.037
23. LP (1) O 2	97. BD*(2) V 1- O 5	4.69	0.91	0.063
24. LP (2) O 2	94. BD*(1) V 1- O 3	1.91	0.42	0.026
24. LP (2) O 2	96. BD*(1) V 1- O 5	9.93	0.37	0.057
24. LP (2) O 2	97. BD*(2) V 1- O 5	53.22	0.23	0.100
25. LP (1) O 3	95. BD*(1) V 1- O 4	1.62	0.85	0.034
25. LP (1) O 3	96. BD*(1) V 1- O 5	2.91	0.79	0.044
25. LP (1) O 3	98. BD*(3) V 1- O 5	3.32	0.80	0.047
26. LP (2) O 3	92. BD*(1) V 1- O 2	4.50	0.40	0.038
26. LP (2) O 3	93. BD*(2) V 1- O 2	0.98	0.42	0.018
26. LP (2) O 3	95. BD*(1) V 1- O 4	2.30	0.47	0.029
26. LP (2) O 3	96. BD*(1) V 1- O 5	1.88	0.41	0.025
26. LP (2) O 3	97. BD*(2) V 1- O 5	3.87	0.27	0.031
26. LP (2) O 3	98. BD*(3) V 1- O 5	0.83	0.42	0.017
27. LP (1) O 4	92. BD*(1) V 1- O 2	2.89	0.78	0.043
27. LP (1) O 4	93. BD*(2) V 1- O 2	3.33	0.80	0.047
27. LP (1) O 4	94. BD*(1) V 1- O 3	1.63	0.84	0.034
28. LP (2) O 4	92. BD*(1) V 1- O 2	2.91	0.40	0.030
28. LP (2) O 4	93. BD*(2) V 1- O 2	0.71	0.42	0.015
28. LP (2) O 4	94. BD*(1) V 1- O 3	1.92	0.46	0.027
28. LP (2) O 4	96. BD*(1) V 1- O 5	3.31	0.41	0.033
28. LP (2) O 4	97. BD*(2) V 1- O 5	5.20	0.27	0.035
28. LP (2) O 4	98. BD*(3) V 1- O 5	0.85	0.42	0.017
29. LP (1) O 5	92. BD*(1) V 1- O 2	1.19	1.04	0.032
29. LP (1) O 5	94. BD*(1) V 1- O 3	1.98	1.10	0.043
29. LP (1) O 5	95. BD*(1) V 1- O 4	3.96	1.11	0.061
29. LP (1) O 5	96. BD*(1) V 1- O 5	1.14	1.05	0.032

Natural bond orbital (NBO)-energies

NBO	Occupancy	Energy
1. BD (1) V 1- O 2	1.94315	-0.32312
2. BD (2) V 1- O 2	1.90287	-0.08688
3. BD (1) V 1- O 3	1.94623	-0.29347
4. BD (1) V 1- O 4	1.94221	-0.29244
5. BD (1) V 1- O 5	1.95820	-0.32890
6. BD (2) V 1- O 5	1.97741	-0.12384
7. BD (3) V 1- O 5	1.90309	-0.08702
8. BD (1) O 3- H 6	1.98982	-0.54614
9. BD (1) O 4- H 7	1.98982	-0.54614
23. LP (1) O 2	1.97711	-0.74395
24. LP (2) O 2	1.71275	-0.06458
25. LP (1) O 3	1.97432	-0.48421
26. LP (2) O 3	1.88058	-0.10394
27. LP (1) O 4	1.97432	-0.48421
28. LP (2) O 4	1.88058	-0.10394
29. LP (1) O 5	1.97711	-0.74396

7.4.2 Monohydrated dihydrogen orthovanadate – adduct 2a

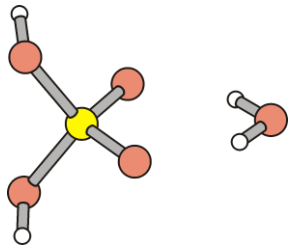

Figure S16. Minimum structure of hydrogen-bonded water to C_2-symmetric dihydrogen orthovanadate.

B3LYP/6-311++G//B3LYP/6-311++G****

Standard orientation:

Center Number	Atomic Number	Atomic Type	Coordinates (Angstroms) X	Y	Z
1	23	0	0.444676	0.000000	0.000000
2	8	0	-0.485920	0.349887	1.287618
3	8	0	1.517362	-1.460506	0.382292
4	8	0	-0.485920	-0.349889	-1.287617
5	8	0	1.517361	1.460507	-0.382292
6	1	0	1.588296	2.079483	0.349977
7	1	0	1.588300	-2.079478	-0.349981
8	1	0	-2.489382	-0.187680	-0.718077
9	8	0	-3.116056	0.000000	0.000000
10	1	0	-2.489383	0.187680	0.718078

```
Zero-point correction=                          0.057388 (Hartree/Particle)
Thermal correction to Energy=                   0.067005
Thermal correction to Enthalpy=                 0.067949
Thermal correction to Gibbs Free Energy=        0.022600
Sum of electronic and zero-point Energies=          -1322.878822
Sum of electronic and thermal Energies=             -1322.869205
Sum of electronic and thermal Enthalpies=           -1322.868261
Sum of electronic and thermal Free Energies=        -1322.913610

Version=AM64L-G03RevE.01\State=1-A\HF-1322.93621\RMSD=3.467e-09\
RMSF=1.247e-07\PG=C01 [X(H4O5V1)]\NImag=0\\@.
```

7.4.3 Methanol bonding to dihydrogen orthovanadate – adduct 2b

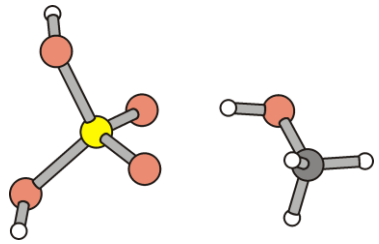

Figure S17. Minimum structure of hydrogen-bonded methanol to C_2-symmetric dihydrogen orthovanadate.

B3LYP/6-311++G//B3LYP/6-311++G****

Standard orientation:

Center Number	Atomic Number	Atomic Type	Coordinates (Angstroms) X	Y	Z
1	23	0	-0.923021	-0.020620	0.037372
2	8	0	-0.510643	-0.869961	1.348094
3	8	0	0.387731	0.552947	-0.759980
4	8	0	-1.899025	-1.117719	-1.091083
5	8	0	-1.981094	1.408670	0.553716
6	1	0	-2.248951	-1.895909	-0.648011
7	1	0	-1.816889	2.197096	0.027766
8	8	0	3.108540	0.631411	-0.477732
9	6	0	3.341627	-0.490602	0.348764
10	1	0	2.139354	0.665644	-0.646226
11	1	0	4.362815	-0.417998	0.739913
12	1	0	2.642983	-0.533706	1.193127
13	1	0	3.256343	-1.440026	-0.202831

```
Zero-point correction=                          0.085170 (Hartree/Particle)
Thermal correction to Energy=                   0.096622
Thermal correction to Enthalpy=                 0.097566
Thermal correction to Gibbs Free Energy=        0.044671
Sum of electronic and zero-point Energies=          -1362.155320
Sum of electronic and thermal Energies=             -1362.143868
Sum of electronic and thermal Enthalpies=           -1362.142924
Sum of electronic and thermal Free Energies=        -1362.195819

Version=AM64L-G03RevE.01\State=1-A\HF-1362.24049\RMSD=5.429e-09\
RMSF=3.300e-07\PG=C01 [X(C1H6O5V1)]\NImag=0\\@.
```

7.4.4 Imidazole bonding to dihydrogen orthovanadate – adduct 2c

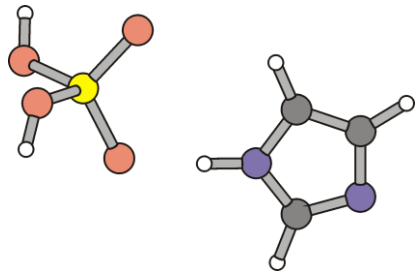

Figure S18. Minimum structure of hydrogen-bonded imidazole to C_2-symmetric dihydrogen orthovanadate.

B3LYP/6-311++G//B3LYP/6-311++G****

Standard orientation:

Center Number	Atomic Number	Atomic Type	Coordinates (Angstroms) X	Y	Z
1	8	0	0.660647	-1.114270	0.156302
2	23	0	1.837696	0.020735	-0.004762
3	8	0	2.895688	0.034124	1.507995
4	8	0	1.196173	1.487845	-0.206091
5	8	0	2.879538	-0.392138	-1.472844
6	1	0	2.841525	-1.321931	-1.716368
7	1	0	3.125690	0.915203	1.816287
8	6	0	-3.121572	-1.104861	0.188484
9	7	0	-1.991446	-0.364832	0.057674
10	6	0	-2.386011	0.931266	-0.157447
11	6	0	-3.761703	0.906952	-0.145251
12	7	0	-4.218510	-0.374894	0.072465
13	1	0	-3.095041	-2.169295	0.367612
14	1	0	-4.444862	1.732581	-0.279630
15	1	0	-1.659278	1.715744	-0.292657
16	1	0	-1.006008	-0.695754	0.105694

```
Zero-point correction=                          0.104533 (Hartree/Particle)
Thermal correction to Energy=                   0.116644
Thermal correction to Enthalpy=                 0.117588
Thermal correction to Gibbs Free Energy=        0.063082
Sum of electronic and zero-point Energies=          -1472.665696
Sum of electronic and thermal Energies=             -1472.653585
Sum of electronic and thermal Enthalpies=           -1472.652641
Sum of electronic and thermal Free Energies=        -1472.707146

Version=AM64L-G03RevE.01\State=1-A\HF-1472.7702285\RMSD=3.761e-09\
RMSF=2.853e-07\PG=C01 [X(C3H6N2O4V1)]\NImag=0\\@.
```

7.4.5 Methylamine bonding to dihydrogen orthovanadate – adduct 2d

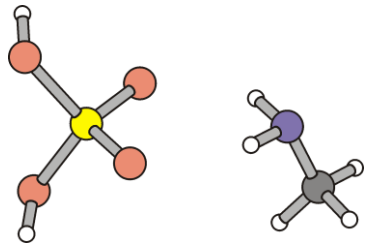

Figure S19. Minimum structure of hydrogen-bonded methylamine to the *anti*/*syn*-conformer of dihydrogen orthovanadate.

B3LYP/6-311++G//B3LYP/6-311++G****

Standard orientation:

Center Number	Atomic Number	Atomic Type	Coordinates (Angstroms) X	Y	Z
1	23	0	0.919377	0.012313	0.001333
2	8	0	0.023066	0.045269	1.356918
3	8	0	0.026347	-0.440454	-1.279208
4	8	0	1.611675	1.708913	-0.298702
5	8	0	2.319179	-1.187953	0.212502
6	1	0	1.620032	2.250125	0.495989
7	1	0	2.495935	-1.695384	-0.584813
8	7	0	-2.793326	-0.754907	0.121105
9	6	0	-3.612118	0.438444	-0.088727
10	1	0	-2.146504	-0.857440	-0.660367
11	1	0	-4.272239	0.592473	0.772685
12	1	0	-3.041163	1.368986	-0.241824
13	1	0	-4.256115	0.297896	-0.964420
14	1	0	-2.161763	-0.592359	0.904638

Zero-point correction= 0.097723 (Hartree/Particle)
Thermal correction to Energy= 0.109517
Thermal correction to Enthalpy= 0.110462
Thermal correction to Gibbs Free Energy= 0.058200
Sum of electronic and zero-point Energies= -1342.262575
Sum of electronic and thermal Energies= -1342.250780
Sum of electronic and thermal Enthalpies= -1342.249836
Sum of electronic and thermal Free Energies= -1342.302097

Version=AM64L-G03RevE.01\State=1-A\HF-1342.3602975\RMSD=7.104e-09\
RMSF=6.498e-07\PG=C01 [X(C1H7N1O4V1)]\NImag=0\\@.

7.4.6 Methylammonium bonding to dihydrogen orthovanadate – adduct 2e

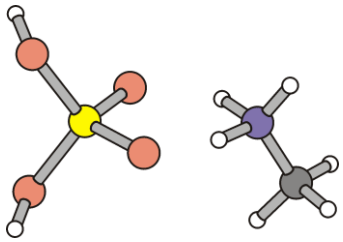

Figure S20. Minimum structure of hydrogen-bonded methylammonium to C_2-symmetric dihydrogen orthovanadate.

B3LYP/6-311++G//B3LYP/6-311++G****

Standard orientation:

Center Number	Atomic Number	Atomic Type	Coordinates (Angstroms) X	Y	Z
1	23	0	-0.878815	0.020906	0.003199
2	8	0	0.143429	-0.059525	-1.293430
3	8	0	0.031991	-0.325730	1.312609
4	8	0	-1.548297	1.693966	0.191215
5	8	0	-2.205758	-1.190773	-0.207478
6	1	0	-1.775293	2.192450	-0.600792
7	1	0	-2.570753	-1.635916	0.563884
8	7	0	2.331234	-0.617243	-0.042042
9	6	0	3.348529	0.458438	0.040674
10	1	0	1.707071	-0.642857	0.799174
11	1	0	3.901685	0.511649	-0.896252
12	1	0	2.830568	1.401181	0.207985
13	1	0	4.033135	0.267849	0.866738
14	1	0	1.567357	-0.412623	-0.789195
15	1	0	2.738255	-1.536005	-0.198208

Zero-point correction= 0.111248 (Hartree/Particle)
Thermal correction to Energy= 0.122336
Thermal correction to Enthalpy= 0.123280
Thermal correction to Gibbs Free Energy= 0.073320
Sum of electronic and zero-point Energies= -1342.777327
Sum of electronic and thermal Energies= -1342.766238
Sum of electronic and thermal Enthalpies= -1342.765294
Sum of electronic and thermal Free Energies= -1342.815254

Version=AM64L-G03RevE.01\State=1-A\HF-1342.8885745\RMSD=4.822e-09\
RMSF=3.971e-07\PG=C01 [X(C1H8N1O4V1)]\NImag=0\\@.

7.4.7 *N*-Methylguanidinium bonding to dihydrogen orthovanadate – adduct 2f

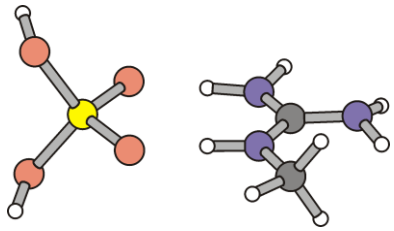

Figure S21. Minimum structure of hydrogen bonded *N*-methylguanidinium to C_2-symmetric dihydrogen orthovanadate.

B3LYP/6-311++G//B3LYP/6-311++G****

Standard orientation:

Center Number	Atomic Number	Atomic Type	Coordinates (Angstroms) X	Y	Z
1	23	0	1.765765	0.011345	0.001388
2	8	0	0.645082	1.208646	-0.048386
3	8	0	0.991629	-1.431463	0.015108
4	8	0	2.833083	0.080849	-1.464169
5	8	0	2.756693	0.211070	1.508129
6	1	0	3.001084	0.941941	-1.860308
7	1	0	3.111606	-0.581282	1.923834
8	7	0	-1.669541	-1.600922	-0.086039
9	6	0	-2.459642	-0.531632	-0.018291
10	1	0	-2.075808	-2.516445	0.015926
11	7	0	-1.959857	0.693002	-0.005691
12	1	0	-0.616471	-1.532295	-0.051343
13	7	0	-3.811053	-0.711309	0.061985
14	6	0	-2.767599	1.900580	0.048707
15	1	0	-0.913173	0.833881	-0.024015
16	1	0	-4.417519	0.075659	-0.098108
17	1	0	-4.192427	-1.609964	-0.184318
18	1	0	-2.082934	2.746601	0.059815
19	1	0	-3.414681	2.004106	-0.830297
20	1	0	-3.377556	1.944965	0.957160

Zero-point correction= 0.148997 (Hartree/Particle)
Thermal correction to Energy= 0.163451
Thermal correction to Enthalpy= 0.164395
Thermal correction to Gibbs Free Energy= 0.107069
Sum of electronic and zero-point Energies= -1491.628052
Sum of electronic and thermal Energies= -1491.613597
Sum of electronic and thermal Enthalpies= -1491.612653
Sum of electronic and thermal Free Energies= -1491.669979

Version=AM64L-G03RevE.01\State=1-A\HF-1491.7770486\RMSD=5.717e-09\
RMSF=6.117e-07\PG=C01 [X(C2H10N3O4V1)]\NImag=0\\@.

7.5 Binding more than one amino acid side chain mimic to orthovanadium compounds

7.5.1 Hydrogen bonding of *N*-methylguanidinium and methanol – adduct $1g_2$

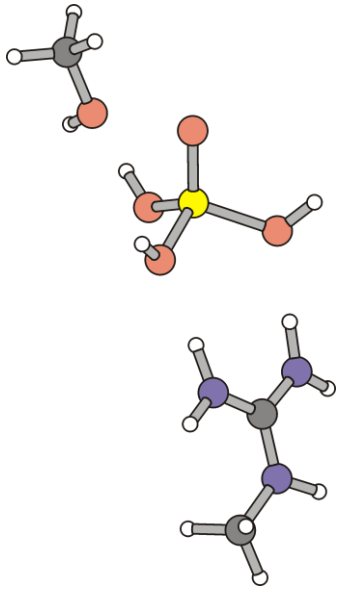

Figure S22. Minimum structure of the hydrogen-bonded adduct of the all-*syn* conformer of orthovanadium acid with *N*-methylguanidium (chelated mode of bonding) and methanol (at the distal hydroxy group).

(*i*) B3LYP/6-311++G**//B3LYP/6-311++G**

```
Zero-point correction=                          0.215397 (Hartree/Particle)
Thermal correction to Energy=                   0.235179
Thermal correction to Enthalpy=                 0.236123
Thermal correction to Gibbs Free Energy=        0.162982
Sum of electronic and zero-point Energies=          -1607.741218
Sum of electronic and thermal Energies=             -1607.721436
Sum of electronic and thermal Enthalpies=           -1607.720492
Sum of electronic and thermal Free Energies=        -1607.793633

Version=AM64L-G03RevE.01\State=1-A\HF=-1607.9566152\RMSD=8.992e-09\
RMSF=9.671e-07\PG=C01 [X(C3H15N3O5V1)]\NImag=0\\@.
```

Standard orientation:

Center Number	Atomic Number	Atomic Type	Coordinates (Angstroms) X	Y	Z
1	1	0	1.787324	-0.257571	-1.069822
2	7	0	2.774167	-0.030562	-0.916414
3	6	0	3.282698	0.188386	0.296282
4	7	0	2.549232	-0.047250	1.389043
5	7	0	4.536705	0.647893	0.426230
6	1	0	3.356521	0.061639	-1.732300
7	6	0	5.408421	1.022632	-0.686902
8	1	0	4.932559	0.655439	1.353261
9	1	0	2.865118	0.280992	2.287675
10	1	0	1.613623	-0.461367	1.348269
11	1	0	4.926544	1.769533	-1.321693
12	1	0	6.311075	1.467508	-0.273364
13	1	0	5.700445	0.153692	-1.283776
14	23	0	-1.151504	-0.677471	-0.067896
15	8	0	-2.289561	-1.725383	-0.292444
16	8	0	-0.000941	-0.662963	-1.472248
17	8	0	-1.820317	0.894668	0.167170
18	8	0	-0.121518	-1.133570	1.354544
19	1	0	-0.171980	-1.204462	-2.252499
20	1	0	-0.318118	-1.918619	1.880227
21	8	0	-4.325994	1.619693	0.344738
22	6	0	-5.454012	0.963121	-0.267492
23	1	0	-5.177751	-0.082942	-0.386853
24	1	0	-5.675637	1.395092	-1.246321
25	1	0	-6.330661	1.029908	0.379908
26	1	0	-4.527176	2.546854	0.507926
27	1	0	-2.784016	1.171168	0.213563

7.5.2 Hydrogen bonding of *N*-methylguanidinium and imidazolium – adduct $2h_2$

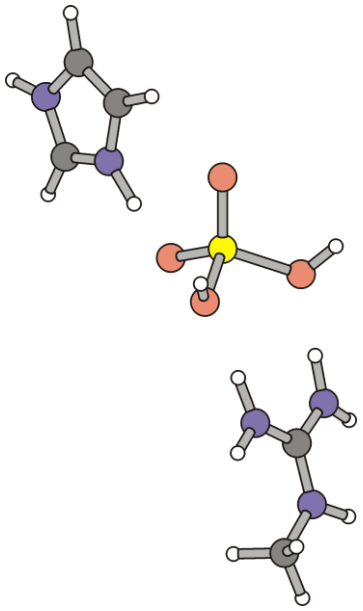

Figure S23. Minimum structure of the hydrogen-bonded adduct of the all-*syn* conformer of dihydrogen orthovanadate with *N*-methylguanidium (chelated mode of bonding) and imidazolium.

(*i*) B3LYP/6-311++G**//B3LYP/6-311++G**

```
Zero-point correction=                          0.235277 (Hartree/Particle)
Thermal correction to Energy=                   0.255197
Thermal correction to Enthalpy=                 0.256141
Thermal correction to Gibbs Free Energy=        0.183091
Sum of electronic and zero-point Energies=          -1718.255093
Sum of electronic and thermal Energies=             -1718.235173
Sum of electronic and thermal Enthalpies=           -1718.234229
Sum of electronic and thermal Free Energies=        -1718.307279

Version=AM64L-G03RevE.01\State=1-A\HF=-1718.4903698\RMSD=9.911e-09\
RMSF=2.767e-07\PG=C01 [X(C5H15N5O4V1)]\NImag=0\\@.
```

Standard orientation:

Center Number	Atomic Number	Atomic Type	Coordinates (Angstroms) X	Y	Z
1	23	0	-0.261318	-0.812446	-0.059770
2	8	0	-1.386390	-1.919883	-0.280376
3	8	0	0.923902	-0.759321	-1.478775
4	8	0	-0.992629	0.653687	0.139351
5	8	0	0.805833	-1.202212	1.397688
6	1	0	0.830447	-1.419648	-2.174147
7	1	0	-2.464766	0.761878	0.098259
8	1	0	0.700463	-2.055625	1.832290
9	1	0	2.567517	-0.228865	-1.081659
10	7	0	3.536100	0.092896	-0.919261
11	6	0	4.040496	0.302657	0.294389
12	7	0	3.352280	-0.037145	1.387141
13	7	0	5.258866	0.860788	0.428588
14	1	0	4.093946	0.291465	-1.732940
15	6	0	6.091822	1.316889	-0.680891
16	1	0	5.664516	0.865445	1.350734
17	1	0	3.668725	0.277948	2.290058
18	1	0	2.423751	-0.487562	1.351616
19	1	0	5.560877	2.052798	-1.289454
20	1	0	6.972824	1.801928	-0.265363
21	1	0	6.426217	0.485398	-1.308768
22	7	0	-3.558499	0.746451	0.053323
23	6	0	-4.320039	-0.385473	-0.150207
24	6	0	-5.628083	-0.003670	-0.142208
25	7	0	-5.628896	1.363434	0.067911
26	6	0	-4.361331	1.791510	0.182846
27	1	0	-3.856234	-1.349037	-0.280480
28	1	0	-6.536423	-0.567300	-0.264053
29	1	0	-6.447400	1.952380	0.126739
30	1	0	-4.056023	2.810453	0.351286

7.5.3 Hydrogen bonding of *N*-methylguanidinium and methylammonium – adduct $2i_2$

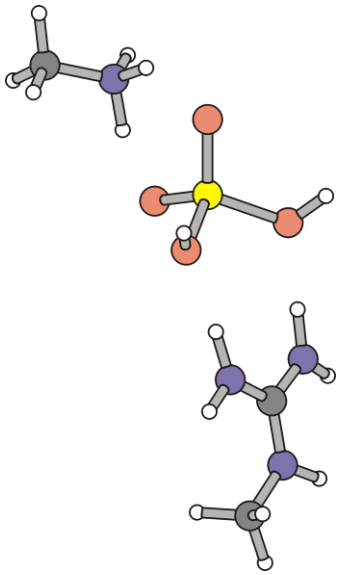

Figure S24. Minimum structure of the hydrogen-bonded adduct of the all-*syn* conformer of dihydrogen orthovanadate with *N*-methylguanidium (chelated mode of bonding) and methylammonium.

(*i*) B3LYP/6-311++G**//B3LYP/6-311++G**

```
Zero-point correction=                          0.230915 (Hartree/Particle)
Thermal correction to Energy=                   0.250018
Thermal correction to Enthalpy=                 0.250962
Thermal correction to Gibbs Free Energy=        0.181405
Sum of electronic and zero-point Energies=          -1587.867267
Sum of electronic and thermal Energies=             -1587.848165
Sum of electronic and thermal Enthalpies=           -1587.847221
Sum of electronic and thermal Free Energies=        -1587.916778

Version=AM64L-G03RevE.01\State=1-A\HF=-1588.0981825\RMSD=3.534e-09\
RMSF=1.551e-07\PG=C01 [X(C3H16N4O4V1)]\NImag=0\\@.
```

Standard orientation:

Center Number	Atomic Number	Atomic Type	Coordinates (Angstroms) X	Y	Z
1	1	0	1.647223	-0.649604	0.902558
2	7	0	2.646906	-0.708331	0.659011
3	6	0	3.229791	0.098836	-0.225387
4	7	0	2.569313	1.142605	-0.734379
5	7	0	4.498247	-0.131224	-0.610067
6	1	0	3.176693	-1.451708	1.082768
7	6	0	5.310291	-1.263097	-0.169599
8	1	0	4.947451	0.578030	-1.167191
9	1	0	2.956343	1.639712	-1.520490
10	1	0	1.603963	1.381701	-0.466299
11	1	0	4.816985	-2.209923	-0.401750
12	1	0	6.251872	-1.235642	-0.714220
13	1	0	5.535078	-1.210918	0.899908
14	23	0	-1.169689	0.405746	0.336495
15	8	0	-2.514057	0.859735	1.100339
16	8	0	-0.088864	-0.661816	1.382576
17	8	0	-1.644316	-0.405245	-1.003293
18	8	0	-0.100898	1.832198	-0.130920
19	1	0	-0.288668	-0.753688	2.320885
20	1	0	-3.279365	-0.431978	-1.098594
21	1	0	-0.281681	2.703876	0.238199
22	7	0	-4.282699	-0.257742	-0.779573
23	6	0	-5.029327	-1.525681	-0.531794
24	1	0	-4.130149	0.285454	0.086093
25	1	0	-4.472788	-2.113065	0.195560
26	1	0	-5.108590	-2.079544	-1.465295
27	1	0	-6.021153	-1.299007	-0.144646
28	1	0	-4.752170	0.337673	-1.460768

7.5.4 Hydrogen bonding of *N*-methylguanidinium and methanol – adduct *iso*-1g$_2$

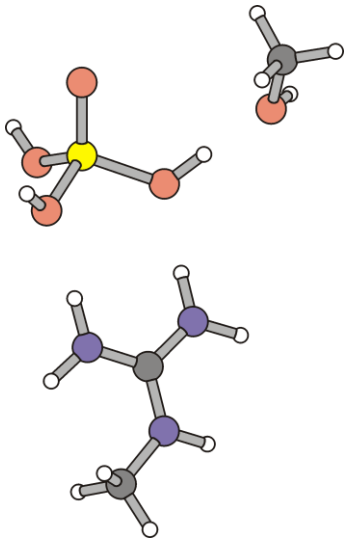

Figure S25. Minimum structure of the hydrogen-bonded adduct of the all-*syn* conformer of orthovanadium acid with *N*-methylguanidium (chelated mode of bonding) and methanol (at the proximal hydroxy group).

(*i*) B3LYP/6-311++G**//B3LYP/6-311++G**

```
Zero-point correction=                          0.215578 (Hartree/Particle)
Thermal correction to Energy=                   0.235249
Thermal correction to Enthalpy=                 0.236194
Thermal correction to Gibbs Free Energy=        0.164044
Sum of electronic and zero-point Energies=          -1607.741492
Sum of electronic and thermal Energies=             -1607.721821
Sum of electronic and thermal Enthalpies=           -1607.720877
Sum of electronic and thermal Free Energies=        -1607.793026

Version=AM64L-G03RevE.01\State=1-A\HF=-1607.9570702\RMSD=1.092e-09\
RMSF=1.205e-07\PG=C01 [X(C3H15N3O5V1)]\NImag=0\\@.
```

Standard orientation:

Center Number	Atomic Number	Atomic Type	Coordinates (Angstroms) X	Y	Z
1	1	0	-1.622126	-0.952712	-0.732360
2	7	0	-2.559227	-0.624438	-0.482201
3	6	0	-2.774617	0.573124	0.063841
4	7	0	-1.743480	1.352293	0.403710
5	7	0	-4.029725	1.006824	0.256308
6	1	0	-3.320408	-1.273890	-0.594005
7	6	0	-5.233271	0.300086	-0.181761
8	1	0	-4.151983	1.840606	0.809425
9	1	0	-1.903118	2.302641	0.697080
10	1	0	-0.778420	1.008921	0.433225
11	1	0	-5.397049	-0.617244	0.391308
12	1	0	-6.086806	0.955592	-0.021709
13	1	0	-5.179193	0.071073	-1.248104
14	23	0	1.381837	-1.189609	0.034945
15	8	0	2.777492	-1.255400	-0.663695
16	8	0	0.061152	-1.650112	-1.118912
17	8	0	1.338721	-2.256539	1.437477
18	8	0	1.010394	0.472305	0.524533
19	1	0	0.259246	-1.974048	-2.006050
20	1	0	2.043392	-2.842471	1.739811
21	1	0	1.670246	1.221756	0.467067
22	8	0	2.700699	2.495268	0.409786
23	6	0	3.578001	2.762378	-0.705044
24	1	0	3.137045	2.742859	1.231951
25	1	0	3.838138	3.822094	-0.738136
26	1	0	3.025056	2.502627	-1.605956
27	1	0	4.482404	2.152747	-0.647727

7.5.5 Hydrogen bonding of *N*-methylguanidinium and imidazole – adduct *iso*-1h$_2$

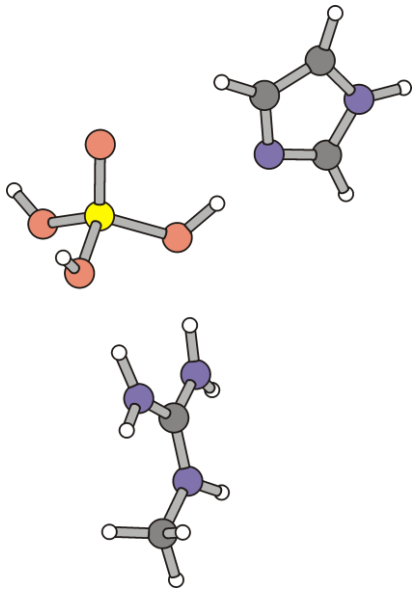

Figure S26. Minimum structure of the hydrogen-bonded adduct of the all-*syn* conformer of orthovanadium acid with *N*-methylguanidium (chelated mode of bonding) and imdiazole (at the proximal hydroxy group).

(*i*) B3LYP/6-311++G**//B3LYP/6-311++G**

```
Zero-point correction=                          0.233642 (Hartree/Particle)
Thermal correction to Energy=                   0.253762
Thermal correction to Enthalpy=                 0.254706
Thermal correction to Gibbs Free Energy=        0.180461
Sum of electronic and zero-point Energies=          -1718.253375
Sum of electronic and thermal Energies=             -1718.233254
Sum of electronic and thermal Enthalpies=           -1718.232310
Sum of electronic and thermal Free Energies=        -1718.306555

Version=AM64L-G03RevE.01\State=1-A\HF=-1718.4870164\RMSD=4.148e-09\
RMSF=2.413e-07\PG=C01 [X(C5H15N5O4V1)]\NImag=0\\@.
```

Standard orientation:

Center Number	Atomic Number	Atomic Type	Coordinates (Angstroms) X	Y	Z
1	1	0	2.372250	0.546544	-0.971709
2	7	0	3.105411	-0.169602	-0.897693
3	6	0	3.113578	-1.085542	0.069246
4	7	0	2.031363	-1.273621	0.831529
5	7	0	4.210291	-1.832086	0.282142
6	1	0	3.881341	-0.104122	-1.535594
7	6	0	5.488825	-1.651392	-0.403612
8	1	0	4.113282	-2.630416	0.889675
9	1	0	2.113282	-1.789246	1.693163
10	1	0	1.140960	-0.788754	0.658784
11	1	0	5.834372	-0.619670	-0.309510
12	1	0	6.223592	-2.295138	0.075692
13	1	0	5.428522	-1.931202	-1.459607
14	23	0	-0.243286	1.801954	0.108117
15	8	0	-1.556347	2.365552	-0.540158
16	8	0	1.144411	1.895004	-1.072022
17	8	0	0.170418	2.692620	1.581545
18	8	0	-0.440014	0.104618	0.467193
19	1	0	1.054570	2.401900	-1.887488
20	1	0	-0.301467	3.457455	1.931178
21	1	0	-1.372734	-0.408997	0.300826
22	7	0	-2.684750	-1.039454	0.059738
23	6	0	-3.140211	-2.201225	0.491639
24	7	0	-4.414183	-2.387461	0.075618
25	6	0	-4.792278	-1.283192	-0.659682
26	6	0	-3.707555	-0.453466	-0.660470
27	1	0	-2.599443	-2.914105	1.092574
28	1	0	-4.988423	-3.192913	0.275108
29	1	0	-5.770263	-1.190486	-1.099421
30	1	0	-3.593081	0.516325	-1.114890

7.5.6 Hydrogen bonding of *N*-methylguanidinium and methylamine – adduct *iso*-1i$_2$

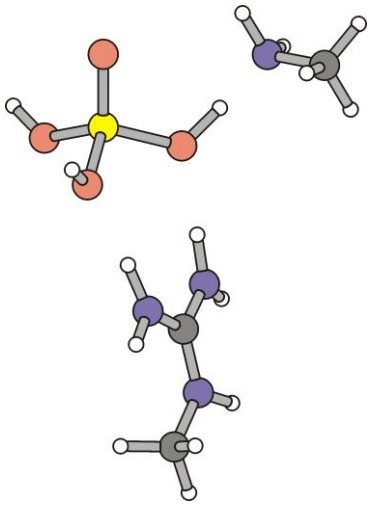

Figure S27. Minimum structure of the hydrogen-bonded adduct of the all-*syn* conformer of orthovanadium acid with *N*-methylguanidium (chelated mode of bonding), and methylamine (at the proximal hydroxy group).

(*i*) B3LYP/6-311++G**//B3LYP/6-311++G**

```
Zero-point correction=                          0.227308 (Hartree/Particle)
Thermal correction to Energy=                   0.246664
Thermal correction to Enthalpy=                 0.247608
Thermal correction to Gibbs Free Energy=        0.176352
Sum of electronic and zero-point Energies=          -1587.866699
Sum of electronic and thermal Energies=             -1587.847343
Sum of electronic and thermal Enthalpies=           -1587.846399
Sum of electronic and thermal Free Energies=        -1587.917655

Version=AM64L-G03RevE.01\State=1-A\HF=-1588.0940072\RMSD=4.289e-09\
RMSF=2.846e-07\PG=C01 [X(C3H16N4O4V1)]\NImag=0\\@.
```

Standard orientation:

Center Number	Atomic Number	Atomic Type	Coordinates (Angstroms) X	Y	Z
1	1	0	1.464345	-0.748129	1.001386
2	7	0	2.396472	-0.339211	0.866959
3	6	0	2.690692	0.450063	-0.165345
4	7	0	1.717538	0.944264	-0.938448
5	7	0	3.969400	0.762007	-0.431979
6	1	0	3.122886	-0.631372	1.499700
7	6	0	5.127371	0.211368	0.271151
8	1	0	4.135099	1.492774	-1.106155
9	1	0	1.949182	1.349576	-1.831366
10	1	0	0.721046	0.788610	-0.742732
11	1	0	5.108313	-0.880457	0.251085
12	1	0	6.025371	0.539637	-0.248201
13	1	0	5.182957	0.566676	1.304353
14	23	0	-1.430947	-1.156379	-0.009149
15	8	0	-2.868743	-1.188097	0.621262
16	8	0	-0.160922	-1.576007	1.228425
17	8	0	-1.313429	-2.263231	-1.385527
18	8	0	-1.076596	0.475965	-0.515652
19	1	0	-0.407017	-1.944757	2.084880
20	1	0	-1.997246	-2.870151	-1.692051
21	1	0	-1.843087	1.252590	-0.428893
22	7	0	-2.921454	2.223434	-0.293754
23	6	0	-2.623555	3.318836	0.659860
24	1	0	-3.741671	1.703615	0.012401
25	1	0	-3.458100	4.015077	0.769120
26	1	0	-1.749042	3.868627	0.310763
27	1	0	-2.394101	2.887980	1.634639
28	1	0	-3.150379	2.602324	-1.210013

7.5.7 Hydrogen bonding of imidazole and methanol – adduct 1j$_2$

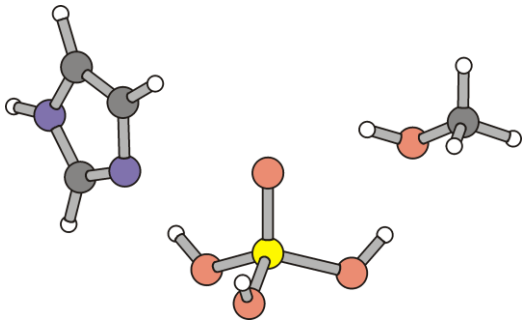

Figure S28. Minimum structure of the hydrogen-bonded adduct of the all-*syn* conformer of orthovanadium acid with methanol and imidazole.

(*i*) B3LYP/6-311++G**//B3LYP/6-311++G**

```
Zero-point correction=                          0.169971 (Hartree/Particle)
Thermal correction to Energy=                   0.186776
Thermal correction to Enthalpy=                 0.187720
Thermal correction to Gibbs Free Energy=        0.119669
Sum of electronic and zero-point Energies=          -1588.893308
Sum of electronic and thermal Energies=             -1588.876504
Sum of electronic and thermal Enthalpies=           -1588.875559
Sum of electronic and thermal Free Energies=        -1588.943610

Version=AM64L-G03RevE.01\State=1-A\HF=-1589.0632791\RMSD=5.554e-09\
RMSF=2.906e-07\PG=C01 [X(C4H11N2O5V1)]\NImag=0\\@.
```

Standard orientation:

Center Number	Atomic Number	Atomic Type	Coordinates (Angstroms) X	Y	Z
1	23	0	1.175969	-1.033743	0.047016
2	8	0	1.017999	0.266688	0.950361
3	8	0	1.807059	-2.390084	1.034997
4	8	0	-0.364566	-1.472264	-0.638663
5	8	0	2.328986	-0.632697	-1.232528
6	1	0	2.039877	-2.284089	1.962452
7	1	0	-1.220775	-0.971126	-0.480926
8	1	0	2.698946	0.274723	-1.216559
9	7	0	-2.657501	-0.094988	-0.191376
10	6	0	-2.783461	0.985806	0.654845
11	6	0	-4.071367	1.446043	0.629827
12	7	0	-4.738120	0.621312	-0.254429
13	6	0	-3.844756	-0.290568	-0.722848
14	1	0	-1.942802	1.355789	1.218836
15	1	0	-4.560752	2.257219	1.140972
16	1	0	-5.711353	0.683341	-0.508852
17	1	0	-4.101571	-1.059302	-1.434363
18	8	0	2.899510	2.005039	-0.508856
19	6	0	4.108110	2.504667	0.061836
20	1	0	2.258070	1.829812	0.194547
21	1	0	3.941462	3.457343	0.575884
22	1	0	4.804718	2.669229	-0.760229
23	1	0	4.553181	1.789750	0.763063

7.5.8 Hydrogen bonding of imidazole and methylamine – adduct $1k_2$

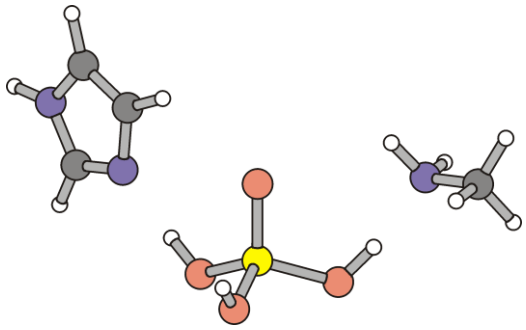

Figure S29. Minimum structure of the hydrogen-bonded adduct of the all-*syn* conformer of orthovanadium acid with imidazole and methylamine.

(*i*) B3LYP/6-311++G**//B3LYP/6-311++G**

```
Zero-point correction=                          0.182747 (Hartree/Particle)
Thermal correction to Energy=                   0.199725
Thermal correction to Enthalpy=                 0.200670
Thermal correction to Gibbs Free Energy=        0.131717
Sum of electronic and zero-point Energies=          -1569.012224
Sum of electronic and thermal Energies=             -1568.995246
Sum of electronic and thermal Enthalpies=           -1568.994301
Sum of electronic and thermal Free Energies=        -1569.063254

Version=AM64L-G03RevE.01\State=1-A\HF=-1569.1949709\RMSD=3.574e-09\
RMSF=7.641e-08\PG=C01 [X(C4H12N3O4V1)]\NImag=0\\@.
```

Standard orientation:

Center Number	Atomic Number	Atomic Type	Coordinates (Angstroms) X	Y	Z
1	23	0	1.047834	-1.009561	0.039595
2	8	0	0.746291	0.199365	1.024057
3	8	0	1.542344	-2.450284	0.998258
4	8	0	-0.394681	-1.375981	-0.888219
5	8	0	2.356327	-0.527116	-1.028192
6	1	0	1.566849	-2.425388	1.959371
7	1	0	-1.260211	-0.908479	-0.728237
8	1	0	2.768398	0.376892	-0.899340
9	7	0	-2.726039	-0.020804	-0.330842
10	6	0	-2.774646	0.922880	0.673438
11	6	0	-4.041512	1.430212	0.772454
12	7	0	-4.775583	0.775657	-0.197274
13	6	0	-3.938735	-0.088043	-0.834250
14	1	0	-1.896635	1.165717	1.250116
15	1	0	-4.477105	2.170928	1.420962
16	1	0	-5.754149	0.910591	-0.396546
17	1	0	-4.255908	-0.730120	-1.640812
18	7	0	3.312342	1.978369	-0.435494
19	6	0	4.684444	2.038043	0.093746
20	1	0	2.632177	2.194777	0.288211
21	1	0	4.961626	3.018059	0.500873
22	1	0	5.387289	1.781750	-0.701137
23	1	0	4.793463	1.292801	0.883660
24	1	0	3.179443	2.653398	-1.182079

7.5.9 Hydrogen bonding of methanol and methylamine – adduct $1m_2$

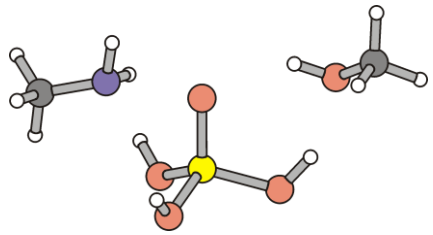

Figure S30. Minimum structure of the hydrogen-bonded adduct of the all-*syn* conformer of orthovanadium acid with methanol and methylamine.

(*i*) B3LYP/6-311++G**//B3LYP/6-311++G**

```
Zero-point correction=                          0.163683 (Hartree/Particle)
Thermal correction to Energy=                   0.179705
Thermal correction to Enthalpy=                 0.180649
Thermal correction to Gibbs Free Energy=        0.115566
Sum of electronic and zero-point Energies=          -1458.511142
Sum of electronic and thermal Energies=             -1458.495120
Sum of electronic and thermal Enthalpies=           -1458.494176
Sum of electronic and thermal Free Energies=        -1458.559259

Version=AM64L-G03RevE.01\State=1-A\HF=-1458.6748251\RMSD=2.586e-09\
RMSF=2.333e-07\PG=C01 [X(C2H12N1O5V1)]\NImag=0\\@.
```

Standard orientation:

Center Number	Atomic Number	Atomic Type	Coordinates (Angstroms) X	Y	Z
1	23	0	0.102374	0.837167	0.056230
2	8	0	0.395479	-0.284156	-1.034000
3	8	0	0.166933	2.460775	-0.699006
4	8	0	-1.472142	0.574772	0.756977
5	8	0	1.359692	0.687821	1.289947
6	1	0	0.422693	2.594704	-1.616790
7	1	0	-2.082979	-0.196043	0.524961
8	1	0	2.024642	-0.019029	1.150910
9	7	0	-3.118343	-1.476856	0.118024
10	6	0	-4.459088	-1.006262	-0.276058
11	1	0	-5.144213	-1.814489	-0.555787
12	1	0	-4.362119	-0.323595	-1.121751
13	1	0	-4.898048	-0.447505	0.551964
14	1	0	-3.176453	-2.110446	0.910039
15	1	0	-2.679315	-1.993664	-0.638676
16	8	0	2.794463	-1.449728	0.218905
17	6	0	4.108053	-1.452483	-0.339544
18	1	0	2.139091	-1.402416	-0.491619
19	1	0	4.269381	-2.332039	-0.971714
20	1	0	4.808687	-1.488971	0.494560
21	1	0	4.303230	-0.546775	-0.924544

7.5.10 Hydrogen bonding of *N*-methylguanidinium, imidazole, and methanol – adduct $\mathbf{1n_3}$

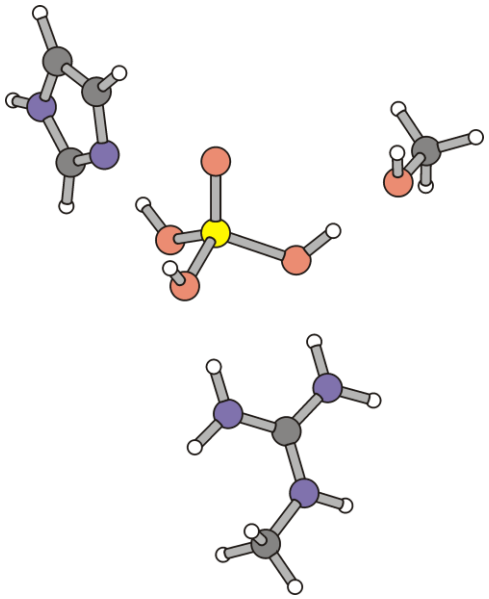

Figure S31. Minimum structure of the hydrogen-bonded adduct of the all-*syn* conformer of orthovanadium acid with *N*-methylguanidium (chelated mode of bonding), imidazole (at the distal hydroxy group) and methanol (at the proximal hydroxy group).

(*i*) B3LYP/6-311++G**//B3LYP/6-311++G**

```
Zero-point correction=                          0.287400 (Hartree/Particle)
Thermal correction to Energy=                   0.312232
Thermal correction to Enthalpy=                 0.313176
Thermal correction to Gibbs Free Energy=        0.224692
Sum of electronic and zero-point Energies=          -1833.984095
Sum of electronic and thermal Energies=             -1833.959263
Sum of electronic and thermal Enthalpies=           -1833.958319
Sum of electronic and thermal Free Energies=        -1834.046802

Version=AM64L-G03RevE.01\State=1-A\HF=-1834.2714948\RMSD=5.585e-09\
RMSF=2.307e-05\PG=C01 [X(C6H19N5O5V1)]\NImag=0\\@.
```

Standard orientation:

Center Number	Atomic Number	Atomic Type	Coordinates (Angstroms) X	Y	Z
1	6	0	-4.405627	-1.778094	-1.262331
2	7	0	-3.716592	-1.031863	-0.420560
3	6	0	-4.632311	-0.424689	0.414005
4	6	0	-5.893743	-0.815798	0.063765
5	7	0	-5.731063	-1.675452	-1.003209
6	8	0	-1.165780	-0.779517	-0.324370
7	23	0	-0.215972	0.186869	0.719683
8	8	0	0.878321	1.257146	-0.221888
9	8	0	-1.146591	1.036928	1.662210
10	8	0	0.911791	-0.871815	1.705285
11	8	0	0.742416	3.940942	-0.043967
12	6	0	0.012619	4.710367	-1.017635
13	7	0	3.348162	-1.585679	0.472308
14	6	0	4.018985	-0.797954	-0.367236
15	7	0	5.218144	-1.185840	-0.837837
16	6	0	5.921402	-2.398705	-0.426330
17	7	0	3.517260	0.383580	-0.732191
18	1	0	0.848322	-0.871807	2.666970
19	1	0	-2.220570	-0.881190	-0.366396
20	1	0	0.814376	2.242581	-0.143109
21	1	0	2.471524	-1.293232	0.926659
22	1	0	3.649711	-2.534474	0.620625
23	1	0	5.618239	-0.643276	-1.586678
24	1	0	4.083646	1.027830	-1.259970
25	1	0	2.547526	0.667633	-0.527176
26	1	0	5.416844	-3.303220	-0.779494
27	1	0	6.918268	-2.376345	-0.862109
28	1	0	6.029510	-2.433001	0.659938
29	1	0	-4.323569	0.243725	1.200502
30	1	0	-6.862373	-0.569809	0.463372
31	1	0	-6.468847	-2.147452	-1.503891
32	1	0	-3.995856	-2.389480	-2.050008
33	1	0	0.365604	5.744118	-1.034284
34	1	0	-1.061722	4.685877	-0.817740
35	1	0	0.206807	4.252542	-1.986309
36	1	0	0.589353	4.307549	0.833237

7.5.11 Hydrogen bonding of *N*-methylguanidinium, imidazole, and methanol – adduct *iso*-1n$_3$

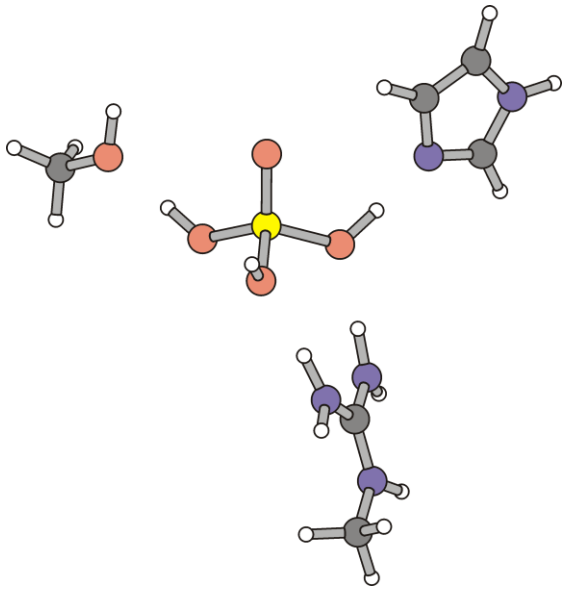

Figure S32. Minimum structure of the hydrogen-bonded adduct of the all-*syn* conformer of orthovanadium acid with *N*-methylguanidium (chelated mode of bonding), methanol (at the distal hydroxy group) and imidazole (at the proximal hydroxy group).

(*i*) B3LYP/6-311++G**//B3LYP/6-311++G**

```
Zero-point correction=                          0.287511 (Hartree/Particle)
Thermal correction to Energy=                   0.312443
Thermal correction to Enthalpy=                 0.313387
Thermal correction to Gibbs Free Energy=        0.224570
Sum of electronic and zero-point Energies=          -1833.982653
Sum of electronic and thermal Energies=             -1833.957721
Sum of electronic and thermal Enthalpies=           -1833.956777
Sum of electronic and thermal Free Energies=        -1834.045594

Version=AM64L-G03RevE.01\State=1-A\HF=-1834.2701636\RMSD=2.942e-09\
RMSF=1.789e-07\PG=C01 [X(C6H19N5O5V1)]\NImag=0 \\@.
```

Standard orientation:

Center Number	Atomic Number	Atomic Type	Coordinates (Angstroms) X	Y	Z
1	1	0	-2.497112	0.277247	1.187720
2	7	0	-3.395202	-0.114032	0.871091
3	6	0	-3.568487	-0.615494	-0.350208
4	7	0	-2.517539	-0.857999	-1.138630
5	7	0	-4.807742	-0.886414	-0.797862
6	1	0	-4.180785	-0.027452	1.494282
7	6	0	-6.040761	-0.575504	-0.077802
8	1	0	-4.883021	-1.431395	-1.642132
9	1	0	-2.662230	-1.024254	-2.121603
10	1	0	-1.543783	-0.740396	-0.820462
11	1	0	-6.075305	0.482879	0.189735
12	1	0	-6.879974	-0.780212	-0.739582
13	1	0	-6.156832	-1.191434	0.819149
14	23	0	0.451615	0.965843	0.618399
15	8	0	1.793909	0.831846	1.425834
16	8	0	-0.974388	1.058383	1.763510
17	8	0	0.484157	2.378948	-0.397879
18	8	0	0.166980	-0.483254	-0.348888
19	1	0	-0.820677	1.167573	2.708790
20	1	0	1.197151	3.070007	-0.422010
21	1	0	0.838812	-1.278244	-0.343168
22	8	0	2.366276	4.268008	-0.433060
23	6	0	2.412458	5.337130	-1.393362
24	1	0	1.387345	5.507376	-1.718314
25	1	0	3.023892	5.066845	-2.258371
26	1	0	2.797170	6.251204	-0.934931
27	7	0	1.911753	-2.428847	-0.279719
28	6	0	2.060250	-3.493384	-1.044722
29	7	0	3.145833	-4.206946	-0.658517
30	6	0	3.722978	-3.558150	0.413294
31	6	0	2.945802	-2.456441	0.635510
32	1	0	1.426988	-3.778856	-1.869201
33	1	0	3.475386	-5.060057	-1.084335
34	1	0	4.607520	-3.927953	0.902567
35	1	0	3.060564	-1.684052	1.377761
36	1	0	3.249116	4.086062	-0.096005

7.5.12 Hydrogen bonding of *N*-methylguanidinium, imidazole, and methanol – adduct $\mathbf{1o_3}$

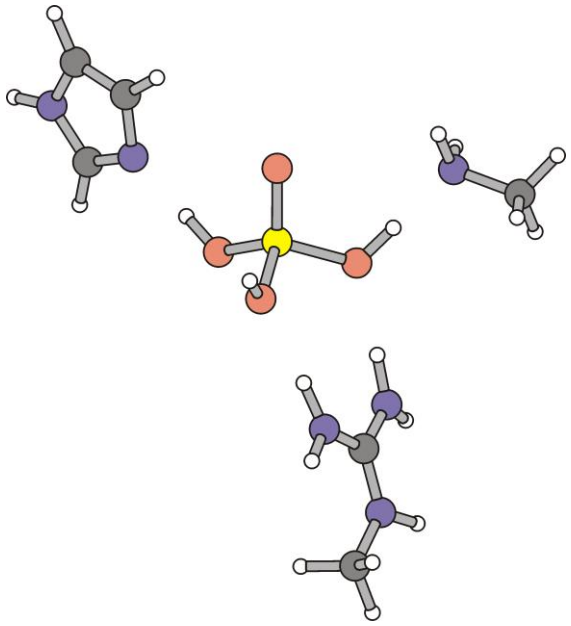

Figure S33. Minimum structure of the hydrogen-bonded adduct of the all-*syn* conformer of orthovanadium acid with *N*-methylguanidium (chelated mode of bonding), imidazole (at the distal hydroxy group) and methylamine (at the proximal hydroxy group).

(*i*) B3LYP/6-311++G**//B3LYP/6-311++G**

```
Zero-point correction=                          0.300292 (Hartree/Particle)
Thermal correction to Energy=                   0.324894
Thermal correction to Enthalpy=                 0.325838
Thermal correction to Gibbs Free Energy=        0.238063
Sum of electronic and zero-point Energies=          -1814.105930
Sum of electronic and thermal Energies=             -1814.081328
Sum of electronic and thermal Enthalpies=           -1814.080384
Sum of electronic and thermal Free Energies=        -1814.168159

Version=AM64L-G03RevE.01\State=1-A\HF=-1814.4062217\RMSD=4.564e-09\
RMSF=2.206e-07\PG=C01 [X(C6H20N6O4V1)]\NImag=0\\@.
```

Standard orientation:

Center Number	Atomic Number	Atomic Type	Coordinates (Angstroms) X	Y	Z
1	23	0	-0.257024	0.378195	0.566724
2	8	0	-1.161506	1.472690	1.253926
3	8	0	0.817641	-0.456221	1.801138
4	8	0	-1.231442	-0.778139	-0.247381
5	8	0	0.872730	1.164617	-0.561909
6	1	0	0.693145	-0.278349	2.739873
7	1	0	-2.275985	-0.846176	-0.279135
8	1	0	0.830982	2.191267	-0.670304
9	1	0	2.434258	-0.947852	1.190678
10	7	0	3.355973	-1.285181	0.876169
11	6	0	3.798098	-1.125061	-0.369782
12	7	0	3.155096	-0.322091	-1.221281
13	7	0	4.906266	-1.770961	-0.777959
14	1	0	3.893338	-1.827461	1.531927
15	6	0	5.654121	-2.733498	0.027342
16	1	0	5.301546	-1.493053	-1.662126
17	1	0	3.376462	-0.362962	-2.203228
18	1	0	2.328310	0.235232	-0.950376
19	1	0	5.002001	-3.538402	0.374054
20	1	0	6.423775	-3.175711	-0.602103
21	1	0	6.145649	-2.257433	0.881269
22	7	0	-3.814061	-0.949481	-0.312542
23	6	0	-4.703158	-0.120924	0.340637
24	6	0	-5.980987	-0.534427	0.088139
25	7	0	-5.856491	-1.635133	-0.734418
26	6	0	-4.535946	-1.850314	-0.950118
27	1	0	-4.365962	0.706853	0.942235
28	1	0	-6.937727	-0.159388	0.408294
29	1	0	-6.614060	-2.185688	-1.109355
30	1	0	-4.154458	-2.652670	-1.560847
31	7	0	0.644454	3.799357	-0.771451
32	6	0	1.796931	4.596812	-0.300603
33	1	0	-0.176384	3.999623	-0.204700
34	1	0	1.614229	5.675126	-0.327811
35	1	0	2.665231	4.375832	-0.923276
36	1	0	2.033557	4.310503	0.725120
37	1	0	0.401239	4.057557	-1.724346

7.5.13 Hydrogen bonding of *N*-methylguanidinium, imidazole, and methanol – adduct *iso*-1o$_3$

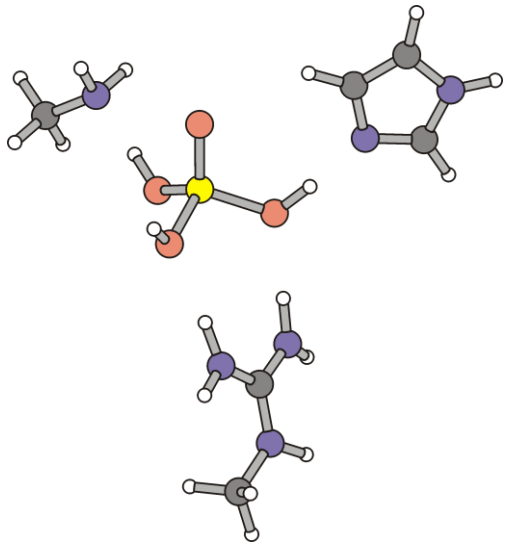

Figure S34. Minimum structure of the hydrogen-bonded adduct of the all-*syn* conformer of orthovanadium acid with *N*-methylguanidium (chelated mode of bonding), methylamine (at the distal hydroxy group) and imddidazole (at the proximal hydroxy group).

(*i*) B3LYP/6-311++G**//B3LYP/6-311++G**

```
Zero-point correction=                          0.300504 (Hartree/Particle)
Thermal correction to Energy=                   0.325036
Thermal correction to Enthalpy=                 0.325981
Thermal correction to Gibbs Free Energy=        0.238645
Sum of electronic and zero-point Energies=          -1814.106085
Sum of electronic and thermal Energies=             -1814.081553
Sum of electronic and thermal Enthalpies=           -1814.080609
Sum of electronic and thermal Free Energies=        -1814.167945

Version=AM64L-G03RevE.01\State=1-A\HF=-1814.4065894\RMSD=9.459e-09\
RMSF=2.448e-07\PG=C01 [X(C6H20N6O4V1)]\NImag=0\\@.
```

Standard orientation:

Center Number	Atomic Number	Atomic Type	Coordinates (Angstroms) X	Y	Z
1	1	0	-2.446145	0.135482	1.153307
2	7	0	-3.315075	-0.349643	0.885344
3	6	0	-3.470636	-0.950371	-0.292811
4	7	0	-2.422864	-1.150768	-1.095846
5	7	0	-4.691231	-1.364421	-0.681047
6	1	0	-4.091508	-0.287615	1.522625
7	6	0	-5.927204	-1.125229	0.060209
8	1	0	-4.737221	-1.969385	-1.485493
9	1	0	-2.577549	-1.409450	-2.057035
10	1	0	-1.454445	-0.916860	-0.820904
11	1	0	-6.060648	-0.058940	0.256056
12	1	0	-6.760774	-1.458315	-0.554934
13	1	0	-5.954693	-1.683549	1.000973
14	23	0	0.404167	1.042654	0.471925
15	8	0	1.779662	1.058338	1.242525
16	8	0	-0.997842	1.071181	1.658804
17	8	0	0.306088	2.395075	-0.588779
18	8	0	0.213369	-0.478236	-0.425826
19	1	0	-0.815526	1.177463	2.599024
20	1	0	1.008101	3.159521	-0.741071
21	1	0	0.936810	-1.209103	-0.380074
22	7	0	2.020961	4.317741	-0.974636
23	6	0	1.441671	5.638683	-0.642955
24	1	0	2.852595	4.143618	-0.415631
25	1	0	1.136856	5.640392	0.404151
26	1	0	0.553349	5.800890	-1.254313
27	1	0	2.139786	6.464103	-0.807819
28	7	0	2.130858	-2.288506	-0.248770
29	6	0	2.349639	-3.412584	-0.902862
30	7	0	3.503811	-3.989689	-0.485705
31	6	0	4.052586	-3.184305	0.490571
32	6	0	3.189188	-2.133383	0.625093
33	1	0	1.720493	-3.836996	-1.668721
34	1	0	3.893158	-4.853423	-0.831918
35	1	0	4.978994	-3.425445	0.982759
36	1	0	3.256522	-1.279447	1.278717
37	1	0	2.319108	4.295299	-1.946627

7.6 Vanadium bonding of amino acid side chain mimics

7.6.1 Methanol binding to vanadium in orthovanadium acid – adduct *iso*$_{trans}$-1b

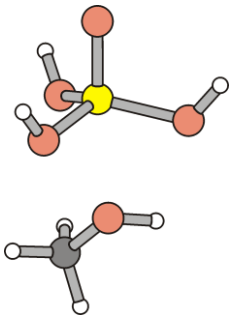

Figure S35. Minimum structure of the *trans*-adduct of methanol with the all-*syn* conformer of orthovanadium acid.

(*i*) B3LYP/6-311++G**//B3LYP/6-311++G**

Standard orientation:

Center Number	Atomic Number	Atomic Type	Coordinates (Angstroms) X	Y	Z
1	23	0	0.650067	-0.034050	-0.008808
2	8	0	2.185998	-0.293963	-0.226946
3	8	0	-0.119183	-1.030508	-1.298094
4	8	0	0.354859	-0.648014	1.649252
5	8	0	0.511947	1.757406	-0.248831
6	1	0	0.462669	-1.551057	-1.862849
7	1	0	1.096303	-1.038162	2.125662
8	1	0	1.319067	2.245260	-0.443723
9	8	0	-1.684328	0.559516	0.280137
10	6	0	-2.805475	-0.263396	-0.054824
11	1	0	-2.720727	-1.164799	0.550118
12	1	0	-2.790822	-0.541893	-1.111707
13	1	0	-3.742226	0.244742	0.192181
14	1	0	-1.737303	1.413952	-0.162301

```
Zero-point correction=                          0.098173 (Hartree/Particle)
Thermal correction to Energy=                   0.109254
Thermal correction to Enthalpy=                 0.110198
Thermal correction to Gibbs Free Energy=        0.061579
Sum of electronic and zero-point Energies=          -1362.659754
Sum of electronic and thermal Energies=             -1362.648674
Sum of electronic and thermal Enthalpies=           -1362.647729
Sum of electronic and thermal Free Energies=        -1362.696348

Version=AM64L-G03RevE.01\State=1-A\HF-1362.7579272\RMSD=6.477e-09\
RMSF=2.491e-07\PG=C01 [X(C1H7O5V1)]\NImag=0\\@.
```

(*ii*) NBO-analysis – B3LYP/6-31G*// B3LYP/6-311++G**

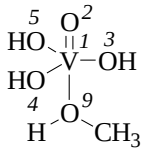

```
=======================================================================
No. (Occupancy) Bond orbital/ Coefficients/ Hybrids
=======================================================================
1.  (1.92350) BD (1) V  1- O  2
    (27.28%) 0.5223* V  1  s(29.46%)   p(0.18%)    d(70.08%)   f(0.29%)
    (72.72%) 0.8528* O  2  s(12.87%)   p(86.95%)   d(0.18%)
2.  (1.99048) BD (2) V  1- O  2
    (22.93%) 0.4789* V  1  s(0.00%)    p(0.81%)    d(98.99%)   f(0.20%)
    (77.07%) 0.8779* O  2  s(0.00%)    p(99.89%)   d(0.11%)
3.  (1.98934) BD (3) V  1- O  2
    (23.08%) 0.4804* V  1  s(0.10%)    p(0.81%)    d(98.89%)   f(0.20%)
    (76.92%) 0.8770* O  2  s(0.04%)    p(99.85%)   d(0.11%)
4.  (1.97619) BD (1) V  1- O  3
    (19.02%) 0.4361* V  1  s(23.95%)   p(0.34%)    d(75.56%)   f(0.15%)
    (80.98%) 0.8999* O  3  s(13.63%)   p(86.28%)   d(0.09%)
5.  (1.97667) BD (1) V  1- O  4
    (19.51%) 0.4417* V  1  s(22.94%)   p(0.37%)    d(76.54%)   f(0.15%)
    (80.49%) 0.8971* O  4  s(13.54%)   p(86.37%)   d(0.10%)
6.  (1.97797) BD (1) V  1- O  5
    (18.72%) 0.4327* V  1  s(22.62%)   p(0.33%)    d(76.91%)   f(0.14%)
    (81.28%) 0.9015* O  5  s(13.77%)   p(86.14%)   d(0.08%)
30. (1.97240) LP (1) O  2  s(87.10%)   p(12.90%)   d(0.00%)
31. (1.96123) LP (1) O  3  s(61.54%)   p(38.40%)   d(0.05%)
32. (1.82545) LP (2) O  3  s(0.01%)    p(99.92%)   d(0.07%)
33. (1.95927) LP (1) O  4  s(61.90%)   p(38.04%)   d(0.06%)
34. (1.81451) LP (2) O  4  s(0.00%)    p(99.92%)   d(0.08%)
35. (1.96185) LP (1) O  5  s(60.96%)   p(38.99%)   d(0.05%)
36. (1.83289) LP (2) O  5  s(0.01%)    p(99.93%)   d(0.07%)
37. (1.97500) LP (1) O  9  s(31.06%)   p(68.87%)   d(0.07%)
38. (1.93053) LP (2) O  9  s(17.50%)   p(82.46%)   d(0.04%)
=======================================================================
```

Second order perturbation theory analysis of Fock-matrix for adduct *iso*$_{trans}$-(**1b**) in NBO-basis(threshold for printing: 0.50 kcal/mol)

Donor NBO (i)	Acceptor NBO (j)	kcal/mol	a.u.	a.u.
30. LP (1) O 2	127. BD*(1) V 1- O 2	2.41	1.12	0.048
30. LP (1) O 2	130. BD*(1) V 1- O 3	1.60	1.03	0.038
30. LP (1) O 2	131. BD*(1) V 1- O 4	1.49	1.03	0.036
30. LP (1) O 2	132. BD*(1) V 1- O 5	1.48	1.03	0.036
31. LP (1) O 3	127. BD*(1) V 1- O 2	3.32	0.82	0.048
31. LP (1) O 3	128. BD*(2) V 1- O 2	2.49	0.63	0.036
31. LP (1) O 3	129. BD*(3) V 1- O 2	3.26	0.63	0.041
31. LP (1) O 3	131. BD*(1) V 1- O 4	1.51	0.73	0.031
31. LP (1) O 3	132. BD*(1) V 1- O 5	1.46	0.72	0.030
32. LP (2) O 3	128. BD*(2) V 1- O 2	1.34	0.24	0.016
32. LP (2) O 3	129. BD*(3) V 1- O 2	1.14	0.24	0.015
32. LP (2) O 3	131. BD*(1) V 1- O 4	10.34	0.34	0.053
32. LP (2) O 3	132. BD*(1) V 1- O 5	10.18	0.34	0.053
33. LP (1) O 4	127. BD*(1) V 1- O 2	3.14	0.81	0.046
33. LP (1) O 4	128. BD*(2) V 1- O 2	6.65	0.63	0.058
33. LP (1) O 4	130. BD*(1) V 1- O 3	1.62	0.73	0.032
33. LP (1) O 4	132. BD*(1) V 1- O 5	1.64	0.72	0.032
34. LP (2) O 4	129. BD*(3) V 1- O 2	2.67	0.24	0.023
34. LP (2) O 4	130. BD*(1) V 1- O 3	10.33	0.34	0.053
34. LP (2) O 4	132. BD*(1) V 1- O 5	11.38	0.34	0.055
35. LP (1) O 5	127. BD*(1) V 1- O 2	2.39	0.81	0.040
35. LP (1) O 5	128. BD*(2) V 1- O 2	0.70	0.63	0.019
35. LP (1) O 5	129. BD*(3) V 1- O 2	5.45	0.63	0.053
35. LP (1) O 5	130. BD*(1) V 1- O 3	1.50	0.73	0.031
35. LP (1) O 5	131. BD*(1) V 1- O 4	1.60	0.73	0.032
36. LP (2) O 5	128. BD*(2) V 1- O 2	2.00	0.24	0.020
36. LP (2) O 5	130. BD*(1) V 1- O 3	9.26	0.34	0.051
36. LP (2) O 5	131. BD*(1) V 1- O 4	10.38	0.34	0.054
37. LP (1) O 9	128. BD*(2) V 1- O 2	0.22	0.44	0.009
37. LP (1) O 9	129. BD*(3) V 1- O 2	0.13	0.44	0.007
37. LP (1) O 9	130. BD*(1) V 1- O 3	0.26	0.54	0.011
37. LP (1) O 9	131. BD*(1) V 1- O 4	0.07	0.54	0.006
37. LP (1) O 9	132. BD*(1) V 1- O 5	0.13	0.53	0.008
37. LP (1) O 9	134. BD*(1) O 4- H 7	0.15	0.96	0.011
38. LP (2) O 9	127. BD*(1) V 1- O 2	13.87	0.56	0.080
38. LP (2) O 9	128. BD*(2) V 1- O 2	0.10	0.37	0.005
38. LP (2) O 9	129. BD*(3) V 1- O 2	0.16	0.37	0.007
38. LP (2) O 9	130. BD*(1) V 1- O 3	0.30	0.47	0.011
38. LP (2) O 9	131. BD*(1) V 1- O 4	0.39	0.47	0.012
38. LP (2) O 9	132. BD*(1) V 1- O 5	0.26	0.47	0.010
38. LP (2) O 9	133. BD*(1) O 3- H 6	0.24	0.89	0.013
38. LP (2) O 9	134. BD*(1) O 4- H 7	0.11	0.89	0.009
38. LP (2) O 9	135. BD*(1) O 5- H 8	0.26	0.90	0.014

Natural bond orbital (NBO)-energies

NBO	Occupancy	Energy
1. BD (1) V 1- O 2	1.92350	-0.59962
2. BD (2) V 1- O 2	1.99048	-0.36174
3. BD (3) V 1- O 2	1.98934	-0.36233
4. BD (1) V 1- O 3	1.97619	-0.52391
5. BD (1) V 1- O 4	1.97667	-0.52323
6. BD (1) V 1- O 5	1.97797	-0.52148
30. LP (1) O 2	1.97240	-0.98485
31. LP (1) O 3	1.96123	-0.68412
32. LP (2) O 3	1.82545	-0.29847
33. LP (1) O 4	1.95927	-0.68146
34. LP (2) O 4	1.81451	-0.29477
35. LP (1) O 5	1.96185	-0.68180
36. LP (2) O 5	1.83289	-0.29780
37. LP (1) O 9	1.97500	-0.49229
38. LP (2) O 9	1.93053	-0.42695

7.6.2 Imidazol binding to vanadium in orthovanadium acid I – adduct *iso*$_{trans}$-(1c)

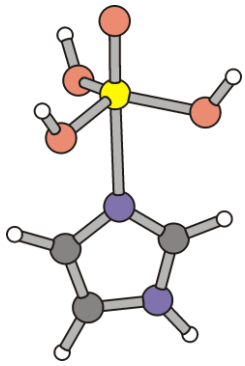

Figure S36. Minimum structure of the *trans*-adduct of imidazol with the all-*syn* conformer of orthovanadium acid

(*i*) B3LYP/6-311++G**//B3LYP/6-311++G**

Standard orientation:

Center Number	Atomic Number	Atomic Type	Coordinates (Angstroms) X	Y	Z
1	6	0	-1.856866	1.043968	-0.019015
2	7	0	-1.074347	-0.012666	-0.029913
3	6	0	-1.899467	-1.114652	-0.008153
4	6	0	-3.205388	-0.712234	0.017799
5	7	0	-3.162610	0.669938	0.011045
6	23	0	1.328483	0.003206	-0.001610
7	8	0	1.002043	-0.541784	1.687463
8	8	0	2.907420	0.050458	-0.022045
9	8	0	0.934954	1.740702	-0.372499
10	8	0	0.996165	-1.240454	-1.271911
11	1	0	-1.497618	-2.113700	-0.021710
12	1	0	-4.131778	-1.260073	0.037015
13	1	0	-1.515569	2.065606	-0.038943
14	1	0	-3.955227	1.291574	0.019807
15	1	0	1.699374	2.315311	-0.488470
16	1	0	1.772848	-1.634457	-1.684601
17	1	0	1.777230	-0.712759	2.234145

```
Zero-point correction=                           0.117761 (Hartree/Particle)
Thermal correction to Energy=                    0.129575
Thermal correction to Enthalpy=                  0.130519
Thermal correction to Gibbs Free Energy=         0.077941
Sum of electronic and zero-point Energies=          -1473.160582
Sum of electronic and thermal Energies=             -1473.148768
Sum of electronic and thermal Enthalpies=           -1473.147824
Sum of electronic and thermal Free Energies=        -1473.200402

Version=AM64L-G03RevE.01\State=1-A\HF-1473.2783433\RMSD=7.043e-09\
RMSF=2.516e-05\ PG=C01 [X(C3H7N2O4V1)]\NImag=0\\@.
```

(*ii*) NBO-analysis – B3LYP/6-31G*// B3LYP/6-311++G**

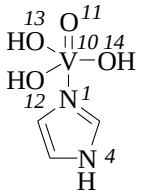


```
=======================================================================
No. (Occupancy) Bond orbital/ Coefficients/ Hybrids
=======================================================================
12. (1.92390) BD (1) V 10- O 11
    (26.48%) 0.5146* V 10  s(30.13%)   p(0.22%)    d(69.36%)   f(0.29%)
    (73.52%) 0.8574* O 11  s(13.45%)   p(86.38%)   d(0.16%)
13. (1.99147) BD (2) V 10- O 11
    (22.96%) 0.4792* V 10  s(0.07%)    p(0.77%)    d(98.96%)   f(0.20%)
    (77.04%) 0.8777* O 11  s(0.03%)    p(99.87%)   d(0.10%)
14. (1.99070) BD (3) V 10- O 11
    (23.00%) 0.4796* V 10  s(0.07%)    p(0.77%)    d(98.97%)   f(0.20%)
    (77.00%) 0.8775* O 11  s(0.02%)    p(99.87%)   d(0.10%)
15. (1.97838) BD (1) V 10- O 12
    (18.81%) 0.4337* V 10  s(22.27%)   p(0.29%)    d(77.30%)   f(0.14%)
    (81.19%) 0.9011* O 12  s(13.43%)   p(86.48%)   d(0.09%)
16. (1.97751) BD (1) V 10- O 13
    (19.25%) 0.4387* V 10  s(22.87%)   p(0.32%)    d(76.67%)   f(0.15%)
    (80.75%) 0.8986* O 13  s(13.41%)   p(86.50%)   d(0.09%)
17. (1.97665) BD (1) V 10- O 14
    (19.25%) 0.4388* V 10  s(23.81%)   p(0.36%)    d(75.69%)   f(0.15%)
    (80.75%) 0.8986* O 14  s(13.45%)   p(86.45%)   d(0.10%)
39. (1.87477) LP (1) N  1  s(31.53%)   p(68.42%)   d(0.05%)
40. (1.57758) LP (1) N  4  s(0.00%)    p(99.98%)   d(0.02%)
41. (1.97075) LP (1) O 11  s(86.50%)   p(13.50%)   d(0.00%)
42. (1.96483) LP (1) O 12  s(61.89%)   p(38.06%)   d(0.05%)
43. (1.83549) LP (2) O 12  s(0.00%)    p(99.92%)   d(0.07%)
44. (1.96422) LP (1) O 13  s(62.18%)   p(37.77%)   d(0.05%)
45. (1.82460) LP (2) O 13  s(0.00%)    p(99.92%)   d(0.08%)
46. (1.96338) LP (1) O 14  s(62.21%)   p(37.74%)   d(0.06%)
47. (1.82308) LP (2) O 14  s(0.00%)    p(99.92%)   d(0.08%)
=======================================================================
```

Second order perturbation theory analysis of Fock-matrix for adduct *iso*$_{trans}$-(**1c**)in NBO-basis(threshold for printing: 0.50 kcal/mol)

Donor NBO (i)	Acceptor NBO (j)	kcal/mol	a.u.	a.u.
39. LP (1) N 1	169. BD*(1) C 2- C 3	4.57	0.99	0.062
39. LP (1) N 1	171. BD*(1) C 2- H 6	1.11	0.90	0.029
39. LP (1) N 1	174. BD*(1) N 4- C 5	7.18	0.86	0.072
39. LP (1) N 1	175. BD*(1) N 4- H 9	0.53	0.83	0.019
39. LP (1) N 1	176. BD*(1) C 5- H 8	1.24	0.87	0.030
39. LP (1) N 1	177. BD*(1) V10- O11	22.02	0.54	0.098
39. LP (1) N 1	178. BD*(2) V10- O11	0.18	0.35	0.007
39. LP (1) N 1	179. BD*(3) V10- O11	0.17	0.35	0.007
39. LP (1) N 1	180. BD*(1) V10- O12	0.28	0.44	0.010
39. LP (1) N 1	181. BD*(1) V10- O13	0.31	0.44	0.011
39. LP (1) N 1	182. BD*(1) V10- O14	0.43	0.44	0.012
39. LP (1) N 1	183. BD*(1) O12- H15	0.25	0.86	0.013
39. LP (1) N 1	184. BD*(1) O13- H16	0.30	0.87	0.015
39. LP (1) N 1	185. BD*(1) O14- H17	0.27	0.87	0.014
40. LP (1) N 4	168. BD*(2) N 1- C 5	52.00	0.28	0.108
40. LP (1) N 4	170. BD*(2) C 2- C 3	29.24	0.31	0.088
41. LP (1) O11	177. BD*(1) V10- O11	2.56	1.11	0.049
41. LP (1) O11	180. BD*(1) V10- O12	1.51	1.01	0.036
41. LP (1) O11	181. BD*(1) V10- O13	1.57	1.01	0.037
41. LP (1) O11	182. BD*(1) V10- O14	1.70	1.02	0.039
42. LP (1) O12	177. BD*(1) V10- O11	2.12	0.82	0.038
42. LP (1) O12	179. BD*(3) V10- O11	5.18	0.63	0.052
42. LP (1) O12	181. BD*(1) V10- O13	1.80	0.72	0.033
42. LP (1) O12	182. BD*(1) V10- O14	1.79	0.73	0.033
43. LP (2) O12	178. BD*(2) V10- O11	1.57	0.24	0.018
43. LP (2) O12	181. BD*(1) V10- O13	10.45	0.34	0.053
43. LP (2) O12	182. BD*(1) V10- O14	9.58	0.34	0.051
44. LP (1) O13	177. BD*(1) V10- O11	2.48	0.82	0.041
44. LP (1) O13	178. BD*(2) V10- O11	3.69	0.63	0.043
44. LP (1) O13	179. BD*(3) V10- O11	1.85	0.63	0.031
44. LP (1) O13	180. BD*(1) V10- O12	1.85	0.72	0.034
44. LP (1) O13	182. BD*(1) V10- O14	1.73	0.73	0.033
45. LP (2) O13	178. BD*(2) V10- O11	0.53	0.24	0.010
45. LP (2) O13	179. BD*(3) V10- O11	1.32	0.24	0.016
45. LP (2) O13	180. BD*(1) V10- O12	11.22	0.33	0.055
45. LP (2) O13	182. BD*(1) V10- O14	9.97	0.34	0.052
46. LP (1) O14	177. BD*(1) V10- O11	3.02	0.82	0.046
46. LP (1) O14	178. BD*(2) V10- O11	4.42	0.63	0.048
46. LP (1) O14	179. BD*(3) V10- O11	0.74	0.63	0.019
46. LP (1) O14	180. BD*(1) V10- O12	1.70	0.72	0.033
46. LP (1) O14	181. BD*(1) V10- O13	1.69	0.72	0.032
47. LP (2) O14	179. BD*(3) V10- O11	1.70	0.24	0.018
47. LP (2) O14	180. BD*(1) V10- O12	10.87	0.33	0.054
47. LP (2) O14	181. BD*(1) V10- O13	10.63	0.34	0.053

Natural bond orbital (NBO)-energies

NBO	Occupancy	Energy
12. BD (1) V 10- O 11	1.92390	-0.58679
13. BD (2) V 10- O 11	1.99147	-0.34515
14. BD (3) V 10- O 11	1.99070	-0.34501
15. BD (1) V 10- O 12	1.97838	-0.50270
16. BD (1) V 10- O 13	1.97751	-0.50434
17. BD (1) V 10- O 14	1.97665	-0.50663
39. LP (1) N 1	1.87477	-0.38874
40. LP (1) N 4	1.57758	-0.27140
41. LP (1) O 11	1.97075	-0.96006
42. LP (1) O 12	1.96483	-0.67078
43. LP (2) O 12	1.83549	-0.28214
44. LP (1) O 13	1.96422	-0.66984
45. LP (2) O 13	1.82460	-0.28064
46. LP (1) O 14	1.96338	-0.67107
47. LP (2) O 14	1.82308	-0.28185

7.6.3 Imidazol binding to vanadium in orthovanadium acid II – adduct *iso*$_{cis}$-(1c)

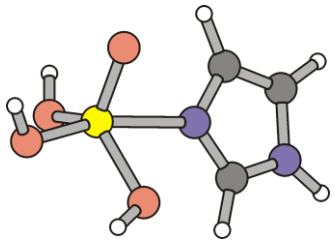

Figure S37. Minimum structure of the *cis*-adduct of imidazol with the all-*syn* conformer of orthovanadium acid.

(*i*) B3LYP/6-311++G**//B3LYP/6-311++G**

Standard orientation:

Center Number	Atomic Number	Atomic Type	Coordinates (Angstroms) X	Y	Z
1	7	0	-3.104385	0.710081	-0.061003
2	6	0	-1.799800	1.062465	-0.145052
3	7	0	-1.036585	-0.009200	-0.063694
4	6	0	-1.876368	-1.094218	0.083864
5	6	0	-3.171848	-0.663333	0.086803
6	23	0	1.207314	-0.057756	0.085563
7	8	0	2.994862	0.161830	-0.150553
8	8	0	0.856430	1.715320	-0.339271
9	8	0	1.147305	-0.386766	1.621406
10	8	0	0.970742	-1.563121	-0.911567
11	1	0	-1.484411	-2.092369	0.181449
12	1	0	-4.106179	-1.189017	0.181738
13	1	0	-1.428235	2.066611	-0.259236
14	1	0	-3.886185	1.344868	-0.099981
15	1	0	0.539132	-1.503401	-1.770720
16	1	0	3.302061	0.261378	-1.059590
17	1	0	1.615778	2.286563	-0.182536

```
Zero-point correction=                          0.117162 (Hartree/Particle)
Thermal correction to Energy=                   0.129063
Thermal correction to Enthalpy=                 0.130007
Thermal correction to Gibbs Free Energy=        0.079247
Sum of electronic and zero-point Energies=          -1473.150857
Sum of electronic and thermal Energies=             -1473.138956
Sum of electronic and thermal Enthalpies=           -1473.138012
Sum of electronic and thermal Free Energies=        -1473.188772

Version=AM64L-G03RevE.01\State=1-A\HF-1473.2680192\RMSD=8.355e-09\
RMSF=4.715e-07\PG=C01 [X(C3H7N2O4V1)]\NImag=0\\@.
```

(*ii*) NBO-analysis – B3LYP/6-31G*// B3LYP/6-311++G**

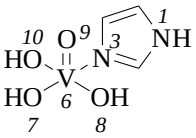


```
=====================================================================
No. (Occupancy) Bond orbital/ Coefficients/ Hybrids
=====================================================================
12. (1.95271) BD (1) V  6- O  7
    (16.72%) 0.4089* V  6  s(39.61%)   p(0.84%)    d(59.36%)   f(0.18%)
    (83.28%) 0.9126* O  7  s(15.52%)   p(84.39%)   d(0.09%)
13. (1.93887) BD (1) V  6- O  8
    (16.27%) 0.4033* V  6  s(30.12%)   p(1.80%)    d(67.83%)   f(0.24%)
    (83.73%) 0.9150* O  8  s(12.42%)   p(87.50%)   d(0.08%)
14. (1.97215) BD (1) V  6- O  9
    (31.74%) 0.5634* V  6  s(12.07%)   p(0.53%)    d(87.20%)   f(0.20%)
    (68.26%) 0.8262* O  9  s(10.65%)   p(89.16%)   d(0.19%)
15. (1.92128) BD (2) V  6- O  9
    (18.19%) 0.4265* V  6  s(2.03%)    p(2.88%)    d(94.59%)   f(0.50%)
    (81.81%) 0.9045* O  9  s(0.20%)    p(99.70%)   d(0.10%)
16. (1.96639) BD (3) V  6- O  9
    (24.33%) 0.4932* V  6  s(2.72%)    p(0.65%)    d(96.39%)   f(0.23%)
    (75.67%) 0.8699* O  9  s(0.00%)    p(99.89%)   d(0.11%)
17. (1.95376) BD (1) V  6- O 10
    (16.53%) 0.4065* V  6  s(11.10%)   p(1.33%)    d(87.33%)   f(0.24%)
    (83.47%) 0.9136* O 10  s(14.43%)   p(85.49%)   d(0.08%)
39. (1.56838) LP (1) N  1  s(0.00%)    p(99.98%)   d(0.02%)
40. (1.81480) LP (1) N  3  s(31.90%)   p(68.06%)   d(0.03%)
41. (1.96025) LP (1) O  7  s(60.38%)   p(39.57%)   d(0.05%)
42. (1.80658) LP (2) O  7  s(0.07%)    p(99.86%)   d(0.08%)
43. (1.96263) LP (1) O  8  s(62.88%)   p(37.08%)   d(0.04%)
44. (1.88882) LP (2) O  8  s(0.19%)    p(99.75%)   d(0.06%)
45. (1.96856) LP (1) O  9  s(89.15%)   p(10.85%)   d(0.00%)
46. (1.95580) LP (1) O 10  s(58.95%)   p(41.00%)   d(0.06%)
47. (1.83875) LP (2) O 10  s(2.07%)    p(97.86%)   d(0.07%)
=====================================================================
```

Second order perturbation theory analysis of Fock-matrix for adduct *iso*$_{cis}$-(**1c**) in NBO-basis(threshold for printing: 0.50 kcal/mol)

Donor NBO (i)	Acceptor NBO (j)	kcal/mol	a.u.	a.u.
39. LP (1) N 1	170. BD*(2) C 2- N 3	56.43	0.27	0.111
39. LP (1) N 1	174. BD*(2) C 4- C 5	29.28	0.30	0.088
40. LP (1) N 3	166. BD*(1) N 1- C 2	6.28	0.88	0.069
40. LP (1) N 3	168. BD*(1) N 1- H14	0.50	0.85	0.019
40. LP (1) N 3	171. BD*(1) C 2- H13	1.06	0.90	0.029
40. LP (1) N 3	173. BD*(1) C 4- C 5	4.12	1.01	0.060
40. LP (1) N 3	175. BD*(1) C 4- H11	0.98	0.92	0.028
40. LP (1) N 3	177. BD*(1) V 6- O 7	33.07	0.56	0.121
40. LP (1) N 3	178. BD*(1) V 6- O 8	0.29	0.52	0.011
40. LP (1) N 3	179. BD*(1) V 6- O 9	0.37	0.49	0.012
40. LP (1) N 3	180. BD*(2) V 6- O 9	0.09	0.41	0.005
40. LP (1) N 3	181. BD*(3) V 6- O 9	7.55	0.39	0.050
40. LP (1) N 3	182. BD*(1) V 6- O10	0.22	0.44	0.009
40. LP (1) N 3	184. BD*(1) O 8- H17	0.28	0.91	0.015
41. LP (1) O 7	177. BD*(1) V 6- O 7	1.02	0.78	0.026
41. LP (1) O 7	178. BD*(1) V 6- O 8	0.90	0.74	0.024
41. LP (1) O 7	181. BD*(3) V 6- O 9	2.03	0.61	0.032
41. LP (1) O 7	182. BD*(1) V 6- O10	0.98	0.66	0.024
42. LP (2) O 7	178. BD*(1) V 6- O 8	2.67	0.37	0.028
42. LP (2) O 7	180. BD*(2) V 6- O 9	6.12	0.26	0.036
42. LP (2) O 7	181. BD*(3) V 6- O 9	0.79	0.24	0.012
42. LP (2) O 7	182. BD*(1) V 6- O10	11.61	0.29	0.052
42. LP (2) O 7	184. BD*(1) O 8- H17	0.59	0.76	0.020
43. LP (1) O 8	177. BD*(1) V 6- O 7	1.67	0.80	0.034
43. LP (1) O 8	178. BD*(1) V 6- O 8	1.01	0.76	0.026
43. LP (1) O 8	179. BD*(1) V 6- O 9	1.40	0.73	0.029
43. LP (1) O 8	181. BD*(3) V 6- O 9	1.80	0.63	0.031
44. LP (2) O 8	179. BD*(1) V 6- O 9	11.26	0.34	0.055
44. LP (2) O 8	180. BD*(2) V 6- O 9	6.52	0.26	0.038
44. LP (2) O 8	182. BD*(1) V 6- O10	0.52	0.29	0.011
45. LP (1) O 9	177. BD*(1) V 6- O 7	5.63	1.11	0.073
45. LP (1) O 9	178. BD*(1) V 6- O 8	5.79	1.07	0.073
45. LP (1) O 9	179. BD*(1) V 6- O 9	0.65	1.04	0.024
45. LP (1) O 9	180. BD*(2) V 6- O 9	0.75	0.96	0.025
45. LP (1) O 9	182. BD*(1) V 6- O10	2.65	1.00	0.048
46. LP (1) O10	177. BD*(1) V 6- O 7	1.53	0.77	0.032
46. LP (1) O10	178. BD*(1) V 6- O 8	15.95	0.74	0.100
46. LP (1) O10	180. BD*(2) V 6- O 9	1.03	0.63	0.024
47. LP (2) O10	178. BD*(1) V 6- O 8	4.87	0.39	0.039
47. LP (2) O10	179. BD*(1) V 6- O 9	0.89	0.36	0.016
47. LP (2) O10	180. BD*(2) V 6- O 9	18.00	0.28	0.065
47. LP (2) O10	182. BD*(1) V 6- O10	0.55	0.31	0.012

Natural bond orbital (NBO)-energies

NBO	Occupancy	Energy
12. BD (1) V 6- O 7	1.95271	-0.50402
13. BD (1) V 6- O 8	1.93887	-0.46538
14. BD (1) V 6- O 9	1.97215	-0.55696
15. BD (2) V 6- O 9	1.92128	-0.32156
16. BD (3) V 6- O 9	1.96639	-0.32335
17. BD (1) V 6- O 10	1.95376	-0.48703
39. LP (1) N 1	1.56838	-0.29094
40. LP (1) N 3	1.81480	-0.42536
41. LP (1) O 7	1.96025	-0.64536
42. LP (2) O 7	1.80658	-0.27046
43. LP (1) O 8	1.96263	-0.66615
44. LP (2) O 8	1.88882	-0.27342
45. LP (1) O 9	1.96856	-0.97658
46. LP (1) O 10	1.95580	-0.64356
47. LP (2) O 10	1.83875	-0.29192

7.6.4 Methylamine binding to vanadium in orthovanadium acid – adduct *iso*$_{trans}$-(1d)

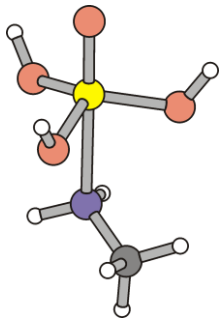

Figure S38. Minimum structure of the *trans*-adduct of methylamine with the all-*syn* conformer of orthovanadium acid.

(*i*) B3LYP/6-311++G**//B3LYP/6-311++G**

Standard orientation:

Center Number	Atomic Number	Atomic Type	Coordinates (Angstroms) X	Y	Z
1	23	0	0.617724	-0.047663	0.000001
2	8	0	2.130229	-0.507372	-0.000001
3	8	0	-0.000679	-0.781701	1.533685
4	8	0	0.776720	1.757939	-0.000066
5	8	0	-0.000711	-0.781833	-1.533612
6	1	0	0.635687	-1.287779	2.051210
7	1	0	1.674921	2.107157	-0.000081
8	1	0	0.635655	-1.287967	-2.051081
9	1	0	-1.728254	1.313973	0.814845
10	1	0	-1.728261	1.313903	-0.814955
11	7	0	-1.659243	0.711271	-0.000028
12	6	0	-2.728343	-0.301832	0.000017
13	1	0	-2.611257	-0.929840	-0.883540
14	1	0	-3.734596	0.132394	-0.000003
15	1	0	-2.611257	-0.929759	0.883632

```
Zero-point correction=                          0.112041 (Hartree/Particle)
Thermal correction to Energy=                   0.122789
Thermal correction to Enthalpy=                 0.123733
Thermal correction to Gibbs Free Energy=        0.076430
Sum of electronic and zero-point Energies=          -1342.781768
Sum of electronic and thermal Energies=             -1342.771020
Sum of electronic and thermal Enthalpies=           -1342.770076
Sum of electronic and thermal Free Energies=        -1342.817379

Version=AM64L-G03RevE.01\State=1-A\HF-1342.893809\RMSD=4.710e-09\
RMSF=3.844e-07\PG=C01 [X(C1H8N1O4V1)]\NImag=0\\@.
```

(*ii*) NBO-analysis – B3LYP/6-31G*// B3LYP/6-311++G**

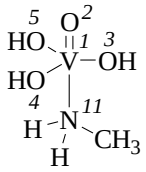

```
=======================================================================
No. (Occupancy) Bond orbital/ Coefficients/ Hybrids
=======================================================================
 1. (1.92591) BD (1) V  1- O  2
    (26.43%) 0.5141* V  1  s(29.79%)   p(0.27%)    d(69.66%)   f(0.29%)
    (73.57%) 0.8577* O  2  s(13.37%)   p(86.47%)   d(0.17%)
 2. (1.99026) BD (2) V  1- O  2
    (23.20%) 0.4817* V  1  s(0.16%)    p(0.85%)    d(98.80%)   f(0.20%)
    (76.80%) 0.8763* O  2  s(0.08%)    p(99.82%)   d(0.10%)
 3. (1.99064) BD (3) V  1- O  2
    (23.11%) 0.4807* V  1  s(0.00%)    p(0.83%)    d(98.98%)   f(0.20%)
    (76.89%) 0.8769* O  2  s(0.00%)    p(99.90%)   d(0.10%)
 4. (1.97779) BD (1) V  1- O  3
    (19.01%) 0.4360* V  1  s(23.00%)   p(0.32%)    d(76.54%)   f(0.15%)
    (80.99%) 0.8999* O  3  s(13.67%)   p(86.24%)   d(0.09%)
 5. (1.97815) BD (1) V  1- O  4
    (18.88%) 0.4345* V  1  s(23.23%)   p(0.33%)    d(76.29%)   f(0.15%)
    (81.12%) 0.9007* O  4  s(13.81%)   p(86.10%)   d(0.09%)
 6. (1.97779) BD (1) V  1- O  5
    (19.01%) 0.4360* V  1  s(23.00%)   p(0.32%)    d(76.54%)   f(0.15%)
    (80.99%) 0.8999* O  5  s(13.67%)   p(86.24%)   d(0.09%)
31. (1.97074) LP (1) O  2  s(86.55%)   p(13.45%)   d(0.00%)
32. (1.96368) LP (1) O  3  s(61.67%)   p(38.28%)   d(0.05%)
33. (1.82701) LP (2) O  3  s(0.00%)    p(99.93%)   d(0.07%)
34. (1.96510) LP (1) O  4  s(61.35%)   p(38.60%)   d(0.05%)
35. (1.83071) LP (2) O  4  s(0.00%)    p(99.93%)   d(0.07%)
36. (1.96368) LP (1) O  5  s(61.67%)   p(38.28%)   d(0.05%)
37. (1.82701) LP (2) O  5  s(0.00%)    p(99.93%)   d(0.07%)
38. (1.88415) LP (1) N 11  s(21.34%)   p(78.64%)   d(0.02%)
=======================================================================
```

Second order perturbation theory analysis of Fock-matrix for adduct *iso*$_{trans}$-(**1d**) in NBO-basis(threshold for printing: 0.50 kcal/mol)

Donor NBO (i)	Acceptor NBO (j)	kcal/mol	a.u.	a.u.
31. LP (1) O 2	128. BD*(1) V 1- O 2	2.51	1.11	0.049
31. LP (1) O 2	131. BD*(1) V 1- O 3	1.64	1.01	0.038
31. LP (1) O 2	132. BD*(1) V 1- O 4	1.64	1.01	0.038
31. LP (1) O 2	133. BD*(1) V 1- O 5	1.64	1.01	0.038
32. LP (1) O 3	128. BD*(1) V 1- O 2	2.87	0.82	0.045
32. LP (1) O 3	129. BD*(2) V 1- O 2	1.09	0.63	0.024
32. LP (1) O 3	130. BD*(3) V 1- O 2	4.23	0.63	0.047
32. LP (1) O 3	132. BD*(1) V 1- O 4	1.67	0.72	0.032
32. LP (1) O 3	133. BD*(1) V 1- O 5	1.72	0.72	0.033
33. LP (2) O 3	129. BD*(2) V 1- O 2	1.56	0.24	0.018
33. LP (2) O 3	130. BD*(3) V 1- O 2	0.50	0.24	0.010
33. LP (2) O 3	132. BD*(1) V 1- O 4	10.36	0.34	0.053
33. LP (2) O 3	133. BD*(1) V 1- O 5	10.38	0.34	0.053
34. LP (1) O 4	128. BD*(1) V 1- O 2	2.05	0.82	0.038
34. LP (1) O 4	129. BD*(2) V 1- O 2	6.03	0.63	0.056
34. LP (1) O 4	131. BD*(1) V 1- O 3	1.64	0.72	0.032
34. LP (1) O 4	133. BD*(1) V 1- O 5	1.64	0.72	0.032
35. LP (2) O 4	130. BD*(3) V 1- O 2	2.01	0.24	0.020
35. LP (2) O 4	131. BD*(1) V 1- O 3	10.19	0.34	0.053
35. LP (2) O 4	133. BD*(1) V 1- O 5	10.19	0.34	0.053
36. LP (1) O 5	128. BD*(1) V 1- O 2	2.87	0.82	0.045
36. LP (1) O 5	129. BD*(2) V 1- O 2	1.08	0.63	0.023
36. LP (1) O 5	130. BD*(3) V 1- O 2	4.24	0.63	0.047
36. LP (1) O 5	131. BD*(1) V 1- O 3	1.72	0.72	0.033
36. LP (1) O 5	132. BD*(1) V 1- O 4	1.67	0.72	0.032
37. LP (2) O 5	129. BD*(2) V 1- O 2	1.56	0.24	0.018
37. LP (2) O 5	131. BD*(1) V 1- O 3	10.38	0.34	0.053
37. LP (2) O 5	132. BD*(1) V 1- O 4	10.36	0.34	0.053
38. LP (1) N11	128. BD*(1) V 1- O 2	24.19	0.49	0.098
38. LP (1) N11	129. BD*(2) V 1- O 2	0.33	0.30	0.009
38. LP (1) N11	131. BD*(1) V 1- O 3	0.28	0.39	0.010
38. LP (1) N11	132. BD*(1) V 1- O 4	0.25	0.39	0.009
38. LP (1) N11	133. BD*(1) V 1- O 5	0.28	0.39	0.010
38. LP (1) N11	134. BD*(1) O 3- H 6	0.33	0.82	0.015
38. LP (1) N11	135. BD*(1) O 4- H 7	0.34	0.82	0.015
38. LP (1) N11	136. BD*(1) O 5- H 8	0.33	0.82	0.015

Natural bond orbital (NBO)-energies

NBO	Occupancy	Energy
1. BD (1) V 1- O 2	1.92591	-0.59314
2. BD (2) V 1- O 2	1.99026	-0.35273
3. BD (3) V 1- O 2	1.99064	-0.35126
4. BD (1) V 1- O 3	1.97779	-0.51593
5. BD (1) V 1- O 4	1.97815	-0.51684
6. BD (1) V 1- O 5	1.97779	-0.51593
32. LP (1) O 3	1.96368	-0.67839
33. LP (2) O 3	1.82701	-0.29144
34. LP (1) O 4	1.96510	-0.67809
35. LP (2) O 4	1.83071	-0.29252
36. LP (1) O 5	1.96368	-0.67839
37. LP (2) O 5	1.82701	-0.29144
38. LP (1) N 11	1.88415	-0.34825

7.6.5 Imidazol binding to vanadium in dihydrogen orthovanadate I – adduct *iso*$_{cis}$-(2c)

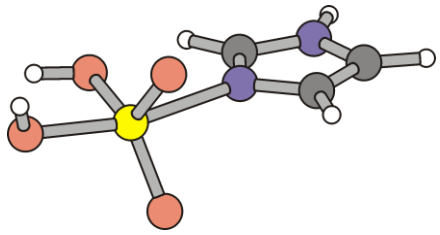

Figure S39. Minimum structure of the *cis*-adduct of imidazol with dihydrogen orthovanadate.

(*i*) B3LYP/6-311++G**//B3LYP/6-311++G**

Standard orientation:

Center Number	Atomic Number	Atomic Type	Coordinates (Angstroms) X	Y	Z
1	7	0	4.218613	-0.374752	0.072710
2	6	0	3.761725	0.906842	-0.146298
3	6	0	2.386028	0.931074	-0.158350
4	7	0	1.991547	-0.364813	0.058216
5	6	0	3.121731	-1.104653	0.189657
6	1	0	4.444822	1.732353	-0.281696
7	1	0	1.659214	1.715346	-0.294328
8	1	0	3.095296	-2.168884	0.370023
9	1	0	1.006093	-0.695623	0.107051
10	23	0	-1.837759	0.020710	-0.004848
11	8	0	-0.660726	-1.113933	0.158911
12	8	0	-2.879905	-0.396055	-1.471605
13	8	0	-1.196220	1.487276	-0.210098
14	8	0	-2.895395	0.038229	1.508123
15	1	0	-2.841779	-1.326441	-1.712831
16	1	0	-3.125231	0.920159	1.814112

```
Zero-point correction=                          0.104515 (Hartree/Particle)
Thermal correction to Energy=                   0.116637
Thermal correction to Enthalpy=                 0.117581
Thermal correction to Gibbs Free Energy=        0.062941
Sum of electronic and zero-point Energies=          -1472.665703
Sum of electronic and thermal Energies=             -1472.653581
Sum of electronic and thermal Enthalpies=           -1472.652636
Sum of electronic and thermal Free Energies=        -1472.707277

Version=AM64L-G03RevE.01\State=1-A\HF-1472.7702178\RMSD=7.312e-09\
RMSF=2.308e-05\PG=C01 [X(C3H6N2O4V1)]\NImag=0 \\@.
```

(*ii*) NBO-analysis – B3LYP/6-31G*// B3LYP/6-311++G**

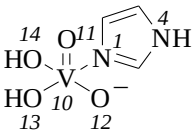


```
==========================================================================
No. (Occupancy) Bond orbital/ Coefficients/ Hybrids
==========================================================================
12. (1.94511) BD (1) V 10- O 11
    (26.72%) 0.5169* V 10  s(13.28%)   p(5.51%)    d(80.63%)   f(0.58%)
    (73.28%) 0.8561* O 11  s(11.25%)   p(88.61%)   d(0.14%)
13. (1.91656) BD (2) V 10- O 11
    (11.46%) 0.3385* V 10  s(5.07%)    p(27.23%)   d(65.77%)   f(1.93%)
    (88.54%) 0.9409* O 11  s(0.47%)    p(99.47%)   d(0.07%)
14. (1.95156) BD (3) V 10- O 11
    (20.56%) 0.4534* V 10  s(1.33%)    p(7.70%)    d(90.44%)   f(0.53%)
    (79.44%) 0.8913* O 11  s(0.01%)    p(99.91%)   d(0.08%)
15. (1.88920) BD (1) V 10- O 12
    (22.99%) 0.4795* V 10  s(12.12%)   p(12.04%)   d(74.74%)   f(1.10%)
    (77.01%) 0.8775* O 12  s(11.29%)   p(88.58%)   d(0.13%)
16. (1.95162) BD (2) V 10- O 12
    (20.25%) 0.4500* V 10  s(0.37%)    p(9.65%)    d(89.25%)   f(0.72%)
    (79.75%) 0.8930* O 12  s(0.02%)    p(99.90%)   d(0.08%)
17. (1.95682) BD (1) V 10- O 13
    (14.15%) 0.3761* V 10  s(43.40%)   p(2.13%)    d(54.28%)   f(0.19%)
    (85.85%) 0.9266* O 13  s(13.70%)   p(86.22%)   d(0.07%)
18. (1.92847) BD (1) V 10- O 14
    (10.83%) 0.3291* V 10  s(27.66%)   p(18.25%)   d(52.77%)   f(1.32%)
    (89.17%) 0.9443* O 14  s(11.80%)   p(88.14%)   d(0.07%)
39. (1.85118) LP (1) N  1  s(32.02%)   p(67.92%)   d(0.06%)
40. (1.60143) LP (1) N  4  s(0.00%)    p(99.99%)   d(0.01%)
41. (1.97110) LP (1) O 11  s(88.27%)   p(11.73%)   d(0.00%)
42. (1.97144) LP (1) O 12  s(87.95%)   p(12.05%)   d(0.00%)
43. (1.73452) LP (2) O 12  s(0.73%)    p(99.20%)   d(0.06%)
44. (1.97615) LP (1) O 13  s(62.38%)   p(37.59%)   d(0.04%)
45. (1.90074) LP (2) O 13  s(0.33%)    p(99.60%)   d(0.07%)
46. (1.96936) LP (1) O 14  s(64.03%)   p(35.94%)   d(0.03%)
47. (1.93121) LP (2) O 14  s(0.00%)    p(99.94%)   d(0.06%)
==========================================================================
```

Second order perturbation theory analysis of Fock-matrix for adduct *iso*$_{cis}$-(**2c**) in NBO-basis(threshold for printing: 0.50 kcal/mol)

Donor NBO (i)	Acceptor NBO (j)	kcal/mol	a.u.	a.u.
39. LP (1) N 1	167. BD*(1) C 2- C 3	4.79	0.97	0.063
39. LP (1) N 1	169. BD*(1) C 2- H 6	1.19	0.88	0.030
39. LP (1) N 1	172. BD*(1) N 4- C 5	7.57	0.84	0.073
39. LP (1) N 1	173. BD*(1) N 4- H 9	0.58	0.79	0.020
39. LP (1) N 1	174. BD*(1) C 5- H 8	1.30	0.86	0.031
39. LP (1) N 1	175. BD*(1) V10- O11	0.32	0.57	0.012
39. LP (1) N 1	176. BD*(2) V10- O11	0.33	0.64	0.013
39. LP (1) N 1	177. BD*(3) V10- O11	2.27	0.46	0.029
39. LP (1) N 1	178. BD*(1) V10- O12	0.35	0.62	0.013
39. LP (1) N 1	179. BD*(2) V10- O12	0.72	0.48	0.017
39. LP (1) N 1	180. BD*(1) V10- O13	23.22	0.58	0.104
39. LP (1) N 1	181. BD*(1) V10- O14	0.45	0.67	0.016
39. LP (1) N 1	183. BD*(1) O14- H16	0.16	0.92	0.011
40. LP (1) N 4	166. BD*(2) N 1- C 5	46.74	0.29	0.106
40. LP (1) N 4	168. BD*(2) C 2- C 3	28.25	0.31	0.085
41. LP (1) O11	175. BD*(1) V10- O11	0.53	1.04	0.022
41. LP (1) O11	176. BD*(2) V10- O11	1.16	1.12	0.034
41. LP (1) O11	180. BD*(1) V10- O13	5.55	1.06	0.071
41. LP (1) O11	181. BD*(1) V10- O14	6.78	1.15	0.081
42. LP (1) O12	175. BD*(1) V10- O11	0.61	1.04	0.023
42. LP (1) O12	176. BD*(2) V10- O11	8.02	1.12	0.090
42. LP (1) O12	180. BD*(1) V10- O13	4.00	1.05	0.060
42. LP (1) O12	181. BD*(1) V10- O14	9.23	1.14	0.095
43. LP (2) O12	175. BD*(1) V10- O11	10.39	0.37	0.057
43. LP (2) O12	176. BD*(2) V10- O11	24.38	0.45	0.093
43. LP (2) O12	177. BD*(3) V10- O11	1.35	0.27	0.018
43. LP (2) O12	181. BD*(1) V10- O14	3.84	0.47	0.039
44. LP (1) O13	178. BD*(1) V10- O12	0.91	0.83	0.025
44. LP (1) O13	179. BD*(2) V10- O12	1.78	0.69	0.032
44. LP (1) O13	181. BD*(1) V10- O14	0.73	0.88	0.023
44. LP (1) O13	183. BD*(1) O14- H16	0.53	1.13	0.022
45. LP (2) O13	175. BD*(1) V10- O11	2.57	0.39	0.029
45. LP (2) O13	177. BD*(3) V10- O11	8.13	0.29	0.043
45. LP (2) O13	179. BD*(2) V10- O12	1.06	0.30	0.016
45. LP (2) O13	183. BD*(1) O14- H16	1.67	0.75	0.032
46. LP (1) O14	175. BD*(1) V10- O11	0.57	0.78	0.020
46. LP (1) O14	177. BD*(3) V10- O11	1.36	0.68	0.028
46. LP (1) O14	178. BD*(1) V10- O12	0.95	0.84	0.026
46. LP (1) O14	179. BD*(2) V10- O12	1.44	0.70	0.029
46. LP (1) O14	180. BD*(1) V10- O13	1.82	0.80	0.035
47. LP (2) O14	175. BD*(1) V10- O11	5.42	0.38	0.041
47. LP (2) O14	177. BD*(3) V10- O11	0.67	0.28	0.012
47. LP (2) O14	178. BD*(1) V10- O12	3.88	0.44	0.037

Natural bond orbital (NBO)-energies

NBO	Occupancy	Energy
12. BD (1) V 10- O 11	1.94511	-0.30004
13. BD (2) V 10- O 11	1.91656	-0.07582
14. BD (3) V 10- O 11	1.95156	-0.08714
15. BD (1) V 10- O 12	1.88920	-0.26865
16. BD (2) V 10- O 12	1.95162	-0.08668
17. BD (1) V 10- O 13	1.95682	-0.26339
18. BD (1) V 10- O 14	1.92847	-0.21319
39. LP (1) N 1	1.85118	-0.25149
40. LP (1) N 4	1.60143	-0.15903
41. LP (1) O 11	1.97110	-0.72733
42. LP (1) O 12	1.97144	-0.72522
43. LP (2) O 12	1.73452	-0.05476
44. LP (1) O 13	1.97615	-0.46473
45. LP (2) O 13	1.90074	-0.07543
46. LP (1) O 14	1.96936	-0.47110
47. LP (2) O 14	1.93121	-0.06552

7.7 Hydrogen-bonded bromide

7.7.1 Bromide monohydrate – adduct 3a

Figure S40. Minimum structure of hydrated bromide (**3a**).

B3LYP/6-311++G//B3LYP/6-311++G****

Standard orientation:

Center Number	Atomic Number	Atomic Type	Coordinates (Angstroms) X	Y	Z
1	35	0	-0.721598	0.002269	0.000000
2	1	0	1.659435	-0.283777	0.000003
3	8	0	2.622818	-0.084152	0.000000
4	1	0	2.613947	0.877580	0.000001

Zero-point correction= 0.023066 (Hartree/Particle)
Thermal correction to Energy= 0.027087
Thermal correction to Enthalpy= 0.028031
Thermal correction to Gibbs Free Energy= -0.003173
Sum of electronic and zero-point Energies= -2650.693657
Sum of electronic and thermal Energies= -2650.689637
Sum of electronic and thermal Enthalpies= -2650.688693
Sum of electronic and thermal Free Energies= -2650.719896

Version=AM64L-G03RevE.01\State=1-A\HF-2650.7167235\RMSD=4.372e-09\
RMSF=3.035e-07\PG=C01 [X(Br1H2O1)]\NImag=0\\@.

7.7.2 Bromide heptahydrate – adduct $3a_7$

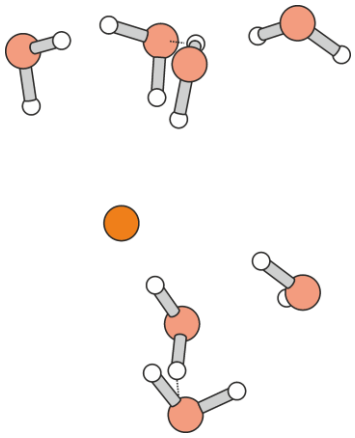

Figure S41. Minimum structure of bromide heptahydrate (**$3a_7$**).

B3LYP/6-311++G//B3LYP/6-311++G****

Standard orientation:

Center Number	Atomic Number	Atomic Type	Coordinates (Angstroms) X	Y	Z
1	8	0	-3.439465	-0.509449	1.273200
2	8	0	-3.525692	1.088766	-1.231984
3	8	0	-1.944091	2.076048	1.058224
4	35	0	-0.514451	-0.564400	-0.609395
5	8	0	2.653635	0.472511	-0.007431
6	8	0	4.249594	2.787502	-0.193367
7	8	0	1.591880	-1.330375	1.981876
8	8	0	2.348789	-2.511549	-0.636236
9	1	0	-2.590567	-0.834121	0.922963
10	1	0	-3.861640	-0.132646	0.480031
11	1	0	-2.742205	0.556226	-1.455922
12	1	0	-1.281953	1.494468	0.639773
13	1	0	3.650157	3.461004	0.148274
14	1	0	0.763716	-1.125845	1.507090
15	1	0	1.434846	-2.234959	-0.833639
16	1	0	3.729895	1.956752	-0.156711
17	1	0	-3.157818	1.760228	-0.628136
18	1	0	1.968696	-2.046082	1.439383
19	1	0	2.844166	-1.680062	-0.720179
20	1	0	-2.489730	1.442271	1.556492
21	1	0	1.757224	0.483330	-0.394857
22	1	0	2.503808	0.065823	0.869993

```
Zero-point correction=                          0.174859 (Hartree/Particle)
Thermal correction to Energy=                   0.195687
Thermal correction to Enthalpy=                 0.196632
Thermal correction to Gibbs Free Energy=        0.120650
Sum of electronic and zero-point Energies=          -3106.809716
Sum of electronic and thermal Energies=             -3106.788888
Sum of electronic and thermal Enthalpies=           -3106.787944
Sum of electronic and thermal Free Energies=        -3106.863925

Version=AM64L-G03RevE.01\State=1-A\HF-3106.9845753\RMSD=3.853e-09\
RMSF=7.735e-07\PG=C01 [X(Br1H14O7)]\NImag=0\\@.
```

7.7.3 Bromide octahydrate – adduct $3a_8$

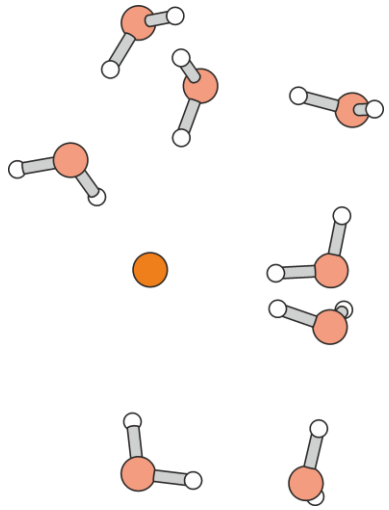

Figure S42. Minimum structure of octahydrated bromide.

B3LYP/6-311++G//B3LYP/6-311++G****

Standard orientation:

Center Number	Atomic Number	Atomic Type	Coordinates (Angstroms) X	Y	Z
1	35	0	0.144265	-0.782650	-0.758654
2	1	0	2.704759	-1.854904	-0.523682
3	8	0	3.625473	-2.062391	-0.310541
4	1	0	3.932355	-1.286281	0.188571
5	1	0	4.609685	1.019922	0.220955
6	1	0	-4.078985	-0.789811	1.992926
7	1	0	-1.258485	-2.171722	0.403710
8	1	0	-2.026524	0.389630	-0.835626
9	1	0	1.277075	0.518662	1.158123
10	8	0	4.367940	0.479211	0.978736
11	8	0	-4.098788	-1.030685	1.062303
12	8	0	-1.969042	-2.744782	0.777964
13	8	0	1.768904	1.292391	1.484345
14	8	0	-2.853627	0.886348	-0.686984
15	1	0	-1.996217	-3.501823	0.184979
16	1	0	3.475576	0.808044	1.235861
17	1	0	-3.386936	0.305422	-0.113316
18	1	0	1.504230	1.980322	0.840114
19	1	0	-3.394485	-1.711268	0.964862
20	1	0	0.606052	1.847333	-1.096356
21	8	0	0.748255	2.730786	-0.720636
22	1	0	-0.152655	3.051584	-0.518497
23	1	0	-1.843362	3.250692	1.065037
24	8	0	-1.922766	3.330308	0.109712
25	1	0	-2.352147	2.487453	-0.173957

```
Zero-point correction=                          0.199318 (Hartree/Particle)
Thermal correction to Energy=                   0.222843
Thermal correction to Enthalpy=                 0.223788
Thermal correction to Gibbs Free Energy=        0.140067
Sum of electronic and zero-point Energies=          -3185.857694
Sum of electronic and thermal Energies=             -3185.834168
Sum of electronic and thermal Enthalpies=           -3185.833224
Sum of electronic and thermal Free Energies=        -3185.916945

Version=AM64L-G03RevE.01\State=1-A\HF-3186.0570118\RMSD=7.171e-09\
RMSF=3.447e-07\PG=C01 [X(Br1H16O8)]\NImag=0\\@.
```

7.7.4 Methanol binding to bromide – adduct 3b

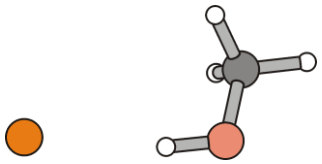

Figure S43. Minimum structure of the hydrogen-bonded methanol to bromide.

B3LYP/6-311++G//B3LYP/6-311++G****

Standard orientation:

Center Number	Atomic Number	Atomic Type	Coordinates (Angstroms) X	Y	Z
1	8	0	2.039211	0.776171	-0.000006
2	6	0	2.589695	-0.521791	-0.000001
3	1	0	1.059611	0.674665	0.000090
4	1	0	3.681031	-0.421811	-0.000438
5	1	0	2.293945	-1.100154	0.887011
6	1	0	2.293245	-1.100442	-0.886584
7	35	0	-1.176563	-0.032311	-0.000001

Zero-point correction= 0.051731 (Hartree/Particle)
Thermal correction to Energy= 0.056925
Thermal correction to Enthalpy= 0.057869
Thermal correction to Gibbs Free Energy= 0.021502
Sum of electronic and zero-point Energies= -2689.971363
Sum of electronic and thermal Energies= -2689.966169
Sum of electronic and thermal Enthalpies= -2689.965225
Sum of electronic and thermal Free Energies= -2690.001592

Version=AM64L-G03RevE.01\State=1-A\HF-2690.023094\RMSD=2.563e-09\
RMSF=8.425e-07\PG=C01 [X(C1H4Br1O1)]\NImag=0\\@.

7.7.5 Imidazole binding to bromide – adduct 3c

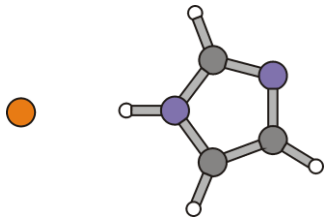

Figure S44. Minimum structure of the hydrogen-bonded imidazole to bromide.

B3LYP/6-311++G//B3LYP/6-311++G****

Standard orientation:

Center Number	Atomic Number	Atomic Type	Coordinates (Angstroms) X	Y	Z
1	7	0	1.065992	-0.009584	0.000694
2	6	0	1.865112	1.103744	0.000094
3	6	0	3.159212	0.634937	-0.000238
4	7	0	3.169005	-0.741760	-0.000374
5	6	0	1.890460	-1.085251	0.000142
6	1	0	0.023509	-0.020651	0.000470
7	1	0	1.449429	2.097648	0.000297
8	1	0	4.076149	1.205898	-0.000528
9	1	0	1.511566	-2.095722	0.000311
10	35	0	-2.234124	0.004333	-0.000079

```
Zero-point correction=                          0.071065 (Hartree/Particle)
Thermal correction to Energy=                   0.076968
Thermal correction to Enthalpy=                 0.077912
Thermal correction to Gibbs Free Energy=        0.038360
Sum of electronic and zero-point Energies=          -2800.482343
Sum of electronic and thermal Energies=             -2800.476441
Sum of electronic and thermal Enthalpies=           -2800.475496
Sum of electronic and thermal Free Energies=        -2800.515048

Version=AM64L-G03RevE.01\State=1-A\HF-2800.5534083\RMSD=4.224e-09\
RMSF=5.976e-05\PG=C01 [X(C3H4Br1N2)]\NImag=0\\@.
```

7.7.6 Methylamine binding to bromide – adduct 3d

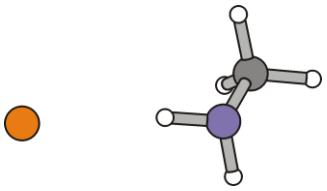

Figure S45. Minimum structure of the hydrogen-bonded methylamine to bromide.

B3LYP/6-311++G//B3LYP/6-311++G****

Standard orientation:

Center Number	Atomic Number	Atomic Type	Coordinates (Angstroms) X	Y	Z
1	7	0	2.223502	0.768221	-0.120974
2	6	0	2.822876	-0.560110	0.021478
3	1	0	1.218444	0.655548	-0.295542
4	1	0	3.889047	-0.467983	0.262627
5	1	0	2.348858	-1.197583	0.783944
6	1	0	2.749266	-1.089801	-0.932717
7	35	0	-1.285129	-0.033507	0.003721
8	1	0	2.272113	1.255658	0.769395

```
Zero-point correction=                          0.064427 (Hartree/Particle)
Thermal correction to Energy=                   0.069978
Thermal correction to Enthalpy=                 0.070922
Thermal correction to Gibbs Free Energy=        0.033674
Sum of electronic and zero-point Energies=          -2670.078452
Sum of electronic and thermal Energies=             -2670.072900
Sum of electronic and thermal Enthalpies=           -2670.071956
Sum of electronic and thermal Free Energies=        -2670.109204

Version=AM64L-G03RevE.01\State=1-A\HF-2670.1428784\RMSD=7.307e-09\
RMSF=6.003e-07\PG=C01 [X(C1H5Br1N1)]\NImag=0\\@.
```

7.7.7 Methylammonium binding to bromide – adduct 3e

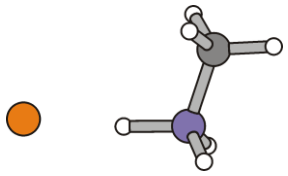

Figure S46. Minimum structure of hydrogen-bonded methylammonium to bromide.

B3LYP/6-311++G//B3LYP/6-311++G****

Standard orientation:

Center Number	Atomic Number	Atomic Type	Coordinates (Angstroms) X	Y	Z
1	7	0	1.766985	0.692964	0.000002
2	6	0	2.513497	-0.590966	-0.000001
3	1	0	0.611156	0.459952	0.000140
4	1	0	3.590666	-0.423747	-0.000192
5	1	0	2.218255	-1.154672	0.883406
6	1	0	2.217961	-1.154830	-0.883210
7	35	0	-1.143574	-0.044048	0.000000
8	1	0	1.968719	1.255093	0.825107
9	1	0	1.968471	1.254948	-0.825263

```
Zero-point correction=                          0.075569 (Hartree/Particle)
Thermal correction to Energy=                   0.080674
Thermal correction to Enthalpy=                 0.081618
Thermal correction to Gibbs Free Energy=        0.046169
Sum of electronic and zero-point Energies=          -2670.591809
Sum of electronic and thermal Energies=             -2670.586704
Sum of electronic and thermal Enthalpies=           -2670.585760
Sum of electronic and thermal Free Energies=        -2670.621209

Version=AM64L-G03RevE.01\State=1-A\HF-2670.6673783\RMSD=3.950e-09\
RMSF=9.124e-07\PG=C01 [X(C1H6Br1N1)]\NImag=0\\@.
```

7.7.8 *N*-Methylguanidinium binding to bromide – adduct 3f

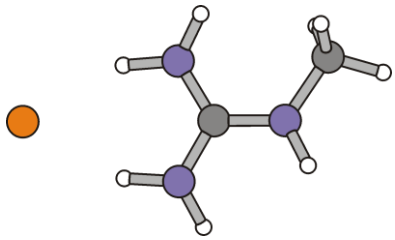

Figure S47. Minimum structure of hydrogen-bonded *N*-methylguanidinium to bromide.

B3LYP/6-311++G//B3LYP/6-311++G****

Standard orientation:

Center Number	Atomic Number	Atomic Type	Coordinates (Angstroms) X	Y	Z
1	7	0	0.623039	1.378705	-0.058293
2	6	0	1.417037	0.306071	-0.028940
3	7	0	0.867350	-0.901306	-0.040815
4	7	0	2.761354	0.461424	0.020158
5	6	0	3.709296	-0.644344	0.052760
6	1	0	0.969727	2.271398	0.254065
7	1	0	-0.405764	1.194115	-0.041778
8	1	0	1.413379	-1.724450	-0.230384
9	1	0	3.116722	1.379645	-0.192397
10	1	0	4.705366	-0.235973	0.216256
11	1	0	3.483361	-1.317004	0.883133
12	1	0	3.720646	-1.212316	-0.884047
13	1	0	-0.181392	-0.944760	-0.031430
14	35	0	-2.209778	-0.112936	0.012466

```
Zero-point correction=                          0.115499 (Hartree/Particle)
Thermal correction to Energy=                   0.124051
Thermal correction to Enthalpy=                 0.124995
Thermal correction to Gibbs Free Energy=        0.080819
Sum of electronic and zero-point Energies=          -2819.439123
Sum of electronic and thermal Energies=             -2819.430571
Sum of electronic and thermal Enthalpies=           -2819.429627
Sum of electronic and thermal Free Energies=        -2819.473803

Version=AM64L-G03RevE.01\State=1-A\HF-2819.5546221\RMSD=6.020e-09\
RMSF=3.574e-07\PG=C01 [X(C2H8Br1N3)]\NImag=0\\@.
```

7.7.9 Ammonia binding to bromide

Figure S48. Minimum structure of hydrogen-bonded ammonia to bromide.

B3LYP/6-311++G//B3LYP/6-311++G****

Standard orientation:

Center Number	Atomic Number	Atomic Type	Coordinates (Angstroms) X	Y	Z
1	35	0	-0.792884	0.000000	0.003552
2	7	0	2.845971	0.000000	-0.112319
3	1	0	2.996453	0.811091	0.482894
4	1	0	2.996613	-0.810987	0.482993
5	1	0	1.836068	-0.000101	-0.303984

Zero-point correction= 0.035428 (Hartree/Particle)
Thermal correction to Energy= 0.039985
Thermal correction to Enthalpy= 0.040929
Thermal correction to Gibbs Free Energy= 0.008084
Sum of electronic and zero-point Energies= -2630.795813
Sum of electronic and thermal Energies= -2630.791257
Sum of electronic and thermal Enthalpies= -2630.790313
Sum of electronic and thermal Free Energies= -2630.823158

Version=AM64L-G03RevE.01\State=1-A\HF=-2630.8312418\RMSD=1.134e-09\
RMSF=5.364e-07\PG=C01 [X(Br1H3N1)]\NImag=0\\@

7.8 Peroxides

7.8.1 Hydrogen peroxide

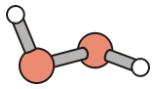

Figure S49. Minimum structure of hydrogen peroxide.

(*i*) B3LYP/6-311++G**//B3LYP/6-311++G**

Standard orientation:

Center Number	Atomic Number	Atomic Type	Coordinates (Angstroms) X	Y	Z
1	8	0	0.000000	0.727018	-0.051877
2	8	0	0.000000	-0.727018	-0.051877
3	1	0	0.828619	0.902776	0.415013
4	1	0	-0.828619	-0.902776	0.415013

```
Zero-point correction=                          0.026433 (Hartree/Particle)
Thermal correction to Energy=                   0.029676
Thermal correction to Enthalpy=                 0.030620
Thermal correction to Gibbs Free Energy=        0.004772
Sum of electronic and zero-point Energies=           -151.575737
Sum of electronic and thermal Energies=              -151.572494
Sum of electronic and thermal Enthalpies=            -151.571550
Sum of electronic and thermal Free Energies=         -151.597397

Version=AM64L-G03RevE.01\State=1-A\HF-151.6021696\RMSD=5.500e-09\
RMSF=2.567e-07\PG=C02 [X(H2O2)]\NImag=0\\@.
```

(*ii*) NBO-analysis – B3LYP/6-31G*// B3LYP/6-311++G**

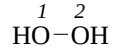

No.	(Occupancy)	Bond orbital/ Coefficients/ Hybrids			
1.	(1.99724)	**BD (1) O 1- O 2**			
	(50.00%)	0.7071* O 1	s(11.26%)	p(88.51%)	d(0.23%)
	(50.00%)	0.7071* O 2	s(11.26%)	p(88.51%)	d(0.23%)
6.	(1.99903)	**LP (1) O 1**	s(57.73%)	p(42.23%)	d(0.04%)
7.	(1.99595)	**LP (2) O 1**	s(9.19%)	p(90.72%)	d(0.09%)
8.	(1.99903)	**LP (1) O 2**	s(57.73%)	p(42.23%)	d(0.04%)
9.	(1.99595)	**LP (2) O 2**	s(9.19%)	p(90.72%)	d(0.09%)

Second order perturbation theory analysis of Fock-matrix for hydrogen peroxide acid in NBO-basis(threshold for printing: 0.50 kcal/mol)

Donor NBO (i)	Acceptor NBO (j)	kcal/mol	a.u.	a.u.
7. LP (2) O 1	34. BD*(1) O 2- H 4	1.00	0.81	0.025
9. LP (2) O 2	33. BD*(1) O 1- H 3	1.00	0.81	0.025

Natural bond orbital (NBO)-energies

	NBO	Occupancy	Energy
1.	BD (1) O 1- O 2	1.99724	-0.71945
6.	LP (1) O 1	1.99903	-0.66815
7.	LP (2) O 1	1.99595	-0.37222
8.	LP (1) O 2	1.99903	-0.66815
9.	LP (2) O 2	1.99595	-0.37222
32.	BD*(1) O 1- O 2	0.00268	0.08319

7.8.2 Orthovanadiumperoxoic acid *end-on*-(4) – *syn*/*syn*/*anticline*-conformation

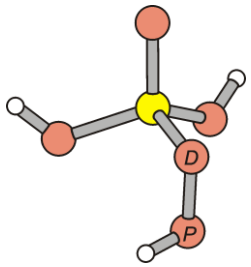

Figure S50. Minimum structure of orthovanadiumperoxoic acid *end-on*-**4** in the *syn*/*syn*/*anticline*-conformation [d(V,O^{P}) = 2.423 Å].

(*i*) B3LYP/6-311++G**//B3LYP/6-311++G**

Standard orientation:

Center Number	Atomic Number	Atomic Type	Coordinates (Angstroms) X	Y	Z
1	23	0	0.327470	0.006798	0.059580
2	8	0	1.416072	0.099083	1.183247
3	8	0	0.349790	1.502134	-0.911528
4	8	0	0.629329	-1.436240	-0.930438
5	8	0	-1.248223	-0.098755	0.954488
6	8	0	-2.068575	-0.192282	-0.242690
7	1	0	0.972220	2.222014	-0.761075
8	1	0	1.347443	-2.056961	-0.764658
9	1	0	-2.478606	0.687066	-0.269226

```
Zero-point correction=                          0.047829 (Hartree/Particle)
Thermal correction to Energy=                   0.056109
Thermal correction to Enthalpy=                 0.057054
Thermal correction to Gibbs Free Energy=        0.015482
Sum of electronic and zero-point Energies=          -1322.083077
Sum of electronic and thermal Energies=             -1322.074797
Sum of electronic and thermal Enthalpies=           -1322.073852
Sum of electronic and thermal Free Energies=        -1322.115424

Version=AM64L-G03RevE.01\State=1-A\HF-1322.1309061\RMSD=5.006e-09\
RMSF=4.839e-07\PG=C01 [X(H3O5V1)]\NImag=0\\@.
```

Mulliken-charges at oxygen (hydrogens and carbons omitted)

number	element symbol	partial charge
5	O^{D}	-0.211410
6	O^{P}	-0.195524

(*ii*) NBO-analysis – B3LYP/6-31G*// B3LYP/6-311++G**

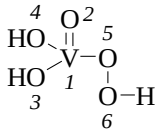


```
=======================================================================
No. (Occupancy) Bond orbital/ Coefficients/ Hybrids
=======================================================================
1.  (1.92471) BD (1) V  1- O  2
    (28.45%) 0.5334* V  1  s(27.81%)   p(0.11%)    d(71.78%)   f(0.30%)
    (71.55%) 0.8459* O  2  s(11.97%)   p(87.83%)   d(0.20%)
2.  (1.98530) BD (2) V  1- O  2
    (22.61%) 0.4755* V  1  s(0.05%)    p(1.03%)    d(98.73%)   f(0.19%)
    (77.39%) 0.8797* O  2  s(0.01%)    p(99.88%)   d(0.11%)
3.  (1.97283) BD (3) V  1- O  2
    (23.43%) 0.4840* V  1  s(0.01%)    p(0.94%)    d(98.86%)   f(0.19%)
    (76.57%) 0.8751* O  2  s(0.00%)    p(99.88%)   d(0.11%)
4.  (1.97253) BD (1) V  1- O  3
    (18.39%) 0.4289* V  1  s(25.67%)   p(0.52%)    d(73.63%)   f(0.18%)
    (81.61%) 0.9034* O  3  s(14.61%)   p(85.31%)   d(0.08%)
5.  (1.97484) BD (1) V  1- O  4
    (18.93%) 0.4351* V  1  s(23.03%)   p(0.50%)    d(76.30%)   f(0.17%)
    (81.07%) 0.9004* O  4  s(14.59%)   p(85.33%)   d(0.08%)
6.  (1.96634) BD (1) V  1- O  5
    (19.78%) 0.4447* V  1  s(22.24%)   p(0.17%)    d(77.38%)   f(0.21%)
    (80.22%) 0.8957* O  5  s(9.84%)    p(90.03%)   d(0.13%)
9.  (1.98616) BD (1) O  5- O  6
    (48.13%) 0.6937* O  5  s(9.75%)    p(90.03%)   d(0.23%)
    (51.87%) 0.7202* O  6  s(11.65%)   p(88.10%)   d(0.25%)
25. (1.97314) LP (1) O  2  s(88.03%)   p(11.97%)   d(0.00%)
26. (1.95180) LP (1) O  3  s(59.56%)   p(40.39%)   d(0.06%)
27. (1.81457) LP (2) O  3  s(0.13%)    p(99.80%)   d(0.07%)
28. (1.94973) LP (1) O  4  s(59.80%)   p(40.14%)   d(0.06%)
29. (1.80649) LP (2) O  4  s(0.02%)    p(99.92%)   d(0.07%)
30. (1.98384) LP (1) O  5  s(80.59%)   p(19.40%)   d(0.01%)
31. (1.83315) LP (2) O  5  s(0.05%)    p(99.87%)   d(0.09%)
32. (1.99371) LP (1) O  6  s(65.49%)   p(34.47%)   d(0.04%)
33. (1.95059) LP (2) O  6  s(0.93%)    p(98.97%)   d(0.10%)
116.(0.00971) BD*(1) O  5- O  6
    (51.87%) 0.7202* O  5  s(9.75%)    p(90.03%)   d(0.23%)
    (48.13%)-0.6937* O  6  s(11.65%)   p(88.10%)   d(0.25%)
=======================================================================
```

Second order perturbation theory analysis of Fock-matrix for *anticline*/*syn*/*syn*-orthovanadiumperoxoic acid *end*-*on*-**4** in NBO-basis(threshold for printing: 0.50 kcal/mol)

Donor NBO (i)	Acceptor NBO (j)	kcal/mol	a.u.	a.u.
9. BD (1) O 5- O 6	108. BD*(1) V 1- O 2	1.03	0.86	0.027
9. BD (1) O 5- O 6	110. BD*(3) V 1- O 2	2.68	0.67	0.039
25. LP (1) O 2	108. BD*(1) V 1- O 2	2.39	1.13	0.047
25. LP (1) O 2	111. BD*(1) V 1- O 3	1.98	1.06	0.043
25. LP (1) O 2	112. BD*(1) V 1- O 4	1.63	1.05	0.039
25. LP (1) O 2	113. BD*(1) V 1- O 5	1.45	1.04	0.036
26. LP (1) O 3	108. BD*(1) V 1- O 2	5.14	0.81	0.059
26. LP (1) O 3	109. BD*(2) V 1- O 2	6.74	0.62	0.059
26. LP (1) O 3	110. BD*(3) V 1- O 2	1.67	0.62	0.029
26. LP (1) O 3	112. BD*(1) V 1- O 4	1.18	0.73	0.027
26. LP (1) O 3	113. BD*(1) V 1- O 5	0.59	0.72	0.019
27. LP (2) O 3	109. BD*(2) V 1- O 2	1.64	0.25	0.018
27. LP (2) O 3	110. BD*(3) V 1- O 2	4.54	0.25	0.030
27. LP (2) O 3	112. BD*(1) V 1- O 4	10.96	0.36	0.056
27. LP (2) O 3	113. BD*(1) V 1- O 5	7.54	0.35	0.046
28. LP (1) O 4	108. BD*(1) V 1- O 2	4.84	0.80	0.057
28. LP (1) O 4	109. BD*(2) V 1- O 2	7.37	0.62	0.061
28. LP (1) O 4	110. BD*(3) V 1- O 2	2.39	0.62	0.035
28. LP (1) O 4	111. BD*(1) V 1- O 3	1.20	0.73	0.027
28. LP (1) O 4	113. BD*(1) V 1- O 5	0.86	0.71	0.023
29. LP (2) O 4	109. BD*(2) V 1- O 2	1.89	0.25	0.020
29. LP (2) O 4	110. BD*(3) V 1- O 2	4.54	0.24	0.030
29. LP (2) O 4	111. BD*(1) V 1- O 3	9.34	0.36	0.052
29. LP (2) O 4	113. BD*(1) V 1- O 5	9.55	0.34	0.051
30. LP (1) O 5	111. BD*(1) V 1- O 3	2.16	0.89	0.041
30. LP (1) O 5	112. BD*(1) V 1- O 4	2.28	0.88	0.042
30. LP (1) O 5	113. BD*(1) V 1- O 5	0.60	0.87	0.021
31. LP (2) O 5	109. BD*(2) V 1- O 2	3.65	0.26	0.028
31. LP (2) O 5	111. BD*(1) V 1- O 3	8.14	0.37	0.049
31. LP (2) O 5	112. BD*(1) V 1- O 4	8.52	0.37	0.050
31. LP (2) O 5	117. BD*(1) O 6- H 9	1.10	0.74	0.027
32. LP (1) O 6	108. BD*(1) V 1- O 2	0.97	0.86	0.026
33. LP (2) O 6	108. BD*(1) V 1- O 2	5.76	0.48	0.048
33. LP (2) O 6	110. BD*(3) V 1- O 2	1.91	0.29	0.021
33. LP (2) O 6	113. BD*(1) V 1- O 5	1.50	0.38	0.022

Natural bond orbital (NBO)-energies

NBO	Occupancy	Energy
1. BD (1) V 1- O 2	1.92471	-0.61105
2. BD (2) V 1- O 2	1.98530	-0.38023
3. BD (3) V 1- O 2	1.97283	-0.37799
4. BD (1) V 1- O 3	1.97253	-0.55318
5. BD (1) V 1- O 4	1.97484	-0.55310
6. BD (1) V 1- O 5	1.96634	-0.52736
9. BD (1) O 5- O 6	1.98616	-0.74469
25. LP (1) O 2	1.97314	-1.01454
26. LP (1) O 3	1.95180	-0.69438
27. LP (2) O 3	1.81457	-0.32297
28. LP (1) O 4	1.94973	-0.69123
29. LP (2) O 4	1.80649	-0.31796
30. LP (1) O 5	1.98384	-0.84683
31. LP (2) O 5	1.83315	-0.33364
32. LP (1) O 6	1.99371	-0.74230
33. LP (2) O 6	1.95059	-0.36239
116. BD*(1) O 5- O 6	0.00971	0.05778

7.8.3 Orthovanadiumperoxoic acid *end-on*-(4) – *syn*/*syn*/*antiperiplanar*-conformation

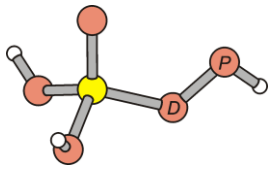

Figure S51. Structure of the *syn*/*syn*/*antiperiplanar*-conformer of orthovanadiumperoxoic acid *end-on*-(**4**) [d(V,O^{P}) = 2.814 Å].

(*i*) B3LYP/6-311++G**//B3LYP/6-311++G**

Standard orientation:

Center Number	Atomic Number	Atomic Type	Coordinates (Angstroms) X	Y	Z
1	8	0	0.222993	-0.000006	1.585806
2	23	0	0.361666	0.000000	0.027644
3	8	0	-2.450923	-0.000006	0.113642
4	8	0	-1.278600	-0.000005	-0.706170
5	8	0	1.236145	1.453364	-0.510950
6	8	0	1.236157	-1.453353	-0.510959
7	1	0	1.545157	2.145753	0.082987
8	1	0	1.545177	-2.145741	0.082975
9	1	0	-3.134821	0.000037	-0.572741

```
Zero-point correction=                          0.046901 (Hartree/Particle)
Thermal correction to Energy=                   0.055901
Thermal correction to Enthalpy=                 0.056845
Thermal correction to Gibbs Free Energy=        0.012681
Sum of electronic and zero-point Energies=          -1322.079642
Sum of electronic and thermal Energies=             -1322.070642
Sum of electronic and thermal Enthalpies=           -1322.069698
Sum of electronic and thermal Free Energies=        -1322.113863

Version=AM64L-G03RevE.01\State=1-A\HF-1322.1265433\RMSD=6.472e-09\
RMSF=1.876e-07\PG=C01 [X(H3O5V1)]\NImag=0\\@.

Mulliken-charges at oxygen (hydrogens and carbons omitted)
==========================================================================
number    element symbol      partial charge
==========================================================================
3               O^P               -0.255169
4               O^D               -0.213454
==========================================================================
```

(*ii*) NBO-analysis – B3LYP/6-31G*// B3LYP/6-311++G**

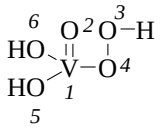

```
=======================================================================
No. (Occupancy) Bond orbital/ Coefficients/ Hybrids
=======================================================================
1.  (1.92518) BD (1) O  1- V  2
    (71.56%) 0.8459* O  1  s(10.71%)   p(89.10%)   d(0.19%)
    (28.44%) 0.5333* V  2  s(25.64%)   p(0.10%)    d(73.98%)   f(0.28%)
2.  (1.92482) BD (2) O  1- V  2
    (80.77%) 0.8987* O  1  s(0.00%)    p(99.89%)   d(0.11%)
    (19.23%) 0.4386* V  2  s(0.00%)    p(21.05%)   d(78.35%)   f(0.60%)
3.  (1.97414) BD (3) O  1- V  2
    (75.47%) 0.8687* O  1  s(0.73%)    p(99.15%)   d(0.12%)
    (24.53%) 0.4953* V  2  s(2.09%)    p(0.83%)    d(96.90%)   f(0.18%)
4.  (1.92803) BD (1) V  2- O  4
    (7.71%)  0.2777* V  2  s(0.00%)    p(37.23%)   d(61.72%)   f(1.05%)
    (92.29%) 0.9607* O  4  s(0.00%)    p(99.96%)   d(0.04%)
5.  (1.96742) BD (2) V  2- O  4
    (17.70%) 0.4207* V  2  s(23.11%)   p(0.36%)    d(76.33%)   f(0.20%)
    (82.30%) 0.9072* O  4  s(13.88%)   p(86.04%)   d(0.08%)
6.  (1.91813) BD (1) V  2- O  5
    (15.65%) 0.3956* V  2  s(23.83%)   p(15.12%)   d(60.64%)   f(0.41%)
    (84.35%) 0.9184* O  5  s(14.68%)   p(85.24%)   d(0.08%)
7.  (1.91813) BD (1) V  2- O  6
    (15.65%) 0.3956* V  2  s(23.83%)   p(15.12%)   d(60.64%)   f(0.41%)
    (84.35%) 0.9184* O  6  s(14.68%)   p(85.24%)   d(0.08%)
8.  (1.98438) BD (1) O  3- O  4
    (48.97%) 0.6998* O  3  s(11.75%)   p(87.98%)   d(0.27%)
    (51.03%) 0.7144* O  4  s(13.91%)   p(85.94%)   d(0.15%)
26. (1.97380) LP (1) O  1  s(88.58%)   p(11.42%)   d(0.00%)
27. (1.99337) LP (1) O  3  s(66.59%)   p(33.38%)   d(0.04%)
28. (1.96798) LP (2) O  3  s(0.00%)    p(99.90%)   d(0.10%)
29. (1.96922) LP (1) O  4  s(72.54%)   p(27.43%)   d(0.03%)
30. (1.95006) LP (1) O  5  s(59.50%)   p(40.44%)   d(0.06%)
31. (1.81386) LP (2) O  5  s(0.00%)    p(99.93%)   d(0.07%)
32. (1.95006) LP (1) O  6  s(59.50%)   p(40.44%)   d(0.06%)
33. (1.81386) LP (2) O  6  s(0.00%)    p(99.93%)   d(0.07%)
114.(0.01322) BD*(1) O  3- O  4
    (51.03%) 0.7144* O  3  s(11.75%)   p(87.98%)   d(0.27%)
    (48.97%)-0.6998* O  4  s(13.91%)   p(85.94%)   d(0.15%)
=======================================================================
```

Second order perturbation theory analysis of Fock-matrix for *syn*/*syn*/*antiperiplanar*-orthovanadiumperoxoic acid *end*-*on*-(**4**) in NBO-basis(threshold for printing: 0.50 kcal/mol)

Donor NBO (i)	Acceptor NBO (j)	kcal/mol	a.u.	a.u.
26. LP (1) O 1	107. BD*(1) O 1- V 2	2.58	1.13	0.049
26. LP (1) O 1	109. BD*(3) O 1- V 2	0.55	0.96	0.021
26. LP (1) O 1	111. BD*(2) V 2- O 4	1.55	1.06	0.038
26. LP (1) O 1	112. BD*(1) V 2- O 5	1.68	1.18	0.041
26. LP (1) O 1	113. BD*(1) V 2- O 6	1.68	1.18	0.041
28. LP (2) O 3	110. BD*(1) V 2- O 4	1.38	0.51	0.025
29. LP (1) O 4	107. BD*(1) O 1- V 2	1.66	0.90	0.035
29. LP (1) O 4	109. BD*(3) O 1- V 2	8.33	0.73	0.071
29. LP (1) O 4	112. BD*(1) V 2- O 5	1.09	0.95	0.029
29. LP (1) O 4	113. BD*(1) V 2- O 6	1.09	0.95	0.029
30. LP (1) O 5	107. BD*(1) O 1- V 2	6.64	0.80	0.066
30. LP (1) O 5	108. BD*(2) O 1- V 2	6.74	0.76	0.065
30. LP (1) O 5	109. BD*(3) O 1- V 2	0.53	0.63	0.017
30. LP (1) O 5	111. BD*(2) V 2- O 4	0.92	0.72	0.024
30. LP (1) O 5	113. BD*(1) V 2- O 6	1.13	0.85	0.028
31. LP (2) O 5	109. BD*(3) O 1- V 2	3.78	0.26	0.028
31. LP (2) O 5	110. BD*(1) V 2- O 4	3.05	0.49	0.035
31. LP (2) O 5	111. BD*(2) V 2- O 4	9.42	0.35	0.051
31. LP (2) O 5	113. BD*(1) V 2- O 6	4.23	0.47	0.041
32. LP (1) O 6	107. BD*(1) O 1- V 2	6.64	0.80	0.066
32. LP (1) O 6	108. BD*(2) O 1- V 2	6.74	0.76	0.065
32. LP (1) O 6	109. BD*(3) O 1- V 2	0.53	0.63	0.017
32. LP (1) O 6	111. BD*(2) V 2- O 4	0.92	0.72	0.024
32. LP (1) O 6	112. BD*(1) V 2- O 5	1.13	0.85	0.028
33. LP (2) O 6	109. BD*(3) O 1- V 2	3.78	0.26	0.028
33. LP (2) O 6	110. BD*(1) V 2- O 4	3.05	0.49	0.035
33. LP (2) O 6	111. BD*(2) V 2- O 4	9.42	0.35	0.051
33. LP (2) O 6	112. BD*(1) V 2- O 5	4.23	0.47	0.041

Natural bond orbital (NBO)-energies

NBO	Occupancy	Energy
1. BD (1) O 1- V 2	1.92518	-0.58732
2. BD (2) O 1- V 2	1.92482	-0.34176
3. BD (3) O 1- V 2	1.97414	-0.39352
4. BD (1) V 2- O 4	1.92803	-0.33146
5. BD (2) V 2- O 4	1.96742	-0.55152
6. BD (1) V 2- O 5	1.91813	-0.52029
7. BD (1) V 2- O 6	1.91813	-0.52029
8. BD (1) O 3- O 4	1.98438	-0.77142
26. LP (1) O 1	1.97380	-1.01890
27. LP (1) O 3	1.99337	-0.73787
28. LP (2) O 3	1.96798	-0.33845
29. LP (1) O 4	1.96922	-0.78653
30. LP (1) O 5	1.95006	-0.68677
31. LP (2) O 5	1.81386	-0.31536
32. LP (1) O 6	1.95006	-0.68677
33. LP (2) O 6	1.81386	-0.31536
114. BD*(1) O 3- O 4	0.01322	0.08934

7.8.4 Orthovanadiumperoxoic acid *side-on*-(4) – *syn*/*syn*/*anticline*-conformation

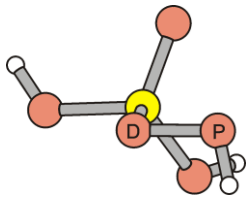

Figure S52. Structure of the *syn*/*syn*/*anticline*-conformer of orthovanadiumperoxoic acid *side-on*-(**4**) at $d(V,O^P)$ = 2.270 Å.

(*i*) B3LYP/6-311++G**//B3LYP/6-311++G**

Standard orientation:

Center Number	Atomic Number	Atomic Type	Coordinates (Angstroms) X	Y	Z
1	8	0	-0.439554	0.034921	1.611940
2	23	0	-0.268022	0.024189	0.052437
3	8	0	-0.213365	1.673403	-0.630493
4	8	0	1.998767	-0.074673	0.107673
5	8	0	1.111598	-1.081247	-0.472430
6	8	0	-1.658744	-0.812575	-0.653136
7	1	0	-2.305979	-1.304783	-0.135368
8	1	0	-0.282224	2.472720	-0.097050
9	1	0	2.363078	0.357087	-0.682075

```
Zero-point correction=                          0.047806 (Hartree/Particle)
Thermal correction to Energy=                   0.056090
Thermal correction to Enthalpy=                 0.057034
Thermal correction to Gibbs Free Energy=        0.015257
Sum of electronic and zero-point Energies=          -1322.075949
Sum of electronic and thermal Energies=             -1322.067666
Sum of electronic and thermal Enthalpies=           -1322.066722
Sum of electronic and thermal Free Energies=        -1322.108499

Version=AM64L-G03RevE.01\State=1-A\HF-1322.1237556\RMSD=8.106e-09\
RMSF=3.103e-07\PG=C01 [X(H3O5V1)]\NImag=0\\@.

Mulliken-charges at oxygen (hydrogens and carbons omitted)
==========================================================================
number    element symbol      partial charge
==========================================================================
4               O^P              -0.131085
5               O^D              -0.266535
==========================================================================
```

(*ii*) NBO-analysis – B3LYP/6-31G*// B3LYP/6-311++G**

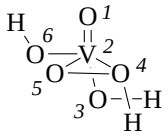

```
=======================================================================
No. (Occupancy) Bond orbital/ Coefficients/ Hybrids
=======================================================================
1.  (1.93022) BD (1) O  1- V  2
    (70.21%) 0.8379* O  1  s(10.86%)   p(88.94%)   d(0.20%)
    (29.79%) 0.5458* V  2  s(22.40%)   p(1.26%)    d(76.07%)   f(0.27%)
2.  (1.97783) BD (2) O  1- V  2
    (77.08%) 0.8780* O  1  s(0.03%)    p(99.85%)   d(0.12%)
    (22.92%) 0.4788* V  2  s(0.24%)    p(3.06%)    d(96.44%)   f(0.25%)
3.  (1.90781) BD (3) O  1- V  2
    (81.02%) 0.9001* O  1  s(0.07%)    p(99.82%)   d(0.11%)
    (18.98%) 0.4356* V  2  s(0.94%)    p(23.54%)   d(74.92%)   f(0.60%)
4.  (1.91961) BD (1) V  2- O  3
    (15.62%) 0.3953* V  2  s(20.50%)   p(17.34%)   d(61.86%)   f(0.29%)
    (84.38%) 0.9186* O  3  s(14.19%)   p(85.73%)   d(0.08%)
5.  (1.91202) BD (1) V  2- O  5
    (16.33%) 0.4041* V  2  s(21.27%)   p(14.92%)   d(63.49%)   f(0.32%)
    (83.67%) 0.9147* O  5  s(8.48%)    p(91.39%)   d(0.14%)
6.  (1.95978) BD (1) V  2- O  6
    (17.32%) 0.4162* V  2  s(33.87%)   p(0.78%)    d(65.11%)   f(0.24%)
    (82.68%) 0.9093* O  6  s(15.84%)   p(84.08%)   d(0.08%)
7.  (1.94062) BD (2) V  2- O  6
    (9.52%)  0.3086* V  2  s(0.31%)    p(29.60%)   d(69.60%)   f(0.48%)
    (90.48%) 0.9512* O  6  s(0.20%)    p(99.74%)   d(0.07%)
9.  (1.98391) BD (1) O  4- O  5
    (54.18%) 0.7360* O  4  s(12.14%)   p(87.62%)   d(0.23%)
    (45.82%) 0.6769* O  5  s(8.22%)    p(91.52%)   d(0.26%)
26. (1.97121) LP (1) O  1  s(89.06%)   p(10.94%)   d(0.00%)
27. (1.94928) LP (1) O  3  s(60.15%)   p(39.79%)   d(0.06%)
28. (1.82581) LP (2) O  3  s(0.03%)    p(99.91%)   d(0.06%)
29. (1.99488) LP (1) O  4  s(62.07%)   p(37.89%)   d(0.04%)
30. (1.90942) LP (2) O  4  s(3.72%)    p(96.19%)   d(0.10%)
31. (1.98512) LP (1) O  5  s(83.50%)   p(16.49%)   d(0.01%)
32. (1.88956) LP (2) O  5  s(0.04%)    p(99.87%)   d(0.09%)
33. (1.94977) LP (1) O  6  s(58.15%)   p(41.79%)   d(0.06%)
=======================================================================
```

Second order perturbation theory analysis of Fock-matrix for *syn*/*syn*/*anti*-orthovanadiumperoxoic acid *side*-*on*-(**4**) in NBO-basis(threshold for printing: 0.50 kcal/mol)

Donor NBO (i)	Acceptor NBO (j)	kcal/mol	a.u.	a.u.
26. LP (1) O 1	107. BD*(1) O 1- V 2	1.94	1.11	0.042
26. LP (1) O 1	110. BD*(1) V 2- O 3	1.34	1.15	0.036
26. LP (1) O 1	111. BD*(1) V 2- O 5	3.18	1.15	0.056
26. LP (1) O 1	112. BD*(1) V 2- O 6	2.75	1.10	0.051
27. LP (1) O 3	107. BD*(1) O 1- V 2	4.16	0.79	0.052
27. LP (1) O 3	109. BD*(3) O 1- V 2	10.76	0.79	0.084
27. LP (1) O 3	111. BD*(1) V 2- O 5	1.24	0.83	0.029
27. LP (1) O 3	112. BD*(1) V 2- O 6	1.58	0.78	0.032
28. LP (2) O 3	108. BD*(2) O 1- V 2	6.44	0.26	0.037
28. LP (2) O 3	111. BD*(1) V 2- O 5	4.78	0.45	0.042
28. LP (2) O 3	112. BD*(1) V 2- O 6	4.88	0.40	0.039
28. LP (2) O 3	113. BD*(2) V 2- O 6	3.99	0.41	0.036
29. LP (1) O 4	112. BD*(1) V 2- O 6	2.12	0.81	0.039
30. LP (2) O 4	111. BD*(1) V 2- O 5	0.55	0.53	0.015
30. LP (2) O 4	112. BD*(1) V 2- O 6	14.68	0.47	0.076
30. LP (2) O 4	113. BD*(2) V 2- O 6	1.56	0.49	0.025
31. LP (1) O 5	107. BD*(1) O 1- V 2	1.91	0.95	0.039
31. LP (1) O 5	109. BD*(3) O 1- V 2	0.74	0.95	0.024
31. LP (1) O 5	110. BD*(1) V 2- O 3	3.54	1.00	0.054
31. LP (1) O 5	112. BD*(1) V 2- O 6	0.90	0.94	0.027
32. LP (2) O 5	107. BD*(1) O 1- V 2	6.24	0.42	0.046
32. LP (2) O 5	108. BD*(2) O 1- V 2	6.63	0.27	0.038
32. LP (2) O 5	109. BD*(3) O 1- V 2	0.54	0.42	0.013
32. LP (2) O 5	110. BD*(1) V 2- O 3	2.61	0.46	0.031
32. LP (2) O 5	116. BD*(1) O 4- H 9	1.01	0.73	0.025
33. LP (1) O 6	107. BD*(1) O 1- V 2	4.00	0.78	0.051
33. LP (1) O 6	108. BD*(2) O 1- V 2	7.24	0.63	0.062
33. LP (1) O 6	109. BD*(3) O 1- V 2	1.09	0.78	0.026
33. LP (1) O 6	112. BD*(1) V 2- O 6	0.62	0.77	0.020

Natural bond orbital (NBO)-energies

NBO	Occupancy	Energy
1. BD (1) O 1- V 2	1.93022	-0.59220
2. BD (2) O 1- V 2	1.97783	-0.36890
3. BD (3) O 1- V 2	1.90781	-0.33403
4. BD (1) V 2- O 3	1.91961	-0.51932
5. BD (1) V 2- O 5	1.91202	-0.47144
6. BD (1) V 2- O 6	1.95978	-0.56293
7. BD (2) V 2- O 6	1.94062	-0.33520
9. BD (1) O 4- O 5	1.98391	-0.73762
26. LP (1) O 1	1.97121	-1.01725
27. LP (1) O 3	1.94928	-0.69820
28. LP (2) O 3	1.82581	-0.32149
29. LP (1) O 4	1.99488	-0.73146
30. LP (2) O 4	1.90942	-0.39549
31. LP (1) O 5	1.98512	-0.86188
32. LP (2) O 5	1.88956	-0.32815
33. LP (1) O 6	1.94977	-0.68665
115. BD*(1) O 4- O 5	0.00666	0.04939

7.8.5 Orthovanadiumperoxoic acid *side-on*-(4)^{activated} – *syn*/*syn*/*anticline*-conformation

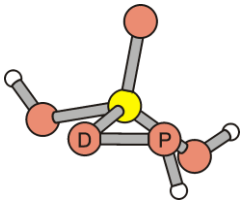

Figure S53. Structure of the *syn*/*syn*/*anticline*-conformer of orthovanadiumperoxoic acid *side-on*-(**4**)^{activated} at $d(V,O^P)$ = 1.876 Å.

(*i*) B3LYP/6-311++G**//B3LYP/6-311++G**

Standard orientation:

Center Number	Atomic Number	Atomic Type	Coordinates (Angstroms) X	Y	Z
1	8	0	-0.544806	0.027307	1.599170
2	23	0	-0.185354	0.021899	0.074853
3	8	0	-0.277327	1.673700	-0.647265
4	8	0	1.686415	0.147281	0.063184
5	8	0	1.208640	-1.172508	-0.314854
6	8	0	-1.448835	-0.929463	-0.765638
7	1	0	-2.108749	-1.431899	-0.275703
8	1	0	-0.679110	2.412733	-0.178418
9	1	0	2.058301	0.544947	-0.744265

```
Zero-point correction=                          0.048488 (Hartree/Particle)
Thermal correction to Energy=                   0.056463
Thermal correction to Enthalpy=                 0.057407
Thermal correction to Gibbs Free Energy=        0.016223
Sum of electronic and zero-point Energies=          -1322.062986
Sum of electronic and thermal Energies=             -1322.055011
Sum of electronic and thermal Enthalpies=           -1322.054067
Sum of electronic and thermal Free Energies=        -1322.095251

Version=AM64L-G03RevE.01\State=1-A\HF-1322.111474\RMSD=3.885e-09\
RMSF=1.504e-02\PG=C01 [X(H3O5V1)]\NImag=0\\@.

Mulliken-charges at oxygen (hydrogens and carbons omitted)
==========================================================================
number    element symbol      partial charge
==========================================================================
1               O^D               -0.277249
2               O^P               -0.052604
==========================================================================
```

(*ii*) NBO-analysis – B3LYP/6-31G*// B3LYP/6-311++G**

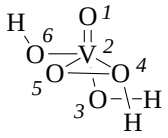

Natural bond orbital (NBO)-energies

NBO	Occupancy	Energy
1. BD (1) O 1- V 2	1.93545	-0.60270
2. BD (2) O 1- V 2	1.92119	-0.33806
3. BD (3) O 1- V 2	1.90088	-0.31570
4. BD (1) V 2- O 3	1.89942	-0.49825
5. BD (1) V 2- O 4	1.88610	-0.54056
6. BD (1) V 2- O 5	1.88229	-0.44427
7. BD (1) V 2- O 6	1.86872	-0.48569
8. BD (2) V 2- O 6	1.94999	-0.32168
28. LP (1) O 3	1.95620	-0.67738
29. LP (2) O 3	1.83018	-0.31702
30. LP (1) O 4	1.98433	-0.70032
31. LP (1) O 5	1.98703	-0.89490
32. LP (2) O 5	1.92099	-0.33194
33. LP (1) O 6	1.95612	-0.65951
115. BD*(1) O 4- O 5	0.03117	0.02557

Table S6. Selected bond lengths, angles, and orbital energies computed for structures associated with change in peroxide binding from end-on to side-on in orthovanadiumperoxoic acid – part 1. [a]

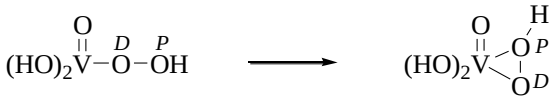

end-on-**4** *side-on*-**4**

entry	d (V,O^P) / Å	d (O^D,O^P) / Å	α [b] / deg	ω [b] / deg	E (**4**) / a.u.	E^{rel} / kJ mol^{-1}	$E\sigma$(O^D,O^P) / a.u.	$E\sigma$*(O^D,O^P) / a.u.	$E\sigma$(V,O^D) / a.u.	$E\sigma$(V,O^P) / a.u.
1 [c]	2.432	1.454	36.7	–179.2	–1322.1309061	≡0.0	–0.74469	0.05778	0.52736	– [d]
2 [d]	2.814	1.431	25.6	0.0	–1322.1265433	11.5	–0.77142	0.08934	0.52029	– [d]
3	2.776	1.429	26.9	0.0	–1322.1264232	11.9	–0.77195	0.09063	0.55167	– [d]
4	2.726	1.428	28.3	0.0	–1322.1258906	13.3	–0.77212	0.09149	–0.55169	– [d]
5	2.676	1.428	29.6	0.0	–1322.1249224	15.9	–0.77145	0.09151	–0.55140	– [d]
6	2.626	1.442	31.6	–43.6	–1322.1245704	16.8	–0.74981	0.08074	–0.49856	– [d]
7	2.576	1.447	33.1	–50.8	–1322.1242322	17.7	–0.74520	0.07472	–0.49427	– [d]
8	2.526	1.450	34.4	–55.7	–1322.1239943	18.3	–0.74164	0.06986	–0.49000	– [d]
9	2.476	1.454	35.6	–59.5	–1322.1238352	18.7	–0.73854	0.06588	–0.48562	– [d]
10	2.426	1.456	36.8	–62.7	–1322.1237472	18.9	–0.73722	0.06116	–0.48340	– [d]
11	2.376	1.459	37.9	–65.5	–1322.1237203	19.0	–0.73643	0.05705	–0.50601	– [d]
12	2.326	1.460	38.9	–68.0	–1322.1237347	19.0	–0.73600	–0.50229	–0.50229	– [d]

[a] Orbital energies from NBO calculations; geometric parameters from energy function minimization (B3LYP/6-311++G**); 1 atom unit (a.u.) = 2625.5 kJ mol^{-1}; deg = degrees. [b] α = (O^D,V,O^P); ω = O^A,V,O^D,O^P. [c] *syn*/*syn*/*anticline*-conformation of *end-on*-**4**. [d] Below threshold of 0.5 kcal mol^{-1}. [e] *syn*/*syn*/*antiplanar*-conformation of *end-on*-**4**.

Table S7. Selected bond lengths, angles, and orbital energies computed for structures associated with change in peroxide binding from end-on to side-on in orthovanadiumperoxoic acid – part 2. [a]

end-on-**4** *side-on*-**4**

entry	d (V,O^P) / Å	d (O^D,O^P) / Å	α [b] / deg	ω [b] / deg	E (**4**) / a.u.	E^{rel} / kJ mol^{-1}	$E\sigma$(O^D,O^P) / a.u.	$E\sigma^*$(O^D,O^P) / a.u.	$E\sigma$(V,O^D) / a.u.	$E\sigma$(V,O^P) / a.u.
13	2.270	1.462	40.0	–70.7	–1322.1237556	18.8	–0.73762	0.04939	–0.47144	–0.39549
14	2.226	1.462	40.8	–72.6	–1322.1237256	19.0	–0.73915	0.04672	–0.46809	–0.40508
15	2.176	1.462	41.6	–74.8	–1322.1235658	19.4	–0.74209	0.04337	–0.46507	–0.41744
16	2.126	1.462	42.4	–76.8	–1322.1231690	20.5	–0.74502	0.04128	–0.46029	–0.43045
17	2.076	1.461	43.2	–78.9	–1322.1223975	22.5	–0.74842	0.03906	–0.45701	–0.44371
18	2.026	1.459	43.8	–81.0	–1322.1210793	25.9	–0.75244	0.03710	–0.45286	–0.45882
19	1.976	1.458	44.5	–83.1	–1322.1190017	31.4	–0.75673	0.03524	–0.44869	–0.47519
20	1.926	1.457	45.0	–85.3	–1322.1159049	39.3	–0.76117	0.03336	–0.44444	–0.49296
21	1.876	1.454	45.6	–87.6	–1322.1114740	51.2	–0.72711	0.02557	–0.44427	–0.54056
22	1.826	1.452	46.1	–89.9	–1322.1053239	67.3	–0.73006	0.02295	–0.43951	–0.56663
23	1.776	1.450	46.5	–92.1	–1322.0969839	89.2	–0.73248	0.01966	–0.43486	–0.59530

[a] Orbital energies from NBO calculations; geometric parameters from energy function minimization (B3LYP/6-311++G**); 1 atom unit (a.u.) = 2625.5 kJ mol^{-1}; deg = degrees. [b] α = (O^D,V,O^P); ω = O^A,V,O^D,O^P. [c] Below threshold of 0.5 kcal mol^{-1}.

7.8.6 Hydrogen orthoperoxovandate (5)

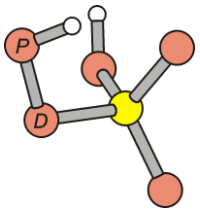

Figure S54. Minimum structure of hydroperoxyhydrogen orthovandate (**5**).

(*i*) B3LYP/6-311++G**//B3LYP/6-311++G**

Standard orientation:

Center Number	Atomic Number	Atomic Type	Coordinates (Angstroms) X	Y	Z
1	23	0	0.406082	-0.089938	0.016882
2	8	0	-0.003080	-0.171622	1.600143
3	8	0	1.001742	1.610872	-0.412232
4	8	0	1.490779	-1.200576	-0.429130
5	8	0	-1.212026	-0.478498	-0.833259
6	8	0	-2.274120	0.208517	-0.097178
7	1	0	0.635811	2.290282	0.162173
8	1	0	-2.002059	0.028751	0.822789

```
Zero-point correction=                          0.036721 (Hartree/Particle)
Thermal correction to Energy=                   0.044407
Thermal correction to Enthalpy=                 0.045351
Thermal correction to Gibbs Free Energy=        0.004659
Sum of electronic and zero-point Energies=          -1321.570739
Sum of electronic and thermal Energies=             -1321.563054
Sum of electronic and thermal Enthalpies=           -1321.562109
Sum of electronic and thermal Free Energies=        -1321.602801

Version=AM64L-G03RevE.01\State=1-A\HF-1321.6074604\RMSD=4.060e-09\
RMSF=1.632e-07\ PG=C01 [X(H2O5V1)]\NImag=0\\@.
```

(*ii*) NBO-analysis – B3LYP/6-31G*// B3LYP/6-311++G**

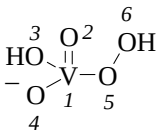


```
=======================================================================
No. (Occupancy) Bond orbital/ Coefficients/ Hybrids
=======================================================================
1.  (1.90266) BD (1) V  1- O  2
    (23.81%) 0.4880* V  1  s(22.30%)   p(6.04%)    d(70.17%)   f(1.49%)
    (76.19%) 0.8729* O  2  s(11.08%)   p(88.78%)   d(0.14%)
2.  (1.89296) BD (2) V  1- O  2
    (12.36%) 0.3516* V  1  s(0.70%)    p(30.57%)   d(64.02%)   f(4.71%)
    (87.64%) 0.9361* O  2  s(0.85%)    p(99.07%)   d(0.07%)
3.  (1.88579) BD (3) V  1- O  2
    (14.29%) 0.3780* V  1  s(2.70%)    p(21.71%)   d(71.31%)   f(4.28%)
    (85.71%) 0.9258* O  2  s(0.02%)    p(99.91%)   d(0.07%)
4.  (1.93701) BD (1) V  1- O  3
    (12.72%) 0.3567* V  1  s(30.81%)   p(14.32%)   d(54.47%)   f(0.41%)
    (87.28%) 0.9342* O  3  s(15.05%)   p(84.87%)   d(0.08%)
5.  (1.89244) BD (1) V  1- O  4
    (25.10%) 0.5010* V  1  s(17.97%)   p(5.93%)    d(73.71%)   f(2.40%)
    (74.90%) 0.8654* O  4  s(11.43%)   p(88.41%)   d(0.16%)
6.  (1.88332) BD (2) V  1- O  4
    (11.63%) 0.3411* V  1  s(1.01%)    p(28.56%)   d(63.61%)   f(6.81%)
    (88.37%) 0.9400* O  4  s(0.02%)    p(99.90%)   d(0.08%)
7.  (1.87865) BD (3) V  1- O  4
    (16.27%) 0.4034* V  1  s(0.52%)    p(32.96%)   d(64.98%)   f(1.54%)
    (83.73%) 0.9150* O  4  s(0.02%)    p(99.89%)   d(0.09%)
8.  (1.93334) BD (1) V  1- O  5
    (13.56%) 0.3682* V  1  s(27.51%)   p(12.18%)   d(59.92%)   f(0.38%)
    (86.44%) 0.9297* O  5  s(12.24%)   p(87.67%)   d(0.09%)
10. (1.98746) BD (1) O  5- O  6
    (48.04%) 0.6931* O  5  s(11.20%)   p(88.62%)   d(0.18%)
    (51.96%) 0.7208* O  6  s(12.17%)   p(87.58%)   d(0.25%)
26. (1.97542) LP (1) O  2  s(88.05%)   p(11.95%)   d(0.00%)
27. (1.97199) LP (1) O  3  s(60.69%)   p(39.27%)   d(0.05%)
28. (1.86803) LP (2) O  3  s(0.23%)    p(99.70%)   d(0.08%)
29. (1.97535) LP (1) O  4  s(88.53%)   p(11.47%)   d(0.00%)
30. (1.98179) LP (1) O  5  s(76.80%)   p(23.19%)   d(0.01%)
31. (1.87284) LP (2) O  5  s(0.07%)    p(99.88%)   d(0.05%)
32. (1.99394) LP (1) O  6  s(61.85%)   p(38.12%)   d(0.03%)
33. (1.98344) LP (2) O  6  s(2.50%)    p(97.41%)   d(0.09%)
114.(0.01627) BD*(1) O  5- O  6
    (51.96%) 0.7208* O  5  s(11.20%)   p(88.62%)   d(0.18%)
    (48.04%)-0.6931* O  6  s(12.17%)   p(87.58%)   d(0.25%)
=======================================================================
```

Second order perturbation theory analysis of Fock-matrix for the *syncline*/*syn*-conformer of hydrogen orthoperoxovandate (**5**) in NBO-basis(threshold for printing: 0.50 kcal/mol)

Donor NBO (i)	Acceptor NBO (j)	kcal/mol	a.u.	a.u.
10. BD (1) O 5- O 6	109. BD*(1) V 1- O 4	0.59	0.89	0.021
10. BD (1) O 5- O 6	111. BD*(3) V 1- O 4	1.18	0.86	0.029
26. LP (1) O 2	105. BD*(1) V 1- O 2	0.93	1.10	0.029
26. LP (1) O 2	107. BD*(3) V 1- O 2	1.72	1.10	0.040
26. LP (1) O 2	108. BD*(1) V 1- O 3	3.02	1.10	0.053
26. LP (1) O 2	109. BD*(1) V 1- O 4	2.41	1.10	0.047
26. LP (1) O 2	110. BD*(2) V 1- O 4	3.35	1.21	0.059
26. LP (1) O 2	112. BD*(1) V 1- O 5	1.46	1.10	0.037
26. LP (1) O 2	115. BD*(1) O 6- H 8	1.21	1.33	0.036
27. LP (1) O 3	105. BD*(1) V 1- O 2	3.68	0.85	0.051
27. LP (1) O 3	106. BD*(2) V 1- O 2	2.34	0.91	0.042
27. LP (1) O 3	112. BD*(1) V 1- O 5	1.75	0.85	0.035
28. LP (2) O 3	105. BD*(1) V 1- O 2	2.98	0.47	0.034
28. LP (2) O 3	106. BD*(2) V 1- O 2	1.46	0.53	0.025
28. LP (2) O 3	109. BD*(1) V 1- O 4	2.14	0.47	0.028
28. LP (2) O 3	110. BD*(2) V 1- O 4	2.80	0.57	0.036
28. LP (2) O 3	112. BD*(1) V 1- O 5	2.30	0.47	0.029
29. LP (1) O 4	105. BD*(1) V 1- O 2	2.75	1.12	0.051
29. LP (1) O 4	106. BD*(2) V 1- O 2	3.56	1.18	0.060
29. LP (1) O 4	107. BD*(3) V 1- O 2	1.22	1.11	0.034
29. LP (1) O 4	108. BD*(1) V 1- O 3	4.59	1.12	0.066
29. LP (1) O 4	109. BD*(1) V 1- O 4	0.76	1.12	0.027
29. LP (1) O 4	110. BD*(2) V 1- O 4	0.56	1.22	0.024
29. LP (1) O 4	111. BD*(3) V 1- O 4	0.55	1.09	0.023
29. LP (1) O 4	112. BD*(1) V 1- O 5	3.01	1.12	0.053
30. LP (1) O 5	107. BD*(3) V 1- O 2	1.69	0.95	0.037
30. LP (1) O 5	108. BD*(1) V 1- O 3	2.52	0.95	0.045
30. LP (1) O 5	115. BD*(1) O 6- H 8	1.11	1.19	0.033
31. LP (2) O 5	105. BD*(1) V 1- O 2	1.27	0.48	0.022
31. LP (2) O 5	107. BD*(3) V 1- O 2	4.55	0.47	0.042
31. LP (2) O 5	108. BD*(1) V 1- O 3	2.68	0.47	0.032
31. LP (2) O 5	109. BD*(1) V 1- O 4	0.99	0.47	0.019
31. LP (2) O 5	110. BD*(2) V 1- O 4	0.56	0.58	0.016
31. LP (2) O 5	111. BD*(3) V 1- O 4	1.34	0.45	0.022
33. LP (2) O 6	109. BD*(1) V 1- O 4	0.50	0.52	0.015

Natural bond orbital (NBO)-energies

NBO	Occupancy	Energy
1. BD (1) V 1- O 2	1.90266	-0.30981
2. BD (2) V 1- O 2	1.89296	-0.10499
3. BD (3) V 1- O 2	1.88579	-0.09842
4. BD (1) V 1- O 3	1.93701	-0.31424
5. BD (1) V 1- O 4	1.89244	-0.31984
6. BD (2) V 1- O 4	1.88332	-0.08819
7. BD (3) V 1- O 4	1.87865	-0.09740
8. BD (1) V 1- O 5	1.93334	-0.30258
10. BD (1) O 5- O 6	1.98746	-0.53783
114. BD*(1) O 5- O 6	0.01627	0.25584

7.8.7 Metavanadiumperoxoic acid (6)

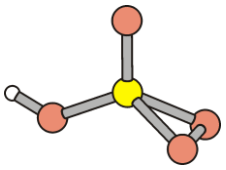

Figure S55. Minimum structure of metavanadiumperoxoic acid (**6**).

(*i*) B3LYP/6-311++G**//B3LYP/6-311++G**

Standard orientation:

Center Number	Atomic Number	Atomic Type	Coordinates (Angstroms) X	Y	Z
1	23	0	-0.157616	0.080495	-0.000012
2	8	0	-0.575749	1.596072	0.000000
3	8	0	1.424671	-0.325595	0.726490
4	8	0	1.424691	-0.325628	-0.726468
5	8	0	-1.513275	-1.067005	0.000013
6	1	0	-2.457529	-0.874132	0.000001

```
Zero-point correction=                          0.022505 (Hartree/Particle)
Thermal correction to Energy=                   0.028358
Thermal correction to Enthalpy=                 0.029303
Thermal correction to Gibbs Free Energy=       -0.007133
Sum of electronic and zero-point Energies=          -1245.596667
Sum of electronic and thermal Energies=             -1245.590814
Sum of electronic and thermal Enthalpies=           -1245.589870
Sum of electronic and thermal Free Energies=        -1245.626305

Version=AM64L-G03RevE.01\State=1-A\HF-1245.6191724\RMSD=4.475e-09\
RMSF=2.397e-06\ PG=C01 [X(H1O4V1)]\NImag=0\\@.
```

(*ii*) NBO-analysis – B3LYP/6-31G*// B3LYP/6-311++G**

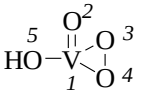


```
=======================================================================
No. (Occupancy) Bond orbital/ Coefficients/ Hybrids
=======================================================================
1.  (1.96964) BD (1) V  1- O  2
    (31.24%) 0.5589* V  1  s(4.64%)    p(0.36%)    d(94.85%)   f(0.16%)
    (68.76%) 0.8292* O  2  s(8.83%)    p(90.94%)   d(0.23%)
2.  (1.91524) BD (2) V  1- O  2
    (18.34%) 0.4282* V  1  s(9.65%)    p(8.53%)    d(81.15%)   f(0.67%)
    (81.66%) 0.9037* O  2  s(0.21%)    p(99.68%)   d(0.11%)
3.  (1.98330) BD (3) V  1- O  2
    (23.35%) 0.4832* V  1  s(0.00%)    p(2.36%)    d(97.45%)   f(0.19%)
    (76.65%) 0.8755* O  2  s(0.00%)    p(99.88%)   d(0.12%)
4.  (1.84671) BD (1) V  1- O  3
    (19.10%) 0.4371* V  1  s(33.51%)   p(5.71%)    d(60.35%)   f(0.43%)
    (80.90%) 0.8994* O  3  s(6.82%)    p(93.00%)   d(0.18%)
5.  (1.84671) BD (1) V  1- O  4
    (19.10%) 0.4371* V  1  s(33.51%)   p(5.71%)    d(60.35%)   f(0.43%)
    (80.90%) 0.8994* O  4  s(6.82%)    p(93.00%)   d(0.18%)
6.  (1.96576) BD (1) V  1- O  5
    (16.07%) 0.4009* V  1  s(2.64%)    p(3.23%)    d(94.00%)   f(0.13%)
    (83.93%) 0.9161* O  5  s(15.42%)   p(84.50%)   d(0.07%)
7.  (1.93982) BD (1) O  3- O  4
    (50.00%) 0.7071* O  3  s(6.36%)    p(93.33%)   d(0.31%)
    (50.00%) 0.7071* O  4  s(6.36%)    p(93.33%)   d(0.31%)
22. (1.97008) LP (1) O  2  s(90.95%)   p(9.05%)    d(0.00%)
23. (1.97708) LP (1) O  3  s(86.52%)   p(13.47%)   d(0.01%)
24. (1.86010) LP (2) O  3  s(0.47%)    p(99.44%)   d(0.09%)
25. (1.97708) LP (1) O  4  s(86.52%)   p(13.47%)   d(0.01%)
26. (1.86011) LP (2) O  4  s(0.47%)    p(99.44%)   d(0.09%)
27. (1.94769) LP (1) O  5  s(57.64%)   p(42.30%)   d(0.06%)
97. (0.04147) BD*(1) O  3- O  4
    (50.00%) 0.7071* O  3  s(6.36%)    p(93.33%)   d(0.31%)
    (50.00%)-0.7071* O  4  s(6.36%)    p(93.33%)   d(0.31%)
=======================================================================
```

Second order perturbation theory analysis of Fock-matrix for metavanadiumperoxoic acid (**6**) in NBO-basis(threshold for printing: 0.50 kcal/mol)

Donor NBO (i)	Acceptor NBO (j)	kcal/mol	a.u.	a.u.
7. BD (1) O 3- O 4	91. BD*(1) V 1- O 2	1.88	0.65	0.032
7. BD (1) O 3- O 4	92. BD*(2) V 1- O 2	8.41	0.66	0.069
7. BD (1) O 3- O 4	94. BD*(1) V 1- O 3	1.23	0.74	0.028
7. BD (1) O 3- O 4	95. BD*(1) V 1- O 4	1.23	0.74	0.028
7. BD (1) O 3- O 4	96. BD*(1) V 1- O 5	6.18	0.62	0.056
22. LP (1) O 2	92. BD*(2) V 1- O 2	3.24	1.04	0.054
22. LP (1) O 2	94. BD*(1) V 1- O 3	4.69	1.11	0.067
22. LP (1) O 2	95. BD*(1) V 1- O 4	4.69	1.11	0.067
23. LP (1) O 3	93. BD*(3) V 1- O 2	0.56	0.81	0.020
23. LP (1) O 3	94. BD*(1) V 1- O 3	1.22	0.97	0.032
23. LP (1) O 3	96. BD*(1) V 1- O 5	1.52	0.85	0.033
23. LP (1) O 3	97. BD*(1) O 3- O 4	0.62	0.95	0.022
24. LP (2) O 3	91. BD*(1) V 1- O 2	8.49	0.33	0.048
24. LP (2) O 3	92. BD*(2) V 1- O 2	0.84	0.34	0.015
24. LP (2) O 3	93. BD*(3) V 1- O 2	6.79	0.24	0.037
24. LP (2) O 3	96. BD*(1) V 1- O 5	7.82	0.29	0.043
25. LP (1) O 4	93. BD*(3) V 1- O 2	0.56	0.81	0.020
25. LP (1) O 4	95. BD*(1) V 1- O 4	1.22	0.97	0.032
25. LP (1) O 4	96. BD*(1) V 1- O 5	1.52	0.85	0.033
25. LP (1) O 4	97. BD*(1) O 3- O 4	0.62	0.95	0.022
26. LP (2) O 4	91. BD*(1) V 1- O 2	8.49	0.33	0.048
26. LP (2) O 4	92. BD*(2) V 1- O 2	0.84	0.34	0.015
26. LP (2) O 4	93. BD*(3) V 1- O 2	6.79	0.24	0.037
26. LP (2) O 4	96. BD*(1) V 1- O 5	7.82	0.29	0.043
27. LP (1) O 5	91. BD*(1) V 1- O 2	1.76	0.69	0.031
27. LP (1) O 5	92. BD*(2) V 1- O 2	17.08	0.70	0.101
27. LP (1) O 5	94. BD*(1) V 1- O 3	1.65	0.77	0.033
27. LP (1) O 5	95. BD*(1) V 1- O 4	1.65	0.77	0.033
28. LP (2) O 5	93. BD*(3) V 1- O 2	9.04	0.25	0.043
28. LP (2) O 5	94. BD*(1) V 1- O 3	5.35	0.41	0.042
28. LP (2) O 5	95. BD*(1) V 1- O 4	5.35	0.41	0.042

Natural bond orbital (NBO)-energies

NBO	Occupancy	Energy
1. BD (1) V 1- O 2	1.96964	-0.58730
2. BD (2) V 1- O 2	1.91524	-0.37292
3. BD (3) V 1- O 2	1.98330	-0.39084
4. BD (1) V 1- O 3	1.84671	-0.47859
5. BD (1) V 1- O 4	1.84671	-0.47859
6. BD (1) V 1- O 5	1.96576	-0.56770
7. BD (1) O 3- O 4	1.93982	-0.66898
22. LP (1) O 2	1.97008	-1.04356
23. LP (1) O 3	1.97708	-0.90686
24. LP (2) O 3	1.86010	-0.34208
25. LP (1) O 4	1.97708	-0.90686
26. LP (2) O 4	1.86011	-0.34208
27. LP (1) O 5	1.94769	-0.70522
28. LP (2) O 5	1.80889	-0.34636
97. BD*(1) O 3- O 4	0.04147	0.03989

7.9 Hydrogen bond donors and acceptors

7.9.1 Water

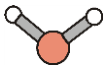

Figure S56. Minimum structure of water.

B3LYP/6-311++G//B3LYP/6-311++G****

Standard orientation:

Center Number	Atomic Number	Atomic Type	Coordinates (Angstroms) X	Y	Z
1	8	0	0.000000	0.000000	0.117057
2	1	0	0.000000	0.763568	-0.468229
3	1	0	0.000000	-0.763568	-0.468229

Zero-point correction= 0.021283 (Hartree/Particle)
Thermal correction to Energy= 0.024119
Thermal correction to Enthalpy= 0.025063
Thermal correction to Gibbs Free Energy= 0.003640
Sum of electronic and zero-point Energies= -76.437249
Sum of electronic and thermal Energies= -76.434413
Sum of electronic and thermal Enthalpies= -76.433469
Sum of electronic and thermal Free Energies= -76.454892

Version=AM64L-G03RevE.01\State=1-A1\HF-76.458532\RMSD=2.938e-09\
RMSF=2.630e-06\PG=C02V [C2(O1),SGV(H2)\\@.

7.9.2 Water tetramer

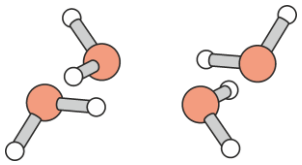

Figure S57. Minimum structure of the water tetramer.

B3LYP/6-311++G//B3LYP/6-311++G****

Standard orientation:

Center Number	Atomic Number	Atomic Type	Coordinates (Angstroms) X	Y	Z
1	8	0	1.475738	-1.259589	-0.090928
2	1	0	1.545602	-0.280438	-0.033546
3	8	0	1.269456	1.468206	0.087436
4	1	0	-0.291787	-1.563352	-0.079322
5	8	0	-1.269825	-1.468690	-0.085744
6	1	0	0.291490	1.563337	0.077172
7	8	0	-1.475596	1.259308	0.088885
8	1	0	-1.545609	0.280253	0.029501
9	1	0	2.114447	-1.613419	0.534071
10	1	0	-2.115704	1.614785	-0.533743
11	1	0	-1.605889	-2.077864	0.577553
12	1	0	1.609274	2.082824	-0.568874

```
Zero-point correction=                          0.098501 (Hartree/Particle)
Thermal correction to Energy=                   0.108340
Thermal correction to Enthalpy=                 0.109284
Thermal correction to Gibbs Free Energy=        0.064836
Sum of electronic and zero-point Energies=           -305.782999
Sum of electronic and thermal Energies=              -305.773160
Sum of electronic and thermal Enthalpies=            -305.772216
Sum of electronic and thermal Free Energies=         -305.816664

Version=AM64L-G03RevE.01\State=1-A\HF-305.8815001\RMSD=4.607e-
09\RMSF=3.047e-05\PG=C01 [X(H8O4)]\NImag=0\\@.
```

7.9.3 Water hexamer

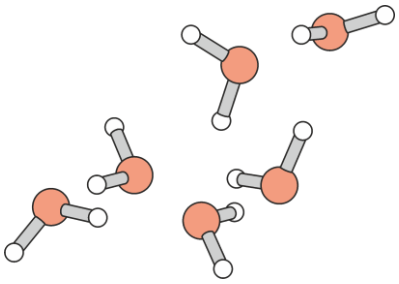

Figure S58. Minimum structure of the water hexamer in the roof-top conformation.

B3LYP/6-311++G//B3LYP/6-311++G****

Standard orientation:

Center Number	Atomic Number	Atomic Type	Coordinates (Angstroms) X	Y	Z
1	8	0	2.253681	1.535370	-0.460164
2	1	0	2.398266	0.578135	-0.605373
3	8	0	2.315490	-1.249393	-0.582675
4	1	0	0.706318	1.562839	0.569923
5	8	0	-0.061060	1.264838	1.097746
6	1	0	1.577086	-1.456498	0.025764
7	8	0	0.050283	-1.346495	1.055148
8	1	0	0.009607	-0.344458	1.168422
9	1	0	2.306280	1.950666	-1.325574
10	1	0	-0.006573	-1.728220	1.936829
11	1	0	-0.862376	1.490901	0.584678
12	8	0	-2.382160	1.348908	-0.452356
13	1	0	3.064605	-1.776208	-0.289825
14	1	0	-3.253245	1.644385	-0.173123
15	1	0	-2.451871	0.382722	-0.600873
16	8	0	-2.187480	-1.414459	-0.629831
17	1	0	-1.406552	-1.552402	-0.055514
18	1	0	-1.991576	-1.862010	-1.458274

```
Zero-point correction=                           0.149740 (Hartree/Particle)
Thermal correction to Energy=                    0.164575
Thermal correction to Enthalpy=                  0.165519
Thermal correction to Gibbs Free Energy=         0.108550
Sum of electronic and zero-point Energies=           -458.680360
Sum of electronic and thermal Energies=              -458.665525
Sum of electronic and thermal Enthalpies=            -458.664580
Sum of electronic and thermal Free Energies=         -458.721549

Version=AM64L-G03RevE.01\State=1-A\HF-458.8300995\RMSD=2.226e-09\
RMSF=1.335e-07\PG=C01 [X(H12O6)]\NImag=0\\@.
```

7.9.4 Water octamer

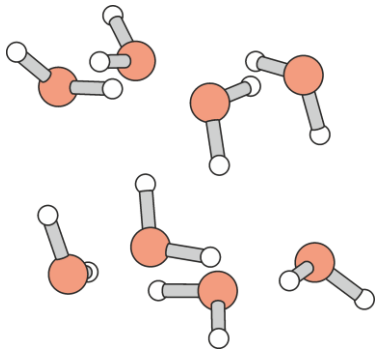

Figure S59. Minimum structure of the water octamer.

B3LYP/6-311++G//B3LYP/6-311++G****

Standard orientation:

Center Number	Atomic Number	Atomic Type	Coordinates (Angstroms) X	Y	Z
1	8	0	2.099833	-1.360374	-0.347437
2	8	0	2.019338	1.398531	-0.189468
3	8	0	-0.356926	1.365646	-1.869440
4	8	0	-2.019123	1.398867	0.188993
5	8	0	0.357160	1.366303	1.868962
6	8	0	-2.100053	-1.359959	0.347894
7	8	0	0.306326	-1.415816	1.954716
8	8	0	-0.306550	-1.416529	-1.954218
9	1	0	0.974550	-1.607857	1.276445
10	1	0	0.345213	0.409063	2.091662
11	1	0	1.454276	1.480002	0.633657
12	1	0	2.257901	-0.390381	-0.340174
13	1	0	-0.526777	1.538978	1.503078
14	1	0	-2.257979	-0.389945	0.340261
15	1	0	-0.545627	-1.595188	1.522791
16	1	0	0.527039	1.538280	-1.503596
17	1	0	-0.345156	0.408325	-2.091805
18	1	0	0.545359	-1.595906	-1.522212
19	1	0	-0.974808	-1.608248	-1.275888
20	1	0	-1.454037	1.479959	-0.634150
21	1	0	2.952950	-1.783495	-0.483972
22	1	0	2.729436	2.042790	-0.110184
23	1	0	-2.953225	-1.782902	0.484638
24	1	0	-2.729152	2.043170	0.109434

```
Zero-point correction=                          0.203417 (Hartree/Particle)
Thermal correction to Energy=                   0.221845
Thermal correction to Enthalpy=                 0.222789
Thermal correction to Gibbs Free Energy=        0.159822
Sum of electronic and zero-point Energies=           -611.584029
Sum of electronic and thermal Energies=              -611.565601
Sum of electronic and thermal Enthalpies=            -611.564657
Sum of electronic and thermal Free Energies=         -611.627625

Version=AM64L-G03RevE.01\State=1-A\HF-611.787446\RMSD=2.710e-09\
RMSF=1.083e-06\PG=C01 [X(H16O8)]\NImag=0\\@.
```

7.9.5 Methanol

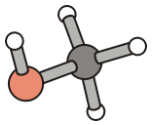

Figure S60. Minimum structure of methanol.

B3LYP/6-311++G//B3LYP/6-311++G****

Standard orientation:

Center Number	Atomic Number	Atomic Type	Coordinates (Angstroms) X	Y	Z
1	6	0	-0.667276	-0.020315	0.000000
2	8	0	0.749564	0.122013	0.000000
3	1	0	-1.083387	0.987342	-0.000005
4	1	0	-1.029339	-0.544639	-0.892906
5	1	0	-1.029339	-0.544630	0.892910
6	1	0	1.149210	-0.752291	0.000000

```
Zero-point correction=                          0.051030 (Hartree/Particle)
Thermal correction to Energy=                   0.054385
Thermal correction to Enthalpy=                 0.055330
Thermal correction to Gibbs Free Energy=        0.028250
Sum of electronic and zero-point Energies=           -115.713969
Sum of electronic and thermal Energies=              -115.710613
Sum of electronic and thermal Enthalpies=            -115.709669
Sum of electronic and thermal Free Energies=         -115.736749

Version=AM64L-G03RevE.01\State=1-A\HF-115.7649986\RMSD=4.315e-09\
RMSF=5.621e-06\]PG=C01 [X(C1H4O1)]\NImag=0\\@.
```

(*ii*) NBO-analysis – B3LYP/6-31G*// B3LYP/6-311++G**

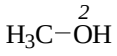

Natural bond orbital (NBO)-energies

NBO	Occupancy	Energy
8. LP (1) O 2	1.98448	-0.58423
9. LP (2) O 2	1.96366	-0.28105

7.9.6 Imidazole

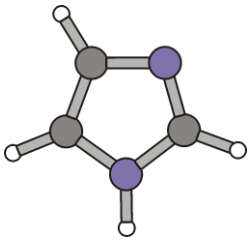

Figure S61. Minimum structure of imidazole.

B3LYP/6-311++G//B3LYP/6-311++G****

Standard orientation:

Center Number	Atomic Number	Atomic Type	Coordinates (Angstroms) X	Y	Z
1	7	0	-0.111029	-1.225863	0.000000
2	6	0	-1.132224	-0.301773	0.000000
3	6	0	-0.628987	0.972925	0.000000
4	7	0	0.742249	0.818441	0.000000
5	6	0	0.997980	-0.524296	0.000000
6	1	0	-2.166837	-0.606741	0.000000
7	1	0	-1.099128	1.941816	0.000000
8	1	0	1.425792	1.558682	0.000000
9	1	0	2.001019	-0.922935	0.000000

```
Zero-point correction=                          0.070832 (Hartree/Particle)
Thermal correction to Energy=                   0.074608
Thermal correction to Enthalpy=                 0.075552
Thermal correction to Gibbs Free Energy=        0.044557
Sum of electronic and zero-point Energies=                -226.212014
Sum of electronic and thermal Energies=                   -226.208237
Sum of electronic and thermal Enthalpies=                 -226.207293
Sum of electronic and thermal Free Energies=              -226.238289

Version=AM64L-G03RevE.01\State=1-A\HF-226.2828452\RMSD=3.800e-09\
RMSF=2.019e-07\PG=C01 [X(C3H4N2)]\NImag=0\\@.
```

(*ii*) NBO-analysis – B3LYP/6-31G*// B3LYP/6-311++G**

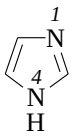

Natural bond orbital (NBO)-energies

NBO	Occupancy	Energy
17. LP (1) N 1	1.92528	-0.34337
18. LP (1) N 4	1.58368	-0.26192

7.9.7 Methylamine

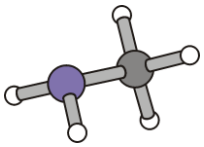

Figure S62. Minimum structure of methylamine.

B3LYP/6-311++G//B3LYP/6-311++G****

Standard orientation:

Center Number	Atomic Number	Atomic Type	Coordinates (Angstroms) X	Y	Z
1	6	0	0.709005	0.000000	0.017633
2	7	0	-0.750167	0.000000	-0.118441
3	1	0	1.116612	0.879164	-0.487357
4	1	0	1.082669	0.000000	1.052626
5	1	0	1.116612	-0.879164	-0.487357
6	1	0	-1.159377	-0.816334	0.322688
7	1	0	-1.159377	0.816334	0.322688

```
Zero-point correction=                          0.063792 (Hartree/Particle)
Thermal correction to Energy=                   0.067230
Thermal correction to Enthalpy=                 0.068174
Thermal correction to Gibbs Free Energy=        0.040860
Sum of electronic and zero-point Energies=            -95.830099
Sum of electronic and thermal Energies=               -95.826661
Sum of electronic and thermal Enthalpies=             -95.825717
Sum of electronic and thermal Free Energies=          -95.853031

Version=AM64L-G03RevE.01\State=1-A\HF-95.8938909\RMSD=8.941e-10\
RMSF=9.433e-07\PG=C01 [X(C1H5N1)]\NImag=0\\@.
```

(*ii*) NBO-analysis – B3LYP/6-31G*// B3LYP/6-311++G**

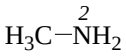

Natural bond orbital (NBO)-energies

NBO	Occupancy	Energy
9. LP (1) N 2	1.96404	-0.28281

7.9.8 Methylammonium

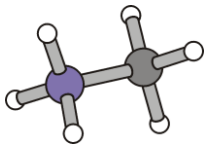

Figure S63. Minimum structure of methylammonium.

B3LYP/6-311++G//B3LYP/6-311++G****

Standard orientation:

Center Number	Atomic Number	Atomic Type	Coordinates (Angstroms) X	Y	Z
1	6	0	0.803351	-0.000001	-0.000001
2	7	0	-0.712374	-0.000002	0.000001
3	1	0	1.143753	-0.756972	-0.703000
4	1	0	1.143749	0.987305	-0.304053
5	1	0	1.143750	-0.230330	1.007059
6	1	0	-1.088246	0.694561	0.653383
7	1	0	-1.088243	0.218580	-0.928196
8	1	0	-1.088254	-0.913129	0.274803

```
Zero-point correction=                          0.079141 (Hartree/Particle)
Thermal correction to Energy=                   0.082599
Thermal correction to Enthalpy=                 0.083543
Thermal correction to Gibbs Free Energy=        0.055952
Sum of electronic and zero-point Energies=                -96.169917
Sum of electronic and thermal Energies=                   -96.166459
Sum of electronic and thermal Enthalpies=                 -96.165515
Sum of electronic and thermal Free Energies=              -96.193106

Version=AM64L-G03RevE.01\State=1-A\HF-96.2490578\RMSD=8.462e-09\
RMSF=1.112e-05\PG=C01 [X(C1H6N1)]\NImag=0\\@.
```

7.9.9 *N*-Methylguanidinium

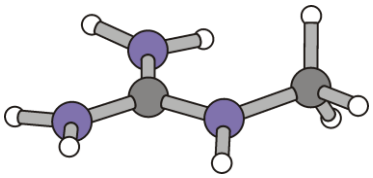

Figure S64. Minimum structure of *N*-methylguanidinium.

B3LYP/6-311++G//B3LYP/6-311++G****

Standard orientation:

Center Number	Atomic Number	Atomic Type	Coordinates (Angstroms) X	Y	Z
1	7	0	-1.673646	-0.679386	0.028551
2	6	0	-0.514596	-0.006540	-0.015652
3	7	0	-0.529556	1.330506	-0.010748
4	7	0	0.641371	-0.667409	-0.052512
5	6	0	1.967731	-0.046829	0.045320
6	1	0	-1.698592	-1.672569	0.199981
7	1	0	0.304757	1.866172	-0.190584
8	1	0	-1.377493	1.844094	0.173275
9	1	0	0.602747	-1.661255	-0.225292
10	1	0	2.700479	-0.840730	0.171966
11	1	0	2.218007	0.509104	-0.862026
12	1	0	2.020362	0.605298	0.918982
13	1	0	-2.556259	-0.215877	-0.121344

Zero-point correction= 0.116202 (Hartree/Particle)
Thermal correction to Energy= 0.123116
Thermal correction to Enthalpy= 0.124060
Thermal correction to Gibbs Free Energy= 0.086663
Sum of electronic and zero-point Energies= -245.040705
Sum of electronic and thermal Energies= -245.033792
Sum of electronic and thermal Enthalpies= -245.032848
Sum of electronic and thermal Free Energies= -245.070245

Version=AM64L-G03RevE.01\State=1-A\HF-245.1569079\RMSD=6.433e-09\
RMSF=4.989e-07\PG=C01 [X(C2H8N3)]\NImag=0\\@.

7.9.10 Ammonia

Figure S65. Minimum structure of ammonia.

B3LYP/6-311++G//B3LYP/6-311++G****

Standard orientation:

Center Number	Atomic Number	Atomic Type	Coordinates (Angstroms) X	Y	Z
1	7	0	0.000000	0.109113	0.000000
2	1	0	-0.947101	-0.254599	0.000000
3	1	0	0.473550	-0.254595	0.820215
4	1	0	0.473550	-0.254595	-0.820215

Zero-point correction= 0.034260 (Hartree/Particle)
Thermal correction to Energy= 0.037134
Thermal correction to Enthalpy= 0.038078
Thermal correction to Gibbs Free Energy= 0.015191
Sum of electronic and zero-point Energies= -56.548463
Sum of electronic and thermal Energies= -56.545589
Sum of electronic and thermal Enthalpies= -56.544645
Sum of electronic and thermal Free Energies= -56.567532

Version=AM64L-G03RevE.01\State=1-A'\HF=-56.5827227\RMSD=2.652e-09\
PG=CS [SG(H1N1),X(H2)]\NImag=0\\@.

7.10 Products and intermediates associated with bromide oxidation

7.10.1 Hydrogen bromide

Figure S66. Minimum structure of hydrogen bromide.

B3LYP/6-311++G//B3LYP/6-311++G****

Standard orientation:

Center Number	Atomic Number	Atomic Type	Coordinates (Angstroms) X	Y	Z
1	35	0	0.000000	0.000000	0.039645
2	1	0	0.000000	0.000000	-1.387561

Zero-point correction= 0.005936 (Hartree/Particle)
Thermal correction to Energy= 0.008296
Thermal correction to Enthalpy= 0.009240
Thermal correction to Gibbs Free Energy= -0.013294
Sum of electronic and zero-point Energies= -2574.747238
Sum of electronic and thermal Energies= -2574.744878
Sum of electronic and thermal Enthalpies= -2574.743933
Sum of electronic and thermal Free Energies= -2574.766468

Version=AM64L-G03RevE.01\State=1-SG\HF-2574.7531735\RMSD=4.447e-10\
RMSF=1.112e-07\ PG=C*V [C*(H1Br1)]\NImag=0\\@.

7.10.2 Hypobromous acid

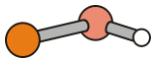

Figure S67. Minimum structure of hypobromous acid.

B3LYP/6-311++G//B3LYP/6-311++G****

Standard orientation:

Center Number	Atomic Number	Atomic Type	Coordinates (Angstroms) X	Y	Z
1	8	0	0.021407	1.481732	0.000000
2	35	0	0.021407	-0.387367	0.000000
3	1	0	-0.920510	1.703991	0.000000

Zero-point correction= 0.012634 (Hartree/Particle)
Thermal correction to Energy= 0.015642
Thermal correction to Enthalpy= 0.016587
Thermal correction to Gibbs Free Energy= -0.011573
Sum of electronic and zero-point Energies= -2649.931076
Sum of electronic and thermal Energies= -2649.928067
Sum of electronic and thermal Enthalpies= -2649.927123
Sum of electronic and thermal Free Energies= -2649.955283

Version=AM64L-G03RevE.01\State=1-A'\HF-2649.9437098\RMSD=3.804e-09\
RMSF=7.793e-06\PG=CS [SG(Br1H1O1)]\NImag=0\\@.

7.10.3 Transition structure 7-O^P for bromide approaching the proximal peroxide oxygen

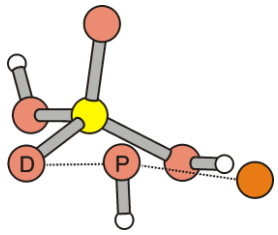

Figure S68. Stationary point for Br,O^P-bond forming and O^D,O^P-bond breaking (dashed lines; imaginary stretching mode i = –289 cm^{-1}).

B3LYP/6-311++G//B3LYP/6-311++G****

Standard orientation:

Center Number	Atomic Number	Atomic Type	Coordinates (Angstroms) X	Y	Z
1	8	0	1.547889	-0.116482	1.636910
2	23	0	1.565905	-0.042997	0.048059
3	8	0	0.703735	-1.450836	-0.713842
4	8	0	-0.426899	0.976718	-0.106672
5	8	0	1.238772	1.592009	-0.505910
6	8	0	3.293865	-0.311540	-0.449932
7	1	0	3.922451	-0.471648	0.259526
8	1	0	-0.236006	-1.535539	-0.492323
9	1	0	-0.664712	1.016260	-1.043520
10	35	0	-2.568470	-0.101117	0.036758

```
Zero-point correction=                          0.046773 (Hartree/Particle)
Thermal correction to Energy=                   0.056549
Thermal correction to Enthalpy=                 0.057493
Thermal correction to Gibbs Free Energy=        0.010346
Sum of electronic and zero-point Energies=          -3896.336496
Sum of electronic and thermal Energies=             -3896.326720
Sum of electronic and thermal Enthalpies=           -3896.325776
Sum of electronic and thermal Free Energies=        -3896.372922

Version=AM64L-G03RevE.01\State=1-A\HF-3896.3832688\RMSD=5.602e-09\
RMSF=4.883e-07\PG=C01 [X(Br1H3O5V1)]\NImag=1\\@.
```

7.10.4 Transition structure 7-O^D for bromide approaching the distal peroxide oxygen

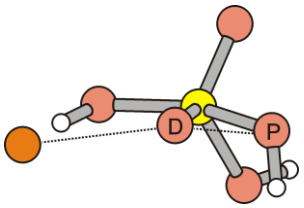

Figure S69. Stationary point for Br,O^D-bond forming and O^D,O^P-bond breaking (dashed lines; imaginary stretching mode i = –219 cm^{-1}).

B3LYP/6-311++G//B3LYP/6-311++G****

Standard orientation:

Center Number	Atomic Number	Atomic Type	Coordinates (Angstroms) X	Y	Z
1	8	0	2.260112	-0.451925	-1.373764
2	23	0	1.365752	-0.217206	-0.085483
3	8	0	0.240383	-1.564108	0.008801
4	8	0	2.405217	-0.297306	1.419192
5	8	0	1.437145	1.832304	-0.091087
6	8	0	-0.025914	1.048640	-0.204594
7	35	0	-2.455163	-0.001366	0.047073
8	1	0	-0.713753	-1.321464	0.159165
9	1	0	3.355310	-0.314578	1.270195
10	1	0	1.341321	2.138759	0.820831

```
Zero-point correction=                          0.046924 (Hartree/Particle)
Thermal correction to Energy=                   0.056252
Thermal correction to Enthalpy=                 0.057197
Thermal correction to Gibbs Free Energy=        0.011104
Sum of electronic and zero-point Energies=          -3896.331905
Sum of electronic and thermal Energies=             -3896.322576
Sum of electronic and thermal Enthalpies=           -3896.321632
Sum of electronic and thermal Free Energies=        -3896.367725

Version=AM64L-G03RevE.01\State=1-A\HF-3896.3788282\RMSD=9.425e-09\
RMSF=1.069e-06\PG=C01 [X(Br1H3O5V1)]\NImag=1\\@.
```

7.10.5 IRC-calculation – part 1: final point on the reaction coordinate of bromide oxidation proceeding via transtion structure 7-O^P

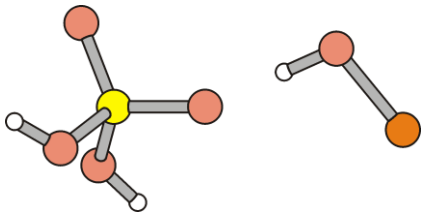

Figure S70. Structure of hydrogen-bonded hypobromous acid to the *anti*/*syn*-conformer of dihydrogen orthovanadate (adduct **2g**), obtained by continuing the reaction coordinate of O^P,Br-bond formation associated wiht transition structure **7-O^P**.

B3LYP/6-311++G//B3LYP/6-311++G****

Standard orientation:

Center Number	Atomic Number	Atomic Type	Coordinates (Angstroms) X	Y	Z
1	8	0	2.748640	-1.072324	-1.066527
2	23	0	2.102734	-0.013592	-0.042059
3	8	0	2.530995	1.689612	-0.608391
4	8	0	-1.856463	-1.091111	-0.493250
5	8	0	0.462592	-0.144130	0.056837
6	8	0	2.841737	-0.295371	1.624752
7	1	0	3.635922	-0.836880	1.606822
8	1	0	1.840638	2.330344	-0.411230
9	1	0	-0.934902	-0.708644	-0.274169
10	35	0	-3.049273	0.195268	0.112531

```
Zero-point correction=                          0.046843 (Hartree/Particle)
Thermal correction to Energy=                   0.057518
Thermal correction to Enthalpy=                 0.058463
Thermal correction to Gibbs Free Energy=        0.006349
Sum of electronic and zero-point Energies=          -3896.382307
Sum of electronic and thermal Energies=             -3896.371632
Sum of electronic and thermal Enthalpies=           -3896.370687
Sum of electronic and thermal Free Energies=        -3896.422801

Version=AM64L-G03RevE.01\State=1-A\HF-3896.4291501\RMSD=3.366e-09\
RMSF=4.981e-05\ PG=C01 [X(Br1H3O5V1)]\NImag=0\\@.
```

7.10.6 IRC-calculation – part 2: initial point on the reaction coordinate of bromide oxidation proceeding via transition structure 7-O^P

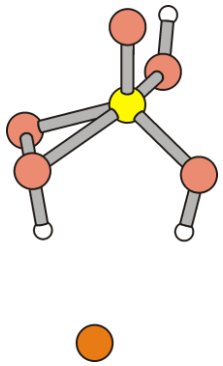

Figure S71. Minimum structure of hydrogen bonded bromide to the *syn*/*anti*/*anticline*-conformer of orthovanadiumperoxoic acid *side-on*-(**4**), obtained by reversing the Br,O^P-attack leading to transition structure **7**-O^P.

B3LYP/6-311++G//B3LYP/6-311++G****

Standard orientation:

Center Number	Atomic Number	Atomic Type	Coordinates (Angstroms) X	Y	Z
1	8	0	-2.670282	0.170968	-1.121481
2	23	0	-1.504756	-0.098100	-0.085334
3	8	0	-0.437961	-1.389727	-0.680697
4	8	0	-0.117066	1.369883	-0.487183
5	8	0	-0.925776	1.467507	0.721163
6	8	0	-2.326462	-0.761360	1.397460
7	1	0	-3.287317	-0.720181	1.396630
8	1	0	0.523833	-1.290429	-0.489968
9	1	0	0.804335	1.033202	-0.191600
10	35	0	2.525398	-0.103556	0.074672

```
Zero-point correction=                          0.048219 (Hartree/Particle)
Thermal correction to Energy=                   0.057760
Thermal correction to Enthalpy=                 0.058704
Thermal correction to Gibbs Free Energy=        0.011879
Sum of electronic and zero-point Energies=          -3896.365574
Sum of electronic and thermal Energies=             -3896.356033
Sum of electronic and thermal Enthalpies=           -3896.355089
Sum of electronic and thermal Free Energies=        -3896.401914

Version=AM64L-G03RevE.01\State=1-A\HF-3896.4137933\RMSD=5.397e-09\
RMSF=6.694e-07\ PG=C01 [X(Br1H3O5V1)]\NImag=0\\@.
```

7.10.7 IRC-calculation – part 3: final point on the reaction coordinate of bromide oxidation proceeding via transtion structure 7-O^D

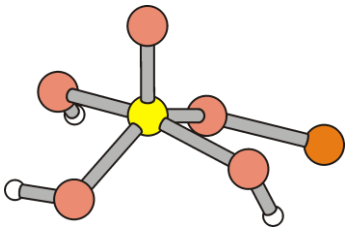

Figure S72. Product obtained by continuing the reaction pathway of O^D,Br-bond formation starting from transition structure **7-O^D**.

B3LYP/6-311++G//B3LYP/6-311++G****

Standard orientation:

Center Number	Atomic Number	Atomic Type	Coordinates (Angstroms) X	Y	Z
1	8	0	-1.883842	-0.316980	1.561318
2	35	0	2.237020	0.002996	-0.035636
3	23	0	-1.248391	-0.085268	0.128113
4	8	0	0.567773	0.827593	0.000564
5	8	0	-1.581602	1.747114	-0.119173
6	8	0	-0.358653	-1.657809	-0.125585
7	8	0	-2.502854	-0.472577	-1.192279
8	1	0	0.328507	-1.662654	-0.801659
9	1	0	-3.011662	0.329594	-1.350675
10	1	0	-0.826146	2.170657	-0.545751

```
Zero-point correction=                          0.047370 (Hartree/Particle)
Thermal correction to Energy=                   0.057459
Thermal correction to Enthalpy=                 0.058403
Thermal correction to Gibbs Free Energy=        0.010788
Sum of electronic and zero-point Energies=          -3896.360009
Sum of electronic and thermal Energies=             -3896.349920
Sum of electronic and thermal Enthalpies=           -3896.348976
Sum of electronic and thermal Free Energies=        -3896.396591

Version=AM64L-G03RevE.01\State=1-A\HF=-3896.407379\RMSD=5.986e-09\
RMSF=2.420e-07\PG=C01 [X(Br1H3O5V1)]\NImag=0\\@.
```

7.10.8 IRC-calculation – part 4: starting point on the reaction coordinate of bromide oxidation proceeding via transition structure 7-O^D

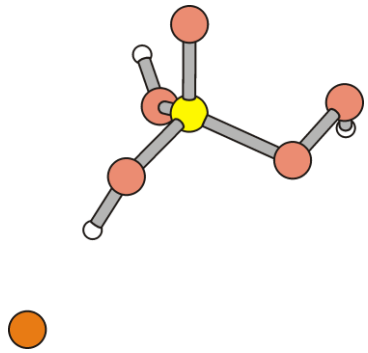

Figure S73. Minimum structure for hydrogen-bonded bromide to the *syn*/*anti*/*syncline*-conformer of peroxoic acid *end-on*-**4**, obtained by reversing Br,O^D-attack leading to transition structure **7**-O^P.

B3LYP/6-311++G//B3LYP/6-311++G****

Standard orientation:

Center Number	Atomic Number	Atomic Type	Coordinates (Angstroms) X	Y	Z
1	8	0	2.337868	-1.456009	-0.718505
2	35	0	-3.009302	0.170765	0.042426
3	23	0	1.367757	-0.362960	-0.095701
4	8	0	1.955745	1.347016	-0.487165
5	8	0	3.301603	1.394562	0.066940
6	8	0	-0.183571	-0.498384	-0.791046
7	8	0	1.349969	-0.528226	1.700952
8	1	0	-1.158566	-0.252926	-0.481728
9	1	0	1.805643	-1.269649	2.110469
10	1	0	3.127179	1.822206	0.918065

```
Zero-point correction=                          0.045871 (Hartree/Particle)
Thermal correction to Energy=                   0.056463
Thermal correction to Enthalpy=                 0.057408
Thermal correction to Gibbs Free Energy=        0.006278
Sum of electronic and zero-point Energies=          -3896.349687
Sum of electronic and thermal Energies=             -3896.339095
Sum of electronic and thermal Enthalpies=           -3896.338150
Sum of electronic and thermal Free Energies=        -3896.389280

Version=AM64L-G03RevE.01\State=1-A\HF=-3896.3955581\RMSD=5.920e-09\
RMSF=8.401e-07\PG=C01 [X(Br1H3O5V1)]\NImag=0\\@.
```

8 Structure References

For assuring that B3LYP/6-311++G**-theory reproduces structures and energetics of orthovanadium compounds, conformers of orthovanadium acid (structure type **Ia**) were initially referenced versus the solid state structure of tri(2-chloroeth-1-yl) vanadate (structure type **Ib**), serving as example for a lower alkyl ester. The latter compound, like most other trialkyl vanadates, forms polymeric adducts in the condensed phase by vanadium-alkoxy oxygen-contacts.[18]

Table S7. Structure parameters of orthovanadium compounds from density functional theory and X-ray diffraction[18]

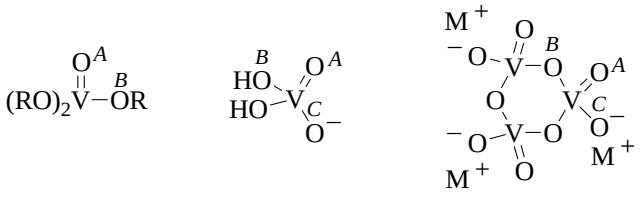

I **II** **III**

type / R or M	V,O^A / Å	V,O^B / Å	V,O^C / Å	O^{A}V,O^B / deg	O^{A}V,O^C / deg
Ia / R = H	1.569	1.778	– [b]	109.3	– [b]
II / – [b]	1.623	1.864	1.623	112.3	109.2
IIIa / – [b]	1.649	1.824	1.649	108.6	111.1
Ib / R = C_2H_5Cl	1.584_2	1.771_2	– [b]	101.8_9	– [b]
IIIb / M = NBu_4	1.625_6	1.80_1	1.638_9	110.4_6	109_1

[a] B3LYP/6-311++G** (0 K). [b] Not available. [c] X-ray diffraction at room temperature; the V,O^C-bond length refers to the monovalent alkoxy substituent in a dimer of tri(2-chloroeth-1-yl) vanadate (type **Ib**) in the solid state. [d] X-ray diffraction at 292±8°C.

In the global minimum of orthovanadium acid (structure type **Ia**), acidic hydrogens are oriented in B3LYP-theory toward oxido oxygen O^A, similar to the experimental structure

of orthophosphorous acid (H_3PO_4) in the solid state.[19] This arrangement is in the Supporing information and the associated article referred to as all-*syn*-conformation. Calculated bond lengths in the minimum structure of orthovanadium acid and experimental structure tri(2-chloroeth-1-yl) vanadate (structure type **Ib**) match with a precision of 99% for vanadium-oxygen single (toward O^B) and multiple bonds (toward O^A). The most significant deviation between predicted and experimental structures are seen for the O^A,V,O^B-angle, being 7% wider in experimental than predicted structures (Table S7).

In natural bond order (NBO)-theory[16] one of the non-bonding electron pairs at O^A overlaps with a vacant *d*-orbital at vanadium raising the bond order to three. The remaining non-bonding electron pair at O^A resides in an *s*-orbital.

For referencing calculated structure parameters of dihydrogen orthovanadate (structure type **II**) we relied on the crystal structure of tris(tetrabutylammonium) cyclotrivanadate[20] (structure type **IIIb**; Table 3, entries 2, 3 and 5), showing similar match as described for uncharged derivatives of orthovanadium acid (vide supra).

In NBO-theory, non-bonding electron pairs at oxygens O^A and O^C, and vacant *d*-orbitals at vanadium overlap leading to bond orders of three and two. In the electronic structure model, O^A and O^C become chemically equivalent.

Appendix: *cyclo*-trisorthovanadate(–3)

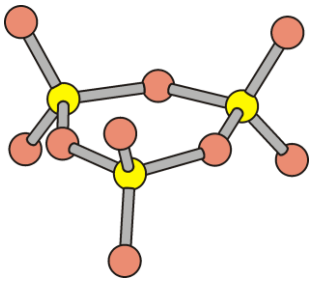

Figure S74. Minimum structure of the *cyclo*-trisorthvanadate trianion.

B3LYP/6-311++G//B3LYP/6-311++G****

Standard orientation:

Center Number	Atomic Number	Atomic Type	Coordinates (Angstroms) X	Y	Z
1	23	0	-0.504349	1.883153	0.000016
2	23	0	1.883036	-0.504796	-0.000036
3	23	0	-1.378688	-1.378349	0.000004
4	8	0	-0.753518	2.812788	-1.338668
5	8	0	-0.753175	2.812991	1.338624
6	8	0	1.177319	1.177031	-0.000174
7	8	0	2.812962	-0.754037	-1.338513
8	8	0	2.812472	-0.754025	1.338777
9	8	0	0.430688	-1.608102	-0.000306
10	8	0	-2.059183	-2.059034	1.338654
11	8	0	-2.059550	-2.058701	-1.338630
12	8	0	-1.608010	0.431067	0.000282

```
Zero-point correction=                           0.030886 (Hartree/Particle)
Thermal correction to Energy=                    0.044503
Thermal correction to Enthalpy=                  0.045447
Thermal correction to Gibbs Free Energy=        -0.011238
Sum of electronic and zero-point Energies=          -3509.659146
Sum of electronic and thermal Energies=             -3509.645528
Sum of electronic and thermal Enthalpies=           -3509.644584
Sum of electronic and thermal Free Energies=        -3509.701270

Version=AM64L-G03RevE.01\State=1-A\HF-3509.6900312\RMSD=7.466e-09\
RMSF=4.040e-05\ PG=C01 [X(O9V3)]\NImag=0\\@.
```

A MAN THINKING OR WORKING IS ALWAYS ALONE,
LET HIM BE WHERE HE WILL.

-- THOREAU

9 References

(1) HyperChem(TM) Professional 7.51, Hypercube, Inc., 1115 NW 4th Street, Gainesville, Florida 32601, US

(2) HyperChem Professional 4.5 in combination with ChemPlus 1.6, Hypercube, Inc., 419 Phillip St., Waterloo, Ontario, Canada, 1995.

(3) Weiss, M.S., Sicker, T., Djinovic K. -Carugo, and Hilgenfeld R. (2001) On the routine use of soft x-rays in macromolecular crystallography. *Acta Cryst.* D57, 689–695.

(4) Vagin, A., and Teplyakov A. (1997) MOLREP. An automated program for molecular replacement. *J. Appl. Cryst*. *30*, 1022–1025.

(5) Winn M, Ballard C, Cowtan K, Dodson E, Emsley P, Evans P, Keegan R, Krissinel E, Leslie A, McCoy A, McNicholas S, Murshudov G, Pannu N, Potterton E, Powell H, Read R, Vagin A, and Wilson K. (2011) Overview of the CCP4 suite and current developments. Acta Crystallogr. *D67*, 235–242.

(6) Emsley, P., Lohkamp, B., Scott, W.G., and Cowtan K. (2010) Features and development of Coot. *Acta Cryst*. *D66*, 486–501.

(7) Vagin, A.A., Steiner, R.A., Lebedev, A.A., Potterton, L., McNicholas, S., Long, F., and Murshudov G.N. (2004) REFMAC5 dictionary. Organization of prior chemical knowledge and guidelines for its use. *Acta Crystallogr*. D 60, 2184–2195

(8) Murshudov, G.N., Skubak, P., Lebedev, A.A., Pannu, N.S., Steiner, R.A., Nicholls, R.A., Winn, M.D., Long F., and Vagin, A.A. (2011) REFMAC5 for the refinement of macromolecular crystal structures. *Acta Cryst. D67*, 355–367.

(9) Murshudov, G.N., Vagin A.A., and Dodson, E.J. (1997). Refinement of Macromolecular Structures by the Maximum-Likelihood Method. *Acta Cryst. D53*, 240–255.

(10) Colin, C., Leblanc, C., Wagner, E., Delage, L., Leize-Wagner, E., Van Dorsselaer, A., Kloareg, B., and Potin, P. (2003) The brown algal kelp *Laminaria digitata* features distinct bromoperoxidase and iodoperoxidase activities. *J Biol Chem. 278,* 23545–23552.

(11) Chen, V.B., Arendall, 3rd, W.B., Headd, J.J., Keedy, D.A., Immormino, R.M., Kapral, G.J., Murray, L.W., Richardson, J.S., and Richardson, D.C. (2010) MolProbity: all-atom structure validation for macromolecular crystallography. Acta Cryst. *D66*, 12–21.

(12) Wischang, D., Radlow, M., Schulz, H. Vilter H., Viehweger, L. Altmeyer, M.O., Kegler, C., Herrmann, J., Müller, R., Gaillard, F., Delage, L., Leblanc, C., and Hartung, J. (2012) Molecular cloning, structure and reactivity of the second bromoperoxidase from *Ascophyllum nodosum*. *Bioorg. Chem*. *44*, 25–34.

(13) Robert, X., and Gouet, P. (2014) Deciphering key features in protein structures with the new ENDscript server. *Nucl. Acids Res. 42*(*W1*), W320–W324.

(14) Frisch, M.J., Trucks, G.W., Schlegel, H.B., Scuseria, G.E., Robb, M.A., Cheeseman, J.R., Montgomery, Jr., J.A., Vreven, T., Kudin, K.N., Burant, J.C., Millam, J.M., Iyengar, S.S., Tomasi, J., Barone, V., Mennucci, B., Cossi, M., Scalmani, G., Rega, N., Petersson, G.A., Nakatsuji, H., Hada, M., Ehara, M., Toyota, K., Fukuda, R., Hasegawa, J., Ishida, M., Nakajima, T., Honda, Y., Kitao, O., Nakai, H., Klene, M., Li, X., Knox, J. E., Hratchian, H.P., Cross, J.B., Bakken, V., Adamo, C., Jaramillo, J., Gomperts, R., Stratmann, R.E., Yazyev, O., Austin, A.J., Cammi, R., Pomelli, C., Ochterski, J.W., Ayala, P.Y., Morokuma, K., Voth, G.A., Salvador, P., Dannenberg, J.J., Zakrzewski, V.G., Dapprich, S., Daniels, A.D., Strain, M.C., Farkas, O., Malick, D.K., Rabuck, A.D., Raghavachari, K., Foresman, J.B., Ortiz, J.V., Cui, Q., Baboul, A.G., Clifford, S., Cioslowski, J., Stefanov, B.B., Liu, G., Liashenko, A., Piskorz, P., Komaromi, I., Martin, R.L., Fox, D.J., Keith, T., Al-Laham, M.A., Peng, C.Y., Nanayakkara, A., Challacombe, M. Gill, P.M.W., Johnson, B., Chen, W., Wong, M.W., Gonzalez, C., and Pople, J.A. (2004). Gaussian, Inc., Wallingford CT, 2004.

(15) Schaftenaar G., and Noordik J.H. (2000) Molden: a pre- and post-processing program for molecular and electronic structures. *J. Comput.-Aided Mol. Design 14* 123–134.

(16) Glendening, E.D., Badenhoop, J.K., Reed, A.E., Carpenter, J.E., Bohmann, J.A., Morales, C.M., Weinhold, F. (2009) NBO 5.9 http://www.chem.wisc.edu/~nbo5. Theoretical Chemistry Institute, University of Wisconsin, Madison, WI.

(17) O'Boyle, N.M., Banck, M., James, C.A., Morley, C., Vandermeersch T., Hutchison, G.R. (2011) Open Babel: An open chemical toolbox. *J. Cheminform*. *3*, 33. DOI: 10.1186/1758-2946-3-33.

(18) Priebsch, W., and Rehder, D. Oxovanadium alkoxides: structure, reactivity, and ^{51}V NMR characteristics. Crystal and molecular structures of $VO(OCH_2CH_2C1)_3$ and $VOCl_2(THF)_2H_2O$. *Inorg. Chem. 29*, 3013–3019.

(19) Dickens, B., Prince, E., Schroeder, L.W. and Jordan T.H. (1974) A refinement of the crystal structure, $H_3PO_4 \cdot ½ H_2O$ with neutron diffraction data. *Acta Cryst. B30* 1470–1473.

(20) Hamilton, E.E., Fanwick, P.E., and Wilker, J.J. (2002) The elusive $(V_3O_9)^{3-}$: isolation, crystal structure and nonaqueous solution behavior. *J. Am. Chem. Soc. 124*, 78–82